UNIVERSIDADE ESTADUAL PAULISTA
"JÚLIO DE MESQUITA FILHO"
INSTITUTO DE QUÍMICA DE ARARAQUARA

A QUÍMICA DE PEPTÍDEOS E O MECANISMO DE INIBIÇÃO DA ATIVIDADE DA DNA GIRASE

Reinaldo Marchetto

Livre-Docência

Araraquara
- 2006 -

A QUÍMICA DE PEPTÍDEOS E O MECANISMO DE INIBIÇÃO DA ATIVIDADE DA DNA GIRASE

Reinaldo Marchetto

Texto sobre as atividades de pesquisa apresentado ao Instituto de Química da Universidade Estadual Paulista, Campus de Araraquara, para obtenção do título de Livre-docente em Bioquímica

Araraquara –S.P
- 2006 –

“Não há maior prova de ignorância
do que acreditar que o inexplicável é impossível”
(S. Bilard)

Aos meus pais Genor e Ermelinda,
que pela graça Divina, me deram a Vida e com ela a
oportunidade do aprimoramento intelectual e espiritual

À Patrícia, minha querida esposa,
grande amiga e companheira,
pelo seu eterno apoio e pela presença
marcante na minha vida.

Aos meus queridos Daniel e Giovanna,
simplesmente por existirem e por mostrarem
que realmente tudo vale a pena.

AGRADECIMENTOS

À Deus, por tudo e sempre.....

Aos Docentes e servidores do Departamento de Bioquímica e Tecnologia Química

Aos colaboradores do IQAr/UNESP, especialmente da DTA, pelo suporte técnico e administrativo.

Às colaboradoras da Seção de Pós-graduação, pela dedicação e convívio amigo.

Às Agências de Fomento, CNPq, CAPES, FUNDUNESP e FAPESP pelo imenso apoio financeiro.

Ao pessoal do Grupo de Síntese, Estrutura e Aplicações de Peptídeos e Proteínas.

Aos grandes mestres Clovis Nakaie, Ernest Giralt e Fernando Albericio, responsáveis diretos pelos alicerces e arranque na minha formação técnica e científica.

Por fim, mas não menos importante, aos meus alunos colaboradores discentes. Todos igualmente contribuíram para mais esta etapa da minha carreira, Em especial, à Andreza, Saulo e Eliane, cujos dados das dissertações e teses foram empregados na confecção deste trabalho.

A todos, meus sinceros agradecimentos.

ÍNDICE

ABREVIATURAS

1. Aminoácidos

Ala (A)	-	Alanina	Arg (R)	-	Arginina
Asn (N)	-	Asparagina	Asp (D)	-	Ácido Aspártico
Glu (E)	-	Ácido Glutâmico	Cys (C)	-	Cisteína
Phe (F)	-	Fenilalanina	Gly (G)	-	Glicina
Gln (Q)	-	Glutamina	His (H)	-	Histidina
Ile (I)	-	Isoleucina	Leu (L)	-	Leucina
Lys (K)	-	Lisina	Met (M)	-	Metionina
Pro (P)	-	Prolina	Ser (S)	-	Serina
Tyr (Y)	-	Tirosina	Thr (T)	-	Treonina
Trp (W)	-	Triptofano	Val (V)	-	Valina
Orn (O)	-	Ornitina			

2. Outras

AAA	-	Análise de Aminoácidos
ACM	-	Acetoamidometila
Ac	-	Acetila
ACN	-	Acetonitrila
AGYRA	-	Análogo da Subunidade A da DNA girase
AGYRAM	-	Análogo Mutado da Subunidade A da DNA girase
AGYRB	-	Análogo da Subunidade B da DNA girase
AGYRBM	-	Análogo Mutado da Subunidade B da DNA girase
AOP	-	Hexafluorfosfato de 7-aza-(1-H-benzotriazol-1-il-oxi)-tris(dimetilamino)-fosfônio
BAR	-	Benzidrilaminoresina
t-Boc	-	tert-Butiloxicarbonila
BOM	-	Benziloximetila

BOP	-	Hexafluorfosfato de (1-H-benzotriazol-1-il-oxi)-tris-(dimetilamino)-fosfônio
BrZ	-	2-bromobenziloxicarbonila
*t*Bu	-	tert-butila
Bzl	-	Benzila
CFX	-	Ciprofloxacina
CLAE	-	Cromatografia Líquida de Alta Eficiência
CLME	-	Cromatografia Líquida de Média Eficiência
cHex	-	Ciclohexila
ClZ	-	2-clorobenziloxicarbonila
DCM	-	Diclorometano
DIC	-	Diisopropilcarbodiimida
DIEA	-	Diisopropiletilamina
DMF	-	Dimetilformamida
DMSO	-	Dimetilsulfóxido
DNP	-	2,4-Dinitrofenila
EDT	-	Etanoditiol
ES	-	Electron Spray
Fmoc	-	9-fluorenilmetiloxicarbonila
For	-	Formila
GyrA	-	Subunidade A da DNA girase
GyrB	-	Subunidade B da DNA girase
HATU	-	Hexafluorfosfato de O-(7-azabenzotriazol-1-il)-1,1,3,3-tetrametilurônio
HBTU	-	Hexafluorfosfato de 2-(1-H-Benzotriazol-1-il) – 1,1,3,3 – tetrametilurônio
HOAt	-	7-aza-1-hidroxibenzotriazol
HOBt	-	1-Hidroxibenzotriazol
HMP	-	Hidroximetilfenoxila
MBAR	-	Metilbenzidrilaminoresina

Meb	-	p-metilbenzila
Mob	-	p-metoxibenzila
NB	-	Novobiocina
PAL	-	Ácido 5-(4-Fmoc-aminometil-3,5-dimetoxi)-fenoxivalérico
PAM	-	Fenilacetamidometila
Pbf	-	2,2,4,6,7-pentametil-dihidrobenzofurano-5-sulfonila
pBS	-	Plasmídeo pBluescript
Pmc	-	2,2,5,7,8-pentametil-cromano-6-sulfonila
PyBOP	-	Hexafluorfosfato de (1-H-benzotriazol-1-il-oxi)-tris-(pirrolidino)fosfônio
PyOAP	-	Hexafluorfosfato de 7-aza-(1-H-benzotriazol-1-il-oxi)-tris(pirrolidino)fosfônio
Rink	-	Ácido 4-(2'-4'-dimetoxifenil-Fmoc-aminometil)-fenoxi-acético
RPE	-	Ressonância Paramagnética Eletrônica
SPFS	-	Síntese de Peptídeos em Fase Sólida
TATU	-	Tetrafluorborato de O-(7-azabenzotriazol-1-il)-1,1,3,3-tetrametilurônio
TBTU	-	Tetrafluorborato de 2-(1-H-Benzotriazol-1-il) – 1,1,3,3 – tetrametilurônio
TFA	-	Ácido Trifluoracético
TIS	-	Triisopropilsilano
Tmob	-	Trimetoxibenzila
TOAC	-	Ácido 4-amino-2,2,6,6-tetrametil-piperidil-N-óxido carboxílico
Tos	-	Tosila
Trt	-	Tritila
UV	-	Ultra-Violeta
Z	-	Benziloxicarbonila

Apresentação

Passaram-se 15 anos de atuação profissional na área acadêmica. Durante este período estive desenvolvendo estudos e pesquisas em duas linhas, porém correlacionadas. A primeira, em continuidade ao trabalho de doutorado, envolvendo estudos sobre a metodologia de síntese de peptídeos em fase sólida, visando o aprimoramento das etapas envolvidas no processo sintético. A segunda, relacionada com a aplicação de peptídeos sintéticos, tanto no estudo do mecanismo de inibição da atividade da DNA girase, quanto na produção de novas famílias de inibidores desta enzima.

Esta tese de Livre-docência representa um compilado e um arrazoado da contribuição que representaram os recentes trabalhos desenvolvidos nestas duas linhas de pesquisa, incluindo dissertações orientadas e teses em orientação, bem como o trabalho desenvolvido durante o estágio de pós-doutorado na Universidade de Barcelona.

O texto ora apresentado foi dividido em três partes: a primeira abordando sucintamente a química de peptídeos, mais especificamente a síntese em fase sólida, já que nossa contribuição está relacionada com o suporte sólido empregado nesta metodologia; a segunda contendo basicamente o campo principal de nossa atuação, que é entender o mecanismo de inibição da DNA girase. Nesta parte, está descrita a obtenção de peptídeos, através da metodologia da fase sólida, empregados como modelos no estudo do processo de interação de diferentes tipos de drogas e a enzima, bem como na tentativa de obtenção de moléculas peptídicas modificadas estruturalmente, de modo a gerar uma nova família potencialmente capaz de inibir a ação da DNA girase. Finalmente, na última parte deste documento, estão anexados os trabalhos científicos publicados ou por publicar, que foram utilizados na elaboração deste texto.

PARTE I

A QUÍMICA DE PEPTÍDEOS

QUÍMICA DE PEPTÍDEOS

1. Métodos de Síntese

A síntese de peptídeos poderia ser explicada, a um nível bastante básico, como a formação química repetida de ligações amida com a finalidade de conectar funções amina e carboxílica de L-α-aminoácidos adjacentes. No entanto, esta definição não permite imaginar o grau de complexidade e ao mesmo tempo a riqueza associada a este campo da ciência. Como seu nome bem indica, todos L-α-aminoácidos possuem ao menos duas funções, e portanto, para que a ligação peptídica ocorra entre as funções desejadas, todas as demais deverão estar protegidas, de modo que a formação de ligações amida posteriores irá requerer, em primeiro lugar, a eliminação de um dos grupos protetores que bloqueiam a função que irá formar a nova ligação peptídica. Além disso, levando-se em conta que muitos dos aminoácidos codificados possuem uma terceira função na cadeia lateral, a síntese de um peptídeo, além da necessidade de dispor de métodos eficazes para completar a reação de formação da ligação peptídica, requer uma correta manipulação dos grupos protetores, tanto das funções em posição α como das funções laterais dos aminoácidos trifuncionais.

Os métodos de síntese de peptídeos se dividem em duas categorias: linear e convergente. A síntese linear se baseia na crescimento seqüencial, aminoácido após aminoácido, da cadeia peptídica (Barany *et al*., 1987; Fields *et al*., 1992). Este crescimento se realiza, ao contrário do que ocorre nos ribossomos, desde a extremidade C-terminal para N-terminal, para evitar a perda de quiralidade do resíduo associado ao grupo carboxílico que se acopla. Na estratégia convergente, as unidades que participam não são aminoácidos protegidos, mas peptídeos igualmente protegidos (Lloyd-Williams *et al.*, 1993; Albericio *et al*., 1997) A etapa final de eliminação dos grupos protetores é comum a ambas estratégias.

Classicamente e desde os trabalhos pioneiros de Fischer (Fischer & Fourneau, 1901) e Curtius (1902), todo processo associado à síntese de um peptídeo ocorria em solução. Há mais de quatro décadas, uma inovadora metodologia para a síntese de peptídeos foi apresentada à comunidade científica por Bruce Merrifield. Tal metodologia veio revolucionar a síntese orgânica por suas características peculiares, uma vez que abandonou a tradicional rotina, própria da síntese em solução, e introduziu o uso de polímeros insolúveis como suporte. Este método, denominado síntese de peptídeos em fase sólida (SPFS) (Merrifield, 1963; Merrifield, 1985), que em princípio foi aplicado exclusivamente à estratégia seqüencial, tem como base o fato do grupo carboxílico C-terminal se encontrar unido covalentemente ao polímero e, portanto, o componente que contém esta extremidade é insolúvel nos solventes utilizados no processo de síntese. Assim, o excesso de reagentes e uma grande maioria dos produtos secundários podem ser eliminados por simples filtração e lavagens do polímero que contém o peptídeo em crescimento. Este fato influencia favoravelmente para que se possam utilizar grandes excessos de reagentes, conseguindo em muitas etapas, rendimentos quase quantitativos. As vantagens adicionais são que se minimizam as perdas por manipulação e que todo processo sintético pode ser automatizado.

A metodologia da fase sólida em sua estratégia seqüencial é atualmente a mais utilizada para a síntese de peptídeos que contém até 50 ou 60 resíduos de aminoácidos. Para a síntese de seqüências maiores, costuma-se empregar a estratégia convergente, seja totalmente em fase sólida ou em solução, ou mediante uma combinação de ambas: síntese dos peptídeos protegidos em fase sólida, e posterior acoplamento dos mesmos em solução.

Neste trabalho dar-se-á maior ênfase a metodologia da fase sólida, especificamente à estratégia seqüencial, a qual estamos envolvidos desde a fase de pós-graduação e tem sido, de certa forma, nossa linha de atuação ao longo dos últimos anos.

2. O Suporte Sólido

Quando se menciona o termo "suporte sólido" deve-se lembrar que tal palavra se aplica a uma série de compostos utilizados em síntese em fase sólida, dos quais muitos se encontram disponíveis comercialmente. Embora muitas vezes sejam chamados vulgarmente de "resinas", apresentam entre si diferenças de fundamental importância, as quais permitem sua classificação de acordo com suas especificações químicas (Früchtel & Jung, 1996).

Genericamente, pode-se descrever uma resina utilizada como suporte sólido como sendo uma estrutura complexa, a qual é formada por polímeros retilíneos compostos por unidades monoméricas constantes, formando uma espécie de rede (Figura I.1). Os feixes desta, são interligados transversalmente através de um monômero bi-funcional (ligações cruzadas, *cross-linking*) formando, na maioria delas, uma esfera (*grão*), de tamanho padronizado. A intervalos mais ou menos regulares surgem funções químicas diferenciadas (ligantes, *linkers*), que podem constituir-se por apenas um átomo ou mesmo serem formadas por moléculas de dimensão considerável com diversos grupos funcionais (Tam *et al.*, 1980).

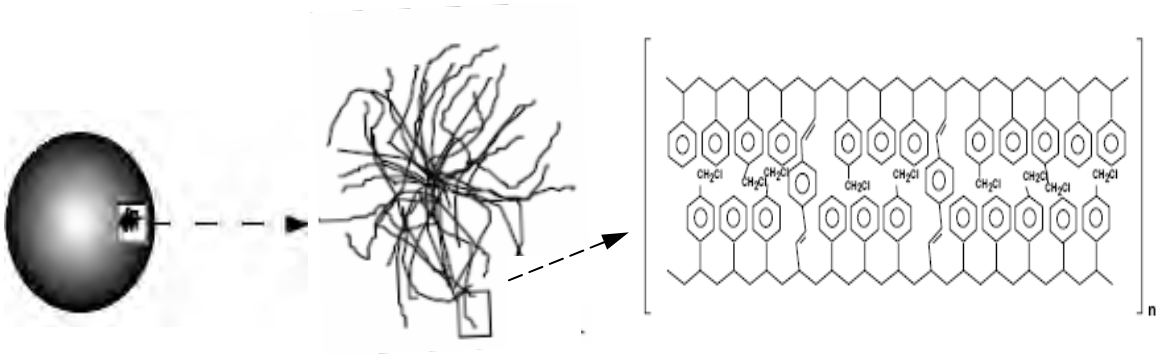

Figura I.1. Visualização progressiva de uma resina, a partir de uma unidade macroscópica e as cadeias poliméricas que a compõem até a fórmula molecular de um determinado polímero.

Em geral, as características físicas da resina são determinadas pelo seu arcabouço, enquanto que as características químicas (tipo de grupo funcional aceitável pelo polímero, condições de clivagem, grupo funcional formado após clivagem, etc.) são determinadas pelo ligante (Lloyd-Willians *et al.*, 1993). Em relação às características físicas, o grau de resistência frente à agitação mecânica, temperatura, pressão e comportamento quando em contato com solventes, são bastante influenciadas pela proporção de ligações cruzadas existentes no polímero; esse último fator também é fortemente determinado pelas características dos ligantes, ainda que em menor extensão .

Os suportes que conduzem aos melhores resultados para a síntese de peptídeos estão muito longe de serem estáticos e as reações químicas em fase sólida não ocorrem exclusivamente na superfície do suporte. Pelo contrário, as reações ocorrem preferencialmente naqueles filamentos do polímero que são móveis, se encontram bem solvatados e são acessíveis aos reagentes químicos (Sarin *et al*., 1980; Marchetto *et al*., 1992). Os suportes que reúnem estas características permitem que as reações químicas ocorram com velocidades muito próximas, embora não iguais, às que ocorrem em solução.

Desde os trabalhos iniciais de Merrifield, o suporte mais utilizado é um polímero microporoso de estireno, que contém 1% de *p*-divinilbenzeno. O grau de substituição destes suportes está compreendido entre 0,2 e 1,0 mmol/g. Enquanto os grãos de poliestireno secos apresentam um diâmetro de aproximadamente 50 μm, na presença dos solventes ou sistemas de solventes mais comuns utilizados na síntese de peptídeos, costumam inchar até 2 a 6 vezes o seu volume inicial (Sarin *et al*., 1980; Marchetto *et al*., 1992). Desta forma é possível conseguir que todos os ligantes, que estão no interior da rede polimérica fiquem expostos e portanto acessíveis aos diferentes solventes e reagentes utilizados na síntese.

3. Formação da Ligação Peptídica

Para a reação de uma função ácida e outra amina, é necessário que o componente eletrófilo (C carbonílico do ácido) esteja ativado, pois em caso contrário, seria formado um sal de amônio. Esta ativação do ácido carboxílico, que é a base da formação da ligação peptídica, tem sido uma das etapas da síntese de peptídeos que mais evoluiu nos últimos anos, resultado da busca incessante de obter bom rendimento na formação da ligação peptídica, mantendo a integridade da cadeia em crescimento, em particular do centro estereogênico em α do grupo carboxílico ativado.

Os reagentes de acoplamento mais utilizados podem ser divididos em dois grandes grupos: carbodiimidas e sais de ônio.

As carbodiimidas são os reagentes de acoplamento mais utilizados, seja em fase sólida ou solução (Sheehan & Hess, 1955). O mecanismo envolve a formação da *O*-acilisourea, que sofre aminólise por parte da amina, para produzir a ligação amida. Se for empregado um segundo equivalente de ácido carboxílico, será formado o anidrido simétrico. Do mesmo modo, na presença de hidroxilaminas (p.ex. Hidroxibenzotriazol – HOBt ou 7-aza-1-hidroxibenzotriazol - HOAt), será obtido um éster ativo. Qualquer uma das três espécies reativas, *O*-acilisourea, anidrido simétrico ou éster ativo, são bons agentes acilantes (Figura I.2).

Embora Kenner (Gawne *et al.*, 1969; Bates *et al.*, 1975) tenha sido o primeiro em descrever os sais de acilfosfonio como reagentes de acoplamento, foi após a divulgação dos trabalhos de Castro e Coste (Castro *et al.*, 1975; Coste *et al.*, 1990; Coste & Campagne, 1995) que a utilização deste tipo de reagente foi amplamente adotada. Os primeiros destes reagentes descritos [hexafluorfosfatos de (benzotriazol -1-il-oxi)-tris(dimetilamino)-fosfônio (BOP) e de (benzotriazol-1-il-oxi)-tris-(pirrolidino)fosfônio (pyBOP)] levam incorporados na molécula, um

equivalente de benzotriazol, portanto a espécie acilante final é o éster de benzotriazol.

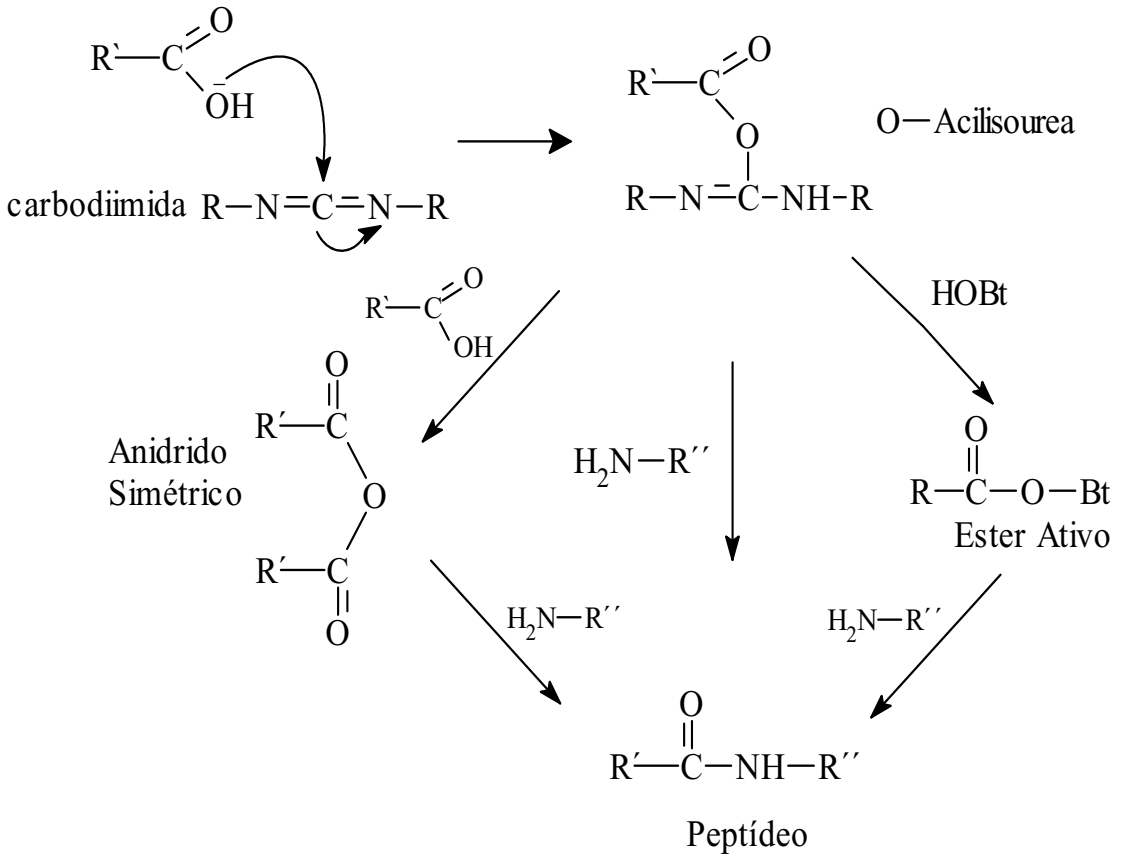

Figura I.2. Mecanismo de formação de ligação peptídica empregando carbodiimidas

Os derivados de HOAt destes sais de fosfônio (AOP e pyOAP) também foram preparados e são melhores agentes acilantes que BOP e pyBOP (Carpino, 1993a; Carpino *et al.*, 1994). Dentre eles, os derivados de pirrolidina (PyBOP e pyOAP) são os mais recomendados pois são mais reativos e não formam produtos secundários tóxicos, como a hexametilfosforotriamida, formada quando se utiliza BOP ou AOP.

Dourtoglou em 1978 descreveu a preparação de derivados análogos aos sais de fosfônio, contendo um átomo de carbono em substituição ao átomo de fósforo (Dourtoglou *et al.*, 1978). A estrutura

proposta, baseada na dos análogos de fosfônio, foi a de um sal de urônio [Hexafluorfosfatos de N-(1H-benzotriazol-1-il)-1,1,3,3-tetrametilurônio (HBTU) e de O-(7-azabenzotriazol-1-il)-1,1,3,3-tetrametiurônio (HATU)] (Figura I.3). Também foi preparado o correspondente tetrafluorborato destes derivados de urônio (TBTU e TATU). Dentre estes últimos reagentes, o HATU tem demonstrado ser o mais eficiente em termos de rendimento e o que provoca menos racemização (Carpino *et al.*, 1995a). HATU assim como o pyOAP é muito indicado para a síntese em fase sólida, de peptídeos que contenham aminoácidos com impedimento estérico (Carpino *et al.*, 1995b) e para preparação de bibliotecas peptídicas mediante o método baseado na utilização de uma mistura de aminoácidos (Kates *et al.*, 1996).

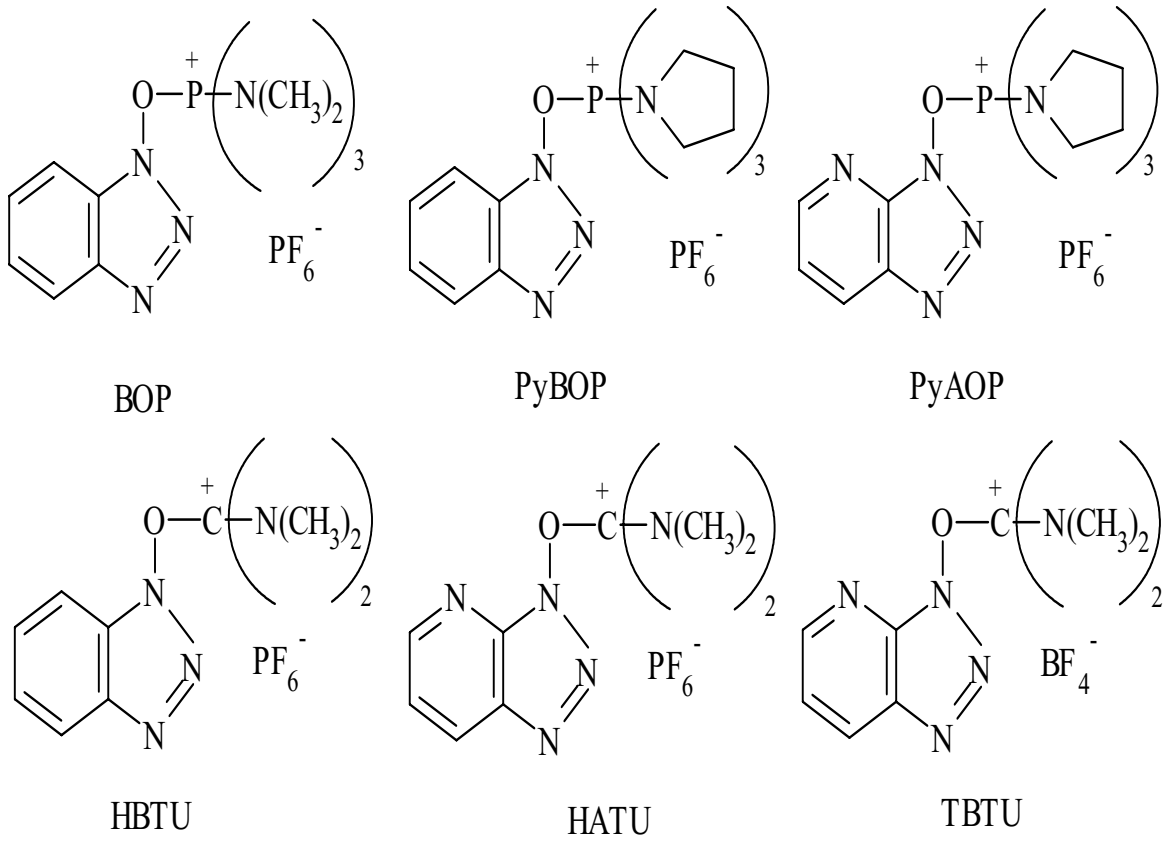

Figura I.3. Sais de fosfônio e urônio empregados como agentes acilantes

4. Esquemas de Proteção

A formação controlada de qualquer ligação peptídica requer que todos os grupos funcionais presentes nas moléculas, exceto os dois que vão participar da formação da ligação, estejam protegidos. Uma vez formada a ligação e antes da incorporação do seguinte aminoácido ou peptídeo, deve-se eliminar o protetor do grupo funcional que irá permitir o crescimento da cadeia peptídica. Por último e ao final do processo sintético, os protetores de todos grupos funcionais devem ser eliminados. Assim, pode-se concluir que o esquema de proteção é crucial para concluir com êxito a síntese de um peptídeo.

Para o processo de síntese seqüencial existem dois tipos diferentes de protetores. Por um lado, está aquele tipo que mascara o grupo funcional que irá participar da nova ligação peptídica e, portanto, deve ser eliminado a cada ciclo sintético, denominado "protetor temporário". Como normalmente a síntese é executada na direção C $\rightarrow$ N, este tipo de protetor é aquele que normalmente protege a função amina. Por outro, estão os "protetores permanentes", que são os que devem permanecer estáveis durante todo processo sintético e que são eliminados no final do mesmo. Neste tipo pode-se diferenciar aqueles da função carboxílica do aminoácido C-terminal dos que protegem as funções laterais dos aminoácidos trifuncionais. Na metodologia da fase sólida, o protetor da função carboxílica C-terminal está unido de forma covalente a um suporte polimérico insolúvel e assim este protetor pode ser considerado como o ancoradouro da cadeia peptídica que vai crescendo ligada ao suporte sólido. A natureza química do grupo protetor da função α-amina marca, de certa forma a estratégia de síntese, uma vez que os protetores permanentes devem ser estáveis às condições utilizadas para eliminar repetidas vezes o protetor temporário. Por sua vez, os protetores permanentes devem ser eliminados eficazmente na última etapa.

Em uma estratégia convergente, durante a síntese dos peptídeos protegidos, se introduz uma nova variante. O protetor da função carboxílica do aminoácido C-terminal deve ser eliminado antes da realização do acoplamento deste peptídeo ao seguinte peptídeo protegido. Este protetor deve ser estável durante o crescimento da cadeia, porém quando da sua eliminação, deve manter inalterados tanto o protetor da função α-amina, como os protetores das cadeias laterais. Neste caso, este protetor, denominado "semi-permanente" introduz ao sistema um novo nível de labilidade química (Figura I.4).

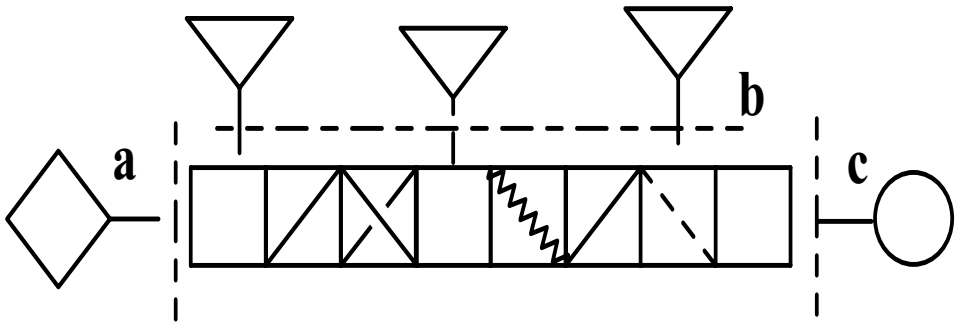

a. Protetor da função α-amina ("temporário")
b. Protetores das cadeias laterais ("permanentes")
c. Protetor da função α-carboxílico:
"permanente" na estratégia seqüencial
"semi-permanente" na estratégia convergente
unido a um suporte insolúvel na metodologia da fase sólida

Figura I.4. Esquema de Proteção

Proteção temporária da função α-amina

Embora existam miríades de excelentes grupos protetores da função amina (Greene & Wuts, 1991), para a proteção do grupo α-amínico dos aminoácidos tem sido usado, quase exclusivamente, protetores tipo uretano. Este tipo de protetores conferem uma resistência marcante à racemização do carbono em α quando o grupo carboxílico se encontra ativado. Concretamente, os grupos *terc*-

butiloxicarbonila (*t*-Boc) (Anderson & McGregor, 1957; Carpino, 1957) e 9-fluorenilmetiloxicarbonila (Fmoc) (Carpino & Han, 1972) são aqueles em que se baseiam os dois principais esquemas de proteção na metodologia da fase sólida (Figura I.5).

O grupo *t*-Boc é eliminado mediante uma acidólise com ácidos de força moderada (TFA 30% em DCM), o que implica que os protetores permanentes que se utilizam juntamente com o grupo *t*-Boc devam ser estáveis nestas condições. Neste caso, em seguida deve-se realizar uma neutralização (normalmente com DIEA 5% em DCM) para liberar a função amina desprotonada. Nesta estratégia, utiliza-se para as funções das cadeias laterais, protetores tipo benzila (Bzl), os quais requerem para sua eliminação, o emprego de ácidos mais fortes como o ácido fluorídrico anidro.

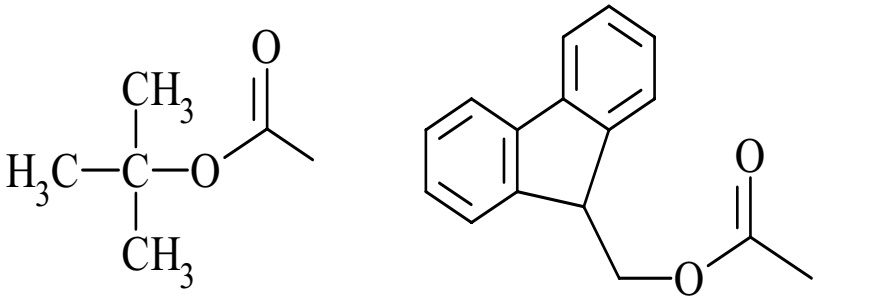

Figura I.5. Protetores usuais para função α-amina na metodologia da fase sólida

Quanto ao grupo Fmoc, este é eliminado com bases de força moderada (piperidina 20% em DMF), através de uma reação de β-eliminação. Isto permite que, para as cadeias laterais dos aminoácidos trifuncionais, podem ser utilizados protetores baseados no

grupo terc-butila (*t*Bu) e que são lábeis na presença de ácidos como o trifluoracético.

Proteção permanente das cadeias laterais funcionalizadas

Alguns dos aminoácidos trifuncionais (Asp, Glu, Lys, Orn e Cys) necessitam imperiosamente de proteção para suas cadeias laterais, enquanto os demais, a decisão de tê-las protegidas depende da estratégia a ser empregada e do tamanho do peptídeo a ser sintetizado.

Na estratégia Boc/Bzl, derivados benzílicos são empregados na proteção da cadeia lateral dos seguintes aminoácidos: Asp, Glu, Ser, Thr, Tyr, Lys e Orn. A função ω-amina da Lys e da Orn é protegida com o grupo 2-clorobenziloxicarbonila (ClZ), que é mais efetivo que o Z. O fenol da Tyr é protegido na forma de carbonato com o grupo 2-bromobenziloxicarbonila (BrZ). Este protetor tem a vantagem frente ao Bzl, uma vez que o carbocátion que se forma durante a acidólise com HF é menos reativa, não permitindo a alquilação do próprio anel aromático (Yamashiro & Li, 1973a). As funções hidroxila da Ser e Thr, assim como a carboxíla do Glu são protegidas com o Bzl, enquanto que para o Asp é preferido utilizar o éster do ciclohexila (cHex), pois o emprego do éster benzílico pode dar lugar a uma eliminação intramolecular que conduz à formação de uma aspartimida, que por sua vez pode hidrolisar para produzir uma mistura de α- e β-peptídeos (Nicolas *et al*., 1989).

Na estratégia Fmoc/*t*Bu são empregados derivados do *t*-butanol para proteger lateralmente estes mesmos aminoácidos: os ésteres ou éteres *t*-butílicos para os cinco primeiros e a correspondente uretana (Boc) para a Lys/Orn.

A Cys é um aminoácido único, pois a função tiol da sua cadeia lateral é capaz de formar pontes disulfeto com outra cadeia lateral de Cys da mesma ou de outra molécula peptídica. Existem dois grupos protetores de Cys, independentemente da estratégia utilizada. De um

lado estão aqueles grupos que são liberados na etapa final da síntese, juntamente com os demais protetores permanentes. De outro, estão aqueles que sua eliminação é independente dos demais, podendo ser liberado antes ou depois deles. Dentro do primeiro grupo estão incluídos o *p*-metilbenzila (Meb) (Erickson & Merrifield, 1973) e *p*-metoxibenzila (Mob) (Akabori *et al*., 1964) que são eliminados com HF e são compatíveis com a estratégia Boc/Bzl. Para a estratégia Fmoc/*t*Bu estão o tritila (Trt) (McCurdy, 1989) e o trimetoxibenzila (Tmob) (Munson *et al*., 1992), que são eliminados com TFA.

A desproteção da função tiol também pode ser feita independentemente da etapa de acidólise. Para isso este grupo deve estar protegido com o grupo acetamidometila (Acm) (Veber *et al*., 1972), que é totalmente estável frente a ácidos e são eliminados mediante oxidação com iodo ou trifluoracetato de tálio (III) para produzir diretamente a ponte disulfeto, ou com acetato de mercúrio (II), seguido de tratamento com β-mercaptoetanol para resultar no grupo tiol livre. Este grupo protetor é compatível com ambas estratégias Boc/Bzl e Fmoc/*t*Bu.

O grupo δ-guanidino da Arg é fortemente básico (pKa = 12,5) e portanto, sua simples protonação, que inclusive ocorre mediante ácidos fracos como o HOBt, previne a acilação não desejada. De qualquer forma, os derivados de Arg sem proteção de cadeia lateral são muito insolúveis e, o que é pior, quando na ativação do grupo carboxílico pode ocorrer a formação de uma δ-lactama. A melhor forma de proteção é mediante grupos tipo arilsulfonilo. O tosila (Tos) (Ramachandran & Li, 1962) que se elimina com HF para a estratégia Boc/Bzl e o 2,2,4,6,7-pentametil-dihidrobenzofurano-5-sulfonila (Pbf) (Carpino *et al*., 1993b) ou o 2,2,5,7,8-pentametilcromano-6-sulfonila (Pmc) (Ramage *et al*., 1991), que são eliminados com TFA 90%, para a estratégia Fmoc/*t*Bu.

Para o grupo imidazol da His, o grupo tritila (Trt) (Sieber & Riniker, 1987) é um bom protetor, na estratégia Fmoc/*t*Bu, pois é estável durante todo processo sintético e é eliminado no final com TFA.

Ao contrário, na estratégia Boc/Bzl não existe um grupo que reúna as condições ótimas para proteção do grupo imidazol da His. O grupo tosila (tos) (Sakakibara & Fujii, 1969) evita a racemização durante a etapa de acoplamento, mas não é estável na presença de HOBt. O benziloximetila (Bom) (Brown & Jones, 1981) tem o inconveniente de gerar formaldeído, durante o tratamento com HF, que pode reagir com as funções amina. Possivelmente o protetor mais útil até o momento seja o 2,4-dinitrofenila (Dnp) (Chillemy & Merrifield, 1969).

As funções amida de Asn e Gln não necessitam estritamente estarem protegidas, embora quando estes resíduos são incorporados empregando carbodiimidas, pode ocorrer uma reação de desidratação com a formação da correspondente nitrila. Na estratégia Fmoc/*t*Bu costuma-se introduzir estes aminoácidos protegidos com o grupo tritila, para aumentar a solubilidade dos Fmoc-aminoácidos e também anular a possibilidade de desidratação.

O indol do Trp é susceptível a reações de substituição aromática eletrofílica durante a acidólise. Por este motivo, costuma-se protegê-lo com grupos que atraem elétrons, como o formila (For) (Yamashiro & Li, 1973b), na estratégia Boc/Bzl, e o Boc (White, 1992) na Fmoc/*t*Bu.

Igualmente ao que ocorre com o Trp, a função tioéter da Met pode sofrer alquilação com os carbocátions formados durante as etapas de acidólise. Além disso pode oxidar-se a sulfóxido. Na estratégia Fmoc/*t*Bu, a oxidação da Met não costuma ser um problema sério e se utiliza sem proteção. Por outro lado, na estratégia Boc/Bzl é recomendável introduzir a Met já na forma de sulfóxido, com posterior regeneração da função tioéter na etapa de clivagem final.

Proteção do grupo α-carboxílico

Na metodologia da fase sólida, o protetor α-carboxílico expressa a união da cadeia peptídica ao suporte polimérico. Para o caso de peptídeos-ácido, esta união é feita mediante uma ligação éster,

enquanto que para peptídeos-amida a união é feita através de uma ligação amida. Um aspecto importante nesta metodologia é como promover esta primeira união, sobretudo para o caso de peptídeos-ácidos, uma vez que a formação de um éster costuma ser mais problemática que a de uma amida. A maneira ótima de realizar esta união é empregando um espaçador (*handle*), que é definido como um composto bifuncional que serve para unir uma cadeia peptídica em crescimento ao suporte polimérico. No caso de síntese de peptídeos-ácidos, o *handle* deve carregar incorporado, o primeiro aminoácido da seqüência, devidamente protegido.

Sem dúvida nenhuma, os protetores permanentes mais comuns para este tipo de peptídeos são os do tipo benzila: *p*-alquilbenzila (na PAM) (Mitchell *et al.*, 1976) para a estratégia Boc/Bzl e *p*-alcoxibenzila (no HMP) (Albericio & Barany, 1985) para a estratégia Fmoc/*t*Bu. Ambos levam incorporado o primeiro aminoácido protegido (Figura I.6).

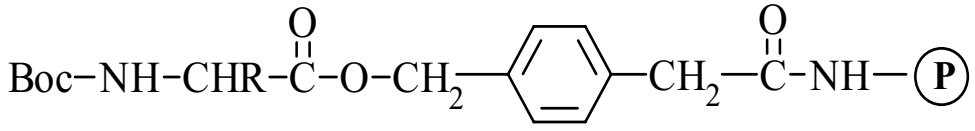

PAM

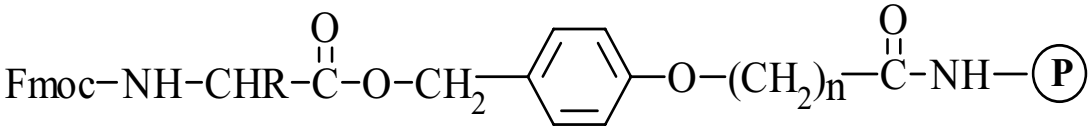

HMP

Figura I.6. *Handles* empregados na síntese de peptídeos-ácido em fase sólida

Nestes denominados *handles*, a formação da ligação éster ocorre normalmente através de uma substituição nucleofílica por parte do carboxilato do aminoácido sobre o correspondente bromobenzilderivado

(Bernatowicz *et al*., 1989). Quando o aminoácido C-terminal é Cys ou His este método não funciona e recorre-se a uma esterificação com o correspondente álcool em condições muito suaves, geralmente com pyOAP (Kates *et al.*, 1996) para evitar a racemização destes dois aminoácidos.

As amidas são mais estáveis que os ésteres frente a acidólise, portanto as posições benzílicas devem estar estabilizadas por outros anéis aromáticos e/ou grupos doadores de elétrons. Assim, para a estratégia Boc/Bzl utiliza-se a resina benzidrilamina (BAR) ou *p*-metilbenzidrilamina (MBAR) (Pietta & Marshall, 1970). Na estratégia Fmoc/*t*-Bu emprega-se principalmente, os *handles* ácido 4-(2'-4'-dimetoxifenil-Fmoc-aminometil)-fenoxiacético (Rink) (Rink 1987) e o ácido 5-(4-Fmoc-aminometil-3,5-dimetoxi)-fenoxivalérico (PAL) (Albericio *et al*., 1990) (Figura I.7), ligados geralmente a uma MBAR.

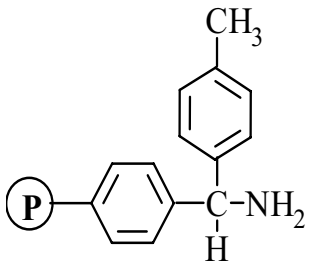

MBAR

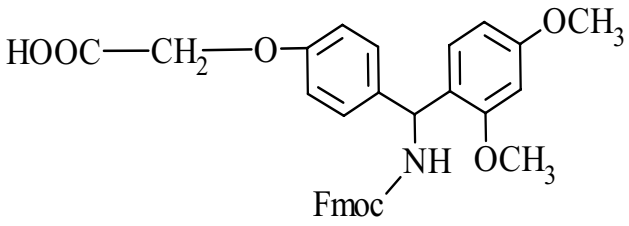

Rink

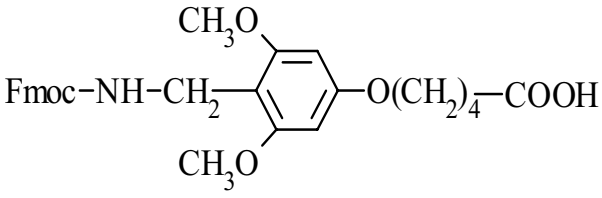

PAL

Figura I.7. Protetores permanentes do grupo α-carboxílico de peptídeos-amida

5. Nossa contribuição à metodologia de síntese em fase sólida

Desde que ingressamos na área de pesquisa científica, atuamos diretamente na parte metodológica da síntese em fase sólida, mais precisamente com o componente principal desta metodologia que é o suporte sólido. Neste contexto, muito havíamos feito até a conclusão do doutorado, porém propriedades como a dinâmica da cadeia polimérica e o processo de agregação entre as cadeias polipeptídicas em crescimento, dependentes da capacidade de inchamento do conjunto polímero-peptídeo, em diferentes sistemas de solventes, ainda permaneciam carentes de uma avaliação mais concreta.

Assim, complementando estudos iniciados na ocasião do doutorado, desenvolvemos um trabalho, que se estendeu por vários anos, o qual culminou com uma publicação recente e que recebeu grande destaque por ter sido escolhido para compor a capa do fascículo 12 do volume 70 do Journal of Organic Chemistry (anexo 1).

Este trabalho, que contou com a participação de importantes colaboradores dentre os quais estagiários e bolsistas de iniciação científica, propõe a determinação de parâmetros essenciais para os processos químicos que ocorrem no interior do polímero, através de um estudo combinado de microscopia e ressonância paramagnética eletrônica (RPE), através de uma estratégia de cálculo inédita.

A estratégia envolveu a medida microscópica inicial dos grãos secos e solvatados, de alguns lotes de benzidrilamina-resinas (BAR) marcadas, resinas usadas na síntese de peptídeo α-carboxi-amidas terminais (Marchetto *et al*., 1992). Subseqüentemente, dados como volume de solvente dentro da estrutura polimérica, número de grupos reacionais por grão de resina, distância entre os grupos reacionais e concentração destes grupos no interior da estrutura polimérica, foram estimados por uma estratégia de cálculo seqüencial.

Em termos de resina marcada, foram estudadas oito amostras de BAR contendo desde 0,003 até 0,988 mmol/g da molécula marcadora

Boc-TOAC. Para obtenção das mesmas, diferentes lotes da resina com grau de substituições iniciais de 0,05, 0,14, 0,80 e 1,40 mmol/g foram usados para o acoplamento do derivado *t*-Boc do ácido 4-amino-2,2,6,6-tetrametil-piperidil-N-óxido carboxílico (Boc-TOAC-OH) (Nakaie *et al*., 1981), empregando o protocolo DIC/HOBt em DCM.

Espectros de RPE das oito amostras de resina (BAR) marcadas, foram traçados e analisados (Figura I.8) como uma forma de checar a estratégia de cálculo proposta. A ocorrência de interação spin-spin foi usada como um critério para avaliar a distância intersítios e a concentração dos mesmos no interior dos grãos de resina. Para isso, foi analisado se o efeito espectral provocado por interações spin-spin, dependentes da distância e concentração da molécula marcadora no interior da estrutura polimérica, era similar ao observado quando da molécula marcadora livre em solução.

Quanto aos parâmetros calculados, a distância média intersítios variou desde um máximo de 170 Å (para a amostra de BAR contendo 0,003 mmol/g de Boc-TOAC, em diclorometano) até um mínimo de 17 Å (para a amostra de BAR contendo 0,988 mmol/g de Boc-TOAC, em dimetilformamida). Além disso, a concentração de sítios dentro dos grãos destas mesmas amostras, variou desde um mínimo de 0,4 M até um máximo de 550 M. Portanto, em condições de elevada quantidade de Boc-TOAC (0,988 mmol/g em DMF), a concentração foi tão alta quanto aquelas empregadas no método de síntese em solução (Gross, E. & Meienhofer, J., 1979)

A relação entre os parâmetros calculados, tal como distância intersítios e concentração de sítios, com o aparecimento de interação spin-spin, foi comparada com dados obtidos a partir de estudos feitos com Boc-TOAC livre em solução (Tabela I.1).

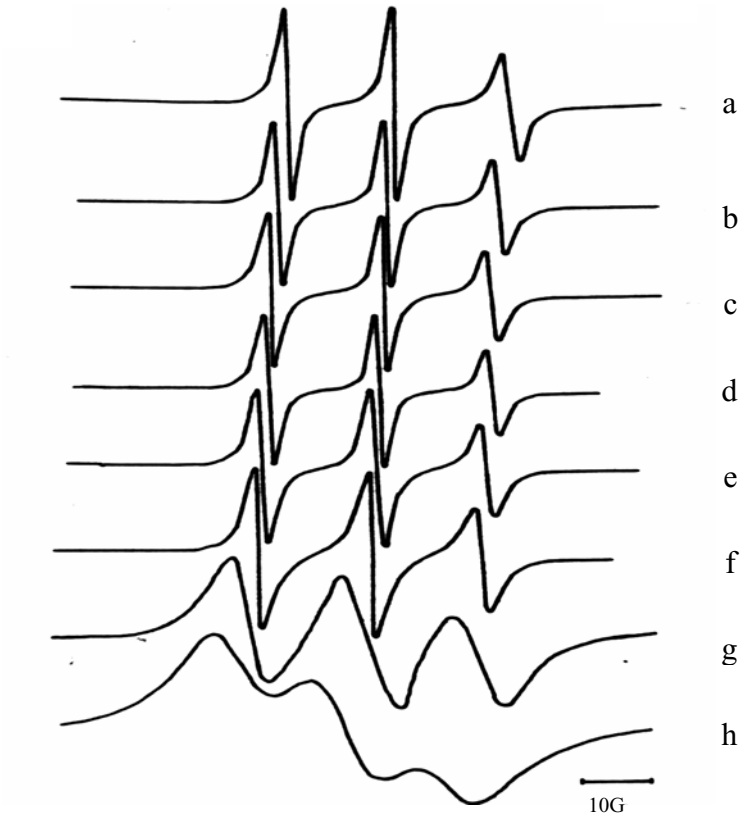

Figura I.8. Efeito do teor de Boc-TOAC no espectro de RPE de Boc-TOAC-BAR em DCM. Teor de Boc-TOAC (mmol/g): a = 0,003; b = 0,019; c = 0,035; d = 0,050; e = 0,065; f = 0,134; g = 0,646; h = 0,988

Tabela I.1: Correlação entre concentração de Boc-TOAC e largura do pico central do espectro de RPE e valores de distância intersítios em solução de DMF

Concentração (M)	ΔH (G)	Distância intersítios (Å)
1×10^{-4}	1,40	255,4
1×10^{-3}	1,40	118,6
5×10^{-3}	1,45	69,3
1×10^{-2}	1,70	55,0
5×10^{-2}	2,40	32,2
1×10^{-1}	3,65	25,5

A Figura I.9 mostra a dependência da largura da linha espectral de campo médio para ambos, resinas marcadas e molécula marcadora livre, em DMF, em função da distância intersítios (A) e a concentração de sítios (B). O alargamento desta linha só ocorreu em distâncias intersítios inferiores a 60 Å (concentração de sítios de aproximadamente 10^{-2} M). A semelhança entre os resultados obtidos seja com a molécula marcadora livre em solução ou imobilizada na malha polimérica, sugere fortemente que a estratégia de cálculo seqüencial adotada para a determinação quantitativa dos parâmetros de inchamento, está correta.

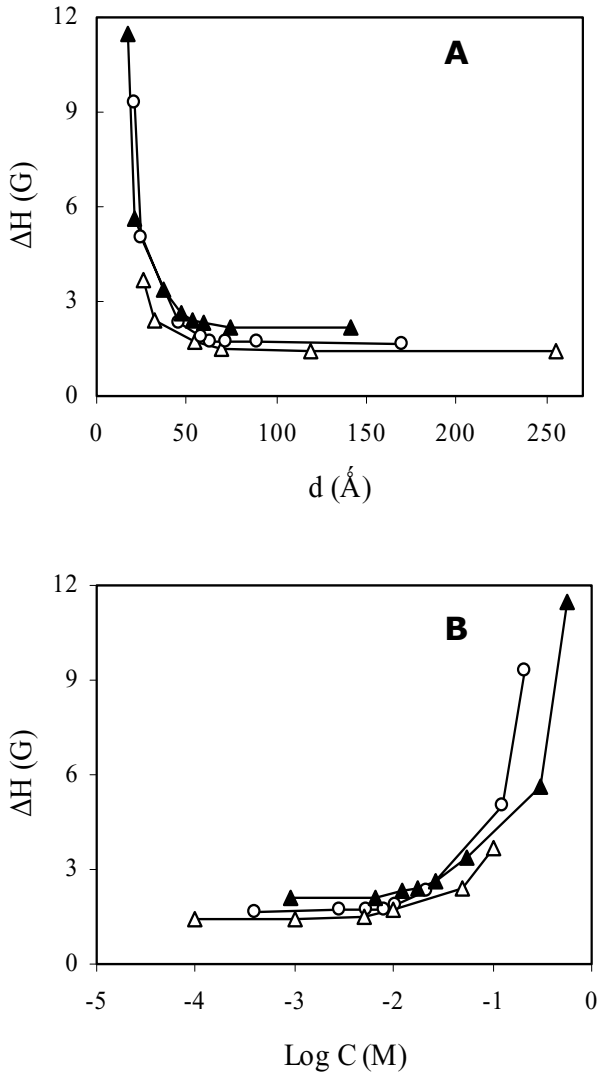

Figura I.9. Efeito da distância intersítios (A) e concentração de sítios (B) na largura do pico central do espectro de RPE de Boc-TOAC em DMF (∆) e Boc-TOAC-BAR em DCM (o) e em DMF (▲).

Para se avaliar a existência de uma relação entre os parâmetros de inchamento, resultantes da estratégia de cálculo proposta e a eficiência da reação de condensação de um aminoácido, um estudo empregando resinas e peptidil-resinas modelo, foi desenvolvido.

A reação de condensação de Boc-Pro para uma BAR contendo 1,40 mmol/g de grupos amina, foi mais eficiente em solventes cujas propriedades de inchamento proporcionam uma maior distância entre os sítios de reação (Tabela I.2), evidenciando que o emprego da estratégia de cálculo, no planejamento de uma síntese, pode ser determinante no sucesso de todo processo sintético.

Tabela I.2: Correlação entre eficiência[a] da reação de acoplamento de Boc-Pro em BAR (1,40 mmol/g) e valores de concentração de sítios e distância intersítios

Solvente	Concentração de sítios (M)	Distância intersítios (Å)	Acoplamento (%)
DCM	0,21	21,7	90
DMF	0,55	17,0	67
DMSO	1,76	14,2	25

[a]Eficiência da reação de acoplamento de Boc-Pro após 30 min, à 25ºC pelo método do anidrido simétrico, em condições equimolares (1 mM de reagentes)

Diferentemente ao estudo com BAR, a eficiência da reação de condensação de um aminoácido a uma peptidil-resina modelo, foi avaliada empregando como componente acilante a própria molécula marcadora, o que permitiu o monitoramento *in situ* desta reação. A molécula de Boc-TOAC foi acoplada à $(NANP)_4$-BAR, e o progresso da reação de acilação à estrutura polimérica foi monitorada diretamente por espectroscopia de ressonância paramagnética eletrônica. Além disso, os parâmetros de inchamento desta peptidil-resina, bem como o efeito da viscosidade do meio, também foram avaliadas nesta

aproximação cinética, cujos resultados estão descritos em um artigo recentemente submetido para publicação (anexo 2).

Na tabela I.3, estão representados os parâmetros de inchamento e a evolução cinética da reação de acoplamento de Boc-TOAC em dois lotes de $(NANP)_4$-BAR, em DCM, DMF e DMSO. O grau de substituição das resinas de partida foi 0,2 e 1,4 mmol/g, os quais renderam ao final da incorporação dos 16 resíduos de aminoácidos, 14 e 68% de conteúdo peptídico, respectivamente.

Tabela I.3: Correlação entre eficiência[a] de acoplamento de Boc-TOAC à $(NANP)_4$-BAR e distância intersítios, em diferentes solventes

Solvente	$(NANP)_4$-BAR[b]				$(NANP)_4$-BAR[c]			
	Distância intersítios (Å)	Acoplamento (%)			Distância intersítios (Å)	Acoplamento (%)		
		30 min	60 min	180 min		30 min	60 min	180 min
DCM	33,6	54	61	78	17,6	24	50	74
DMF	37,3	83	88	93	23,6	43	82	92
DMSO	33,6	33	46	65	27,7	80	87	95

[a]Eficiência do acoplamento de Boc-TOAC em tempos diferentes à 25ºC, pelo método do anidrido simétrico em condições equimolares (2 mM de reagentes); [b]obtida a partir de uma BAR de 0.20 mmol/g; [c]obtida a partir de BAR de 1.40 mmol/g.

Tal como observado para BAR, a eficiência da reação de condensação de um aminoácido a uma peptidil-resina apresentou uma relação direta com o inchamento, independentemente da amostra estudada. Assim, DMF e DMSO permitiram uma acilação mais rápida para as peptidil-resinas com baixo e alto conteúdo peptídico respectivamente. Entretanto, quando o grau de inchamento foi equivalente (distância intersítios iguais), a reação de acilação foi mais rápida no solvente menos viscoso (DCM). Este resultado mostra claramente que a viscosidade é um fator que afeta a eficiência da

reação de acoplamento de um aminoácido e que deve ser considerado no planejamento de um processo sintético.

Seguindo estes resultados iniciais, o monitoramento direto da reação de acoplamento de Boc-TOAC à $(NANP)_4$-BAR (1,40 mmol/g), empregando espectroscopia de ressonância paramagnética eletrônica, foi testado em DMF, usando o mesmo protocolo de acilação empregado para os experimentos detalhados na tabela I.3.

A análise inicial dos espectros de RPE traçados, revelou alargamento crescente das linhas espectrais com o curso da reação de acoplamento, atribuído ao aumento da imobilização da molécula de Boc-TOAC ao suporte polimérico.

Na Figura I.10 está representada a correlação entre os valores de largura da linha de campo médio do espectro de RPE (ΔH) e o tempo de reação. Este parâmetro tem sido geralmente empregado na determinação do grau de mobilidade de moléculas marcadoras em um dado sistema (Cilli, *et al*., 1999; Oliveira, *et al.*, 2002).

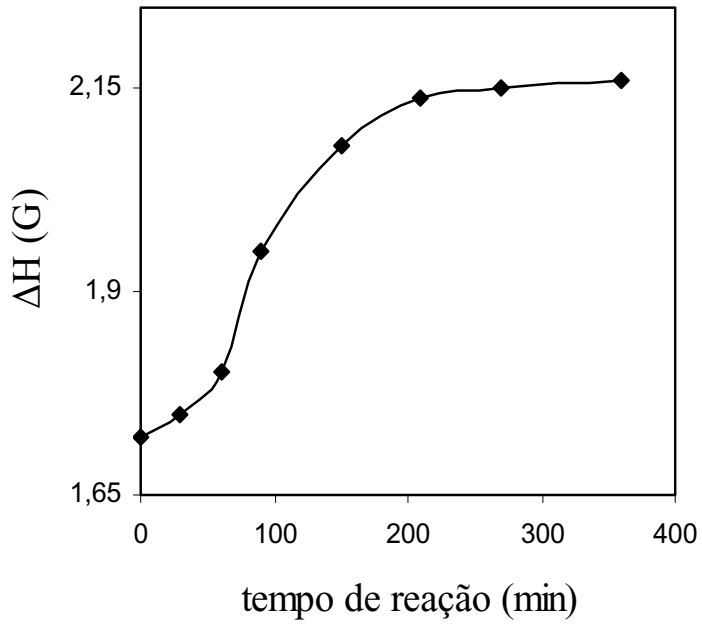

Figura I.10. Acoplamento de Boc-TOAC à $(NANP)_4$-BHAR (1.40 mmol/g) em DMF à 25ºC, empregando o método do anidrido simétrico em condições equimolares (2 mM de reagentes), monitorado por RPE

Como pode ser visto, uma completa estabilização dos valores de ΔH ocorreu após 3 a 4 horas de acoplamento, valores estes comparáveis àqueles obtidos sem o monitoramento por RPE, no qual o acoplamento chegou próximo ao máximo de eficiência após este tempo (Tabela I.3).

Deste modo, os resultados descritos neste artigo (anexo 2) demonstram a viabilidade de se acompanhar diretamente, monitorando *in situ* uma reação química no interior da estrutura polimérica na qual o reagente é a própria sonda espectral.

O campo de aplicação de materiais poliméricos, tais como resinas, tem crescido progressivamente, e vai desde o uso simples como um suporte sólido para cromatografia líquida até métodos complexos de síntese de macromoléculas, como peptídeos e oligonucleotídeos, assim como em química combinatória e desenvolvimento de novas drogas. Nossa contribuição na área, está diretamente relacionada com os fatores físico-químicos e estruturais que influenciam o rendimento de reações no interior das estruturas poliméricas.

Acreditamos assim, que nossos estudos representam um passo importante na compreensão mais profunda e conseqüente melhoria dos processos químicos que envolvam estruturas poliméricas.

6 Referências Bibliográficas

AKABORI, S., SAKAKIBARA, S.; SHIMONISHI, Y.; NOBUHARA, Y. A new method for the protection of the sulphydryl group during peptide synthesis. *Bull. Chem. Soc. Jap.*, v. 37, p. 433 – 434, 1964.

ALBERICIO, F.; BARANY, G. Improved approach for anchoring N^{α}-9-fluorenylmethyloxycarbonylamino acids as p-alkoxybenzyl esters in solid-phase peptide synthesis. *Int. J. Peptide protein Res.*, v. 26, p. 92 – 97, 1985.

ALBERICIO, F.; KNEIB-CORDONIER, N.; BIANCALANA, S.; GERA, L.; MASADA, R. I.; HUDSON, D.; BARANY, G. Preparation and application of the 5-(4-(9-fluorenylmethoxycarbonyl)aminomethyl-3,5-dimethoxyphenoxy)-valeric acid (PAL) handle for the solid-phase synthesis of C-terminal Peptide amides under mild conditions. *J. Org. Chem.*, v. 55, p. 3730 – 3743, 1990.

ALBERICIO, F.; LLOYD-WILLIAMS, P.; GIRALT, E. Convergent solid-phase peptide synthesis. *Methods Enzymol.*, v. 289, p. 313 – 336, 1997.

ANDERSON, G.W.; McGREGOR, A.C. t-Butyloxycarbonylamino acids and their use in peptide synthesis. *J. Am. Chem. Soc.*, v. 79, p. 6180 – 6183, 1957.

BARANY, G.; KNEIB-CORDONIER, N.; MULLEN, D.G. Solid phase peptide synthesis: a silver anniversary report. *Int. J. Peptide Protein Res.* v. 30, p. 705 – 739, 1987.

BATES, A.J.; GALPIN, I.J.; HALLETT, A.; HUDSUN, D.; KENNER, G.W.; RAMAGE, R.; SHEPPARD, R.C. A new reagent for polypeptide synthesis: μ-Oxo-bis-[tris-(dimethylamino)-phosphonium]-bis-tetrafluoroborate. *Helv. Chim. Acta,* v. 58, p. 688 – 696, 1975.

BERNATOWICZ, M.S.; KEARNEY, T.; NEVES, R.S.; KÖSTER, H. An efficient method for racemization free attachment of 9-fluorenylmethyloxycarbonyl-amino acids to peptide synthesis supports. *Tetrahedron Lett.*, v. 30, p. 4341 – 4344, 1989.

BROWN, T.; JONES, J.H. Protection of histidine side-chains with π-benzyloxymethyl or π-bromobenzyloxymethyl-groups. *J. Chem. Soc. Chem. Commun.*, p. 648 – 649, 1981.

CARPINO, L.A. Oxidative reactions of hydrazides. IV. Elimination of nitrogen from 1,1-disubstituted-2-arenesulfonylhydrazides. *J. Am. Chem. Soc.*, v. 79, p. 4427 – 4431, 1957.

CARPINO, L.A.; HAN, G.A. The 9-fluorenylmethyloxycarbonyl amino-protecting group. *J. Org. Chem.*, v. 37, p. 3404 – 3409, 1972.

CARPINO, L.A. 1-Hydroxy-7-azabenzotriazole. An efficient peptide coupling additive. *J. Am. Chem. Soc.*, v. 115, 4397 – 4398, 1993a.

CARPINO, L.A.; SCHROFF, H.; TRIOLO, S.A.; MANSOUR, E.-S, M.E. The 2,2,4,6,7-pentamethyldihydrobenzofuran-5-sulphonyl group (Pbf) as arginine side-chain protectant. *Tetrahedron Lett.*, v. 34, p. 7829 – 7832, 1993b.

CARPINO, L.A.; EL-FAHAN, A.; MINOR, C.A.; ALBERICIO, F. Advantageous applications of azabenzotriazole (triazolopyridine)-based coupling reagents to solid-phase peptide synthesis. *J. Chem. Soc. Chem. Commun.,* p. 201 – 203, 1994.

CARPINO, L.A.; EL-FAHAN, A.; ALBERICIO, F. Efficiency in peptide coupling: 1-hydroxy-7-azabenzotriazole vs 3,4-dihydro-3-hydroxy-4-oxo-1,2,3-benzotriazine. *J. Org. Chem.,* v. 60, p. 3561 – 3564, 1995a.

CARPINO, L.A.; EL-FAHAN, A.; TRURAN, G.A.; MINOR, C.A.; KATES, S.A.; GRIFIN, G.W.; SHROFF, H.; TRIOLO, S.A.; ALBERICIO, F. New approaches for extending the scope of solid-phase peptide synthesis. Em: R. Epton (Ed.) Innovation and perspectives in solid-phase synthesis. Peptides, proteins and nucleic acids. Biological and Biomedical applications, Mayflower Worldwide Ltd, Birmingham, p. 95 – 104, 1995b.

CASTRO, B.; DORMOY, J.R.; EVIN, G.; SELVE, C. Reactifs du couplage peptidique IV. (1)-L'-Hexafluorophosphate de benzotriazolyl N-oxytris-dimethylamno phosphonium (BOP). *Tetrahedron Lett.*, v. 16, p. 1219 – 1222, 1975.

CHILLEMY, F.; MERRIFIELD, R.B. Use of N^{im}-Dinitrophenylhistidine in the solid-phase synthesis of the tricosapeptides 124-146 of human hemoglobin β-chain. *Biochemistry*, v. 8, p. 4344 – 4346, 1969.

COSTE, J.; LE-NGUYEN, D.; CASTRO, B. PyBOP: A new peptide coupling reagent devoid of toxic by-product. *Tetrahedron Lett.,* v. 31, p. 205 – 208, 1990.

COSTE, J.; CAMPAGNE, J.-M. A propôs de l'esterification de acides carboxyliques par le BOP ou le PyBOP. *Tetrahedron Lett.* v. 36, p. 4253 – 4256, 1995.

CURTIUS, T. Synthetische versuche mit hippurazid. *Ber. Dtsch. Chem. Ges.* v. 35, p. 3226 – 3228, 1902.

DOURTOGLOU, V.; ZIEGLER, J.-C.; GROSS, B. L'-Hexafluorophosphate de O-benzotriazolyl-N,N'-tetramethyluronium: um Reactif de couplage peptidique nouveau et efficace. *Tetrahedron Lett.,* v. 19, p. 1269 – 1272, 1978.

ERICKSON, B.W.; MERRIFIELD, R.B. Acid stability of several benzylic protecting groups used in solid-phase peptide synthesis. Rearrangement of o-benzyltyrosine to 3-benzyltyrosine. *J. Am. Chem. Soc.*, v. 95, p. 3750 – 3756, 1973.

FIELDS, G.B.; TIAN, Z.; BARANY, G. Principles and practice of solid-phase peptide synthesis. Em: Synthetic peptides. A user's guide (ed. G.A. Grant), W.H.Freeman and Company, New York, p. 77 – 183, 1992.

FISCHER, E.; FOURNEAU, E. Ueber einige derivate glykolls. *Ber. Dtsch. Chem.. Ges.* v. 34, p. 2868 – 2877, 1901.

FRÜCHTEL, J.S.; JUNG, G.; Organic chemistry on solid supports. *Angew.Chem. Int. Ed. Engl.* v. *35*, p. 17 – 42, 1996.

GAWNE, G.; KENNER, G.; SHEPPARD, R.C. Acyloxyphosphonium salts as aylating agents. A new synthesis of peptides. *J. Am. Chem. Soc.* v. 91, p. 5669 – 5671, 1969.

GREENE, T.W.; WUTS, P.G.M. Protective groups in organic synthesis. 2nd. Edition. John Wiley & Sons, New York, 1991.

GROSS, E.; MEIENHOFER, J. (Eds.) *The Peptides,* Academic Press, New York, v. 1, 1979.

KATES, S.A., TRIOLO, S.A., GRIFFIN, G.W., HERMAN, L.W., TARR, G., SOLE, N.A., DIEKMANN, E., EL-FAHAM, A., IONESCU, D., ALBERICIO, F. & CARPINO, L.A. Advances in the use of onium-based coupling reagents: Application for solid phase peptide synthesis and combinatorial libraries. Em: R. Epton (Ed.), Innovation and Perspectives in Solid Phase Synthesis & Combinatorial Libraries. Mayflower Scientific Limited, Birmingham, p. 41 – 50, 1996.

LLOYD-WILLIANS, P.; ALBERICIO, F.; GIRALT, E. Convergent solid-phase peptide synthesis. *Tetrahedron*, v. 49, p. 11065 – 11133, 1993.

McCURDY, S.N. The investigation of Fmoc-Cysteine derivatives in solid phase peptide synthesis. *Peptide Res.*, v. 2, p. 147 – 152, 1989.

MARCHETTO, R.; ETCHEGARAY, A.; NAKAIE, C.R. Kinetics of synthesis and swelling studies of highly substituted benzhydrylamine-resins: Implications for peptide synthesis and perspectives for use as anion exchanger resin. *J. Braz. Chem. Soc.*, v. 3, p. 30 – 37, 1992.

MERRIFIELD, R.B. Solid-phase peptide synthesis. I. The synthesis of a tetrapeptide. *J. Am. Chem. Soc.*, v. 85, p. 2149 – 2154, 1963.

MERRIFIELD, R.B. Solid-phase peptide synthesis (Nobel Lecture). *Angew. Chem. Int. Ed. Engl.* v. 24, p. 799 – 810, 1985.

MITCHELL, A.R.; ERICKSON, B.W.; RYABTSEV, M.N.; HODGES, R.S.; MERRIFIELD, R.B. tert-butyloxycarbonylaminoacyl-4-(oxymethyl)-phenyl-acetamidomethyl-resin, a more acid-resistant support for solid-phase peptide synthesis. *J. Am. Chem. Soc.*, v. 98, p. 7357 – 7362, 1976.

MUNSON, M.C.; GARCIA-ECHEVERRÍA, C.; ALBERICIO, F.; BARANY, G. S-2,4,6-trimethoxybenzyl (Tmob): A novel cysteine protecting group for the N-9-fluorenylmethoxycarbonyl (Fmoc) strategy of peptide synthesis. *J. Org. Chem.*, v. 57, p. 3013 – 3018, 1992.

NAKAIE, C. R.; GOISSIS, G.; SCHREIER, S.; PAIVA, A. C. M. pH-dependence of ESR spectra of nitroxides containing ionizable groups. *Braz. J. Med. Biol. Res*., v. 14*,* p. 173 – 180, 1981.

NICOLAS, E.; PEDROSO, E.; GIRALT, E. Formation of aspartimide peptides in AspGly sequences. *Tetrahedron Lett.*, v. 30, p. 497 – 500, 1989.

PIETTA, P.G.; MARSHALL, G.R. Amide protection and amide supports in solid-phase peptide synthesis. *J. Chem. Soc. Chem. Commun.*, p. 650 – 651, 1970.

RAMACHANDRAN, J.; LI, C.H. Preparation of crystalline N^G-tosylarginine derivatives. *J. Org. Che.*, v. 27, p. 4006 – 4009, 1962.

RAMAGE, R.; GREEN, J.; BLAKE, A.J. An acid labile arginine derivative for peptide synthesis: N^G-2,2,7,8-pentamethylchroman-6-sulphonyl-L-arginine. *Tetrahedron*, v. 47, p. 6353 – 6370, 1991.

RINK, H. Solid-phase synthesis of protected peptide fragments using a trialkoxy diphenyl methylester resin. *Tetrahedron Lett.*, v. 28, p. 3787 – 3790, 1987.

SAKAKIBARA, S.; FUJII, T. Synthesis and use of N^{im}-tosyl-L-histidine. *Bull. Chem. Soc. Jap.*, v. 42, p. 1466 – 1468, 1969.

SARIN, V.K.; KENT, S.B.H.; MERRIFIELD, R.B.; Solvation and swelling of peptide-containing resins in solid phase peptide synthesis. *J. Am. Chem. Soc.*. v.102, p. 5463 – 5470, 1980.

SHEEHAN, J.C.; HESS, G.P. A new method of forming peptide bonds. *J. Am. Chem. Soc.,* v. 77, p. 1067 – 1068, 1955.

SIEBER, P.; RINIKER, B. Protection of histidine in peptide synthesis: a reassessment of the trityl group. *Tetrahedron Lett.,* v. 28, p. 6031 – 6034, 1987.

TAM, J.; TJOENG, F.; MERRIFIELD, R. B.; Design and synthesis of multi-detachable resin supports for solid phase peptide synthesis. *J. Am. Chem. Soc.* v. 102, p. 6117 – 6127, 1980.

VEBER, D.F.; MILKOWSKI, J.D.; VARGA, S.L.; DENKEWALTER, R.G.; HIRSCHMANN, R. Acetamidomethyl. A novel thiol protecting group for cysteine. *J. Am. Chem. Soc.*, v. 94, p. 5456 – 5461, 1972.

WHITE, P. Fmoc-Trp(Boc)-OH: A new derivative for the synthesis of peptides containing tryptophan. Em: Peptides. Chemistry and Biology. Proceedings of the 12th American peptides Symposium. (Smith, J.A & Rivier, J.E, Eds). ESCOM, Leiden, p. 537 – 538, 1992.

YAMASHIRO, D.; LI, C.H. Protection of tyrosine in solid phase peptide synthesis. *J. Org. Chem.*, v. 38, p. 591 – 592, 1973a.

YAMASHIRO, D.; LI, C.H. Protection of tryptophan with formyl group in peptide synthesis. *J. Org. Chem.*, v. 38, p. 2594 – 2597, 1973b.

PARTE II

MECANISMO DE INIBIÇÃO DA ATIVIDADE DA DNA GIRASE

DNA GIRASE

1. Introdução

A enzima bacteriana DNA girase foi descoberta em 1976, especificamente por possuir a habilidade única de catalisar a introdução de voltas helicoidais negativas no DNA circular (Gellert, *et. al*., 1976). Desde então, esta enzima tem sido o foco de grande atenção em relação a sua estrutura, mecanismo de ação, interação com agentes antibacterianos e seu papel fisiológico. Aparte o interesse intrínseco da girase, ela também serve como um sistema modelo útil para o estudo de interações DNA-proteína e acoplamento de energia biológica.

A DNA girase pertence a uma classe de proteínas denominada DNA topoisomerases, que compartilham a propriedade de catalisar interconversões entre diferentes formas topológicas do DNA. Todas topoisomerases são capazes de relaxar o DNA superenrolado, mas somente a girase pode também introduzir super-hélices negativas no DNA, usando a energia livre liberada pela hidrólise do ATP (Reece & Maxwell, 1991a).

2. Estrutura

A DNA girase tem sido isolada de muitas espécies de bactérias, porém a enzima mais estudada em termos estruturais e funções bioquímicas, é a girase de *Escherichia coli*. Esta enzima, consiste de duas proteínas A (GyrA) e B (GyrB), as quais estão unidas formando um heterotetrâmero A_2B_2, que corresponde à sua forma ativa (Wigley, 1995). A proteína A tem um peso molecular de 97-kDa e é funcionalmente constituída de um domínio amino-terminal (64-kDa), o qual é essencial para o mecanismo de quebra-união do DNA, cuja etapa intermediária envolve o ataque covalente do resíduo Tyr-122 da GyrA às extremidades 5', previamente rompidas, de cada fita do DNA, além

de um domínio carboxi-terminal (33-kDa), o qual está envolvido nas interações DNA-proteína (Reece & Maxwell, 1989, 1991b) (Figura II.1). A subunidade B tem um peso molecular de 90-kDa, e contém um domínio amino-terminal (43-kDa), o qual inclui o sítio de ligação do ATP, bem como um domínio carboxi-terminal (47-kDa) o qual está envolvido na interação com GyrA e o DNA (Wigley, *et al.*, 1991; Ali, *et al.*, 1993). O domínio amino-terminal inclui dois subdomínios (uma parte N-terminal de 24-kDa e uma parte C-terminal de 19-kDa). O sítio de ligação do ATP está localizado no primeiro subdomínio (Ali, *et al.*, 1993).

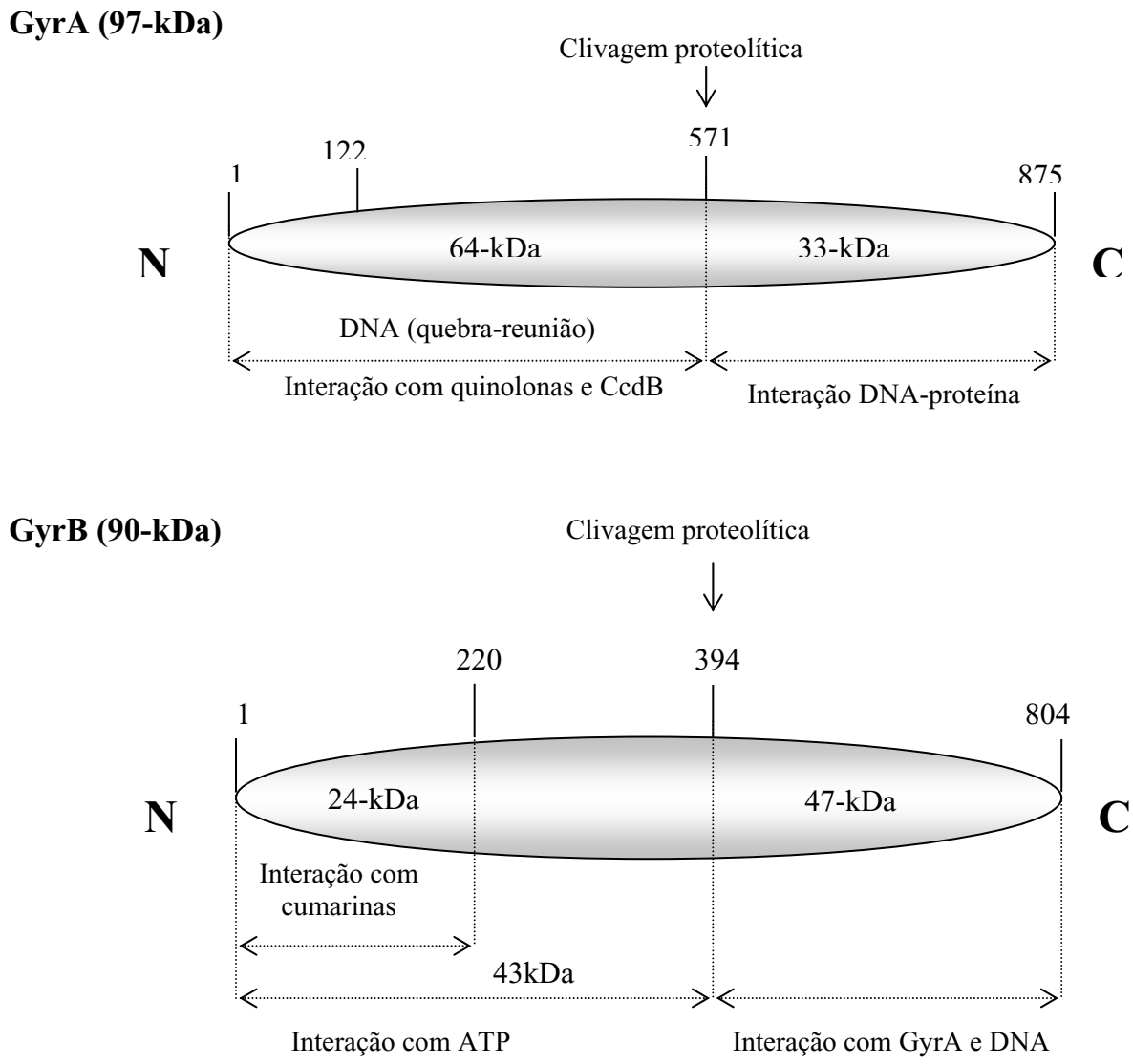

Figura II.1 - Diagramas esquemáticos das estruturas de GyrA e GyrB.

3. Reações da Girase

A DNA girase executa uma série de interconversões topológicas na molécula de DNA. Somada à habilidade única de catalisar a introdução de voltas helicoidais negativas no DNA circular, a girase também pode aliviar o superenrolamento do DNA, na ausência de ATP (Gellert, *et al.,* 1977), bem como promover o "catenation" ou "decatenation" (encadeamento ou desencadeamento) de dois DNA duplex cíclicos (Kreuzer & Cozzarelli, 1980; Marians, 1987), além de desfazer o "knotted" (emaranhado) topológico de uma única molécula de DNA duplex circular (Liu, *et al.,* 1980) (Figura II.2). Na presença de ATP, ou do análogo não hidrolisável 5'-adenilil-β,γ-imidodifosfato (ADPNP), a girase também pode relaxar positivamente o DNA superenrolado (reduzindo assim seu número de ligações) através de uma reação considerada análoga à introdução de super-hélices negativas (Brown, *et al.,* 1979).

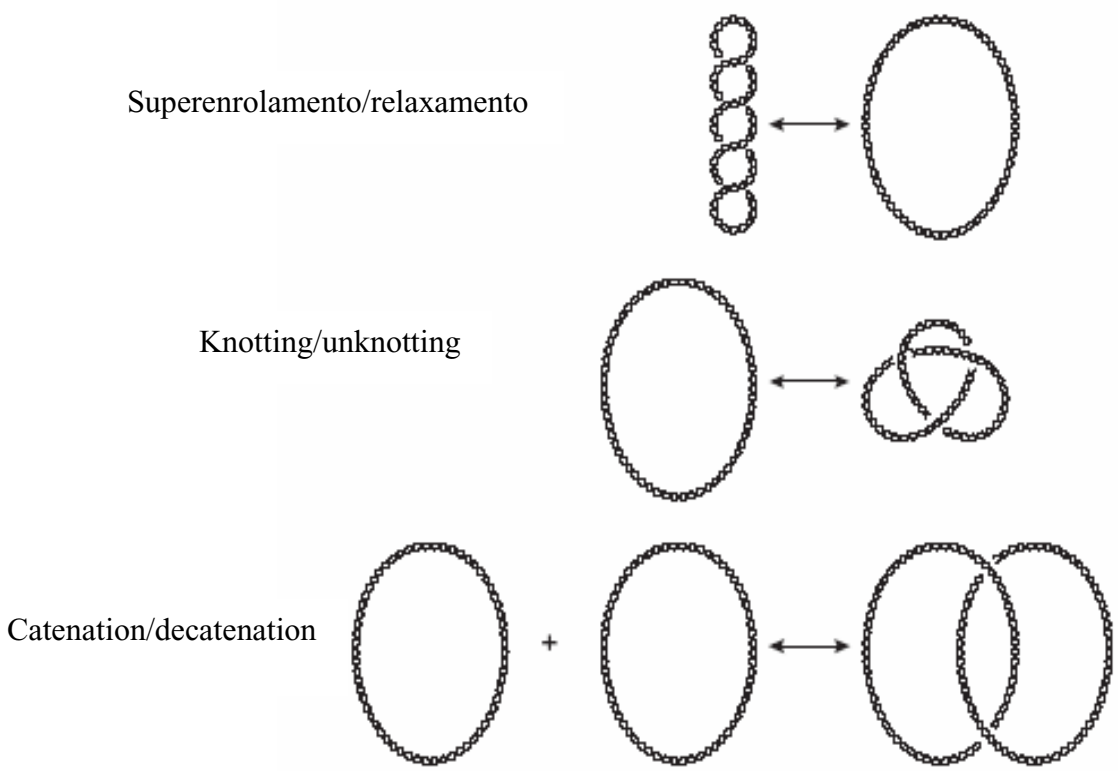

Figura II.2. Reações da DNA girase

Superenrolamento e relaxamento

Todas reações catalisadas pelas topoisomerases envolvem a ligação da proteína ao DNA, clivagem do DNA, a passagem das fitas, religação do DNA, e em muitos casos a hidrólise do ATP. Embora a girase compartilhe do mecanismo geral das topoisomerases, ela também deve possuir características mecanísticas especiais, as quais determina sua habilidade em superenrolar ativamente o DNA. A reação de superenrolamento do DNA requer, além de ATP, um cátion bivalente, tal como o Mg^{2+}, e é estimulada na presença de espermidina (Gellert, *et al.,* 1976).

No superenrolamento, a girase age catalisando uma quebra transitória em uma molécula de DNA, a passagem de outro segmento da mesma molécula através dessa abertura e a posterior religação das fitas do DNA. Para que esse processo ocorra, inicialmente a DNA girase liga-se a um segmento de DNA, de aproximadamente 130 bp, envolvendo-o ao redor do tetrâmero e formando nele uma super-hélice positiva (Figura II.3a). A seguir, ocorre a ligação de uma molécula de ATP à subunidade GyrB. O ATP produz então mudanças conformacionais na enzima, que sofre uma rotação. GyrB dimeriza e captura um segmento desse DNA denominado segmento T. Simultaneamente GyrA catalisa uma clivagem nas duas fitas de um outro segmento, denominado segmento G (Figura II.3b). O complexo intermediário formado entre DNA e girase é denominado complexo clivável e nele o DNA está covalentemente ligado à enzima por uma ligação entre a terminação 5’ do DNA clivado e o resíduo de tirosina 122 da GyrA. O segmento T é transportado através da abertura produzida no segmento G (Figura II.3c e II.3d), que depois desta passagem tem suas fitas religadas (Figura II.3e). O segmento T é então liberado da enzima por uma abertura transitória na GyrA. Com o religamento do DNA clivado, duas super-hélices negativas são introduzidas na molécula. O retorno da enzima à sua conformação original é promovido pela hidrólise da

molécula de ATP (Roca, 1995; Berger, 1996; Morais Cabral *et al*., 1997; Smith & Maxwell, 1998).

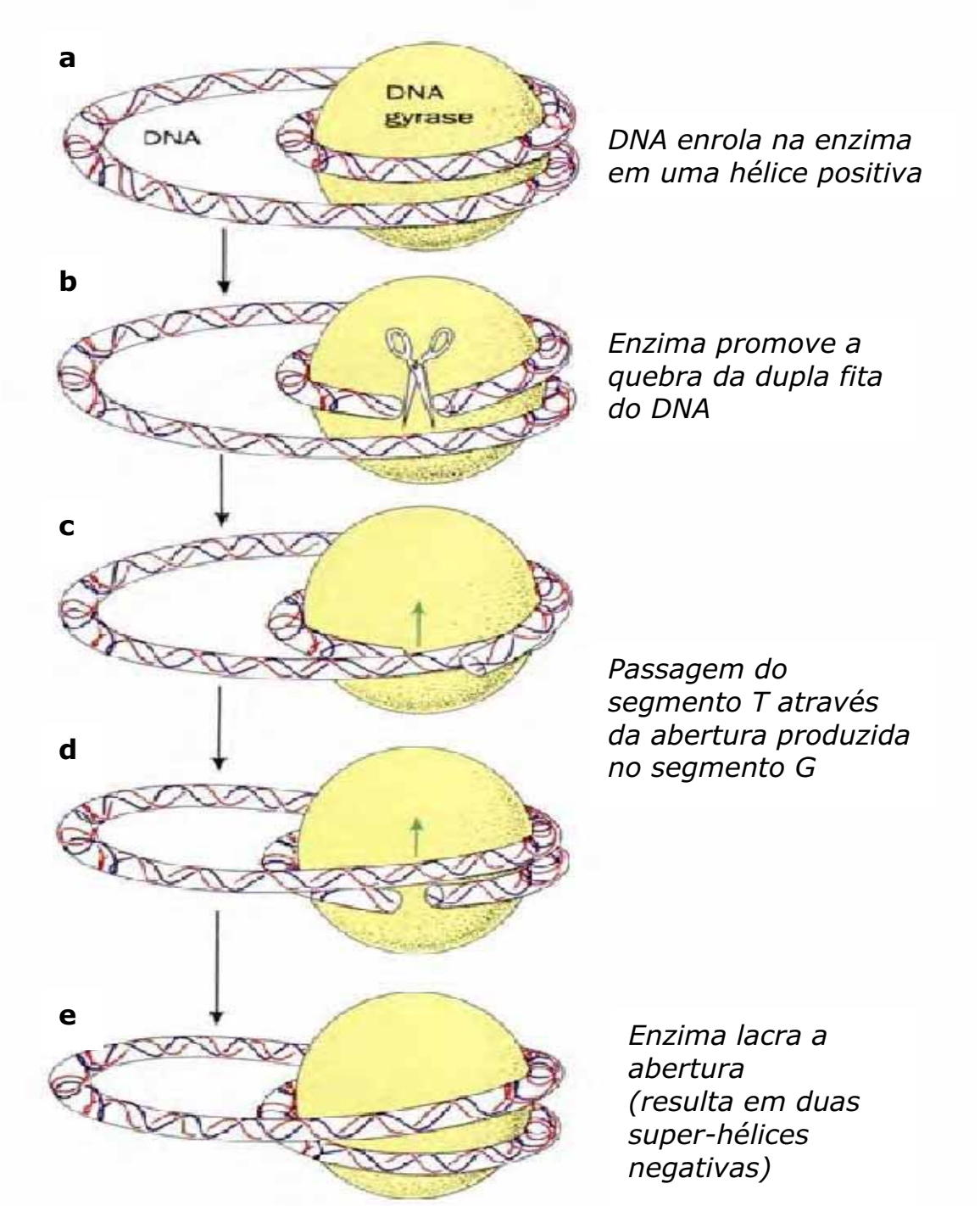

Figura II.3. Modelo molecular para ação da DNA Girase.

Na ausência de ATP, a girase relaxa negativamente o DNA superenrolado. A atividade de relaxamento da girase é muito menos eficiente que a reação de superenrolamento, sendo requerida uma quantidade de aproximadamente 20 a 40 vezes maior de enzima, para uma taxa de reação comparável (Higgins, *et al.,* 1978).

É possível que o relaxamento do DNA seja simplesmente o inverso da reação de superenrolamento, e que a hidrólise do ATP é requerida para dirigir a passagem de uma fita de DNA em apenas uma direção.

"Catenation", "Decatenation" e "unknotting"

A DNA girase pode catalisar a formação e resolução de DNA encadeados ("catenate DNA") e pode desatar o DNA emaranhado ("knotted DNA"). Em princípio, acreditava-se que a girase também poderia emaranhar o DNA dupla fita circular, porém esta reação não foi citada até o momento. Essas reações requerem ATP e são inibidas por drogas tipo quinolonas e cumarinas.

"Catenation" e "decatenation", assim como a reação de superenrolamento, são estimuladas por espermidina (Kreuzer & Cozzarelli, 1980).

Teoricamente, as reações de "catenation" e de "decatenation" não deveriam requerer a hidrólise de ATP uma vez que, sob condições de concentração de DNA apropriadas, estas reações são energeticamente favoráveis. Porém, tem sido descrito que ambas reações requerem ATP. De fato, foi mostrado que a reação de decatenation catalisada pela girase, não ocorre na presença do análogo não hidrolisável ADPNP (Reece & Maxwell, 1991a).

Uma possibilidade é que estas reações devam ocorrer por um mecanismo similar ao superenrolamento do DNA onde a hidrólise do ATP assegura a passagem eficiente das fitas do DNA. Se as reações ocorressem pelas vias do relaxamento, ou seja independentemente da

hidrólise do ATP, elas poderiam ser muito lentas para serem detectadas através de métodos convencionais (Reece & Maxwell, 1991a).

4. Interação com antibióticos

A natureza indispensável da girase para as células bacterianas e a ausência aparente de atividade em eucariotos faz da DNA girase um alvo ideal para a ação de diversos tipos de drogas. Realmente, um grande número de agentes antibacterianos girase-específicos têm sido descrito nos últimos anos. Muitos deles classificados basicamente em dois grupos, o das quinolonas e o das cumarinas, embora existam outros compostos classificados fora destas duas classes, tais como as moléculas peptídicas da classe das microcinas e a toxina bacteriana CcdB.

Quinolonas

Existem atualmente mais de 5000 compostos antibacterianos derivados do 4-oxo-1,4-dihidroquinolina (Figura II.4), coletivamente denominados 4-quinolonas ou simplesmente quinolonas.

É importante salientar que as quinolonas não são produtos naturais, mas sim totalmente sintéticos. O primeiro componente desta classe a ser sintetizado foi o ácido nalidíxico (Lesher, *et al.,* 1962), o qual apresentou atividade contra muitas espécies de bactérias Gram-negativas, mas não contra células eucarióticas, porém sua atividade tem sido superada, por derivados 1000 vezes mais potentes, em particular as fluorquinolonas tal como a ciprofloxacina (Figura II.4).

Essas drogas são amplamente usadas clinicamente contra uma variedade de infecções bacterianas, incluindo aquelas do trato urinário e respiratório. O considerável sucesso das fluorquinolonas pode ser atribuído pelo seu amplo espectro de atividade, mínima toxidade em

eucariotos, fácil penetração nas células bacterianas, e boas propriedades farmacocinéticas.

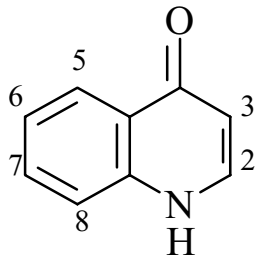

Estrutura básica das 4-quinolonas

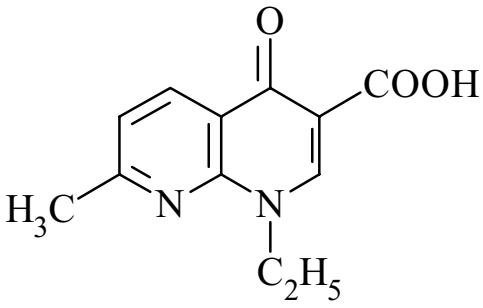

Ácido Nalidíxico

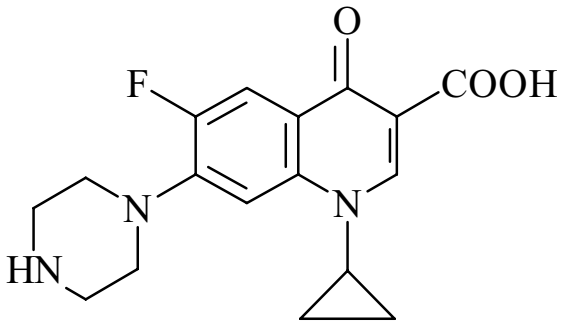

Ciprofloxacina

Figura II.4. Estrutura de antibióticos quinolônicos

Substituições sistemáticas a várias posições no núcleo quinolônico sugeriram características especiais que contribuem para a eficácia antimicrobiana. Por exemplo, o grupo carboxílico na posição 3 e o grupo carbonílico na posição 4 parecem ser essenciais para a atividade antibacteriana e possivelmente devem estar envolvidos na interação enzima-droga ou DNA-droga. O substituinte na posição 1 é também importante, e é geralmente um pequeno grupo alifático tal como etila (ácido nalidíxico e norfloxacina) ou ciclopropila (ciprofloxaxina). A presença de um átomo de flúor na posição 6 aumenta

significativamente a potencialidade da droga (Koga, *et al.,* 1980) e virtualmente todos novos análogos incluem este substituinte. O ácido nalidíxico, por exemplo, apresenta atividade limitada a certas espécies Gram-negativas enquanto as novas fluorquinolonas apresentam um espectro de atividade muito mais amplo que inclui bactérias Gram-positivas e Gram-negativas.

Diferentemente de muitos outros antibióticos, as quinolonas não parecem estar sujeitas à resistência transferível mediada por plasmídeos. Quando ocorre resistência, a mutação é cromossomal e é freqüentemente encontrada no gene *gyrA*, o gene estrutural que codifica a proteína A da DNA girase. Muitos mutantes resistentes à quinolonas foram mapeados no gene *gyrA* embora alguns tenham sido mapeados em *gyrB* ou em outros locais (Tabela II.1), como o gene *parC* (equivalente a *gyrA*) de várias espécies de bactérias (Drlica & Zhao, 1997).

Tabela II.1. Mutantes resistentes à quinolonas na DNA girase de *Escherichia coli*

Subunidade	Aminoácido alterado
GyrA	Ala-67 → Ser
GyrA	Gly-81 → Asp, Cys
GyrA	Ser-83 → Ala, Leu, Trp, Tyr
GyrA	Ala-84 → Pro
GyrA	Asp-87 → Asn, Gly, His, Thr, Val
GyrA	Gln-106 → Arg, His
GyrB	Asp-426 → Asn
GyrB	Lys-447 → Glu

Mutações em *gyrA*, aparecem em grande proporção em uma pequena região da proteína A da girase, especificamente entre os aminoácidos 67 e 106, a qual está muito próximo do resíduo Tyr-122, o centro ativo da enzima. Isto caracteriza a proteína A (GyrA) como o local primário de ligação das quinolonas. Porém a existência de mutações em *gyrB* e a observação de que as quinolonas também podem se ligar ao DNA (Shen & Pernet, 1985), gerou por um bom período, algumas dúvidas sobre esta teoria.

O efeito das quinolonas na girase é o bloqueio da reação de quebra-união do DNA, portanto a inibição do superenrolamento do DNA. Se SDS é adicionado para uma reação entre girase, DNA e uma quinolona, o DNA é encontrado rompido em ambas fitas e as subunidades GyrA presas ao grupo 5'-fosfato no local de quebra via Tyr-122, a tirosina do sítio ativo. A habilidade da quinolona em estabilizar o denominado "complexo clivável" entre a girase e o DNA é essencial para seu efeito bactericida. Esta habilidade também é compartilhada por um grande número de drogas antitumorais, cujo alvo é a DNA topoisomerase II (Topo II), a enzima equivalente à girase em células eucarióticas.

Evidências de que as quinolonas também atuam na DNA topoisomerase IV (Topo IV) têm sido estabelecidas recentemente (Scholar & Pratt, 2000). Esta enzima também é uma DNA topoisomerase bacteriana tipo II, que diferentemente da girase, não pode superenrolar o DNA. A topoisomerase IV catalisa o relaxamento do DNA, dependente de ATP, e é mais potente que a DNA girase na catálise da reação de "decatenation" do DNA. Assim, ela ajuda na separação das moléculas de DNA filhas, após o processo de replicação do DNA.

Está muito bem aceito que a inibição destas duas enzimas pelas quinolonas é uma importante etapa em seus mecanismos de ação. Porém, ainda não está muito claro como as quinolonas ligam-se às

topoisomerases ou precisamente como a inibição da enzima leva as células à morte.

Muitos modelos para a interação enzima-DNA-quinolona têm sido sugeridos. Um deles, envolve a ligação cooperativa entre a droga e uma fita relaxada do DNA, em uma cavidade induzida pela ação da própria DNA girase (Shen, *et al.,* 1989). Entretanto, este modelo parece ser um tanto desfavorável, uma vez que DNA girase com mutações no seu centro ativo (Tyr-122 para Ser ou Phe) pode ainda se ligar à droga, apesar de não possuir habilidade para clivar o DNA (Critchlow & Maxwell, 1996).

Um modelo alternativo envolve a ligação das quinolonas para os grupos fosfatos do DNA, via pontes de Mg^{+2}, e interação por sobreposição de anéis das quinolonas e das bases nitrogenadas do DNA (Palumbo, *et al.,* 1993). Ainda um outro modelo, baseado na interação de drogas antitumorais com Topo II de células eucarióticas e bacteriófago T4, sugere a intercalação de inibidores no espaço internucleotídico, próximo à ligação fosfodiéster clivável, do DNA (Capranico, *et al.,* 1990; Freudenreich & Kreuzer, 1993).

Todos os estudos dão suporte a idéia de que as quinolonas ligam-se ao complexo "clivável" formado entre a enzima e o DNA, o que o estabiliza e causa o efeito letal destas drogas ou conduz à indução de uma quebra na fita de DNA e o congelamento da forquilha de replicação (Drlica & Zhao, 1997). Neste contexto, complexos de DNA, quinolona e topoisomerase IV parecem formar barreiras físicas para a replicação do DNA. Em 1999, um complexo induzido por quinolona, de DNA e topoisomerase IV também foi descrito por inibir a atividade de várias helicases de DNA em *E. coli*, inclusive a helicase DnaB, que é um componente do complexo de replicação (Shea & Hiasa, 1999). O bloqueio na passagem da RNA polimerase que conduz a uma terminação prematura da transcrição também acontece com o complexo quinolona-girase-DNA (Willmott, *et al.,*1994). A conclusão que emerge

destes estudos é que a colisão envolvendo uma helicase no lugar de uma polimerase, pode estar envolvida na resposta citotóxica.

Ainda há várias perguntas relativas à ação das quinolonas sobre a girase que permanecem sem respostas, mas a falta de compreensão das bases moleculares da ação destas drogas não foi suficiente para evitar que elas se tornassem agentes antibacterianos de grande sucesso.

Cumarinas

Drogas cumarínicas são agentes antimicrobianos originariamente isolados de espécies de *Streptomyces*. O primeiro membro desta classe a ser identificado, há cerca de 50 anos, foi a novobiocina (Figura II.5), seguido posteriormente pela cumermicina A_1 e clorobiocina. Muitos derivados sintéticos destes compostos têm sido obtidos desde então, sendo classificados como agentes inibidores da síntese de ácidos nucléicos em bactérias (Maxwell, 1997).

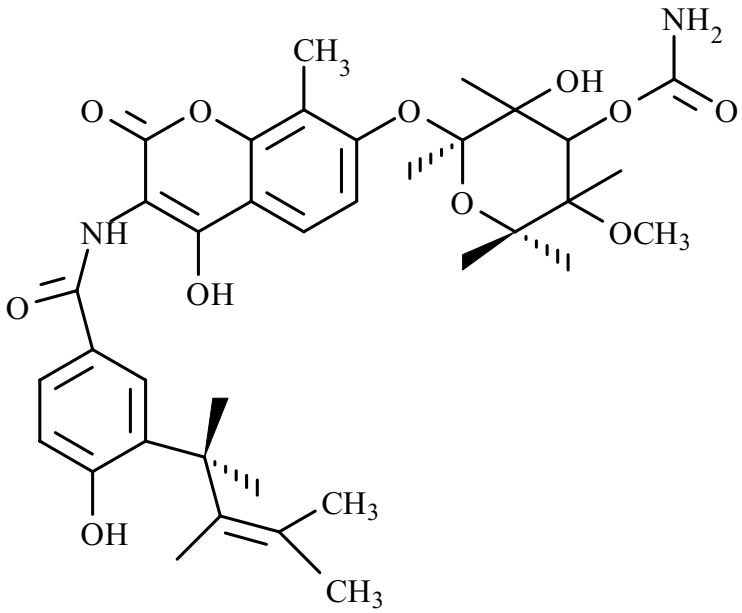

Figura II.5. Estrutura molecular da novobiocina

Com a descoberta da DNA girase, estudos de inibição do superenrolamento do DNA, catalisada pela girase, *in vitro*, levaram a concluir que esta enzima era o principal alvo das cumarinas. Mais especificamente, essas drogas atuam como inibidores competitivos da reação de hidrólise do ATP, catalisada pela proteína B da girase (GyrB) (Gormley, *et al.,* 1996).

Cumarinas são potentes inibidores das reações de superenrolamento e ATPase, catalisadas pela girase, com valores de K_i (constante de inibição) entre 10^{-7} e 10^{-9} M (Maxwell, 1993). Entretanto por diversas razões, incluindo baixa atividade contra bactérias Gram-negativas (resultante da baixa permeabilidade), toxidade em eucariotos e pouca solubilidade em água, elas não tem tido muito sucesso como drogas. No entanto, o interesse em relação à produção de novos produtos biologicamente ativos tem estimulado estudos adicionais do mecanismo molecular envolvidos na ligação das cumarinas à girase, incluindo um melhor entendimento dos contatos chave entre a droga e a enzima.

A natureza da inibição da função ATPásica da DNA girase, por cumarinas, tem sido objeto de muitos debates. Alguns autores sugeriram que a novobiocina comporta-se como um inibidor competitivo em estudos cinéticos da reação de superenrolamento e da atividade de ATPase da girase, porém estes mesmos autores também mostraram que a droga pode bloquear o acesso do ATP, sem compartilhar seu sítio de ligação, possivelmente estabilizando uma conformação incompatível com o *binding* do ATP (Sugino *et al*., 1978; Sugino & Cozzarelli, 1980). Mizuuchi e colaboradores (1978) concluíram, porém, que a novobiocina pode prevenir o *binding* do ATP à GyrB, o que corresponde à idéia de que os dois ligantes compartilham o mesmo sítio de ligação. Estudos cinéticos posteriores, envolvendo a função ATPásica da girase também sustentam a idéia de que a novobiocina funciona como um inibidor competitivo da DNA girase (Tamura *et al*., 1992).

Em outros estudos, também foi sugerido (Ali, *et al.*, 1993) que a interação de GyrB com a droga é aparentemente muito mais forte do que com nucleotídeos e que um fragmento N-terminal de 43-kDa da GyrB exibe uma cinética em desacordo com a equação de Michaelis-Menten, de modo que o efeito da novobiocina é aparentemente inconsistente, com uma simples ação competitiva.

O que emerge de todos esses estudos é que a cinética de hidrólise do ATP pela DNA girase não é simples e que o efeito das cumarinas não é facilmente caracterizado através de estudos cinéticos.

Através de análises de um número de cepas bacterianas resistentes às cumarinas, identificou-se pontos de mutação em um domínio N-terminal de 24-kDa da GyrB (Del Castillo, *et al.*, 1991; Contreras & Maxwell, 1992). A mais proeminente destas mutações é a de um resíduo de arginina (Arg-136 em GyrB de *Escherichia coli*), o qual é proposto estar envolvido na interação droga/proteína. A proteína GyrB, que carrega uma mutação em Arg-136, apresenta uma perda substancial na capacidade de superenrolar o DNA, bem como de hidrolisar o ATP (Contreras & Maxwell, 1992).

Há cerca de 10 anos, um fragmento amino-terminal de GyrB (24-kDa; resíduos 2 a 220) foi clonado e expressado, encontrando-se o sítio de ligação das drogas tipo cumarinas (Gilbert & Maxwell, 1994). O complexo formado entre este fragmento e a novobiocina foi cristalizado (Lewis, *et al.,* 1994) e sua estrutura determinada (Lewis, *et al.,* 1996). Somado a isso, a estrutura de um outro complexo formado entre a novobiocina e um fragmento de 24-kDa contendo a mutação Arg-136 $\rightarrow$ His também foi elucidada (Holdgate, *et al.,* 1997). A análise destas estruturas cristalinas mostrou claramente que o complexo formado entre a droga e a proteína envolve interações hidrofóbicas e uma rede de ligações de hidrogênio, especialmente com a molécula de açúcar da droga. O resíduo de Arg-136 liga-se por ligações de hidrogênio com o anel cumarínico, o que parece ser a chave da interação em termos de estabilidade do complexo proteína-droga. Os sítios de ligação da enzima

com o ATP e com a droga se sobrepõem, de modo que o açúcar da droga ocupa o lugar do anel de adenina do ATP, o que torna viável a idéia de ação competitiva das drogas cumarínicas e que é muito provável que essas drogas ajam prevenindo o acesso do ATP ao seu sítio de ligação.

Estudos de *binding* de cumarinas, empregando a proteína de 43-kDa carregando a mutação Arg-136 $\rightarrow$ His mostraram, como resultado desta mutação, uma redução nos valores de K_d de aproximadamente duas ordens de grandeza (Holdgate, *et al.,* 1997). Estudos empregando ressonância de superfície de plasma e mutantes produzidos por mutagênese sítio-dirigida, também confirmaram redução no *binding* para resíduos de aminoácidos envolvidos na interação com cumarinas.

Apesar de todo conhecimento gerado ao longo dos anos, acerca da ação das drogas tipo cumarinas, especificamente quanto ao mecanismo de inibição da reação de superenrolamento catalisada pela girase, estudos quanto o processo de interação com a enzima, ainda devem receber atenção especial, pois armado de informações estruturais é possível redesenhar racionalmente estes compostos e criar uma nova geração de cumarinas que mantenham as características importantes para a interação droga-proteína, mas que apresentem maior capacidade para penetrar nas bactérias e toxidade reduzida em sistemas eucarióticos.

Outros Compostos

Embora a maioria dos compostos conhecidos cujo alvo seja a DNA girase, pertençam à classe das quinolonas e cumarinas, existe um número crescente de inibidores desta enzima que não estão classificados nestes dois grupos.

A Microcina B17 (MccB17) é um deles. Trata-se de um peptídeo rico em glicina (PM = 3,2-kDa) produzido por uma enterobactéria que

carrega o plasmídeo pMccB17 ou outros correlacionados. Estes plasmídeos contêm seis genes estruturais para a produção do antibiótico, e um sétimo gene que confere imunidade para o mesmo. MccB17 é ativo contra muitas enterobactérias e tem sido apresentado como um inibidor da replicação do DNA, que leva a uma rápida interrupção na síntese de DNA, indução da resposta SOS, degradação do DNA e morte celular (Heddle, *et al.,* 2001). Dois isolados independentes de mutantes resistentes à MccB17 de *Escherichia coli*, foram mapeados e ambos contém um simples ponto de mutação no gene *gyrB* que converte Trp-751 em Arg, na proteína B (Vizán, *et al.,* 1991). A microcina B17 é também capaz de induzir a clivagem do DNA, de um modo semelhante as quinolonas, quando incubada com DNA e extratos de células de linhagens de bactérias sensíveis, mas não resistentes. Estes resultados sugerem portanto que o alvo intracelular da microcina B17 é a DNA girase, porém muitos estudos adicionais ainda devem ser feitos para esclarecer o modo exato de ação deste antibiótico.

Ciclotialidina é um peptideo cíclico isolado de *Streptomyces*. Estudos *in vitro* mostraram que inibem as reações de superenrolamento e de hidrólise do ATP, catalisadas pela DNA girase. Linhagens resistentes de *Staphylococcus aureus* têm mutações mapeadas em GyrB, próximo aos sítios de ligação do ATP e das cumarinas, e estudos de *binding* sugerem que o sítio de ligação das ciclotialidinas sobrepõe aos sítios de ligação do ATP e das cumarinas em GyrB. Realmente, a estrutura cristalina de um complexo formado entre o composto correlacionado GR122222X e o fragmento 24-kDa de GyrB, foi recentemente determinada e mostrou que o anel do resorcinol da droga ocupa uma posição semelhante àquela ocupada pelo anel de adenina do ADPNP no complexo com o fragmento 43-kDa da girase. Assim, ciclotialidinas agem de uma maneira análoga as cumarinas, embora seus sítios de ligação sejam distintos, e que mutantes resistentes às cumarinas não são resistentes a ciclotialidinas. Deste modo, parece que

as ciclotialidinas são pelo menos tão potentes quanto as cumarinas mas apresentam um modo de ação um pouco diferente. Embora elas não apresentem atividade antibacteriana significante, há muito espaço para desenvolvimento futuro (Maxwell, 1997).

Clerocidina é um antibiótico terpenóide isolado de *Fusidium viridae*. É conhecido como um agente citotóxico e tem sido descrito como um agente que estabiliza o complexo "clivável" de Topo II de mamíferos. *In vitro*, a clerocidina inibe a reação de superenrolamento do DNA e causa a clivagem do DNA de uma maneira similar a quinolonas. Análise de mutantes resistentes à clerocidina de *Escherichia coli* sugere que a mutação se encontra em *gyrA*, portanto a classifica como inibidor da DNA girase.

Embora não estritamente uma droga, a proteína *killer* CcdB, proporciona uma comparação interessante com os compostos descritos acima. CcdB é uma proteína de 11,7-kDa produzida pelo plasmideo F como parte de um sistema de morte celular programada formado por dois componentes. CcdB age como uma toxina e CcdA como o antídoto. Na ausência de CcdA, CcdB pode matar bactérias por um mecanismo que envolve a DNA girase. *In vitro*, CcdB pode formar um complexo "clivável" com a girase de uma maneira análoga às drogas tipo quinolonas; diferentemente das quinolonas, a clivagem do DNA linear requer ATP. Mutações que conferem resistência ao CcdB foram mapeadas em *gyrA* e produzem substituições no aminoácido Arg-462 para Cys e Gly-214 para Glu (Bernard & Couturier, 1992; Miki, *et al.,* 1992). Girase que carrega a mutação 462 em *gyrA* não consegue manter a clivagem do DNA, induzida pelo CcdB, mas ainda pode manter a clivagem induzida por quinolonas. Parece provável então, que CcdB e quinolonas interagem em locais diferentes em GyrA, bem como atuam por mecanismos distintos. Estudos desta pequena proteína, tais como seu modo de ação e interação com a enzima, podem render novas idéias para o desenvolvimento de novos inibidores peptídicos da DNA girase.

5. Nossa contribuição ao mecanismo de ação da DNA girase

5.1. Estudos com Quinolonas

Nosso interesse pelas DNA topoisomerases, mais especificamente a DNA girase, teve inicio em meados de 1996, quando passamos a desenvolver um estágio de pós-doutorado no Departamento de Química Orgânica, da Faculdade de Química da Universidade de Barcelona.

Os antecedentes do grupo anfitrião em relação ao tema de interesse resumem-se apenas à identificação de linhagens de *Escherichia coli*, resistentes à ação de duas quinolonas, o ácido nalidíxico e a ciprofloxacina. Neste estudo, mutações na denominada região determinante de resistência as quinolonas nos genes *gyrA* e *gyrB* em 27 isolados clínicos de *E. coli*, foram determinadas por sequenciamento de DNA. Uma alteração em apenas um resíduo de aminoácido (Ser-83) foi suficiente para produzir um alto nível de resistência ao ácido nalidíxico, enquanto uma segunda mutação em Asp-87, na subunidade A da DNA girase, foi encontrada em linhagens com elevados níveis de resistência à ciprofloxacina, evidenciando a região que contém estes dois resíduos em GyrA como sendo essencial para a interação com as quinolonas (Vila, *et al.,* 1994).

Considerando que as quinolonas inibem a atividade da DNA girase, através da formação de um complexo ternário quinolona-enzima-DNA e que este é a chave de todo processo de inibição, as vias pelas quais os substratos interagem, bem como as funções desenvolvidas por este complexo, a nível molecular, são pontos cruciais a serem esclarecidos e que ainda permanecem em debate.

Sob o ponto de vista estrutural, estudos desta natureza implicam em enormes dificuldades, devido basicamente ao tamanho do complexo formado. Este fato prontamente levou-nos a considerar a possibilidade de usar pequenos peptídeos contendo segmentos da subunidade A da DNA girase envolvidos no reconhecimento do DNA e das quinolonas,

como modelos no estudo de *binding*, o que resultou em nosso projeto de pós-doutorado, onde tivemos a oportunidade orientar nossa primeira aluna de mestrado, Núria Castillo, cuja contribuição foi intensa e decisiva para a qualidade dos resultados alcançados.

Para projetar os peptídeos usados nos estudos de interações do complexo quinolona/peptídeo/DNA, focalizamos nossa atenção em GyrA, a subunidade da DNA girase onde as quinolonas desempenham seu efeito inibitório. Reece e Maxwell (1991b) identificaram o fragmento 7 - 523 como o menor domínio de GyrA de *E. coli* com atividade de quebra do DNA, quando complexado com GyrB. A determinação da estrutura cristalina deste domínio revelou detalhes estruturais, tais como uma dobra hélice-volta-hélice, nas proximidades da região N-terminal e um agrupamento de resíduos carregados positivamente, próximos à Tyr-122, propostos como sendo o sítio de ligação da droga e o sítio ativo da reação de quebra-reunião, respectivamente, sendo que os dois locais estão muito próximos um do outro (Morais Cabral, *et al.,* 1997). Esta denominada dobra hélice-volta-hélice é também considerada a região determinante de resistência às quinolonas, uma vez que um grande número de mutações em linhagens resistentes estão localizadas nesta seqüência, mais especificamente no fragmento helicoidal C-terminal, constituído pelos resíduos 81 ao 92.

De acordo com estes dados pensamos que um bom ponto de partida para nossos estudos seria considerar, no planejamento da nossa seqüência peptídica, a hélice mencionada acima, bem como uma pequena seqüência da proteína nativa contendo o sítio ativo Tyr-122 (Horowitz & Wang, 1987). Deste modo, dois fragmentos da seqüência da proteína, uma incluindo a hélice C-terminal da dobra hélice-volta-hélice e uma outra incluindo o resíduo Tyr-122, foram escolhidos para comporem a estrutura primária do peptídeo modelo. O tamanho destes fragmentos foi fixado considerando a presença de resíduos básicos nas seqüências correspondentes. Finalmente, decidimos substituir a longa seqüência nativa de 23 aminoácidos que conecta os dois fragmentos,

por um *linker* flexível, para facilitar o processo de síntese. Levando em conta todas estas considerações, o peptídeo modelo denominado AGYRA foi sintetizado, pela metodologia da fase sólida, usando os fragmentos naturais 75 – 92 e 116 – 130, e dois resíduos de ácido aminohexanóico para conectá-los (Figura II.6).

A resistência bacteriana às quinolonas parece ser uma conseqüência da perda de ligação da droga ao complexo girase/DNA, induzida por mutações na seqüência de aminoácidos da enzima (Willmott & Maxwell, 1993). Este fato prontamente levou-nos a incluir, neste trabalho, a síntese de um análogo mimético da GyrA mutada. De acordo com o descrito na literatura, mutações têm sido encontradas nas posições 83 e 87, em particular as mutações Ser-83 $\rightarrow$ Leu e Asp-87 $\rightarrow$ Asn por produzirem elevados índices de resistência a ciprofloxacina (CFX) (Vila, *et al.,* 1994). Assim, incluímos em nossos estudos, além de AGYRA e CFX, o análogo AGYRM, o peptídeo mimético da GyrA mutada, contendo as citadas mutações (Figura II.6).

Ac-^{75}GKYHPHGD**S**$^{\mathbf{83}}$AVY**D**$^{\mathbf{87}}$TIVRX^{92}-ZZ-^{116}SAAAXR**Y**TEIRLAKI^{130}

AGYRA

Ac-^{75}GKYHPHGD**L**$^{\mathbf{83}}$AVY**N**$^{\mathbf{87}}$TIVRX^{92}-ZZ-^{116}SAAAXR**Y**TEIRLAKI^{130}

AGYRM

X = Norleucina e Z = ácido aminohexanóico

Figura II.6. Estrutura primária dos miméticos da GyrA

Ambos peptídeos foram acetilados na extremidade N-terminal e possuem um grupo carboxamida na C-terminal, para simular a presença de ligações amida nestas posições na proteína. Além disso, os

resíduos de Met foram substituídos por Norleucina (considerado isóstero da Met) para prevenir processos indesejados de oxidação e/ou alquilação durante a síntese dos peptídeos.

Empregamos ensaios de cromatografia de afinidade, para atingir a principal meta do nosso trabalho, que era determinar, a exemplo da girase, se a CFX poderia formar um complexo ternário com DNA e AGYRA, bem como averiguar se o mesmo poderia ou não ser formado com AGYRM. Para isso, consideramos a possibilidade de ter tanto uma quinolona como os peptídeos covalentemente ancorados em um suporte polimérico. Para imobilizar os peptídeos AGYRA e AGYRM, os análogos com um resíduo de cisteína (Cys) na posição N-terminal foram também preparados (CAGYRA e CAGYRM, respectivamente), uma vez que este resíduo permite a ligação da cadeia peptídica para uma resina através do grupo tiol da cadeia lateral da Cys (Figura II.7).

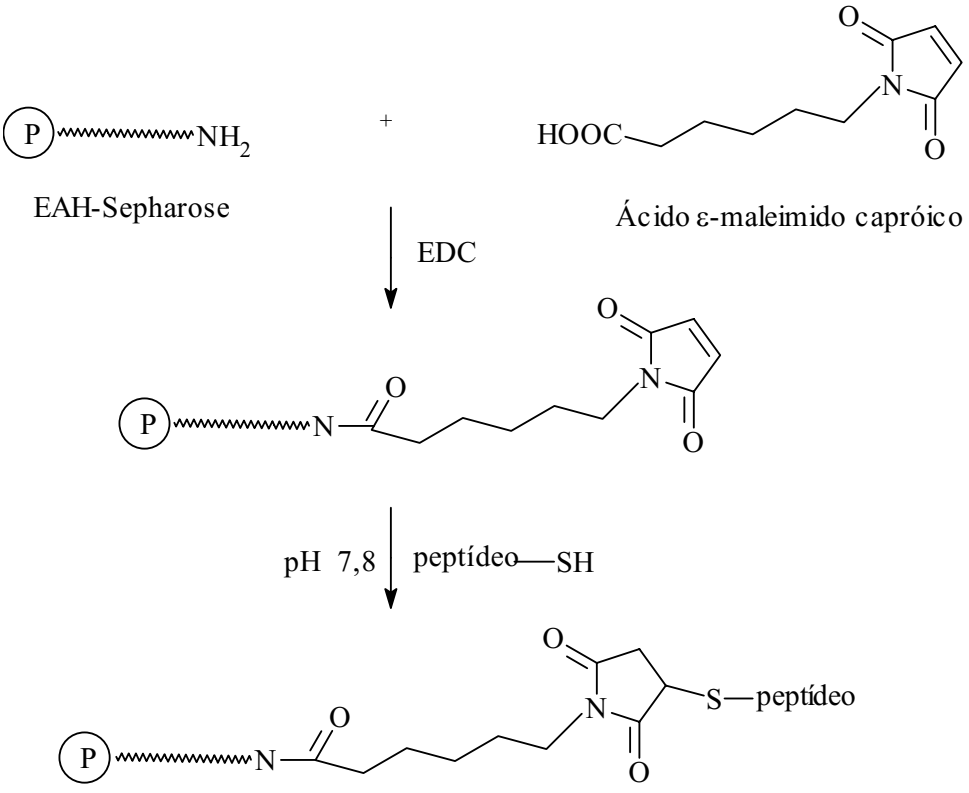

Figura II.7. Imobilização de AGYRA e AGYRM no suporte polimérico (EDC = 1-Etil-3-(3'-dimetilaminopropil)carbodiimida)

Quanto a ciprofloxacina, esta foi imobilizada a um suporte sólido, empregando uma Sepharose epoxi-ativada, na qual a droga foi ancorada por alquilação do seu grupo amino secundário (Figura II.4) sob condições padrões.

Os ensaios de cromatografia de afinidade mostraram que o DNA apresenta interações com AGYRA e com ciprofloxacina. O mais interessante é que as três espécies foram capazes de interagir uma com a outra de alguma forma, que pode ter resultado na formação de um complexo ternário quando o peptídeo mimético AGYRA foi usado. Entretanto, este comportamento não foi observado no caso do mimético mutado AGYRM (Figura II.8A).

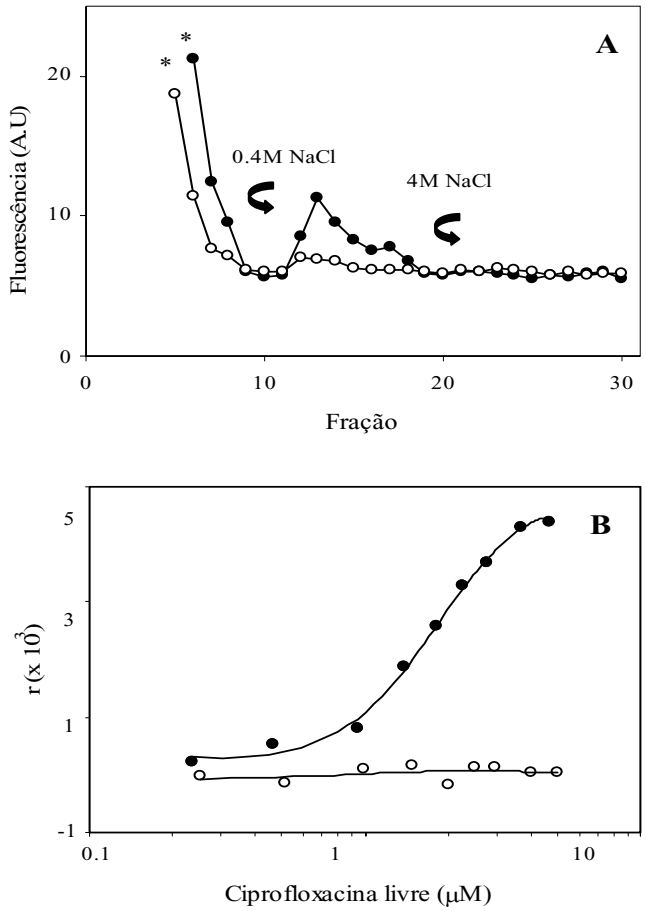

Figura II.8. (A) Experimentos de cromatografia de afinidade com (●) AGYRA ou (o) AGYRM imobilizado, aplicando uma mistura de CFX e pBS; *indica fluorescência maior que 20; AU = unidade arbitrária; (B) *Binding* do pBS pelo método de filtração em membranas: CFX foi adicionado a uma mistura pré-incubada contendo (●) AGYRA/pBS e (o) AGYRM/pBS; O ponto médio da curva de saturação equivale à constante de dissociação aparente (K_d) (Klotz, 1974).

Os resultados de cromatografia de afinidade foram confirmados através de ensaios para determinação dos parâmetros de *binding*, executados pelo método de filtração em membranas (Shen, *et al.,* 1989b), para os diferentes sistemas possíveis. Ciprofloxacina liga-se ao DNA, porém somente na presença do íon Mg^{2+}. Resultado semelhante foi obtido com a interação do DNA com os peptídeos testados (AGYRA e AGYRM), porém AGYRM se ligou mais eficientemente ao DNA que AGYRA (Tabela II.2).

Tabela II.2 – *Binding* do plasmídeo pBS a diferentes ligantes empregando o método de filtração em membranas

Ligante	K_d (x 10^{-7} M)
AGYRA	10,0
AGYRM	2,5
Ciprofloxacina	18,0
CFX/AGYRA[a]	16,0
CFX/AGYRM[a]	-[b]

[a] CFX foi adicionado a uma mistura pré-incubada de pBS e peptídeo
[b] nenhuma interação foi observada

Em relação à interação da droga com DNA, na presença de peptídeo, experimentos executados com misturas das três espécies, produziram resultados interessantes. A droga ligou-se ao DNA na presença de AGYRA, tal como esperado a partir dos resultados de cromatografia de afinidade obtidos com a molécula peptídica imobilizada no suporte polimérico (Figura II.8A), com uma constante de dissociação (K_d) de 16 x 10^{-7} M (Figura II.8B e Tabela II.2). Entretanto este valor de K_d é similar ao obtido na ausência de AGYRA, o que sugere que o DNA pode ter diferentes sítios de ligação para a droga e

para o peptídeo. Finalmente, nenhum tipo de interação entre a droga e o DNA foi detectada na presença do peptídeo mimético da GyrA mutada (AGYRM), de acordo portanto com os resultados obtidos usando cromatografia de afinidade (Figura II.8).

Os ensaios de *binding*, empregando ciprofloxaxina, DNA e peptídeos modelo projetados como miméticos da GyrA (selvagem e mutante), confirmaram características importantes já conhecidas a respeito do mecanismo de ação das quinolonas. Do ponto de vista das técnicas experimentais empregadas, conclusões similares podem ser esboçadas a partir dos resultados de cromatografia de afinidade e filtração em membranas.

Atualmente, é de consenso que as quinolonas inibem a ação da DNA girase ligando-se ao complexo enzima-DNA (formação chave da atividade biológica das topoisomerases), formando um complexo ternário. Estudos promovidos na ausência de girase revelaram que a droga interage com o DNA (Shen & Pernet, 1985; Shen, *et al.,* 1989b; Freudenreich & Kreuzer, 1993). Por outro lado, sabe-se que as quinolonas possuem baixa ou nenhuma afinidade para as topoisomerases na ausência de DNA (Shen & Pernet, 1985; Willmott & Maxwell, 1993; Khac & Moreau, 1994), porém detalhes moleculares da ligação da droga com a enzima no complexo ternário ainda permanecem não muito claros.

De um ponto de vista qualitativo, um comportamento paralelo foi observado para AGYRA. Este mimético peptídico de GyrA é incapaz de interagir com CFX, não importando qual componente se encontrava imobilizado no suporte sólido, droga ou peptídeo. Entretanto, ambos ligaram-se ao DNA. A cromatografia de afinidade também revelou a formação de um complexo ternário quando AGYRA (CFX imobilizado) e CFX (AGYRA imobilizada) ficaram retidos na coluna, na presença de DNA. Como já descrito na literatura, Mg^{2+} foi necessário para promover a interação da droga com o DNA (Palù, *et al.,* 1992; Palumbo, *et al.,* 1993; Fan, *et al.,* 1995). Estes resultados qualitativos foram

corroborados pela técnica de filtração em membranas, que permitiu a obtenção de valores de K_d para a ligação da CFX e AGYRA ao DNA, bem como da quinolona ao complexo AGYRA-DNA (Tabela II.2). O fato da AGYRA e CFX apresentarem afinidade para colunas contendo quinolona imobilizada e peptídeo imobilizado, respectivamente, na presença de DNA e Mg^{2+} indicam a formação de um complexo ternário. Este resultado não é surpreendente se a retenção é uma conseqüência da interação simultânea do DNA com o peptídeo e a droga.

A ligação do peptídeo mimético da GyrA mutada, AGYRM, ao DNA mostrou ser mais eficiente que AGYRA (Tabela II.2). A variação da carga efetiva do peptídeo de +2 para +3, como conseqüência da mutação de Asp para Asn na posição 87, o que resulta em uma adicional interação eletrostática com os grupos fosfatos carregados negativamente, pode explicar a maior afinidade de AGYRM ao DNA. Porém, o resultado mais intrigante foi obtido quando a ciprofloxacina foi usada com AGYRM. Diferentemente do que foi observado para AGYRA, CFX não ligou ao DNA, na presença de AGYRM, como pode ser observado pelos dados de cromatografia de afinidade e pela técnica de filtração em membranas (Figura II.8 e Tabela II.2). Este comportamento está de acordo com aqueles encontrados por Willmott e Maxwell (1993) para a norfloxacina e girase A com uma mutação que confere resistência à quinolonas (Ser-83 $\rightarrow$ Trp). Neste caso, a enzima apresentou grande redução na capacidade de ligação da droga.

Nossos resultados indicam que o peptídeo modelo AGYRA contém informações estruturais suficientes para induzir a formação de um complexo ternário com CFX e DNA através de interações mútuas entre as três espécies. Mutações nas posições críticas 83 e 87 produzem mudanças estruturais que resultam na desestabilização do complexo, como ocorre provavelmente no ambiente natural da enzima. Assim, o uso de pequenas seqüências peptídicas, tal como AGYRA e AGYRM, em estudos de interação com DNA pode ser uma aproximação satisfatória

para uma avaliação preliminar de diferentes quinolonas, como drogas com potencial antibacteriano.

Portanto, nossa contribuição ao estudo do mecanismo de ação e inibição da DNA girase, resume-se na sugestão do uso de pequenas moléculas peptídicas como um meio alternativo para estudar a interação entre as quinolonas com o complexo DNA-girase, bem como para melhor entender o mecanismo de resistência a estes antibióticos. Além disso, acreditamos que AGYRA constitui um importante ponto de partida para o planejamento de novas seqüências peptídicas capazes de manter características estruturais do sítio de ligação das quinolonas em GyrA e, usar esta potencialidade na pesquisa de novas drogas com atividade antibacteriana.

5.2. Estudos com Cumarinas

As cumarinas e a sua potencialidade clínica não tem sido muito explorada nos últimos anos, devido basicamente a problemas de toxidade, permeabilidade e solubilidade (Maxwell, 1997). Porém, o fato destes compostos serem significativamente mais potentes que as quinolonas, na inibição da DNA girase, *in vitro*, despertou-nos o interesse em estudá-los, uma vez que o entendimento das propriedades moleculares envolvidas na formação dos complexos enzima-droga e enzima-ATP, pode fornecer subsídios para a produção de compostos estruturalmente relacionados e mais viáveis para a prática clinica.

Neste sentido, dois mestrandos, Andreza Costa Scatigno e Saulo Santesso Garrido, propuseram-se a investigar a possibilidade do uso de pequenos peptídeos sintéticos, contendo segmentos da subunidade B da girase (GyrB) envolvidos no reconhecimento das cumarinas, ATP e DNA, como modelos para estudos estruturais e de interações moleculares. A principio foi sintetizado um peptídeo de 4,2-kDa, denominado AGYRB, formado por uma região C-terminal contendo os resíduos envolvidos na interação com o DNA (Funatsuki, *et al.,* 1997) e uma região N-terminal

contendo o resíduo de arginina na posição 136 (Arg-136), o qual acredita-se estar envolvido no processo de interação com as cumarinas (Maxwell, 1999). Técnicas de cromatografia de afinidade e supressão de fluorescência foram empregadas nos estudos de *binding*, deste peptídeo com a novobiocina, ATP e DNA.

Para projetar AGYRB foi considerado o fato de que um grande número de linhagens bacterianas resistentes a cumarinas, apresenta mutação no resíduo Arg-136. Além disso, as regiões de contato das cumarinas com a girase, estão localizadas em uma região que sobrepõe o sítio de ligação do ATP, o que inclui os resíduos ao redor de Arg-136. Não obstante, tem sido proposto que os resíduos vizinhos a um outro resíduo de arginina, o 760 (Funatsuki, *et al.,* 1997) estão relacionados diretamente com o reconhecimento e/ou transporte de DNA para o domínio de ligação do DNA na subunidade A da girase. Assim, AGYRB foi projetado considerando duas folhas β, formadas pelos resíduos 131 – 135 e 139 – 146 e os resíduos da alça (136 – 138) que as conectam, bem como uma pequena seqüência da proteína nativa que contém o resíduo Arg-760. Portanto, dois fragmentos da seqüência da proteína, uma incluindo as duas folhas β e uma alça, e uma outra incluindo Arg-760, foram escolhidas para comporem a estrutura primária do peptídeo modelo AGYRB. Finalmente, para simplificar e evitar problemas sintéticos, decidiu-se pela substituição da longa seqüência nativa de 607 aminoácidos que conecta estes dois fragmentos, por um *linker* flexível. Levando em conta todas estas considerações, AGYRB foi construído usando os fragmentos naturais 131 -146 e 753 – 770, e um resíduo de ácido ε-aminohexanóico para conectá-los (Figura II.9).

De acordo com a literatura, o aminoácido usualmente mutado em linhagens resistentes a cumarinas é Arg-136 de GyrB (Contreras & Maxwell, 1992; Maxwell, 1993, 1997, 1999), especialmente Arg-136 $\rightarrow$ Leu, o que resulta em uma perda substancial na capacidade de ligação da droga à enzima. Este fato, levou-nos a considerar um estudo

comparativo entre AGYRB e seu análogo mutado AGYRBM, o peptídeo mimético do mutante Leu-136 de GyrB (Figura II.9).

Ambos peptídeos foram acetilados nas respectivas extremidades N-terminal, e para simular a presença de ligação amida na extremidade C-terminal, ambos foram sintetizados de modo a conterem um grupo carboxiamida nesta posição. Finalmente, decidimos em não adicionar qualquer sonda fluorescente aos peptídeos, basicamente para manter a estrutura primária o mais próximo possível das características estruturais dos sítios de ligação das cumarinas, do ATP e do DNA, na proteína B da girase.

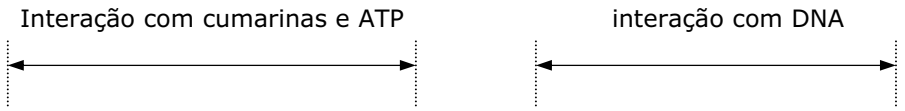

Ac-^{131}ELVIQ**R**$^{\mathbf{136}}$EGKIHRQIYE^{146}-Z-^{753}ITXDPESRRXLRVTVKDA^{770}-NH_2

AGYRB

Ac-^{131}ELVIQ**L**$^{\mathbf{136}}$EGKIHRQIYE^{146}-Z-^{753}ITXDPESRRXLRVTVKDA^{770}-NH_2

AGYRBM

X = Norleucina e Z = ácido aminohexanóico

Figura II.9. Estrutura primária dos peptídeos miméticos de GyrB

O objetivo para o estudo proposto era determinar se a novobiocina (Figura II.5) ou o ATP poderia formar um complexo estável com AGYRB, bem como se este complexo seria ou não estabilizado pela presença de DNA. Além disso, o efeito da alteração do aminoácido Arg-136, em AGYRBM, na formação deste complexo, também era parte integrante dos objetivos propostos. Para este fim, inicialmente partiu-se

para os ensaios de cromatografia de afinidade, utilizando suportes contendo novobiocina, ATP e DNA imobilizados.

Foram empregados adenosina 5'-trifosfato agarose (1,3 μmol/mL) e DNA fita simples ligado à celulose (3,5 μg/g), ambas comerciais. No caso de novobiocina, esta foi imobilizada usando uma Sepharose epoxi-ativada, na qual a droga foi imobilizada por um grupo hidroxila fenólico da parte da molécula que contém o ácido 4-hidroxi-3-(3-metil-2-butenil)- benzóico, sob condições alcalinas brandas (Figura II.10).

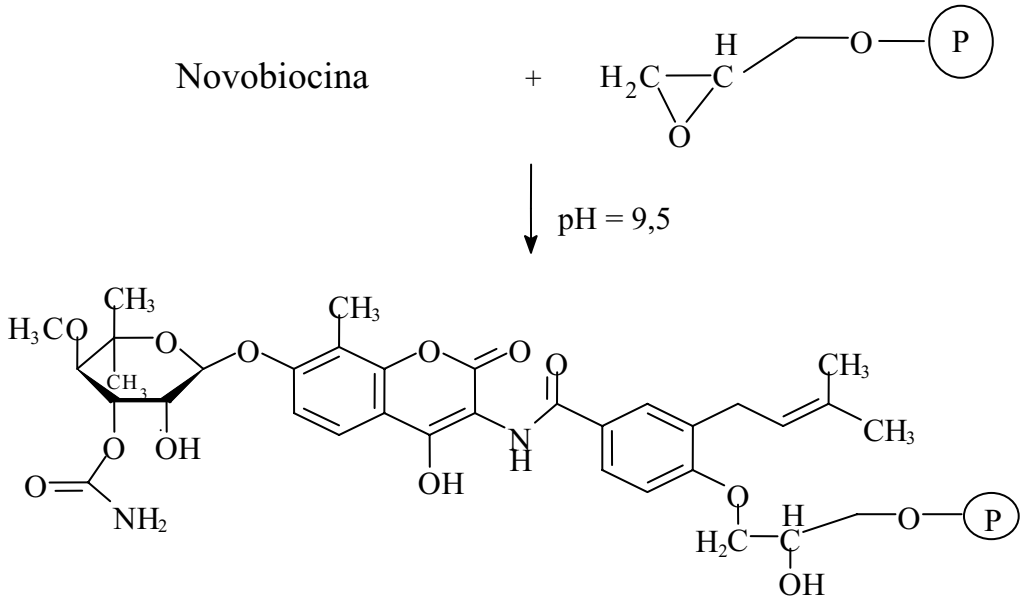

Figura II.10. Imobilização da novobiocina em uma epoxi-sepharose

Os experimentos de cromatografia de afinidade revelaram interações entre o peptídeo mimético AGYRB e novobiocina e ATP, uma vez que o mesmo apresentou retenção às respectivas colunas cromatográficas, sendo eluído das mesmas, utilizando soluções com força iônica relativamente baixa. O interessante foi que as interações foram independentes da presença de DNA. Entretanto, este comportamento não foi seguido no caso do peptídeo mimético AGYRBM, o que nos levou a determinar os parâmetros de *binding* para os sistemas mencionados.

Os parâmetros de *binding* foram estudados através do acompanhamento da supressão da fluorescência intrínseca do peptídeo, produzido após interação com a novobiocina, ATP ou DNA. A representação gráfica da intensidade de fluorescência relativa dos peptídeos (excitação a 280 nm e emissão a 304 nm) em função da quantidade de novobiocina, está mostrada na Figura II.11. Os dados estão mostrados na forma de representação gráfica de Stern-Volmer, para supressão estática, onde a fluorescência relativa dos peptídeos (Fo/F) é medida em função da concentração de novobiocina [NB]. Deste modo, a inclinação da respectiva curva é igual à constante de associação (k_a) do complexo formado (Lakowicz, 1987), de acordo com a equação: $Fo/F = 1 + k_a[NB]$, onde Fo e F são a intensidade de fluorescência na ausência e presença de novobiocina, respectivamente.

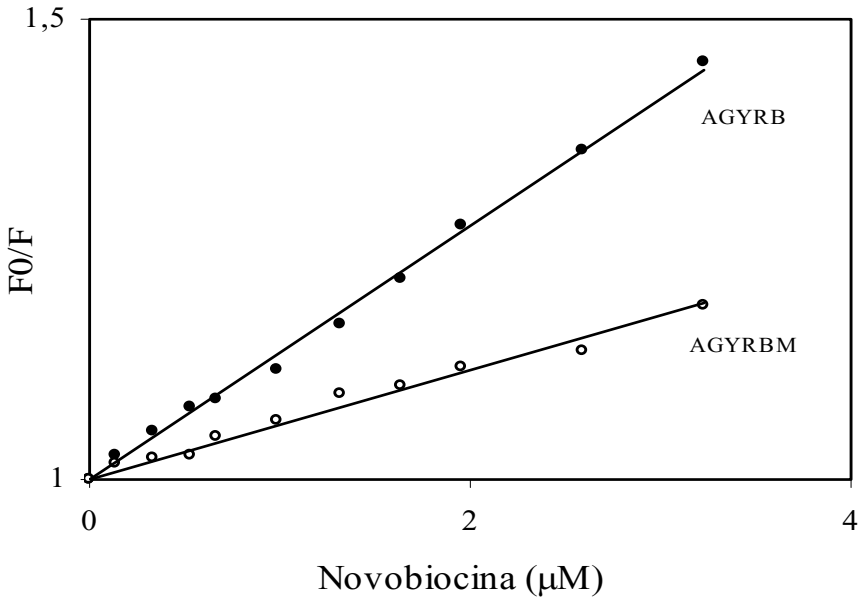

Figura II.11. Representação de Stern-Volmer para determinação dos parâmetros de *Binding*. Peptídeo (30 nmol) e novobiocina (0,13 – 3,23 μM).

Os parâmetros de *binding* com ATP e DNA, foram determinados através de medidas da diminuição da intensidade de fluorescência dos peptídeos em função da concentração de ATP e DNA, respectivamente,

sendo as medidas e a análise dos resultados as mesmas empregadas para a novobiocina.

Os valores das constantes de associação obtidas pela representação gráfica de Stern-Volmer, para os diferentes complexos formados, estão apresentados na Tabela II.3.

Tabela II.3. Binding comparativo[a]

Ligante	k_a (x 10^3 M^{-1})		k_d (μM)	
	AGYRB	AGYRBM	AGYRB	AGYRBM
Novobiocina	140 ± 30	-[b]	7,1± 1,2	-[b]
ATP	1,9 ± 0,4	1,7 ± 0,3	530 ± 95	590 ± 90
pBS	1600 ± 200	1400 ± 100	0,63 ± 0.08	0,71 ± 0,07

[a]Resultados obtidos por medidas de supressão na fluorescência de AGYRB e AGYRBM. Misturas de reação contendo 20 μM de um dos peptídeos e quantidades variáveis do ligante. A constante de associação (K_a) foi determinada pelo gráfico de Stern-Volmer. Os valores da constante de dissociação, k_d (= $1/k_a$), também estão representados; [b]Supressão identificada como sendo dinâmica, portanto não há *binding*. pBS = plasmídeo pBluescript.

Como observado por cromatografia de afinidade, novobiocina e ATP ligam-se ao peptídeo AGYRB, na presença de Mg^{2+}. Um *binding* preferencial da droga foi observado neste caso (cerca de 70 vezes em relação ao ATP). Por outro lado, não foi observado nenhum tipo de ligação da novobiocina ao AGYRBM, entretanto, a ligação do ATP foi idêntica para ambos AGYRB e AGYRBM, de acordo portanto com os resultados de cromatografia de afinidade, e consistente com a idéia de que a parte N-terminal da proteína B, que inclui o resíduo de Arg-136 está envolvida nas interações com as cumarinas e com o ATP e o DNA

não é requerido para promover estas interações. Além disso, a importância da presença de Mg^{2+} para promover as interações entre as espécies envolvidas, já havia sido descrita na literatura, no caso da proteína B da girase (Wigley, *et al.,* 1991; Noble & Maxwell, 2002).

A eluição de AGYRB da coluna de afinidade contendo novobiocina, sob condições brandas sugere que ligações de hidrogênio são as forças predominantes na formação do complexo peptídeo-droga. A importância do resíduo Arg-136 sugere interações iônicas entre este resíduo e a droga, mas nas condições dos experimentos a droga foi incapaz de interagir por este tipo de interação devido a ausência de uma carga efetiva negativa na sua estrutura. Estudos com uma proteína com 24-kDa também sugerem a ausência deste tipo de interação no *binding* com a droga (Gilbert & Maxwell, 1994). Neste caso, o íon Mg^{2+} pode estar desempenhando um papel importante na interação peptídeo-droga, servindo de ponte entre o grupo guanidinio da Arginina e o anel de lactona da novobiocina.

A interação de AGYRB com novobiocina produziu uma supressão na fluorescência, identificada através da análise dos espectros de absorção, como sendo do tipo estático, com um k_a de 1,4 x 10^5 M^{-1}, menor que o obtido para os fragmentos de DNA girase de 24 e 43-kDa (aprox. 10^7 M^{-1}) (Wigley, *et al.,* 1991; Holdgate, *et al.,* 1997, Tsai, *et al.,* 1997), o que não é surpreendente considerando o tamanho desses fragmentos (6 e 10 vezes maiores, respectivamente).

Em contraste, no *binding* do ATP, interações eletrostáticas devem estar envolvidas. Neste caso, grupos fosfatos ligam-se com Mg^{2+} por interações eletrostáticas e as moléculas de água coordenadas a este íon, através de ligações de hidrogênio, interagem com o peptídeo. As condições de eluição na cromatografia de afinidade já sugeriam uma fraca interação do ATP ao peptídeo, o que foi confirmado pela pequena constante de associação do complexo ATP-AGYRB (1,9 x 10^3 M^{-1}).

Em relação à interação dos peptídeos com o DNA, os resultados de fluorescência foram consistentes com a cromatografia de afinidade,

ou seja, ambos apresentaram interações com o DNA. A alteração da carga efetiva de +1 para 0, como conseqüência da mutação de Arg para Leu, na posição 136 em AGYRBM, não foi suficiente para promover qualquer alteração na afinidade, mesmo com a redução das interações eletrostáticas com os grupos fosfatos carregados negativamente. Isso sugere que o fragmento C-terminal, comum aos dois peptídeos, é o que realmente está envolvido com a interação com o DNA, de acordo portanto, com resultados obtidos com o fragmento de 43-kDa da proteína B, que foi incapaz de interagir com o DNA (Ali, *et al.,* 1993).

Diferentemente de AGYRB, a novobiocina não apresentou interação com AGYRBM, como mostrado pelas técnicas de cromatografia de afinidade e supressão de fluorescência. Este comportamento está de acordo com diversos dados experimentais obtidos com novobiocina e fragmentos da DNA girase com uma mutação no resíduo Arg-136, que confere resistência às cumarinas (Contreras & Maxwell, 1992; Maxwell, 1993; Holdgate, *et al.,* 1997; Kampranis, *et al.,* 1999). Como ocorrido com AGYRB, uma diminuição na intensidade de fluorescência de AGYRBM, em função da concentração de droga, foi observada (Figura II.11), mas a análise dos espectros de absorção e dependência da temperatura, mostrou que se tratava de supressão do tipo dinâmico, resultante de encontros colisionais entre as espécies e não devido a formação de um complexo. Portanto a inclinação da reta de Stern-Volmer não equivale a constante de associação, mas apenas a constante de supressão.

A reduzida afinidade exibida pelo peptídeo mutante sugere que a perda de ligações de hidrogênio entre Arg-136 e a droga resulta em uma diminuição no *binding*, presumivelmente devido a ausência deste tipo de interação quando este resíduo é substituído por Leu. Por outro lado, a mutação nesta posição não produziu qualquer alteração no *binding* do ATP. Isto implica que possivelmente este resíduo não faz parte do sítio de ligação do ATP.

Muitos estudos descrevem que a atividade de ATPase da DNA girase é inibida de uma maneira competitiva pela novobiocina (Sugino, *et al.,* 1978; Sugino & Cozzarelli, 1980; Gormley, *et al.,* 1996). Assim, para averiguar se a novobiocina liga-se ao peptídeo AGYRB competitivamente com o ATP, o *binding* da novobiocina e ATP foram examinados por experimentos de supressão na fluorescência (Figura II.12).

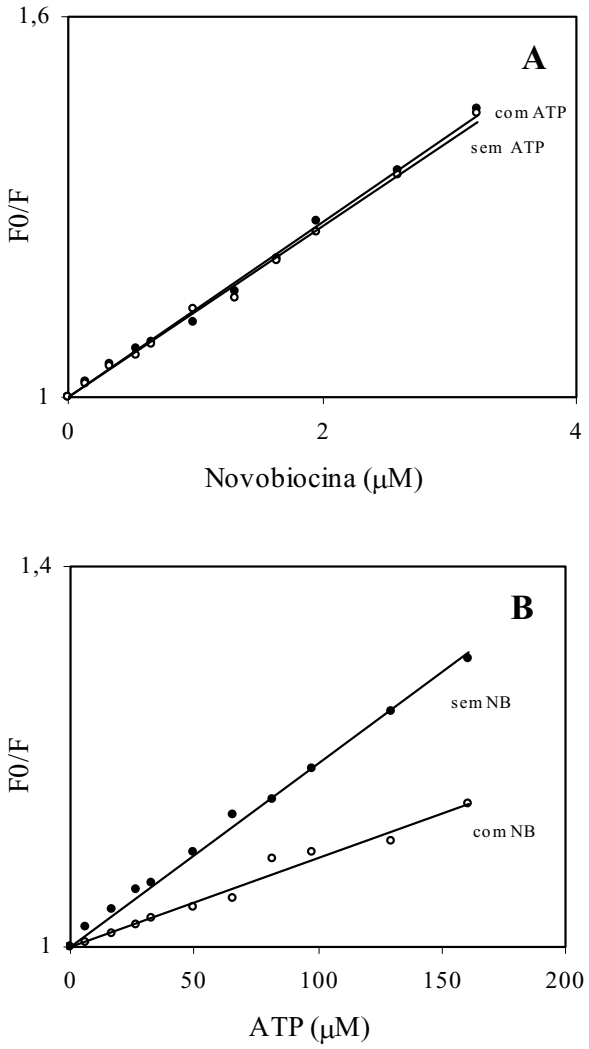

Figura II.12. *Binding* da novobiocina (A) e ATP (B) com AGYRB. O peptídeo (20 μM) foi pré-incubado com o mesmo excesso molar de ATP por 1 h e novobiocina (NB) (0,13 – 3,23 μM) foi adicionado (A). O peptídeo (20 μM) foi pré-incubado com o mesmo excesso molar de NB por 1 h e ATP (6,65 – 161,30 μM) foi adicionado (B). Fluorescência foi medida (exc. 280 nm, emis. 304 nm) após adição de cada alíquota.

Quando AGYRB foi pré-incubado com ATP e novobiocina adicionada subseqüentemente, para análise de fluorescência, nenhuma

alteração na representação de Stern-Volmer foi observada, quando comparada com a representação gráfica obtida sem pré-incubação de ATP (Figura II.12A). Conseqüentemente a constante de associação foi aparentemente a mesma para ambos casos (1,4 x 10^5 M^{-1}), sugerindo que o ATP não afeta a ligação da droga. Por outro lado, quando AGYRB foi pré-incubada com novobiocina e ATP adicionado subseqüentemente para análise de intensidade de fluorescência, uma diminuição na inclinação da reta de Stern-Volmer foi observada e a constante de associação menor que o valor correspondente obtido na ausência de pré-incubação com novobiocina (Figura II.12B).

Os resultados dos ensaios de competitividade indicaram que, dentro dos limites de erros experimentais, a novobiocina previne a ligação do ATP, indicando sobreposição dos sítios de ligação destes dois ligantes, o que suporta a idéia do *binding* competitivo. Esta conclusão está de acordo com dados de cristalografia obtidos por raios X, da estrutura do complexo formado entre o fragmento de 24-kDa da GyrB e a novobiocina (Lewis, *et al.,* 1996).

A conclusão que emerge dos resultados aqui comentados e que constituem o Anexo 5, é que o uso de pequenos peptídeos contendo seqüências de GyrB fornece um caminho alternativo para estudar e melhor entender os contatos chave entre as cumarinas ou ATP e a enzima, o que é especialmente importante para o desenvolvimento racional de novas drogas. Além disso, acreditamos que estes estudos forneceram uma prova adicional de que o modelo de inibição das drogas tipo cumarinas é competitivo e que os sítios de ligação do ATP e da droga não são os mesmos, porém estão bastante próximos.

Para confirmar tais conclusões e obter maiores detalhes a respeito da importância do resíduo Arg-136 nas interações droga-proteína e ATP-proteína, os parâmetros de *binding* da droga e do ATP com pequenos peptídeos sintéticos (Figura II.13), carregando uma série de mutações nesta posição também foram determinados, cujos dados foram detalhados na revista Journal of Peptide Research (Garrido,

Scatigno, Trovatti, Carvalho & Marchetto, 2005 – Anexo 6). Os resultados apresentados confirmaram que o resíduo Arg-136 pertence ao sítio de ligação das cumarinas e não do ATP, porém ambos estão sobrepostos.

Ac-E^{131}LVIQ**R**$^{\mathbf{136}}$EGKIHRQIYE^{146}-NH_2 ***agbN***

Ac-E^{131}LVIQ**S**$^{\mathbf{136}}$EGKIHRQIYE^{146}-NH_2 ***agbS***

Ac-E^{131}LVIQ**H**$^{\mathbf{136}}$EGKIHRQIYE^{146}-NH_2 ***agbH***

Ac-E^{131}LVIQ**L**$^{\mathbf{136}}$EGKIHRQIYE^{146}-NH_2 ***agbL***

Figura II.13. Estrutura primária dos fragmentos peptídicos de GyrB

Quatro peptídeos de baixo peso molecular foram selecionados e sintetizados pelo método da fase sólida (Figura II.13). O peptídeo *agbN* foi selecionado porque sua seqüência de aminoácidos reproduz a seqüência do segmento 131 – 146 (16 resíduos) da proteína B da girase de *Escherichia coli*, onde está incluído o resíduo Arg-136, reconhecidamente essencial para as interações com as cumarinas.

De acordo com as considerações já aventadas anteriormente, a respeito da importância do resíduo Arg-136 e a relação das mutações nesta posição e a resistência as cumarinas, *agbS, agbH* e *agbL* foram preparados como análogos de *agbN*, com o resíduo de arginina na posição 136, substituído por Ser, His e Leu, respectivamente. Do mesmo modo que para AGYRB e AGYRBM, estas quatro seqüências foram sintetizadas de modo a gerar grupos carboxiamidas terminais, bem como foram acetiladas na extremidade N-terminal, para que ao final, pudesse simular a presença de ligações amida nestas posições.

Considerando que cromatografia de afinidade é um bom método de análise qualitativa, ensaios baseados nesta técnica, a exemplo de AGYRB, foram projetados para identificar processos de interação. Um primeiro ensaio foi feito, usando a mesma coluna cromatográfica, obtida pela imobilização da novobiocina em uma sepharose (Figura II.10). Os peptídeos foram detectados por medidas de intensidade de emissão de fluorescência a 304 nm (excitação a 280 nm), e o comportamento cromatográfico dos peptídeos representados na Figura II.14A.

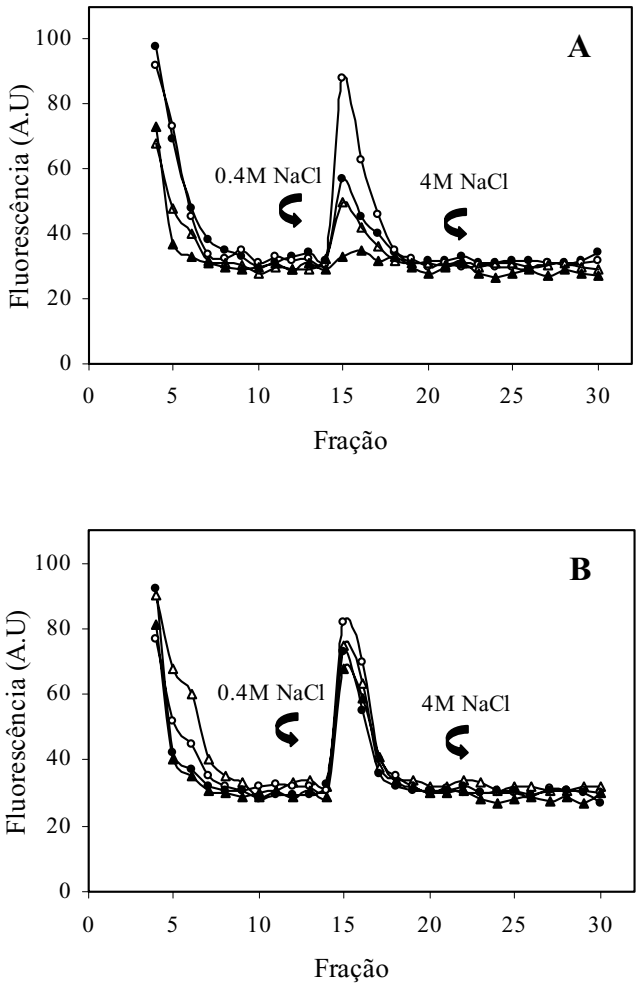

Figura II.14. Cromatografia de afinidade com novobiocina (A) e ATP (B) imobilizados em um suporte polimérico. Amostras: *agbN* (○); *agbS* (●); *agbH* (Δ); *agbL* (▲). Colunas foram equilibradas com 5 mM Tris.HCl, pH 7.2 /20 mM NaCl/5 mM $MgCl_2$. Eluição foi feita com mesmo tampão contendo 0,4 ou 4 M de NaCl como indicado. Frações com valores de fluorescência fora da escala não foram considerados. A.U = Unidade arbitrária.

Na presença de Mg^{2+}, *agbN* teve afinidade pela coluna de novobiocina, como demonstrado pela sua eluição quando a força iônica do meio foi aumentada. Para os peptídeos miméticos da GyrB mutada (*agbS* e *agbH*) a afinidade foi relativamente menor que *agbN*. Quanto ao peptídeo mutante *agbL*, diferentemente dos demais, não apresentou nenhum tipo de afinidade para a coluna empregada.

No caso da interação com ATP, o *binding* foi avaliado empregando a mesma coluna preenchida com adenosina 5'-trifosfato agarose comercial (1,3 µmol/mL), utilizada nos estudos com AGYRB. De acordo com os perfis cromatográficos mostrados na Figura II.14B, todos peptídeos, independentemente do resíduo presente na posição 136, foi retido na coluna. Deste modo, o ATP parece se ligar, com uma afinidade similar para os quatro peptídeos testados, porém sempre dependente da presença do íon magnésio.

Diferentemente dos resultados anteriores, *agbN* e suas formas mutagênicas não foram retidos em colunas contendo DNA imobilizado, independentemente da presença de Mg^{2+}.

Em relação aos parâmetros de *binding*, foram determinados como já descrito anteriormente, pela técnica de supressão da fluorescência intrínseca dos peptídeos, como uma função da concentração de novobiocina ou ATP (Figura II.15). Os valores de constante de associação (k_a), apresentados na Tabela II.4, foram obtidos igualmente, a partir da inclinação da representação gráfica de Stern-Volmer para supressão identificada como sendo do tipo estática, de acordo com a equação já apresentada: $Fo/F = 1 + k_a[NB]$.

Os dados se mostraram totalmente de acordo com a técnica de cromatografia de afinidade: novobiocina e ATP ligaram-se a *agbN*, na presença de magnésio. Um *binding* preferencial da droga aos peptídeos foi também observado neste caso (cerca de 80 vezes em relação ao ATP). O *binding* da novobiocina a*o agbS* e *agbH* foram muito próximos, porém menores que *agbN*, entretanto não foi observado nenhum tipo de ligação da novobiocina com *agbL*. Por outro lado, o *binding* com o

ATP foi muito parecido, independentemente da seqüência peptídica (k_a = 2,0 x 10^3 M^{-1}), o que está de acordo com os resultados obtidos por cromatografia de afinidade.

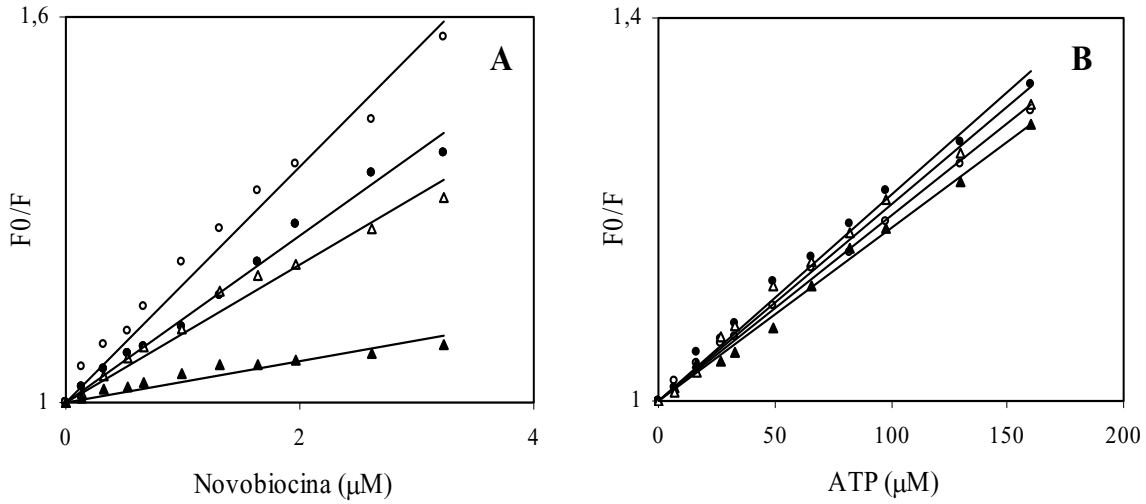

Figura II.15. Determinação dos parâmetros de *Binding*, usando gráfico de Stern-Volmer. 150 nmol de *agbN* (○), *agbS* (●), *agbH* (Δ), *agbL* (▲) e (A) novobiocina (0,13 – 3,23 μM) ou (B) ATP (6,65 – 161,30 μM). Fluorescência foi medida (excitação, 280 nm; emissão, 304 nm) após adição de cada alíquota em cada amostra. A inclinação da curva de Stern-Volmer representa a constante de associação para supressão do tipo estática. Para supressão do tipo dinâmica a inclinação representa a constante de supressão de Stern-Volmer.

TABELA II.4. *Binding* comparativo[a]

peptideo	k_a (×10^3 M^{-1})	
	Novobiocina	ATP
agbN	180 ± 20	1,9 ± 0.4
agbS	130 ± 10	2,1 ± 0.3
agbH	100 ± 20	2,0 ± 0.3
agbL	-[b]	1,8 ± 0.2

[a]Ensaios de supressão na fluorescência. Misturas de reação contendo 100 μM de um dos peptídeos e quantidades variáveis de novobiocina (0,13 – 3,23 μM) ou ATP (6,65 – 161,30 μM). A constante de associação (k_a) foi determinada pelo gráfico de Stern-Volmer.
[b] Supressão identificada com sendo dinâmica, portanto não há interação.

A exemplo de AGYRB, o novo peptídeo mimético da GyrB, *agbN*, apresentou um comportamento similar, sob o ponto de vista qualitativo, às propriedades de interação da DNA girase. *agbN* foi capaz de se ligar à novobiocina e ao ATP, independentemente da presença de DNA, consistente com a idéia de que a parte N-terminal da proteína B, que inclui o resíduo Arg-136 é a responsável pela interação da proteína com estas duas espécies, e que DNA não é requerido para promover estas interações.

Como já observado para AGYRB, as condições moderadas de eluição de *agbN* da coluna com novobiocina imobilizada, sugerem que ligações de hidrogênio são os principais determinantes na manutenção do complexo peptídeo-droga. Como Mg^{2+} desempenha papel fundamental no processo de interação, é possível que este íon aja como uma ponte entre o grupo guanidinio da Arg-136 e o anel de lactona da novobiocina, hipótese aventada anteriormente com AGYRB e que resultou na proposta de um modelo de interação, descrito detalhadamente neste estudo com *agbN* (Figura II.16).

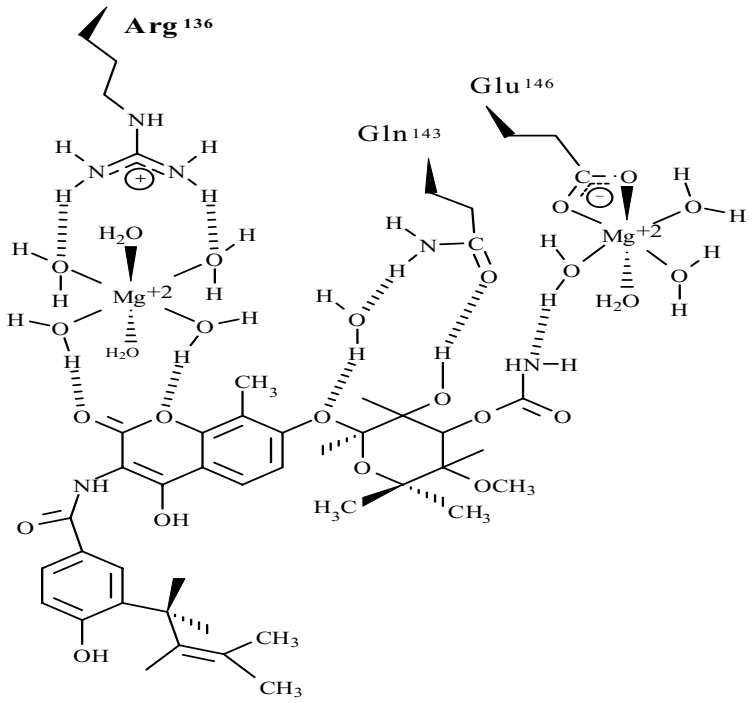

Figura II.16. Modelo proposto para a interação novobiocina-*agbN*

Neste modelo, duas moléculas de água coordenadas com Mg^{2+} formam ligações de hidrogênio com o grupo guanidinio da Arg-136 e outras duas com o grupo éster e oxigênio carbonílico do anel cumarínico. Também é possível que no ajuste molecular, o grupo 2'-hidroxílico da novobiose forme uma ligação de hidrogênio direta com o oxigênio carbonílico da Gln-143. O grupo 3'-carbamoil da novobiose forma uma ligação de hidrogênio mediada por uma molécula de água com Mg^{2+} coordenado com a cadeia lateral do resíduo Glu-146. Além disso, o oxigênio da função éter que liga o anel cumarínico e o açúcar novobiose pode formar uma ligação de hidrogênio com uma molécula de água ordenada, a qual por sua vez forma uma outra ligação de hidrogênio com a cadeia lateral da Gln-143.

Para as formas mutagênicas de *agbN*, a ligação com a novobiocina, foi progressivamente reduzida com o aumento da hidrofobicidade do resíduo presente na posição 136 (aprox. 30 e 50% para Ser e His, respectivamente). Novobiocina não se ligou a *agbL*, como revelado pelos ensaios de cromatografia de afinidade e supressão de fluorescência. Aparentemente, a afinidade da novobiocina pelos peptídeos está relacionada com o número de ligações de hidrogênio entre a droga e o resíduo de aminoácido na posição 136. Ser e His, diferentemente de Arg, formam uma única ligação de hidrogênio com as moléculas de água coordenadas com o Mg^{2+}, o qual forma duas ligações de hidrogênio com o grupo éster e oxigênio carbonílico do anel cumarínico. Porém, nas condições experimentais empregadas, a serina age como um doador de ligações de hidrogênio enquanto a histidina como aceptor deste tipo de ligação, o que explica a pequena diferença no *binding* da novobiocina observado para *agbS* e *agbH*. A carência de ligações de hidrogênio entre a novobiocina e o peptídeo mutante contendo Leu, pode explicar a reduzida afinidade exibida por este peptídeo. Com o aumento da hidrofobicidade dos resíduos na posição 136 (Arg $<$ Ser $\leq$ His $<$ Leu) (Guy, 1985; Abraham & Leo, 1987;

Roseman, 1988), há uma diminuição na tendência de formação de ligações de hidrogênio e conseqüentemente no *binding* da novobiocina.

Diferentemente dos complexos formados com a novobiocina, o *binding* do ATP envolve interações eletrostáticas, e como em AGYRB, o grupo fosfato liga-se ao Mg^{2+}, por interações eletrostáticas, o qual por sua vez liga-se igualmente por interações eletrostáticas, com os resíduos de ácido glutâmico, especificamente localizados nas posições 131 e 146. Neste caso, o *binding* deve também ser estabilizado por outras interações, considerando que os anéis de adenina pode efetuar muitos contatos polares com o peptídeo, em particular com o resíduo Tyr-145.

As mutações, na posição crítica 136, ao contrário da novobiocina, não produziram qualquer alteração na ligação do ATP. Isso implica que este resíduo não faz parte do sítio de ligação do ATP. De fato, um número considerável de mutações que conferem resistência a cumarinas, na DNA girase ficam na periferia do sítio de ligação do ATP (Del Castilho, *et al.,* 1991; Contreras & Maxwell, 1992).

Em relação a interações com o DNA, os estudos com AGYRB e AGYRBM, peptídeos contendo o fragmento C-terminal invariável 753 - 770, havia confirmado a proposta de que os resíduos vizinhos ao resíduo Arg-760 estão relacionados diretamente com o reconhecimento e/ou transporte do DNA para o domínio de interação do DNA da subunidade A da girase. A ausência de interação entre o pequeno peptídeo *agbN* e o DNA, intensificou esta hipótese.

Os resultados obtidos com *agbN* e seus análogos mutados fortaleceram a idéia de que o uso de pequenos peptídeos, contendo segmentos da GyrB fornece uma via alternativa para o estudo dos pontos importantes de contato entre as cumarinas, o ATP e a enzima. Além disso, nossos estudos também produziram provas adicionais a respeito do modo de inibição das cumarinas, que é competitivo e que os sítios de interação da droga e do ATP, não são os mesmos, porém devem estar muito próximos.

Talvez a contribuição mais importante que emerge de nossos estudos com cumarinas é o suposto papel que o íon magnésio e suas moléculas de água de coordenação desempenham, na formação da rede de ligações de hidrogênio, tão importante para a estabilidade do complexo cumarina-enzima. O modelo de ponte de Mg^{2+} proposto, fornece pistas importantes para o real papel do resíduo de Arg-136, no *binding* das cumarinas à DNA girase.

5.3. Estudos com CcdB

Como conseqüência do nosso interesse pela DNA girase, incluindo seu modo de ação e inibição, bem como nossa experiência em síntese química de peptídeos, iniciamos recentemente um trabalho, com a participação direta de uma aluna de doutorado, Eliane Trovatti, juntamente com outras duas de iniciação científica, Maria Ap. Loureiro Spósito e Camila Ap. Cotrim, que visa basicamente a obtenção de seqüências peptídicas análogas ao CcdB, para melhor caracterizar o processo de inibição da DNA girase, bem como tentar produzir um novo grupo de moléculas com potencialidade antibiótica.

Embora ainda não tenham sido publicados, os resultados obtidos até o momento são bastante animadores, os quais passo a descrever:

5.3.1. *Design das seqüências*

As seqüências sintetizadas foram projetadas com base na estrutura cristalina de CcdB proposta por Loris e colaboradores (1999). Para tal, considerou-se as regiões de importância significativa na interação com a DNA girase (região Ser-84 a Ile-101) e com o antídoto CcdA (região Arg-41 a Leu-50), além da região envolvida na formação de dímeros (região Met-68 – Pro-72), bem como o segmento N-terminal (Met-1 a Lys-9) da toxina. Este último, além de conter uma estrutura em folha β, pode servir como seqüência de reconhecimento no

mecanismo de penetração através da parede celular. A seqüência de aminoácidos da molécula de CcdB alinhada com sua estrutura secundária, representando seus diversos segmentos (S), está esquematizada na Figura II.17.

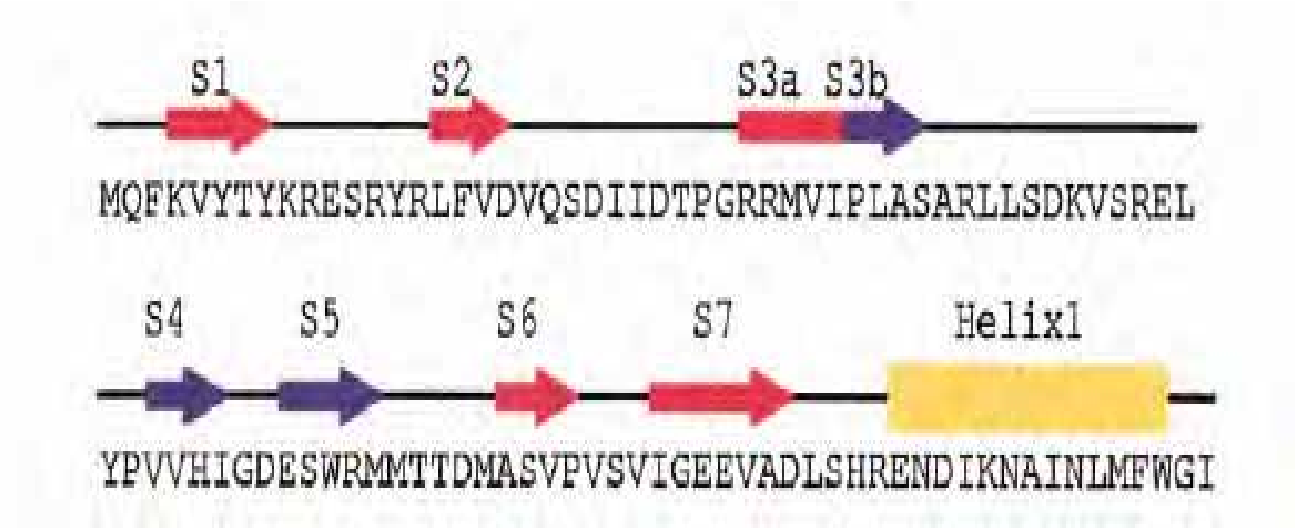

Figura II.17. Seqüência de aminoácidos de CcdB bacteriano alinhado com sua estrutura secundária.

Segundo Loris e colaboradores (1999), os três resíduos da extremidade C-terminal (Trp-99, Gly-100 e Ile-101) desempenham papel fundamental na formação do complexo CcdB-GyrA. Mutantes identificados com substancial perda de atividade *killer* e, portanto, menor habilidade de formar um complexo com GyrA, apresentaram mutações localizadas nesta região. Por outro lado, tais mutações não provocaram qualquer efeito na função de auto-repressão de CcdB, dependente de CcdA, evidenciando que estes aminoácidos não devem estar envolvidos na formação do complexo CcdB-CcdA. Além disso, o resíduo Trp-99, juntamente com outros doze resíduos da extremidade C-terminal (Glu-87 a Phe-98), faz parte da composição da única α-hélice presente na estrutura do CcdB (Figuras II.17 e II.18).

Além da α-hélice e das estruturas em folha β principais, a molécula de CcdB também apresenta, entre os seguimentos S6 e S3a

da folha β principal, 3 segmentos menores em forma de folha, as quais se projetam para fora da molécula como uma "asa". Esta "asa" envolve os resíduos 41-50 que formam uma alça e permanecem protegidos da ação de proteases, na presença de CcdA (Van Melderen, *et al.,* 1996). Isso indica que este segmento forma um local de reconhecimento provável para o CcdA (Figura II.18).

MQFKVYTYKRESRYRLFVDVQSDIIDTPGRRMVIPLASARLLSDKVSRELYPVVH
IGDESWRMMTTDMASVPVSVIGEEVADLSHRENDIKNAINLMFWGI

CcdB

MKQRITVTVDSDSYQLLKAYDVNISGLVSTTMQNEARRLRAERWKAENQEGMA
EVARFIEMNGS FADENRDW

CcdA

Figura II.18. Estrutura primária do CcdB e do CcdA

O monômero CcdB consiste de cinco principais estruturas antiparalelas denominadas folhas β. Entre elas, o segmento S6, que é formado pelos resíduos Met-68 – Pro-72 e desempenha papel importante na formação da estrutura do dímero de CcdB. A interface do dímero é formada pelos resíduos que compõem o fragmento S6, além dos 3 resíduos C-terminais da α-hélice. No dímero, o segmento S6 de um monômero interage com o segmento S6 do monômero oposto, de maneira antiparalela. A cadeia lateral do resíduo Trp-99 forma uma fraca ligação de hidrogênio com Asn-95, além de contatos hidrofóbicos com Lys-91, ambos do monômero oposto, estabilizando, assim, o dímero formado, representado a seguir, na Figura II.19.

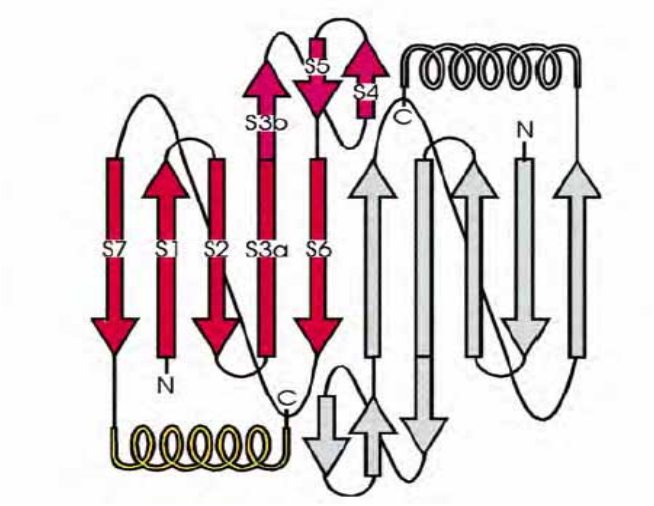

Figura II.19. Diagrama representativo do dímero de CcdB. Elementos da estrutura secundária são marcados e codificados por cores. Vermelho - estrutura em dobra β antiparalela principal; lilás - estrutura em dobra β menores formando a denominada "asa"; amarelo - α-hélice C-terminal.

De acordo com as considerações anteriores, o análogo CcdB1 (Figura II.20), foi sintetizado, mantendo a seqüência de resíduos de aminoácidos de Ile-101 a Ser-84 da molécula de CcdB bacteriano. Esta seqüência inicial foi mantida em todos os análogos devido à sua importância estrutural e possibilidade de interação com GyrA e ausência de interação com CcdA, como citado anteriormente.

^{32}MQNEARRLRAERWKAENQEGMAEVARFIEMNGSFADENRDW^{72} (CcdA41)

^{84}SHRENDIKNAINLMFWGI^{101} (CcdB1)

^{1}MQFKVYTYK^{9}-Z-^{40}RLLSDKVSREL^{50}-Z-^{84}SHRENDIKNAINLMFWGI^{101} (CcdB2)

^{1}MQFKVYTYK^{9}-Z-^{84}SHRENDIKNAINLMFWGI^{101} (CcdB3)

^{68}MASVPVSVPVSVIGEEVADLSHRENDIKNAINLMFWGI^{101} (CcdB4)

Figura II.20**.** Estrutura primária do CcdA41 e dos análogos do CcdB

Para compor a estrutura primária do segundo análogo (CcdB2), uma seqüência maior foi projetada, incluindo, além do fragmento que contém a α-hélice C-terminal (Ser-84 a Ile-101), a seqüência de reconhecimento do antídoto CcdA (Arg-40 – Leu-50) e uma terceira seqüência contendo o segmento N-terminal (Met-1 a Lys-9). Estes 3 fragmentos foram conectados por um *linker* flexível (ácido ε-amino-capróico), em substituição aos 63 resíduos de aminoácidos da seqüência nativa. Destaca-se a importância da extremidade N-terminal no possível reconhecimento molecular com a parede celular bacteriana e a importância do fragmento que contém os resíduos Arg-40 – Leu-50 no reconhecimento do CcdA como antídoto da possível ação tóxica do análogo proposto. O análogo CcdB3 foi projetado mantendo-se a seqüência C-terminal (Ser-84 a Ile-101) e a seqüência N-terminal (Met-1 a Lys-9), porém, sem a seqüência de reconhecimento do CcdA, com o intuito de um estudo comparativo entre os análogos em relação à interação com a enzima e com o inibidor enzimático CcdB.

A seqüência CcdB4, por sua vez, foi escolhida por manter o segmento S6 que, segundo Loris e colaboradores (1999), desempenha papel fundamental na formação da estrutura do dímero de CcdB . Desta forma é possível analisar se a atividade antibacteriana de CcdB ou de seus análogos é dependente da formação deste dímero ou a estrutura monomérica dos análogos por si só já desenvolve a ação esperada.

No caso da seqüência do CcdA escolhida para síntese (Figura II.20), decidiu-se por considerar regiões nas quais acredita-se estarem envolvidas na formação do complexo CcdA-CcdB, segundo Van Melderen e colaboradores (1996).

De acordo com estes autores, predições da estrutura secundária do CcdA sugerem a existência de duas ou três α-hélices no domínio C-terminal de 41 resíduos de aminoácidos. A proteção deste domínio, pelo CcdB, frente à degradação promovida por proteases, leva a acreditar que a interação do CcdA com o CcdB ocorre nesta região, a qual centralizamos nossa atenção.

Segundo Bernard & Couturier (1992), uma seqüência truncada do CcdA, contendo 41 resíduos de aminoácidos (Met-32 a Trp-72), ainda mantém a atividade inibitória da ação do CcdB. Desta forma, decidiu-se por sintetizar esta seqüência e constatar o possível efeito antídoto em análogos do CcdB e posteriormente no CcdB intacto.

5.3.2. *Síntese*

Os análogos do CcdB, foram sintetizados manualmente pelo método da fase sólida (maiores detalhes na Parte I), de acordo com o protocolo padrão que emprega o grupamento base-lábil Fmoc como protetor dos α-amino grupos, e derivados t-butilicos (*t*-Bu) para a proteção da maioria das cadeias laterais de resíduos de aminoácidos (Fields & Noble, 1990), usando uma Fmoc-Ile-Wang resina e DIC/HOBt como agentes de condensação. Os grupos funcionais das cadeias laterais dos Fmoc-aminoácidos foram protegidos pelos seguintes grupos: tBu para Asp, Glu, Ser, Tyr e Thr; Trt para Asn, Gln e His, Boc para Lys e Pmc para Arg. Na etapa de acoplamento de cada aminoácido, empregou-se o excesso molar de 3 equivalentes para o Fmoc-aminoácido e 3 equivalentes para os reagentes de acoplamento em DCM:DMF (1:1), por 2 horas. A eficiência das etapas de acoplamento foi monitorada pelo teste de Kaiser e, se positivo, o processo era repetido com 50% dos reagentes. Acetilação, quando necessária, foi feita com anidrido acético e DIEA (10 equivalentes cada) em DMF, por 30 minutos.

A clivagem final dos peptídeos das respectivas resinas e a desproteção dos grupos protetores das cadeias laterais, foi efetuada pelo tratamento das peptidil-resinas com uma solução de clivagem contendo TFA (94%), água deionizada (2,5%), EDT (2,5%) e TIS (1,0%), a 25ºC por 1h30min. Peptídeos brutos, foram precipitados com éter dietílico gelado e centrifugados (quatro vezes), dissolvidos em solução aquosa de ácido acético 10% e liofilizados. O rendimento dos

peptídeos brutos (em peso) situou-se entre 70 e 90%, para todas amostras.

A purificação dos peptídeos foi feita por Cromatografia Líquida de Média Eficiência (CLME), usando uma coluna de fase reversa Nucleosil C_{18} (25 x 2,5 cm; 15 μm; 300 Å) com um gradiente convexo de 30 a 60% de componente orgânico (acetonitrila; água; 0,1% TFA) e fluxo de 2,0 mL/min e detecção a 220 nm. CLAE analítica foi feita em um cromatógrafo Varian ProStar, empregando uma coluna de fase reversa Nucleosil C_{18} (25 x 0,46 cm; 5 μm; 300 Å), com um gradiente linear de 5 a 95% de solvente B (A: água, 0,045% TFA; B: ACN, 0,036% TFA) em 30 min, fluxo de 1,5 mL/min e detecção a 220 nm (Figura II.21).

Análises de aminoácidos resultaram em valores em concordância com os valores teóricos (hidrólise: HCl 6M a 110°C por 72 horas; analisador: Shimadzu LC-10A/C-47A com método de funcionalização pós-coluna usando orto-phtalaldeído). A identidade dos peptídeos foi confirmada por determinação dos correspondentes pesos moleculares, 2156, 4754, 3459 e 4137 g/mol, determinados pela técnica ES-MS positivo [ES m/z = 1079 $(M + 2H)^{+3}$; 1190 $(M + 4H)^{+4}$; 1154 $(M + 3H)^{+3}$, 1380 $(M + 3H)^{+3}$] para CcdB1, CcdB2, CcdB3, CcdB4, respectivamente.

Na síntese do CcdA41, empregou-se as mesmas condições de acoplamento e clivagem, descritas para os análogos do CcdB, porém partindo-se de uma resina de Wang, com Fmoc-Trp pré-incorporado. O peptídeo bruto também foi purificado por CLME e analisado por CLAE, nas mesmas condições já descritas. O perfil cromatográfico do análogo CcdA41 purificado por CLAE, exibido na Figura II.22B, mostra a presença de pico único com t_r = 7,731 min. O peso molecular teórico 4.943,50 g/mol foi confirmado por espectrometria de massas, empregando a técnica ES-MS positivo [ES m/z = 1648 $(M + 3H)^{+3}$; 1236 $(M + 4H)^{+4}$; 989 $(M + 5H)^{+5}$].

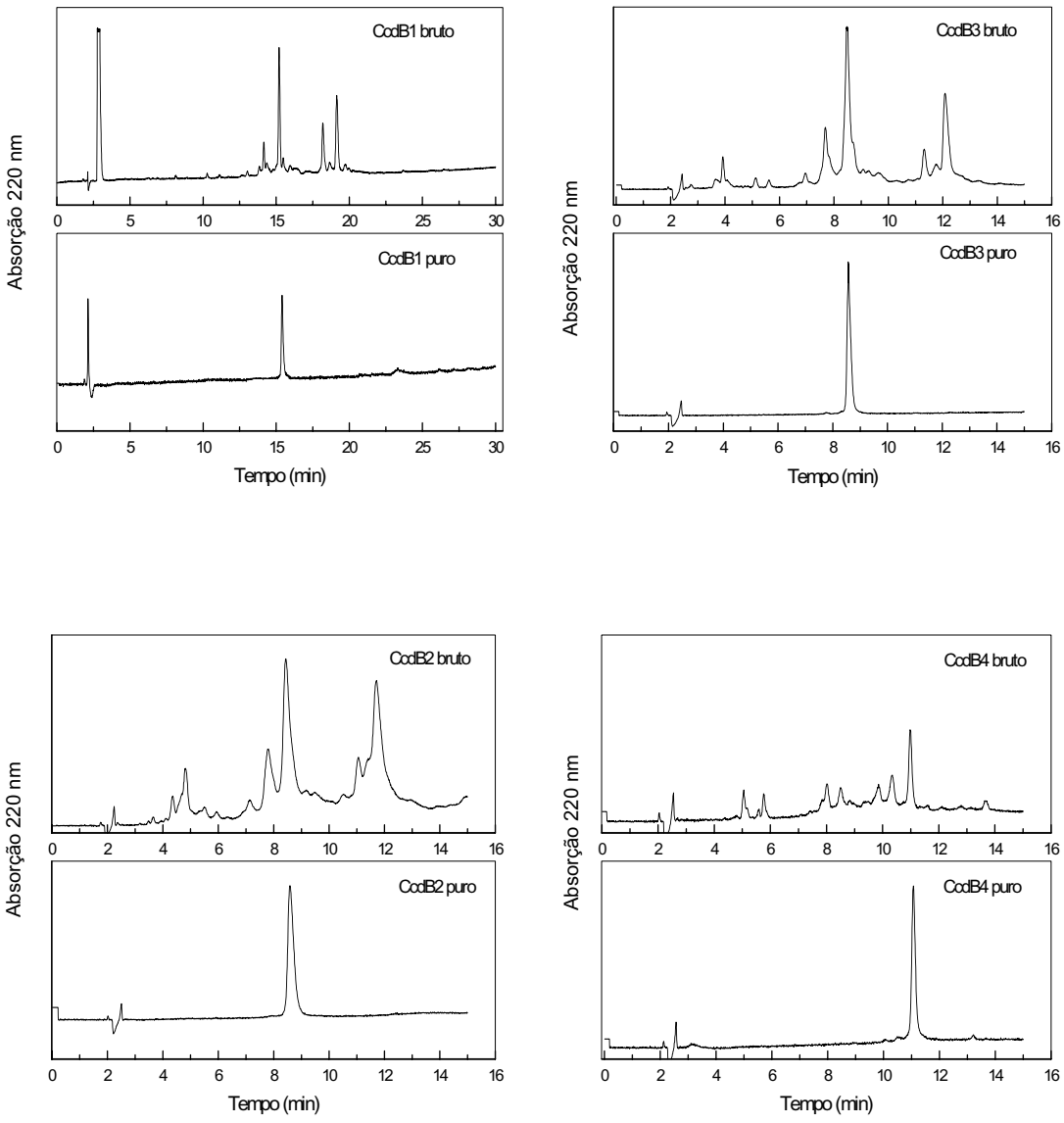

Figura II.21. Cromatogramas obtidos em escala analítica para os análogos peptídicos sintetizados CcdB1, CcdB2, CcdB3 e CcdB4. Antes (superior) e após purificação (inferior), respectivamente.

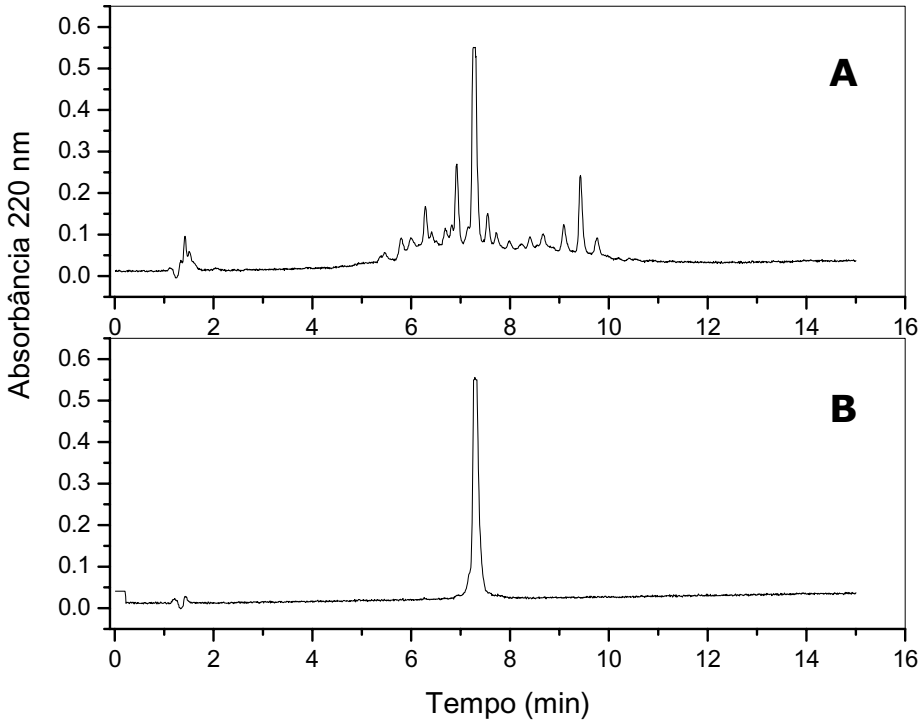

Figura II.22. Cromatogramas obtidos em escala analítica para o análogo peptídico CcdA41, antes (A) e após (B) purificação.

5.3.3. *Ensaios de inibição da atividade da DNA girase*

Os ensaios de inibição da atividade da DNA girase, pelos análogos sintéticos do CcdB, foram feitos através da observação do efeito inibitório dos mesmos, na reação de superenrolamento do DNA, catalisada pela enzima. Desta forma, foram incubados 2 unidades (U) de DNA girase com 0,5 µg de plasmídeo pBR322 relaxado em um volume de reação de 30 µl a 37°C por 30 minutos em tampão de ensaio. As concentrações de peptídeos foram variáveis. A reação foi interrompida pela adição de 1 µL de uma solução de proteinase K (2,5 mg/mL) e posterior incubação por 30 min a 37^{o}C. Em seguida as amostras foram submetidas à eletroforese em gel de agarose, cuja análise inicial está representada na Figura II.23.

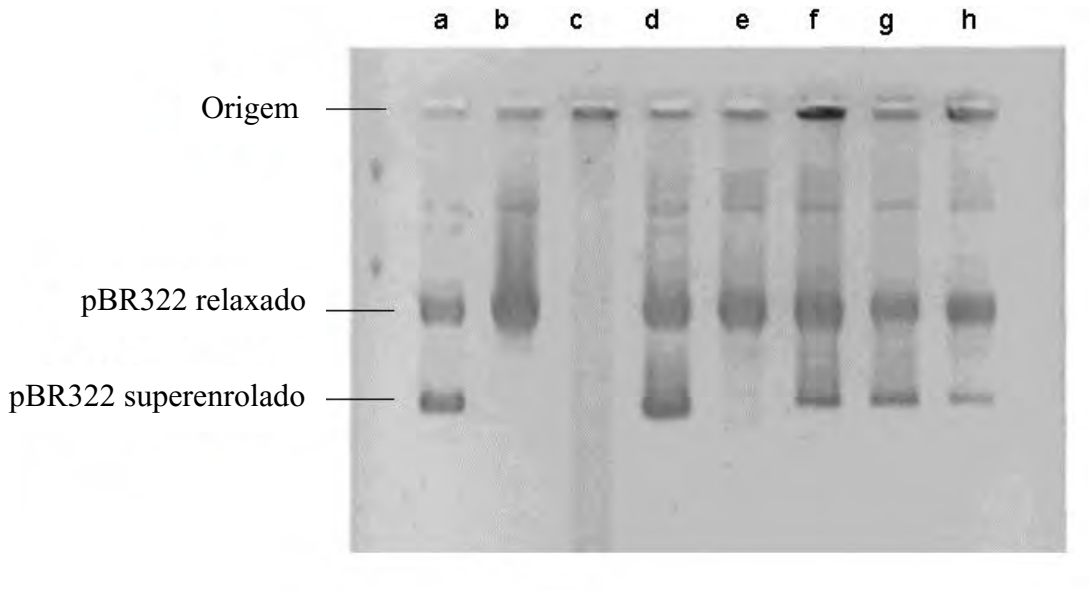

Figura II.23. Inibição da atividade de superenrolamento da DNA girase por análogos do CcdB. Volume de reação de 20 µL contendo: linha **a**, plasmídeo pBr322 superenrolado controle; linha **b**, plasmídeo pBr322 relaxado controle; linha **c**, DNA fita simples controle; linha **d**, plasmídeo pBr322 relaxado e DNA girase (2 U); linhas **e** até **h**, plasmídeo pBR322 relaxado, DNA girase (2 U) e 2 mg/mL de CcdB2, CcdB1, CcdB4, e CcdB3, respectivamente.

Nesta figura podemos observar o efeito dos diferentes análogos sintéticos do CcdB, na reação de superenrolamento do DNA mediado pela DNA girase. A ação da DNA girase foi inibida completamente pela presença do análogo CcdB2 (linha e), não sendo possível identificar a banda do plasmídeo superenrolado, evidenciando a capacidade de interação deste fragmento com a enzima, inibindo sua ação, assim como ocorre com a molécula de CcdB intacta. No caso dos demais análogos (linhas f, g, h), estes apresentaram inibição menos efetiva, o que permite concluir que o análogo denominado CcdB2, deve conter informações estruturais suficientes para induzir a formação de um complexo com a girase, o qual não possui atividade de topoisomerase.

A partir deste primeiro ensaio, os que seguem foram elaborados, com o intuito de se determinar a concentração mínima de inibição, para cada um dos análogos sintetizados. O procedimento, os tampões empregados e a concentração do gel, foram os mesmos do ensaio anterior, porém o volume final de reação foi de 30 µL. As Figuras II.24, II.25 e II.26, mostram as análises por eletroforese em gel, na presença

dos análogos CcdB1, CcdB2, e CcdB3, respectivamente, variando-se a concentração dos mesmos. Para o CcdB4, não foi encontrado um valor de concentração mínima, compreendido na faixa de 10 a 500 μM, para inibição da DNA girase.

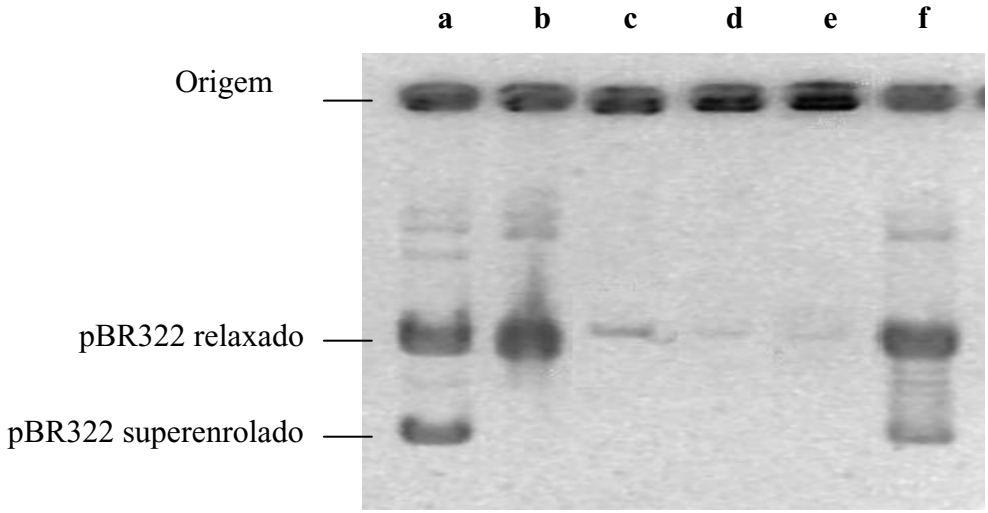

Figura II.24. Inibição do superenrolamento do DNA pelo **CcdB1**. Volume de reação 30 μL; ensaios contendo plasmídeo pBR322 relaxado (0,5 μg) e DNA girase (2U). linhas **a** e **b**, pBR322 superenrolado e relaxado controles, respectivamente; linhas **c** até **e**, contendo CcdB1 nas concentrações de 120, 240 e 360 μM, respectivamente; linha **f**, ausência do CcdB1.

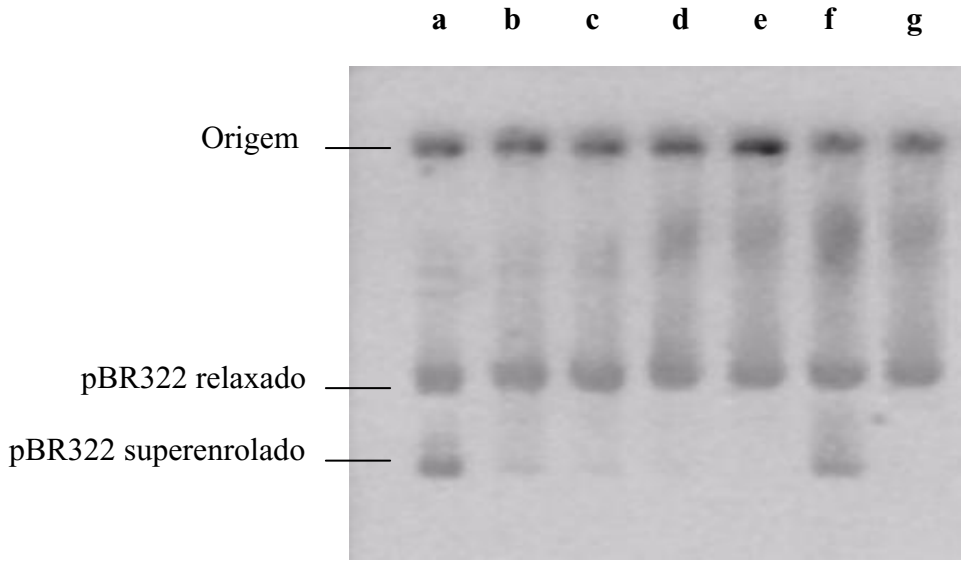

Figura II.25. Inibição do superenrolamento do DNA pelo **CcdB2**. Volume de reação 30 μL; ensaios contendo plasmídeo pBR322 relaxado (0,5 μg) e DNA girase (2U). linhas **a** e **g**, pBR322 superenrolado e relaxado controles, respectivamente; linhas **b** até **e**, contendo CcdB2 nas concentrações de 14, 19, 35 e 70 μM, respectivamente; linha **f**, ausência do CcdB2.

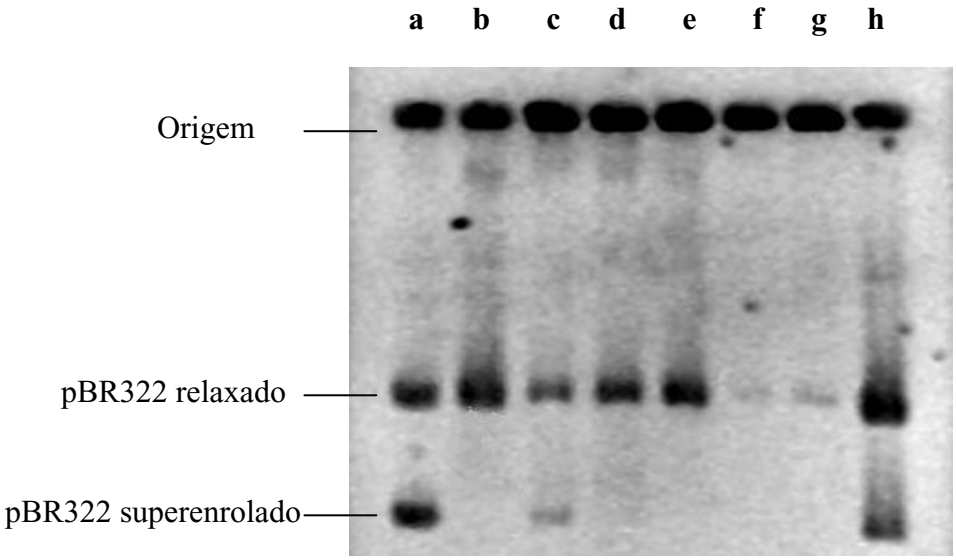

Figura II.26**.** Inibição do superenrolamento do DNA pelo **CcdB3**. Volume de reação 30 µL; ensaios contendo plasmídeo pBR322 relaxado (0,5 µg) e DNA girase (2U). linhas **a** e **b**, pBR322 superenrolado e relaxado controles, respectivamente; linhas **c** até **g**, contendo CcdB3 nas concentrações de 80, 160, 250, 310 e 360 µM, respectivamente; linha **h** ausência do CcdB3.

Uma avaliação das Figuras II.24, II.25 e II.26, confirmam os resultados prévios de inibição da DNA girase, ou seja, o análogo CcdB2 foi o que apresentou a menor concentração para inibição da reação de superenrolamento do DNA. Foi possível observar uma grande diferença entre os análogos sintetizados e testados. A ação da DNA girase foi inibida pelo CcdB2, a uma concentração de 19 µM, enquanto CcdB1 e CcdB3 somente acima de 100 µM. Fato interessante foi o desaparecimento total das bandas atribuídas ao pBR322 relaxado e superenrolado, quando na presença de CcdB1 e CcdB3, em concentrações superiores a 200 e 300 µM, respectivamente. Nestes casos, foi possível observar um aumento de intensidade das bandas presentes na origem das respectivas eletroforeses, as quais podem ser explicadas através de duas hipóteses.

Existem na literatura (Critchlow, *et al.*, 1997), alguns estudos envolvendo a clivagem de pBR322 linear, induzida pelo CcdB. Clivagem

esta dependente da hidrólise do ATP pela DNA girase. Desta forma, a primeira hipótese a ser aventada para o resultado observado com os peptídeos, seria o mesmo, ou seja em altas concentrações, CcdB1 e CcdB3, induzem a hidrólise do DNA, formando fragmentos que não migram quando submetido a um campo elétrico. Uma outra hipótese, seria que a presença destes dois peptídeos, nas condições do experimento, deve promover a formação de um complexo peptídeo-enzima-DNA insolúvel, o que impossibilitaria a migração do DNA quando submetido à análise por eletroforese. Van Melderen e colaboradores. (1996) já haviam observado fenômeno semelhante causado pela insolubilidade de um complexo CcdA-CcdB e girase, quando ensaiado em concentrações crescentes de CcdB.

A partir destes resultados, ensaios de atividade antibacteriana dos peptídeos, foram executados empregando bioensaio por difusão em agar (antibiograma), baseado no método descrito por Bauer e colaboradores (1966). Foram testadas as bactérias *Klebsiella pneumoniae, Staphilococcus aureus, Salmonella sp., Enterococcus sp.* e *Pseudomonas sp*, porém não foi possível detectar atividade para nenhum dos peptídeos.

Esta ausência de inibição do crescimento das bactérias pode estar relacionada coma a baixa permeabilidade da membrana bacteriana, aos fragmentos peptídicos testados. Desta forma, uma fase de viabilização de introdução destes fragmentos no interior da bactéria, por encapsulamento já foi iniciada, porém os resultados ainda não estão disponíveis.

Apesar, do resultado negativo quanto a atividade antibacteriana, os resultados de inibição de atividade da DNA girase *in vitro*, permitem concluir que os análogos do CcdB sintetizados constituem um bom ponto de partida para o melhor entendimento da chave das interações do CcdB natural e a enzima, além do mecanismo de ação desta toxina, assim como no desenvolvimento de novos inibidores da DNA girase.

6. Referências Bibliográficas

ABRAHAM, D.J.; LEO, A.J. Extension of the fragment method to calculate amino acid zwitterion and side chain partition coefficients. *Proteins*, v. 2, p. 130 – 152, 1987.

ALI, J.A.; JACKSON, A.P.; HOWELLS, A.J.; MAXWELL, A. The 43-kilodalton N-terminal fragment of DNA gyrase B protein hydrolyses ATP and binds coumarin drugs. *Biochemistry*, v. 32, p. 2717 – 2724, 1993.

BAUER, A.W.; KIRBY, W.M.M.; SHERRIS, J.C./ TURCK, M. Antibiotic susceptibility testing by a standardized single disk method., *Am. J. Clin. Path.,* v. 45, p. 493 – 496, 1966.

BERGER, J. M.; GAMBLIM, S. J.; HARRISON, S. C.; WANG, J.C. Structure and mechanism of DNA Topoisomerase II. *Nature*, v. 379, p. 225 – 232, 1996.

BERNARD, P.; COUTURIER, M. Cell killing by the F-Plasmid CcdB protein involves poisoning of DNA-topoisomerase-II complexes. *J. Mol. Biol.*, v. 226, p. 735 – 745, 1992.

BROWN, P.O.; PEEBLES, C.L.; COZZARELLI, N.R. A topoisomerase from Escherichia coli related DNA gyrase. *Proc. Natl. Acad. Sci. USA.*, v. 76, p. 6110 – 6114, 1979.

CAPRANICO, G.; KOHN, K.W.; POMMIER, Y.; Local sequence requirements for DNA cleavage by mammalian topoisomerase II in the presence of doxorubicin. *Nucleic Acids Res.* v. 18*,* p. 6611 – 6619, 1990.

CRITCHLOW, S.E.; MAXWELL, A. DNA cleavage is not require for the binding of quinolone drugs to the DNA gyrase-DNA complex. *Biochemistry*, v. *35*, p. 7387 – 7393, 1996.

CRITCHLOW, S.E.; O'DEA, M.H.; HOWELLS, A.J.; COUTURIER, M.; GELLERT, M.; MAXWELL, A. The interaction of the F plasmid killer protein, CcdB, with DNA Gyrase: Induction of DNA cleavage and blocking of transcription. *J. Mol. Biol*., v. 273, p. 826 – 839, 1997.

CONTRERAS, A.; MAXWELL, A. GyrB mutations which confer coumarin resistence also affect DNA supercoiling and ATP hydrolysis by Escherichia coli DNA gyrase. *Mol. Microbiol.*, v. 6, p. 1617 – 1624, 1992.

Del CASTILLO, I.; VIZÁN, J.; RODRIGUEZ-SAINZ, M.; MORENO, F. An usual mechanism for resistance to the antibiotic coumermycin-A1. *Proc. Natl. Acad. Sci. U.S.A.*, v. 88, p. 8860 – 8864, 1991.

DRLICA, K.; ZHAO, X. DNA gyrase, topoisomerase IV and the 4-quinolones. *Microbiol. Mol. Biol. Rev.*, v. 61, p. 377 – 392, 1997.

FIELDS, G.; NOBLE, R. L. Solid-phase peptide-synthesis utilizing 9-fluorenyl-methoxycarbonyl amino-acids, *International Journal of Peptide and protein Reearch,* v. 35, p. 161 – 214, 1990.

FREUDENREICH, C.H.; KREUSER, K.N. Mutational analysis of a type II topoisomerase cleavage site: distinct requirements for enzyme and inhibitors. *EMBO J.*, v. 12, p. 2085 – 2097, 1993.

FUNATSUKI, K.; TANAKA, R.; INAGAKI, S.; KONNO, H.; KATOH, K.; NAKAMURA H. *acrB* Mutation located at carboxy-terminal region of gyrase B subunit reduces DNA binding of DNA Gyrase. *J. Biol. Chem.*, v. 272, p. 13302 – 13308, 1997.

GELLERT, M.; MIZUUCHI, K.; O'DEA, M.H.; NASH, H.A. DNA gyrase: An enzyme that introduces superhelical turns into DNA. *Proc. Natl. Acxad. Sci. USA.,* v. 73, p. 3872 – 3876, 1976.

GELLERT, M.; MIZUUCHI, K.; O'DEA, M.H.; ITOH, T.; TOMIZAWA, J. Nalidixic acid resistance: a second genetic character in DNA gyrase activity. *Proc. Natl. Acxad. Sci. USA.,* v. 74, p. 4772 – 4776, 1977.

GILBERT, E.J.; MAXWELL, A. The 24 kDa N-terminal sub-domain of the DNA gyrase B protein binds coumarin drugs. *Mol. Microbiol.*, v. 12, p. 365 – 373, 1994.

GORMLEY, N.A.; ORPHANIDES, G.; MEYER, A.; CULLIS, P.M.; MAXWELL, A. The interaction of coumarin antibiotics with fragments of the DNA gyrase B protein. *Biochemistry,* v. 35, p. 5083 – 5092, 1996.

GUY, H.R. Amino acid side-chain partition energies and distribution of residues in soluble proteins. *Biophys. J.* v. 47, p. 61 – 70, 1985.

HEDDLE, J. G.; BLANCE, S. J.; ZAMBLE, D. B.; HOLLFELDER, F.; MILLER, D. A.; WENTZELL, L. M.; WALSH, C. T.; MAXWELL, A. The antibiotic microcin B17 is a DNA gyrase poison: characterisation of the mode of inhibition. *J. Mol. Biol.*, v. 307, p. 1223 – 1234, 2001.

HIGGINS, N.P.; PEEBLES, C.L.; SUGINO, A.; COZZARELLI, N.R. Purification of subunits of *Escherichia coli* DNA gyrase and reconstitution of enzymatic activity. *Proc. Natl. Acad. Sci. USA.*, v. 75, p. 1773 – 1777, 1978.

HOLDGATE, G.A.; TUNNICLIFFE, A.; WARD, W.H.J.; WESTON, S.A.; ROSEMBROCK, G.; BARTH, P.T.; TAYLOR, I.W.F.; PAUPTIT, R.A.; TIMMS, D. The entropy penalty of ordered water accounts for weaker binding of the antibiotic novobiocin to a resistant mutant of DNA gyarse: A thermodynamic and crystallographic study. *Biochemistry*, v. 36, p. 9663 – 9673, 1997.

HOROWITZ, D.S.; WANG, J.C. Mapping the active site tyrosine of *Escherichia coli* DNA gyrase. *J. Biol. Chem.* v. 262, p. 5339 – 5344, 1987.

KAMPRANIS, S.C.; GORMLEY, N.A.; TRANTER, R.; ORPHANIDES, G.; MAXWELL, A. Probing the binding of coumarins and cyclothialidines to DNA gyrase. *Biochemistry*, v. 38, p. 1967 – 1976, 1999.

KLOTZ, I.M. Protein interactions with small molecules. *Acc. Chem. Res.* v. 7, p. 162 – 168, 1974.

KOGA, H.; ITOH, A.; MURAYAMA, S.; SUZUE, S.; IRIKURA, T. Structure activity relationships of antibacterial 6,7- and 7,8-disubstituted 1-alkyl-1,4-dihydro-4-oxoquinolone-3-carboxylic acids. *J. Med. Chem.,* v. 23, p. 1358 – 1363, 1980.

KREUZER, K.N.; COZZARELLI, N.R. Formation and resolution of DNA catenates by DNA gyarse. *Cell*, v. 20, p. 245 – 254, 1980.

LACOWICZ, J.R. ed. *Principles of fluorescence spectroscopy*, Plenum Press, New York, USA, p. 496, 1987.

LESHER, G.; FORELICH, E.; GRUETT, M.; BAILEY, J.; BRUNDAGE, R. 1,8-naphthyridine derivatives, a new class of chemotherapy agents. *J. Med. Pharm. Chem.* v. 5, p. 1063 – 1065, 1962.

LEWIS, R.J.; SINGH, O.M.P.; SMITH, C.V.; SKARYNSKI, T.; MAXWELL, A.; WONACOTT, A.J. e WIGLEY, D.B. Crystallization of inhibitor complexes of na N-terminal 24 kDa fragment of the DNA gyrase B protein. *J. Mol. Biol.*, v. 241, p. 128 – 130, 1994.

LEWIS, R.J.; SINGH, O.M.P.; SMITH, C.V.; SKARYNSKI, T.; MAXWELL, A.; WONACOTT, A.J.; WIGLEY, D.B. The nature of inhibition of DNA gyrase by the coumarins and the cyclothialidines revealed by X-ray crystallography. *EMBO J.*, v. 15, p. 1412 – 1420, 1996.

LIU, L.F.; LIU, C.-C.; ALBERTS, B.M. Type II DNA topoisomerases? Enzymes that can unknot topolologically knotted DNA molecule via a reversible double-strand break. *Cell*, v. 19, p. 697 – 707, 1980.

LORIS, R.; DAO-THI, M. H.; BAHASSI, E. M.; VAN MELDEREN, L.; POORTMANS, F.; LIDDINGTON, R.; COUTURIER, M.; WYNS, L. Crystal structure of CcdB, a topoisomerase poison from E-coli. *J. Mol. Biol.* v. 285, p. 1667 – 1677, 1999.

MARIANS, K.J. DNA gyrase-catalysed decatenation of multiply linked DNA dimmers. *J. Biol. Chem.* v. 262, p. 10362 – 10368, 1987.

MAXWELL, A. The interaction between coumarin drugs and DNA gyrase. *Mol. Microbiol.*, v. 9, p. 681 – 686, 1993.

MAXWELL, A. DNA gyrase as a drug target. *Trends in Microbiology*. v. 5, p. 102 – 109, 1997.

MAXWELL A. DNA gyrase as a drug target. *Biochem. Soc. Trans*., v. 27, p. 48 – 53, 1999.

MIKI, T.; PAER, J.A.; NAGAO, K., MURAYAMA, N. HORIUCHI, T. Control of segregation of chromosomal DNA by sex factor F in *Escherichia coli*. Mutants of DNA gyrase subunit A suppress *let*D (*ccdB*) product growth inhibition. *J. Mol. Biol.*, v. 255, p. 39 – 52, 1992.

MIZUUCHI, K.; O'DEA, M.H.; GELLERT, M. DNA gyrase-subunit structure and ATPase activity of the purified enzyme. *Proc. Natl. Acad. Sci. U.S.A.*, v. 75, p. 5960 – 5963, 1978.

MORAIS CABRAL, JH.; JACKSON, AP.; SMITH, CV.; SHIKOTRA, N.; MAXWELL, A.; LIDDINGTON, R.C. Crystal structure of the breakage-reunion domain of DNA gyrase. *Nature*, v. 388, p. 903 – 906, 1997.

NOBLE, C.G.; MAXWELL, A. The role of GyrB in the DNA cleavage-religation reaction of DNA gyrase: a proposed two metal-ion mechanism. *J. Mol. Biol.*, v. 318, p. 361 – 371, 2002.

PALUMBO, M.; GATTO, B.; ZAGATTO, Z.; PALÙ, G. On the mechanism of action of quinolone drugs. *Trends Microbiol.*, v. 1, p. 232 – 235, 1993.

REECE, R.J.; MAXWELL, A. Tryptic fragments of the *Escherichia coli* DNA gyrase A protein. *J. Biol. Chem.* v. 264, p. 19648 – 19653, 1989.

REECE, R.J.; MAXWELL, A. DNA Gyrase: Structure and Function. *Crit. Rev. Biochem. Mol. Biol.,* v. 26, p. 335 – 375, 1991a.

REECE, R.J.; MAXWELL, A. Probing the limits of the DNA breakage-reunion domain of the *Escherichia coli* DNA gyrase A protein. *J. Biol.Chem.* v. 266, p. 3540 – 3546, 1991b.

ROCA, J. The mechanisms of DNA Topoisomerases. *Trends Biochem. Sci*., v. 20, p. 156 – 160, 1995.

ROSEMAN, M.A. Hydrophilicity of polar amino acid side-chains is markedly reduced by flanking peptide bonds. *J. Mol. Biol*. v. 200, p. 513 – 522, 1988.

SCHOLAR, E.M.; PRATT, W. *The Antimicrobial Drugs,* 2nd ed., Oxford University Press, New York NY, 2000.

SHEA, M.E.; HIASA, H. Interactions between DNA helicases and frozen topisomerase IV-quinolone-DNA ternary complexes. *J. Biol. Chem.,* v. 274, p. 22747 – 22754, 1999.

SHEN, L.L.; PERNET, A.G. Mechanism of inhibition of DNA gyrase ny analogues of nalidixic acid: the target of the drugs is DNA. *Proc. Natl. Acad. Sci. U.S.A* v. 82, p. 307 – 311, 1985.

SHEN, L.L.; MITSCHER, L.A.; SHARMA, P.N.; O'DONNELL, T.J.; CHU, D.T.W.; COOPER, C.S.; ROSEN, T. AND PERNET, A.G. Mechanism of inhibition of DNA gyrase by quinolone antibacterials: a co-operative drug-DNA binding model. *Biochemistry*, v. 28, p. 3886 – 3894, 1989a.

SHEN, L.L., BARANOWSKI, J. AND PERNET, A.G. Mechanism of inhibition of DNA gyrase by quinolone antibacterials: specificity and cooperativity binding to DNA. *Biochemistry*, v. 28, p. 3879 – 3885, 1989b.

SMITH, C. V.; MAXWELL, A.; Identification of a residue involved in transition-state stabilization in the ATPase reaction of DNA gyrase. *Biochemistry,* v. 37, p. 9658 – 9667, 1998.

SUGINO, A.; HIGGINS, N.P.; BROWN, P.O.; PEEBLES C.L.; COZZARELLI, N.R. Energy coupling in DNA gyrase and mechanism of action of novobiocin. *Proc. Natl. Acad. Sci. U.S.A.,* v. 75, p. 4838 – 4842, 1978.

SUGINO, A.; COZZARELLI, N.R. The intrinsic ATPase of DNA gyrase. *J. Biol. Chem.*, v. 255, p. 6299 – 6306, 1980.

TAMURA, J.K.; BATES, A.D.; GELLERT, M. Slow interaction of 5'-adenylyl-beta,gamma-imidodiphosphate with Escherichia coli DNA gyrase. Evidence for cooperativity in nucleotide binding. *J. Biol. Chem.*, v. 267, p. 9214 – 9222, 1992.

TSAI, F.T.F.; SINGH, O.M.P.; SKARZYNSKY, T.; WONACOTT, A.J.; WESTON, S.; TUCKER, A.; PAUPTIT, R.A.; BREEZE, A.L.; POYSER, J.P.; O'BRIEN, R.; LADBURY, J.E.; WIGLEY, D.B. The high-resolution crystal structure of a 24-kDa gyrase B fragment from *E. coli* complexed with one of the most potent coumarin inhibitors, clorobiocin. *Proteins*, v. 28, 41 – 52, 1997.

VAN MELDEREN, L; THI, M.H.D.; LECCHI, P.; GOTTESMAN, S.; COUTURIER, M.; MAURIZI, M. R. ATP-dependent degradation of CcdA by Lon protease - Effects of secondary structure and heterologous subunit interactions. *J. Biol. Chem.,* v. 271, p. 27730 – 27738, 1996.

VILA, J.; RUIZ, J.; MARCO, F.; BARCELO, A.; GOÑI, P.; GIRALT, E.; JIMENEZ DE ANTA, T. Association between double mutation in *gyrA* gene of ciprofloxacin-resistant clinical isolates of *Escherichia coli* and MICs. *Antimicrob. Agents Chemother.*, v. 38, p. 2477 – 2478, 1994.

VIZÁN, J.; HERNÁNDEZ-CHICO, C.; DEL CASTILLO, I.; MORENO, F. The peptide antibiotic microcin B17 induces double-strand cleavage of DNA mediated by *E. coli* DNA gyrase. *EMBO J.,* v. 10, p. 467 – 476, 1991.

WIGLEY, D.B.; DAVIES, G.J.; DODSON, E.J.; MAXWELL, A.; DODSON, G. Crystal structure of an N-terminal fragment of the DNA gyrase B protein. *Nature*, v. 351, p. 624 – 629, 1991.

WIGLEY, D.B. Structure and mechanism of DNA Gyrase. In: *Nucleic Acids and Molecular Biology*, vol 9 (Eckstein, F. & Lilley, D.M.J., Eds.), pp. 165 - 176 Springer-Verlag, Heidelberg, Berlin, 1995.

WILLMOTT, C.J.R.; MAXWELL, A. A single point mutation in the DNA gyrase A protein greatly reduced binding of fluoroquinolones to the gyrase-DNA complex *Antimicrob. Agents Chemother.*, v. 37, p. 126 – 127, 1993.

WILLMOTT, C.J.; CRITCHLOW, S.E.; EPERON, I.C.; MAXWELL, A., The complex of DNA gyrase and quinolone drugs with DNA forms a barrier to transcription by RNA polymerase. *J. Mol. Biol.,* v. 242, p. 351 – 366, 1994.

PARTE III

ANEXOS

ANEXOS

1. Marchetto, R.; Cilli, E.M.; Jubilut, G.N.; Schreier, S.; Nakaie, C.R. Determination of site-site distance and site concentration within polymer beads: A combined swelling-electron paramagnetic resonance study. *J. Org. Chem.*, v. 70, p. 4561 – 4568, 2005.

2. Nakaie, C.R.; Malavolta, L.; Schereir, S.; Trovatti, E.; Marchetto, R. Direct electron paramagnetic resonance monitoring of the peptide synthesis coupling reaction in polymeric support. *Polymer,* v. 47, p. 4531 – 4536, 2006.

3. Marchetto, R.; Castillo, N.; Nicolas, E.; Navia, M.; Vila, J.; Giralt, E. Interaction between quinolone, DNA and a peptide analog of DNA gyrase. *Peptides 1998*, Sandor Bajusz aand Ferenc Hudecz (Eds.), Akadémiai Kiadó, Budapest, p. 582 – 583, 1999.

4. Marchetto, R.; Nicolas, E.; Castillo, N.; Bacardit, J.; Navia, M.; Vila, J.; Giralt, E. Two short peptides including segments os subunit A of *Escherichia coli* DNA Gyrase as potential probes to evaluate the antibacterial activity of quinolones. *J. Peptide. Sci.*, v. 7, p. 27 – 40, 2001.

5. Scatigno, A.C.; Garrido, S.S.; Marchetto, R. A 4.2 kDa synthetic peptide as a potential probe to evaluate the antibacterial activity of coumarins drugs. *J. Peptide. Sci.* v. 10, p. 566 – 577, 2004.

6. Garrido, S.S.; Scatigno, A.C.; Trovatti, E.; Carvalho, D.C.; Marchetto, R. Probing the binding of the coumarin drugs using peptide fragments of DNA gyrase B protein. *J. Peptide Res.*, v. 65, p. 502 – 511, 2005.

ANEXO 1

VOLUME 70, NUMBER 12 JOC Articles JUNE 10, 2005

Determination of Site−Site Distance and Site Concentration within Polymer Beads: A Combined Swelling-Electron Paramagnetic Resonance Study

Reinaldo Marchetto,[†] Eduardo M. Cilli,[†] Guita N. Jubilut,[‡] Shirley Schreier,[§] and Clovis R. Nakaie*,[‡]

Department of Biochemistry and Technological Chemistry, Institute of Chemistry, UNESP, Araraquara, São Paulo 14800-900, Brazil, Department of Biophysics, Universidade Federal de São Paulo, Rua 3 de Maio 100, CEP 04044-020 São Paulo, Brazil, and Department of Biochemistry, Institute of Chemistry, Universidade de São Paulo, CP 26077, 05513-970 São Paulo, SP, Brazil

clovis.biof@epm.br

Received September 20, 2004

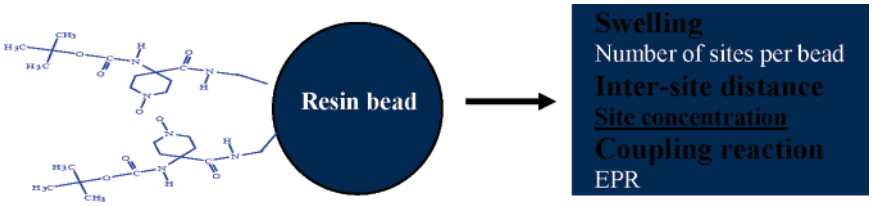

This work proposes a combined swelling-electron paramagnetic resonance (EPR) approach aiming at determining some unusual polymer solvation parameters relevant for chemical processes occurring inside beads.Batches of benzhydrylamine-resin (BHAR), a copolymer of styrene−1% divinylbenzene containing phenylmethylamine groups were, labeled with the paramagnetic amino acid 2,2,6,6-tetramethylpiperidine-1-oxyl-4-amine-4-carboxylic acid (TOAC), and their swelling properties and EPR spectra were examined in DCM and DMF. By taking into account the BHARs labeling degrees, the corresponding swelling values, and some polymer structural characteristics, it was possible to calculate polymer swelling parameters, among them, the volume and the number of sites per bead, site−site distances and site concentration. The latter values ranged from 17 to 170 Å and from 0.4 to 550 mM, respectively. EPR spectroscopy was applied to validate the multistep calculation strategy of these swelling parameters. Spin−spin interaction was detected in the labeled resins at site−site distances less than approximately 60 Å or probe concentrations higher than approximately 1×10^{-2} M, in close agreement with the values obtained for the spin probe free in solution. Complementarily, the yield of coupling reactions in different resins indicated that the greater the inter-site distance or the lower the site concentration, the faster the reaction. The results suggested that the model and the experimental measurements developed for the determination of solvation parameters represent a relevant step forward for the deeper understanding and improvement of polymer-related processes.

Introduction

The innovation of performing chemical processes within an insoluble polymer matrix came into use about four decades ago with the development of the solid-phase peptide synthesis method[1,2] and has been successfully expanded to create efficient synthetic methodologies for other macromolecules.[3] More recently, progressively greater knowledge of solid-phase supported processes has been crucial in successfully launching the unique com-

* To whom correspondence should be addressed. Phone: 55-11-5539 0809. Fax: 55-11-5575 9617.
[†] UNESP.
[‡] Universidade Federal de São Paulo.
[§] Universidade de São Paulo.

(1) Merrifield, R. B. *J. Am. Chem. Soc.* **1963**, *85*, 2149.

10.1021/jo0483318 CCC: $30.25 © 2005 American Chemical Society
Published on Web 01/13/2005

binatorial chemistry approach[4] that has allowed the generation of peptide libraries and has had a remarkable impact on the development of new therapeutic agents.[5]

With the scope of using polymers for an ever-widening array of purposes, a large number of different resins has been formulated.[6] In addition, spectroscopic techniques have been applied with the aim of reaching a deeper understanding of polymer-based processes. Among these, investigations based on nuclear magnetic resonance,[7] infrared,[8] fluorescence,[9,10] Raman,[10] and electron paramagnetic resonance (EPR)[11] have been of great value since they provide relevant information about the solvated polymeric network. Properties such as diffusion, adsorption, and distribution of sites within beads were all examined in these reports. We and other groups have described and exploited the use of the paramagnetic amino acid 2,2,6,6-tetramethylpiperidine-1-oxyl-4-amino-4-carboxylic acid (TOAC) to investigate the conformation and dynamics of labeled peptides.[12,13] The use of TOAC has been extended to structural investigations of solvated resins and peptide resins.[14]

The interaction between the solvent system and any type of solute is of utmost relevance when examining chemical or physicochemical processes.[15] In the case of polymers or peptide-polymers, the solvent system affects polymer swelling, the average distance between chains (and, as a result, the degree of chain association), controls the rate of motion of components, and regulates reaction kinetics. For this reason, polymer solvation has been investigated with a variety of experimental procedures, among them the microscope measurement of beads.[16]

This latter experimental approach has been of value in the examination of the solvation characteristics of a great number of polymeric materials, adopted as solute models in a large amount of solvents. This approach proved very fruitful since it allowed us to obtain consistent results regarding polymer solvation and to propose a novel amphoteric solvent parameter (AN + DN),[17] which is the sum of Gutmann's solvent electron acceptor (AN) and electron donor (DN) numbers[18] at a ratio of 1:1. The use of the AN and DN concepts was recently extended to predict the potential of a given solvent to dissociate peptide chains not only when bound to a polymer matrix but also when free in solution.[19]

When making use of polymeric matrixes to perform chemical processes it is desirable to understand as much as possible, at a molecular level, the properties of the environment created by these matrixes. In this context, many studies have assessed properties such as dynamics of the polymer backbone, site−site aggregation, and swelling capacity in each solvent system.[7−11,14] To continue these polymer-focused studies, the strategy described in the present work relied primarily on a novel approach to calculate some structural characteristics of

(2) (a) Barany, G.; Merrifield, R. B. *The Peptides*; Academic Press Inc.: New York, 1979; Vol. 2, pp 1−284. (b) Stewart, J. M.; Young, J. D. *Solid-Phase Peptide Synthesis*; Pierce Chemical Co.: Rockford, IL, 1984. (c) Fields, G. B.; Noble, R. L. *Int. J. Peptide Protein Res.* **1990**, *35*, 161. (d) Kates, S. A., Albericio, F. *Solid-Phase Synthesis. A Practical Guide*; Marcel Dekker: New York, Basel, 2000; pp 275−330. (e) Kent, S. B. H. *Annu. Rev. Biochem*. **1988**, *57*, 957.

(3) (a) Fréchet, J. M.; Schuerch, C. *J. Am. Chem. Soc.* **1971**, *93*, 492. (b) Zehavi, U.; Patchornik, A. *J. Am. Chem. Soc*. **1973**, *95*, 5673. (c) Letsinger, R. L.; Finnan, J. L.; Heavner, G. A.; Lunsford, W. B. *J. Am. Chem. Soc*. **1975**, *85*, 3278. (d) Amarnath, V., Broom, A. D. *Chem. Rev.* **1977**, *77*, 183.

(4) (a) Hermkens, P. H. H.; Ottenheim, H. C. J.; Rees, D. *Tetrahedron* **1996**, *52*, 4527 (b) Thompson, L. A.; Ellman, J. A. *Chem. Rev*. **1996**, *95*, 555, (c) Hermkens, P. H. H.; Ottenheim, H. C. J.; Rees, D. *Tetrahedron* **1996**, *52*, 4527.

(5) (a) Lam, K. S.; Salmon, S. E.; Hersh, E. M.; Hruby, V. J.; Kazmierski, W. M.; Knapp, R. J. *Nature* **1991**, *354*, 82. (b) Jung, G.; Beck-Sickinger, A. G. *Angew. Chem., Int. Ed. Engl*. **1992**, *31*, 367. (c) Lam, K. S., Salmon, S. E., Hersh, E. M., Hruby, V. J., Kasmierski, W. M., Knapp, R. J. *Nature* **1991**, *354*, 82.

(6) (a) Lebl, M. *Biopolymers* **1998**, *47*, 397. (b) Kates, S. A.; McGuiness, B. F.; Blackburn, C.; Griffin, G. W.; Solé, N. A.; Barany, G.; Albericio, F. *Biopolymers* **1998**, *47*, 365. (c) Meldal, M. In *Methods in Enzymology*: *Solid-Phase Peptide Synthesis*; Fields, G., Ed.; Academic Press: New York 1997; pp 83−103.

(7) (a) Ludwick, A. G.; Jelinski, L. W.; Live, D.; Kintamar, A.; Dumais, J. J. *J. Am. Chem. Soc.* **1986**, *108*, 6493. (b) Deber, C. M.; Lutek, M. K.; Heimer, E. P.; Felix, A. M. *Peptide Res.* **1989**, *2*, 184. (c) Warrass, R.; Wieruszeski, M.; Bouitillon, C.; Lippens, G. *J. Am. Chem. Soc* **2000**, *122*, 1789. (d) Furrer, J.; Piotto, M.; Bourdonneau, M.; Limal, D.; Guichard, G.; Elbayed, K.; Briand, J. P.; Bianco, A. *J. Am. Chem. Soc*. **2001**, *123*, 4130. (e) Gambs, C.; Dickerson T. J.; Mahajan, S.; Pasternack L. B.; Janda, K. D. *J. Org. Chem*. **2003**, *68*, 3673. (f) Zhao, T. J.; Beckham, H. W. (g) Zhao, T. J.; Beckham, H. W.; Gibson, H. W. *Macromolecules* **2003** *13*, 4833.

(8) (a) Milton, R. C. L.; Milton, S. C. F.; Adams, P. A. *J. Am. Chem. Soc*. **1990**, *112*, 5039. (b) Hendrix, J. C., Halverson, K. J., Jarret, J. T.; Lansbury, P. T., Jr. *J. Org. Chem.* **1990**, *55*, 4517. (c) Yan, B. *Acc. Chem. Res*. **1998**, *31*, 621.

(9) (a) Li, Y. H.; Chan, L. M.; Tyler, L.; Moody, R. T.; Himel, C. M.; Hercules, D. M. *J. Am. Chem. Soc.* **1975**, *97*, 3118. (b) Shea, K. J.; Sassaki, D. Y.; Stoddarard, G. J. *Macromolecules* **1989**, *22*, 1722. (c) Vaino, A. R.; Janda, K. D. *J. Comb. Chem.* **2000**, *2*, 579.

(10) (a) Kress, J.; Rose, A.; Frey, J. G.; Brocklesby, W. S.; Ladlow, M.; Mellor, G. W.; Bradley, M. *Chem. Eur. J.* **2001**, *7*, 3880. (b) Rademann, J.; Barth, M.; Brock, R.; Egelhaaf, H. J.; Jung, G. *Chem. Eur. J*. **2001**, *7*, 3884. (c) Kress, J., Zanaletti, R.; Rose, A.; Frey, J. G.; Brockesby, W. S.; Ladlow, M.; Bradley, M. *J. Comb. Chem*. **2003**, *5*, 28.

(11) (a) Regen, S. L. *J. Am. Chem. Soc.* **1974**, *96*, 5275. (b) Ward, T. C.; Brooks, J. T. *Macromolecules* **1974**, *7*, 207. (c) Vaino, A. R.; Goodin, D. B.; Janda, K. D. *J. Comb. Chem.* **2000**, *2*, 330.

(12) (a) Nakaie, C. R.; Schreier, S.; Paiva, A. C. M. *Braz. J. Med. Biol. Res.* **1981**, *14*, 173. (b) Marchetto, R.; Schreier, S.; Nakaie, C. R. *J. Am. Chem. Soc.* **1993**, *117*, 11042. (c) Barbosa, S. R.; Cilli, E. M.; Lamy-Freund, M. T.; Castrucci, A. M. L., Nakaie, C. R. *FEBS Lett.* **1999**, *446*, 45. (d) Pertinhez, T. A.; Nakaie, C. R.; Carvalho, R. S. H.; Paiva, A. C. M.; Tabak, M.; Toma, E.; Schreier, S. *Biopolymers* **1977**, *42*, 821. (e) Nakaie, C. R.; Silva, E. G.; Cilli, E. M.; Marchetto, R.; Schreier, S.; Paiva, T. B.; Paiva, A. C. M. *Peptides* **2002**, *23*, 65. (f) Schreier, S.; Barbosa, S. R.; Casallanovo, F., Vieira, R. F. F., Cilli, E. M.; Paiva, A. C. M.; Nakaie, C. R. *Biopolymers* **2004**, *74*, 389.

(13) (a) Smithe, M. L.; Nakaie, C. R.; Marshall, G. R. *J. Am. Chem. Soc.* **1995**, *117*, 10555. (b) Toniolo, C.; Valente, E.; Formaggio, F.; Crisma, M.; Pilloni, G.; Corvaja, C.; Toffoletti, A.; Martinez, G. V.; Hanson, M. P.; Millhauser, G. L.; George, C.; Flippen-Anderson, J. *J. Pept. Sci.* **1995**, *1*, 45. (c) McNulty, J. C.; Silapie, J. L.; Carnevali, M.; Farrar, C. T.; Griffin, R. G.; Formaggio, F.; Crisma, M.; Toniolo, C.; Millhauser, G. L. *Biopolymers* **2000**, *55*, 479. (d) Victor, K. G., Cafiso, D. S. *Biophys. J*. **2001**, *81*, 2241. (e) Pispisa, B., Palleschi, L., Stella, M., Venanzi, M., Toniolo, C. *J. Phys. Chem. B* **1998**, *102*, 7890.

(14) (a) Cilli, E. M.; Marchetto, R.; Schreier, S.; Nakaie, C. R. *Tetrahedron Lett.* **1997**, *38*, 517. (b) Cilli, E. M.; Marchetto, R.; Schreier, S.; Nakaie, C. R. *J. Org. Chem.* **1999**, *64*, 9118. (c) Ribeiro, S. C. F., Schreier, S., Nakaie, C. R., Cilli, E. M. *Tetrahedron Lett.* **2001**, *42*, 3243. (d) Oliveira, E.; Cilli, E. M.; Miranda, A.; Jubilut, G. N.; Albericio, F.; Andreu, A.; Paiva, A. C. M.; Schreier, S.; Tominaga, M.; Nakaie, C. R. *Eur. J. Org. Chem*. **2002**, *21*, 3686.

(15) (a) Katritzky, A. R., Fara, D. C., Hongfang, Y., Tämm, K. *Chem. Rev*. **2004**, *104*, 175, (b) Markus, Y. *Chem. Soc. Rev*. **1993**, *22*, 409. (c) Reichardt, C. *Chem. Rev*. **1994**, *94*, 2319. (c) Pytela, O. *Collect. Czech. Chem. Commun*. **1988**, *53*, 1333. (d) Burton, A. F. M. *Chem. Rev*. **1975**, *75*, 731.

(16) (a) Sarin, V. K.; Kent, S. B. H.; Merrifield, R. B. *J. Am. Chem. Soc.* **1980**, *102*, 5463. (b) Fields, G. B.; Fields, C. G. *J. Am. Chem. Soc.* **1991**, *113*, 3, 4202. (c) Tam, J. P.; Lu, Y. A. *J. Am. Chem. Soc*. **1995**, *117*, 12058. (d) Pugh, K. C.; York, E. J.; Stewart, J. M. *Int. J. Peptide Protein Res*. **1992**, *40*, 208.

(17) (a) Cilli, E. M.; Oliveira, E.; Marchetto, R.; Nakaie, C. R. *J. Org. Chem.* **1996**, *61*, 8992. (b) Malavolta, L.; Oliveira, E.; Cilli, E. M.; Nakaie C. R. *Tetrahedron* **2002**, *58*, 4383.

(18) (a) Gutmann, V. *Electrochim. Acta* **1976**, *21*, 661. (b) Gutmann, V. *The Donor−Acceptor Approach to Molecular Interactions*; Plenum Press: New York, 1978.

(19) Malavolta, L.; Nakaie, C. R. *Tetrahedron* **2004**, *60*, 9417.

TABLE 1. Swelling Parameters of Differently Labeled Boc-TOAC-BHAR in DCM

	sample									
	col 1	col 2	col 3	col 4	col 5	col 6	col 7	col 8	col 9	col 10
BHAR[a] (mmol/g)	diam dry bead (μm)	diam swollen bead (μm)	vol solvent/ bead (10^5 μm^3)	vol dry sample/g copol[b] (mL)	wt dry sample/g copol (g)	vol dry sample/g sample (mL)	no. of beads/g sample (10^7)	no. of sites/bead (10^{12})	site−site distance (Å)	site concn (mM)
0.003[c]	57	98	4.0	1.8	1.17	1.54	1.59	0.1	169.8	0.4
0.019[c]	57	98	4.0	1.8	1.18	1.53	1.58	0.7	88.9	2.9
0.035[c]	57	98	4.0	1.8	1.18	1.53	1.58	1.3	72.2	5.4
0.050[c]	57	98	4.0	1.8	1.18	1.53	1.58	1.9	63.7	7.9
0.065[d]	57	98	4.0	1.8	1.19	1.51	1.56	2.5	58.1	10.4
0.134[d]	57	98	4.0	1.8	1.22	1.48	1.53	5.2	45.5	21.7
0.646[e]	57	98	4.0	1.8	1.45	1.24	1.28	30.3	25.3	126.3
0.988[f]	58	99	4.1	1.9	1.66	1.14	1.12	52.9	21.2	215.0

[a] Degree of Boc-TOAC-OH labeling. [b] Copolymer of styrene−1% divinylbenzene: d = 0.99 g/mL; average diameter of dry beads = 47 μm. [c] Obtained from 0.050 mmol/g of BHAR. [d] Obtained from 0.14 mmol/g of BHAR. [e] Obtained from 0.80 mmol/g of BHAR. [f] Obtained from 1.40 mmol/g of BHAR.

polymers in solvated conditions. Making use of TOAC labeling, EPR spectroscopy was applied to check the validity of the calculation protocol. The calculation strategy involved the initial microscopic measurement of dry and swollen beads of several spin-labeled batches of the benzhydrylamine resin (BHAR) used to synthesize α-carboxamide peptides.[20] Subsequently, data such as solvent volume inside the bead, number of sites per bead, site−site distance, and site concentration within beads were estimated through a sequential calculation strategy.

EPR spectra of BHAR batches, labeled with *tert*-butyloxycarbonyl-TOAC derivative (Boc-TOAC-OH),[12a] were obtained in order to check the proposed calculation approach. The occurrence of spin−spin interaction was used as a criterion to assess site−site distances and site concentrations inside the beads. The strategy was to verify if this spectral effect is observed at similar probe−probe distances or probe concentrations within the resin beads and when the probe was free in solution.

In addition, experiments were performed to evaluate the relationship between the calculated polymer swelling data, such as site−site distance, site concentration, and the rate of amino acid coupling reactions in model resins or peptide-resins. The results demonstrate that the practical-conceptual approach presented in this work for quantifying resin swelling properties can be applied to other polymeric materials.

Results

Swelling Studies. BHAR batches, with phenylmethylamine group loading ranging from 0.05 to 1.4 mmol/g at the polystyrene−1% divinylbenzene backbone, were synthesized according to a previously described protocol.[20] Boc-TOAC-OH was coupled to BHAR batches under controlled conditions in order to produce resins spin-labeled to different extents.

Approximately 0.5 g of BHAR with substitution degrees of 0.05, 0.14, 0.80, and 1.40 mmol/g were used to couple the Boc-TOAC-OH residue using the conventional Boc-peptide synthesis strategy.[2a,b] If necessary, a 3-fold molar excess was applied to guarantee quantitative spin label incorporation using the diisopropylcarbodiimide/*N*-hydroxybenzotriazole (DIC/HOBt) coupling protocol in DCM. In all BHAR batches, the coupling was complete in about 2 h. When partial incorporation was desired, the coupling step was deliberately carried out with less than equimolar amounts of Boc-TOAC-OH. The exact degree of incorporation was determined by quantitative picric acid method.[21] Using this experimental protocol, eight batches of Boc-TOAC-BHAR with paramagnetic labeling degrees ranging from 0.003 to 0.988 mmol/g were synthesized.

Calculation Strategy To Determine Polymer Bead Swelling Parameters. By starting from simple swelling parameters such as diameters of dry and swollen beads as reference points, a sequence of calculations was designed to determine the resin parameters given in Tables 1 and 2. The tables summarize the data calculated for eight batches of Boc-TOAC-BHAR in DCM and in DMF, respectively.

To illustrate how the various resin parameters were sequentially calculated, the detailed procedure will be described below for the 0.134 mmol/g of Boc-TOAC-BHAR batch in DCM (Table 1, row 6).

Example: 0.134 mmol/g of Labeled Boc-TOAC-BHAR Swollen in DCM (Table 1). Columns 1 and 2 list the average diameters of the dry (57 μm) and DCM swollen (98 μm) beads, respectively, measured under the light microscope. The volumes of the dry (0.97×10^5 μm^3) and swollen (4.93×10^5 μm^3) beads were calculated, and the volume of solvent/bead (4×10^5 μm^3, column 3) was obtained by subtracting the dry bead volume from the swollen bead volume.

Column 4: Volume of Dry Sample/Gram of Copolymer (1.8 mL/g of Copolymer). The ratio (diameter dry sample/diameter dry copolymer)^3 represents the relationship between the volume of the dry macroscopic working sample (0.134 mmol/g of Boc-TOAC-BHAR) and that of the dry copolymer used to synthesize the sample. In the example, since the average diameters of beads of dry sample and dry copolymer are 57 and 47 μm, respectively, the ratio between the dry volumes of both resins is $(57/47)^3 = 1.78$. Considering that the number of beads in 1 g of copolymer is the same as in the sample synthesized from this amount of copolymer and taking

(20) (a) Pietta, P. G.; Cavallo, P. F.; Takahashi, K.; Marshall, G. R. *J. Org. Chem*. **1974**, *39*, 44. (b) Marchetto, R.; Etchegaray, A.; Nakaie, C. R. *J. Braz. Chem. Soc.* **1992**, *3*, 30.

(21) Gisin, B. F. *Anal. Chim. Acta* **1972**, *58*, 248.

TABLE 2. Swelling Parameters of Differently Labeled Boc-TOAC-BHAR in DMF

	sample									
	col 1	col 2	col 3	col 4	col 5	col 6	col 7	col 8	col 9	col 10
BHAR[a] (mmol/g)	diam dry bead (μm)	diam swollen bead (μm)	vol solvent/ bead (10^5 μm^3)	vol dry sample/g copol[b] (mL)	wt dry sample/g copol (g)	vol dry sample/g sample (mL)	no. of beads/g sample (10^7)	no. of sites/bead (10^{12})	site−site distance (Å)	site concn (mM)
0.003[c]	57	81	1.8	1.8	1.17	1.54	1.59	0.1	140.9	0.9
0.019[c]	57	81	1.8	1.8	1.18	1.53	1.58	0.7	73.7	6.5
0.035[c]	57	81	1.8	1.8	1.18	1.53	1.58	1.3	60.0	12.0
0.050[c]	57	81	1.8	1.8	1.18	1.53	1.58	1.9	52.8	17.6
0.065[d]	57	79	1.6	1.8	1.19	1.51	1.56	2.5	47.0	26.0
0.134[d]	57	79	1.6	1.8	1.22	1.48	1.53	5.2	36.8	54.2
0.646[e]	57	80	1.7	1.8	1.45	1.24	1.28	30.3	20.5	297.1
0.988[f]	58	79	1.6	1.9	1.66	1.14	1.12	52.9	17.0	551.0

[a] Degree of Boc-TOAC-OH labeling. [b] Copolymer of styrene−1% divinylbenzene: d = 0.99 g/mL; average diameter of dry beads = 47 μm. [c] Obtained from 0.050 mmol/g of BHAR. [d] Obtained from 0.14 mmol/g of BHAR. [e] Obtained from 0.80 mmol/g of BHAR. [f] Obtained from 1.40 mmol/g of BHAR.

into account that the volume of 1 g of copolymer is 1.01 mL (d = 0.99 g/mL),[16a] the total volume of dry sample containing 1 g of copolymer is therefore 1.78 × 1.01 mL, or 1.80 mL.

Column 5: Weight of Dry Sample/Gram of Copolymer (1.22 g/g of Copolymer). The 0.134 mmol Boc-TOAC-BHAR sample was synthesized by quantitative incorporation of the Boc-TOAC-OH in the 0.140 mmol/g of BHAR batch. This resin originated from partial phenylmethylamino incorporation into a heavily substituted 1.4 mmol/g benzoyl group-containing copolymer. This copolymer derivative is synthesized in the first step (Friedel−Crafts acylation) necessary to obtain BHAR.[20] Thus, the Boc-TOAC-BHAR sample under consideration still contains (1.4−0.14) mmol = 1.26 mmol/g of remaining benzoyl groups attached to its backbone. Considering the total weight of groups added in all the synthetic steps, one can calculate that the sum of Boc-TOAC-OH and benzoyl groups attached to the initial copolymer corresponds to 0.182 g. Therefore, in 1 g of sample, the mass of copolymer is 1 − 0.182 g = 0.818 g. Thus, for 1 g of starting copolymer, the weight of the 0.134 mmol Boc-TOAC−BHAR is 1.22 g.

Column 6: Volume of Dry Sample/Gram of Sample (1.48 mL/g). This parameter is calculated by dividing the value of (volume of dry sample/gram of copolymer), column 4, by (weight of dry sample/gram of copolymer), column 5. The value obtained (1.48 mL/g) represents the ratio between the volume of the dry sample (1.8 mL) and its total weight (1.22 g) and corresponds to the volume occupied by 1 g of sample in the dry form.

Column 7: Number of Beads/Gram of Sample (1.53×10^7 Beads/g of Sample). This value is calculated by dividing the volume of 1 g of dry sample (1.48 mL, column 6) by the average volume of one dry bead, which is calculated from its diameter (57 μm, column 1). Thus, the volume of one dry bead is 9.7×10^{-8} mL. The ratio 1.48 mL/9.7×10^{-8} mL yields 1.53×10^7 beads in 1 g of sample.

Column 8: Number of Sites/Bead (5.2×10^{12}). The number of sites per bead is calculated by dividing the number of sites/gram of sample by the number of beads/gram of sample (column 7). The former value corresponds to $0.134 \times 6.02 \times 10^{20}$ sites/g. Dividing this number by the number of beads in 1 g of sample (1.53×10^7, column 7) gives 5.2×10^{12} sites/bead.

Column 9: Site−Site Distance (45.5 Å). To evaluate this important parameter, we first calculate the average volume per site. This is done by dividing the volume of one swollen bead (4.9×10^{-5} μm^3, calculated from the measured diameter of one swollen bead, 98 μm, column 2) by the number of sites/bead (5.2×10^{12}, column 8). Thus, the average volume per site is 9.4×10^4 Å^3. By assuming a uniformly distributed cubic lattice for the sites within the bead, the site−site distance corresponds to the side of a cube and is given by the cubic root of the volume occupied by one site, i.e., $(9.4 \times 10^4$ Å$^3)^{1/3}$ = 45.5 Å.

Column 10: Site Concentration Inside the Bead (21.7 mM). Finally, making use of the parameters calculated in the previous steps, it is possible to determine the site concentration within the bead. Thus, for the 0.134 mmol/g of substituted Boc-TOAC-BHAR, the site concentration is obtained by dividing the number of sites/bead (5.2×10^{12}, column 8) by the volume of solvent/bead (4×10^5 μm^3, column 3), that is, 1.3×10^7 sites/μm^3, or 1.3×10^{19} sites/mL. Considering that 6.02×10^{20} sites/mL correspond to 1 M concentration, we find that that the site concentration corresponds to an effective Boc-TOAC−OH concentration of 21.7 mM.

By examining the parameters calculated in Tables 1 and 2, it can be seen that the average inter-site distance ranged from a maximum of about 170 Å (for 0.003 mmol/g of Boc-TOAC-BHAR in DCM, Table 1) to a minimum of 17 Å (for 0.988 mmol/g of Boc-TOAC-BHAR in DMF, Table 2). Furthermore, the site concentration within the beads varied from a minimum of approximately 0.4 mM to a maximum of approximately 550 mM. Under very highly loaded conditions (0.988 mmol/g of Boc-TOAC-BHAR in DMF), the concentrations were as high as those typically used during the solution peptide synthesis method.[22]

Some of the parameters calculated in Tables 1 and 2, such as the number of beads per gram of the resin or the number of sites per bead, are relevant for application in polymer studies. Interestingly, values of this latter parameter ranged from approximately 0.3×10^{12} to 50×10^{12} (0.003 mmol/g and 0.988 mmol/g of Boc-TOAC-labeled resins, respectively). A linear correlation between

(22) Gross, E., Meienhofer, J., Eds. *Peptides: Analysis, Synthesis, Biology*; Academic Press: New York, 1989; Vol. 1.

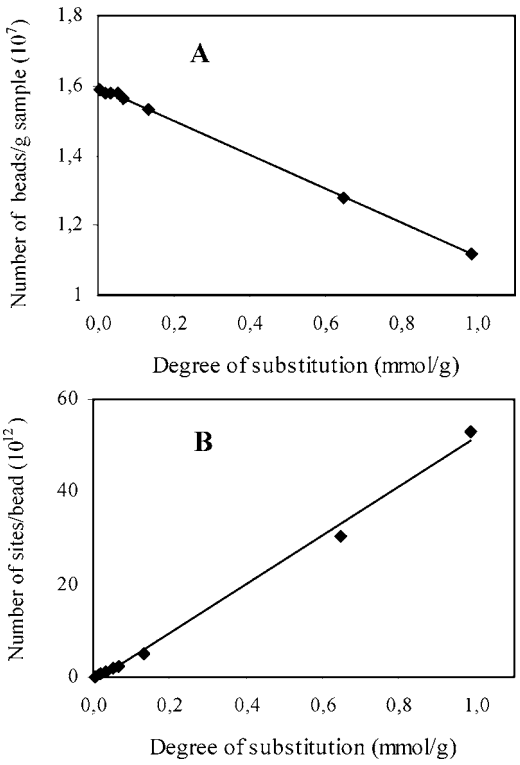

FIGURE 1. Correlation between number of beads per gram of sample (A) and number of sites per bead (B) and the degree of substitution of Boc-TOAC-BHARs.

these two parameters (columns 7 and 8) and the degree of resin labeling is observed in Figure 1. As expected, while the number of beads per gram of resin decreased, the number of sites per bead increased with the increasing degree of substitution.

It should be pointed out that this calculation strategy can be extended to resins containing other chemical groups, including peptides. Besides the dry and swollen bead diameters, it is only necessary to know the density of the starting resin (and therefore the volume occupied by 1 g of resin) and to calculate the overall weight variation due to the incorporation of the desired groups in the composite derivative.

EPR Studies. Figure 2 shows the EPR spectra of eight labeled resins in DCM and DMF (panels A and B, respectively). Spectral line broadening due to spin−spin interaction was observed in both solvents and increased with increasing Boc-TOAC-OH substitution.

The dependence of probe−probe interaction on resin calculated parameters, such as site−site distance and site concentration, was compared with data obtained for Boc-TOAC-OH in solution. Figure 3 shows the EPR spectra of the spin probe in DMF as a function of concentration. Spectral line broadening due to spin−spin interaction can be clearly observed as the probe concentration increases.

Table 3 correlates the Boc-TOAC-OH concentration with the line width of the mid-field line (ΔH) measured for the spectra in Figure 3 and with the average distance between probe molecules free in solution. Similarly to the analysis for the labeled resins (column 9 in Tables 1 and 2), a static model of probe distribution in solution was assumed, namely, the probes are uniformly distributed within a cubic lattice. The average distance between adjacent Boc-TOAC-OH molecules in solution was estimated by calculating the amount of probe molecules at each concentration combined with the average volume occupied by each molecule. Assuming a cubic lattice distribution of probe molecules, the average intermolecular distance between adjacent molecules corresponds to the side of a cube and is given by the cubic root of the volume occupied by the probe. As an example, for 10^{-3} M Boc-TOAC-OH, the average volume occupied by each molecule is 1.7×10^6 Å^3 and the average distance between adjacent molecules is 118.6 Å (Table 3).

Figure 4 displays the dependence of the mid-field spectral line width of both labeled resins and of the spin label in DMF solution on site−site distance (panel A) and site concentration (panel B). Line broadening did not occur for site−site distances larger than approximately 60 Å (probe concentration of ca. 1×10^{-2} M). Similar results were obtained for the probe free in solution and spread throughout resin backbone, strongly suggesting that the sequential calculation designed for quantitative determination of the swelling parameters in Tables 1 and 2 is a valid approach.

Correlation between Resin-Swelling Parameters and the Rate of Coupling Reactions. To emphasize the usefulness of the strategy developed to determine resin swelling parameters, the relationship between site−site distance and site concentration and the rate of coupling reactions throughout a polymer network was examined. Table 4 shows the coupling yield of Boc-Pro-OH in DCM to the 1.4 mmol/g of BHAR batch. One can observe that the greater the site−site distance and lower the site concentration, the faster the coupling reaction. The rate of coupling follows the order: DCM > DMF > DMSO. Complementary swelling data of the 1.4 mmol/g of BHAR batch are given in the Supporting Information.

PSA Method in Equimolar Conditions (1 mM Reactants). Table 5 displays another example of the application of this approach, this time extended to peptidyl-resins. Four batches of the aggregating Ile-Asn-Gly sequence[23] bound to BHAR in varying amounts (up to 1.59 mmol/g) were compared under equivalent conditions with respect to the frequency of Boc-(2BrZ)-Tyr-OH coupling. Other swelling parameters of these four peptide resins are also available in the Supporting Information Section. Closely paralleling the results outlined in the previous paragraph, faster coupling reactions occurred systematically with resins that presented larger site−site distance and lower site concentration.

Discussion

The main objective of the present work was to design a novel swelling-EPR approach aimed at multiple goals. First, we intended to develop a sequential calculation that would allow the estimation of polymer swelling parameters for further practical application. Second, we applied EPR spectroscopy to paramagnetically labeled resins in order to determine at what site−site distance or site concentration values significant spin−spin interactions begin to occur. Finally, we verified the correlation between the calculated properties of solvated polymer

(23) Hancock, W. S.; Prescott, D. J.; Vagelos, P. R.; Marshall, G. R. *J. Org. Chem.* **1973**, *38*, 774.

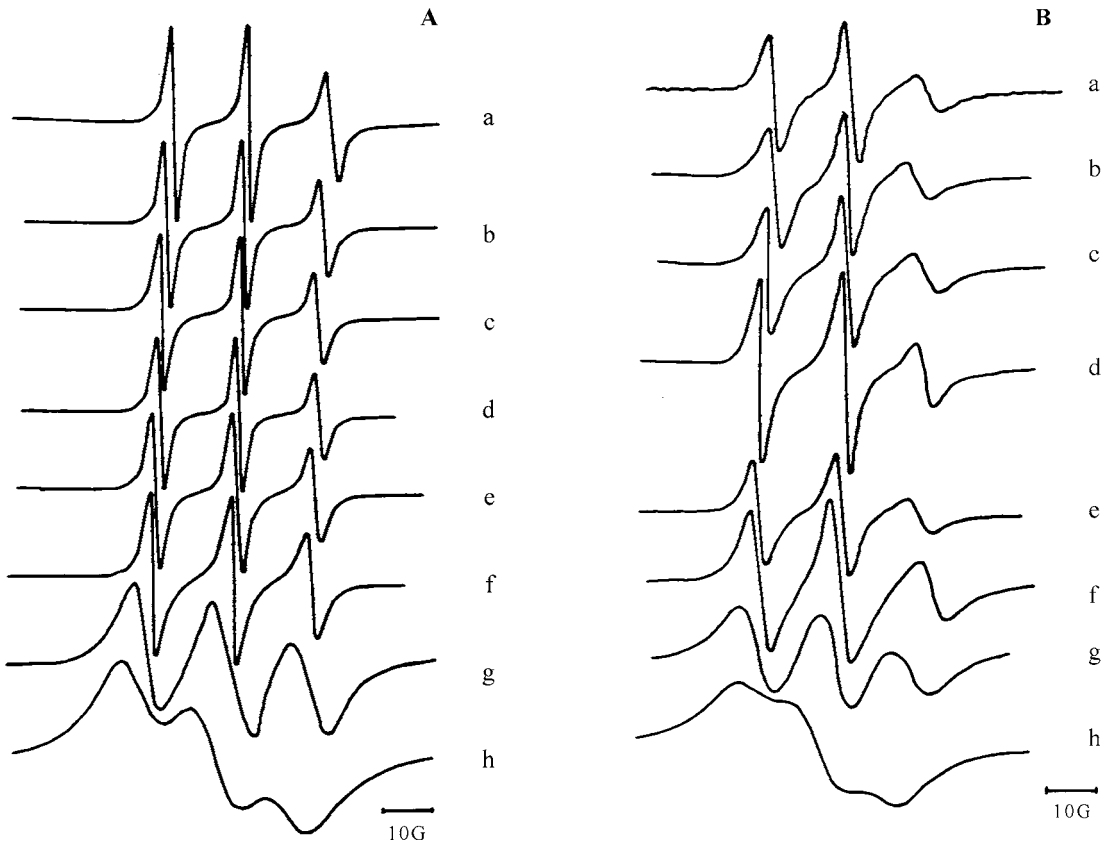

FIGURE 2. Effect of Boc-TOAC-OH loading on the EPR spectra of Boc-TOAC-BHAR in DCM (**A**) and DMF (**B**). Probe loading (mmol/g): a = 0.003; b = 0.019; c = 0.035; d = 0.050; e = 0.065; f = 0.134; g = 0.646; h = 0.988.

and the efficiency of chemical processes taking place in the polymer matrix.

The initial step in this study comprised synthesis and microscopic measurement of the swelling properties of several BHAR batches labeled with the Boc-TOAC-OH spin probe for further EPR studies. By combining swelling and structural data of these resins, a sequential calculation strategy was designed to estimate resin swelling parameters that can be useful in the polymer field (Tables 1 and 2). Among these parameters, the number of sites per bead, average volume occupied by each site, site−site distance, site concentration within beads, should be mentioned.

The combination of EPR spectroscopy with the swelling data of TOAC-labeled resins aimed at testing the validity of the calculation strategy for gauging bead-swelling information. By comparing EPR data for the probe in DMF solution with those for the paramagnetic probe attached to the polymer core at variable degrees in the same solvent, it was possible to estimate the maximum site−site distance (∼60 Å) or minimum site concentration ($\sim 1 \times 10^{-2}$ M) for the onset of spin−spin interaction. Similar values were found for the paramagnetic probe attached to the polymer core when the solvent was DCM.

The good agreement between the results obtained with this approach and those obtained making use of the sequential protocol for calculation of swelling parameters (Figure 4) strongly suggest that the proposed protocol is correct. Several geometrical models could be adopted to estimate the average site distribution−spherical, cylindrical, etc. We chose to use a cubic distribution of sites or probes in solution or bound to the resin, based on the classical report by Barany and Merrifield designed to estimate site−site distance within beads.[2a] In this context, it should be recalled that more than 99% of sites are located inside the bead structure and not at its surface.[24]

In previous EPR-solvation studies, we[14] and other groups[11] have monitored the dynamics of resins and peptide-resins with the aim of improving the peptide synthesis methodology. In these studies the mobility of the labeled sites was analyzed by calculating rotational correlation times from measurement of line widths and line heights in the absence of spin−spin interactions, that is, at low label concentrations. Here we took advantage of the occurrence of spin−spin interactions to assess site−site distances and site concentrations inside the polymeric matrixes.

The spectral line broadening obtained with increased labeling of the resins and increased probe concentration in solution provided a clear evidence of the occurrence of increasing spin−spin interaction. The interaction could be due to exchange and/or dipolar mechanisms. The dipolar interaction has been found to be the predominant broadening mechanism in the case of doubly labeled enzymes.[25] In these cases the two paramagnetic centers are located at a fixed distance from each other. Moreover,

(24) Merrifield, B. R.; Littau, V. In *Peptides 1968*; Bricas, E., ed.; North-Holland Publishing Co.: Amsterdam, 1968; p 179.

(25) (a) Taylor, J. S.; Leigh, J. S., Jr.; Cohn, M. *Proc. Natl. Acad. Sci. U.S.A.* **1969**, *64*, 219. (b) Mchaourab, H. S.; Oh, K. J.; Fang, C. J.; Hubbell, W. L. *Biochemistry* **1997**, *36*, 307.

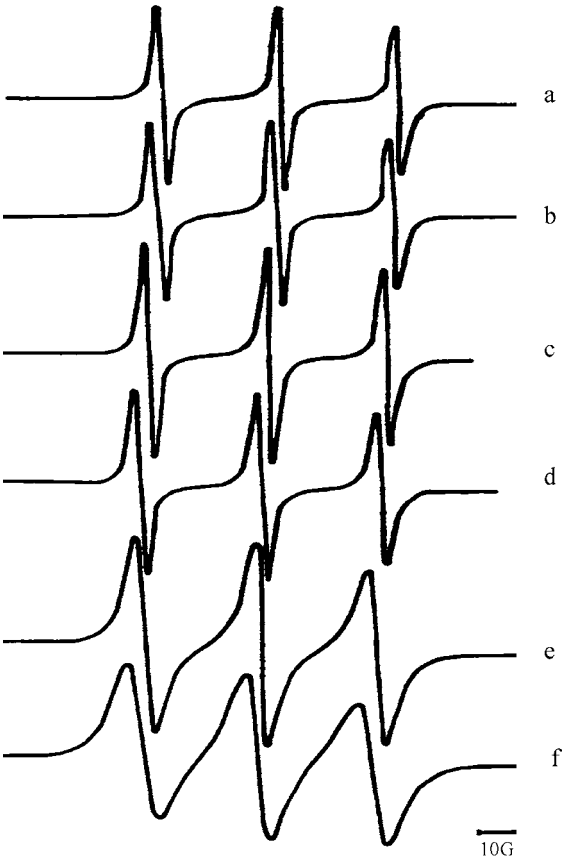

FIGURE 3. EPR spectra of Boc-TOAC-OH in DMF. Concentration (M): a = 0.0001; b = 0.001; c = 0.005; d = 0.01; e = 0.05; f = 0.1.

TABLE 3. Correlation between Concentration of Boc-TOAC-OH in DMF and the EPR Spectra's Central Peak Linewidth and the Site−Site Distance Values

concn (M)	ΔH (G)	site−site distance (Å)
1×10^{-4}	1.40	255.4
1×10^{-3}	1.40	118.6
5×10^{-3}	1.45	69.3
1×10^{-2}	1.70	55.0
5×10^{-2}	2.40	32.2
1×10^{-1}	3.65	25.5

the dipolar interaction has been shown to be detectable up to about 25 Å.[25b] Although the resin beads are formed by a polymeric matrix, the characteristics of these polymers are quite different from those of a protein. In the polystyrene-divinylbenzene branched copolymer, the $-NH_2$ reactive groups are distributed at random, that is, the distances between pairs of attached nitroxides vary. Moreover, these polymers, immersed in solvent, are flexible (as indicated by the spectra at low resin loading, spectra a in Figure 3, panels A and B) and undergo intramolecular motions that lead to variation in the distances separating individual nitroxide groups. In addition, Boc-TOAC-OH bound to one polymer chain can encounter Boc-TOAC moieties bound to other polymer chains in the same bead.

Taking these facts into account, it is seen that the polymeric matrix is a highly dynamic structure and that the distances between Boc-TOAC-OH groups vary in space and time. Thus, the values obtained in the calculations are average values. In this context, it seems plausible to draw an analogy with the situation found in membranes, where their constituent lipid molecules undergo lateral diffusion. Studies at high label concentrations have shown that in model[26] and biological[27] membranes the main contribution to spin−spin interaction is provided by the exchange mechanism. Although in fluid systems the exchange interaction is modulated

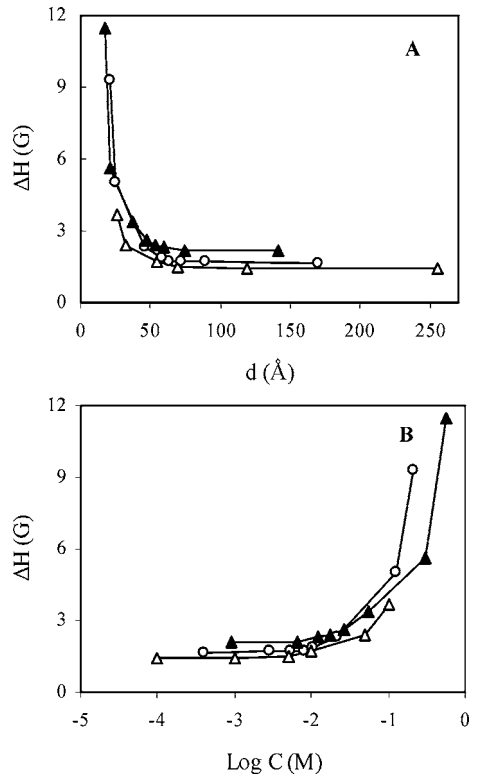

FIGURE 4. Effect of site−site distance (**A**) and site concentration (**B**) on the central peak line width of EPR spectra of Boc-TOAC-OH in DMF solution (Δ) and Boc-TOAC-BHAR in DCM (○) and in DMF (▲).

TABLE 4. Correlation between Yield[a] of Boc-Pro-OH Coupling to BHAR (1.40 mmol/g) and Site Concentration and Site−Site Distance Values

solvent	site concn (M)	site−site distance (Å)	coupling (%)
DCM	0.21	21.7	90
DMF	0.55	17.0	67
DMSO	1.76	14.2	25

[a] Yield of Boc-Pro-OH coupling after 30 min, at 25 °C with PSA method in equimolar conditions (1 mM of reactants).

TABLE 5. Correlation between Boc-(2BrZ)-Tyr-OH Coupling[a] Yield to ING-BHAR in DCM and Site Concentration and Site−Site Distance Values

ING-BHAR[a] (mmol/g)	site concn (mM)	site−site distance (Å)	coupling yield[b] (%)
0.19	39	38	86
0.54	89	33	63
1.16	625	17	21
1.59	1963	14	1

[a] Degree of ING substitution. [b] Yield of Boc-(2BrZ)-Tyr-OH coupling after 15 min, at 25°C with PSA method in equimolar condition (10 mM concentration of reactants).

by the collision frequency between molecules, calculations were performed using a static model to estimate critical distances for the onset of spin−spin interaction.[26b−d] These calculations yielded results in good agreement with the site−site distances found in the present study.

The data regarding the swelling parameters shown in Tables 1 and 2, when compared to those generated in previous swelling approaches to peptide resins,[16a] represent a step forward in the gauging of differentiated physicochemical factors that govern polymer solvation. In this context, the various swelling parameters evaluated in this study could be of great help in deepening the understanding of the resin solvation phenomenon at the microenvironment level. Accordingly, a clear relationship between site−site distance and site concentration values and the rate of the acylation reaction is demonstrated for the first time in the present report (Tables 4 and 5).

Modern science has progressively broadened the scope of the use of polymeric materials for a variety of purposes. Resin applications range from simple use as a solid support for liquid chromatography to complex methods for synthesizing macromolecules such as peptides[2] and oligonucleotides,[3a,b] as well as in combinatorial chemistry[4] conducted for the development of new drugs. The present report describes an alternative method for the determination of polymer swelling properties in combination with the investigation of model resins by means of EPR spectroscopy. We believe that this dual approach can be of great applicability in many areas involving the use of polymeric matrixes.

Experimental Section

Materials. Reagents and solvents were of analytical grade, were collected from recently opened containers and were not further purified. Boc-TOAC-OH was synthesized according to previous reports[12a]

Methods. Peptide Synthesis. The Ile-Asn-Gly sequence was synthesized manually by standard Boc chemistry[2a,b] on about 0.5 g of 0.22, 0.62, 1.62, and 2.62 mmol/g of BHAR. Coupling was performed using a 2.5 excess of Boc-amino acid/DIC/HOBt (1:1:1) in DCM/DMF for approximately 2 h. All couplings were monitored by qualitative ninhydrin test, and when positive, acetylation was performed with 50% acetic anhydride in DCM for 15 min. A small portion of the peptide-resin was cleaved in anhydrous HF and the crude peptide was characterized with regard to identity and homogeneity using mass spectrometry, amino acid analysis, and analytical HPLC.

Measurement of Peptide-Resin Swelling. Before swelling measurements of Boc-TOAC-OH-labeled resins, all batches of synthesized BHAR were sized by suspension in ethanol and fine material was decanted. The suspension was allowed to stand until approximately 90−95% had settled before decanting the supernatant. This procedure was repeated five times and was followed by suspending the beads in DCM. Solvent containing fine particles was withdrawn; this latter procedure was also repeated five times. To develop the swelling study with as narrowly sized population of beads as possible, the last resin purification step involved repeated sifting of dry beads through several 44−88 μm pore metal sieves. This sieving procedure lowered the standard deviation of the resin diameter to about 4%.

Swelling studies of the small-diameter bead populations were performed as published elsewhere[16a,17] after the resins were dried in a vacuum using an Abderhalden-type apparatus. Subsequently, about 200 dry and swollen (allowed to solvate overnight) beads from each resin were spread over a microscope slide and measured directly with a microscope coupled with Image-Pro Plus software. The values of bead diameter distribution were estimated by the geometric means and geometric standard deviations, as published elsewhere.[28]

EPR Studies. EPR measurements were carried out at 9.5 GHz on a Bruker ER 200D-SRC spectrometer at room temperature (22 ± 2 °C) using flat quartz cells from Wilmad Glass Co. (Buena, NJ). The magnetic field was modulated with amplitudes less than one-fifth of the line widths, and the microwave power was 5 mW to avoid saturation effects. Details of the procedure for TOAC-labeling of resins have been reported.[14] Labeled peptide resins were pre-swollen overnight in the solvent under study.

Yield of the Coupling Reaction. In a reaction vessel thermostated at 25 °C, 50−100 μmol of BHAR or ING-BHAR was equilibrated with the desired solvent. Preformed symmetrical anhydride (PSA) of the Boc-Pro-OH and Boc-2-Br-carbobenzoxyl (2BrZ)-Tyr-OH residues, respectively, were produced by mixing with DCC in equimolar conditions (for 1 h, at 0 °C). The white precipitate was removed by filtration and the solution was evaporated for further dissolution with the desired solvent for comparative coupling experiments. The PSA method was deliberately chosen for these experiments as it is less susceptible to the effect of solvent polarity.[2a,b] The rate of rotation of the reaction flask was 20 rpm. The acylating reagents were dissolved in the solvent under investigation and added in equimolar condition (at 10^{-2} M concentration of reactants) to the reaction vessel containing peptide resin pre-swollen in the same solvent. The coupling yield was monitored by the picric acid method,[21] and each experiment was performed in duplicate.

Acknowledgment. This work was funded by grants from Fapesp, CNPq, and Capes. R.M., E.M.C., S.S., and C.R.N. are recipients of CNPq research fellowships.

Supporting Information Available: Tables with swelling parameters for the 1.4 mmol/g of BHAR and ING-BHAR (four batches) are available. This material is available free of charge via the Internet at http://pubs.acs.org.

JO0483318

(26) (a) Devaux, P., McConnell, H. M. *J. Am. Chem. Soc.* **1972**; *94*, 4475. (b) Sackmann, E.; Träuble, H. *J. Am. Chem. Soc.* **1972**, *94*, 4482. (c) Träuble, H. J.; Sackmann, E. *J. Am. Chem. Soc.* **1972**, *94*, 4492. (d) Sackmann, E.; Träuble, H. *J. Am. Chem. Soc.* **1972**, *94*, 4499.

(27) (a) Scandella, C. J.; Devaux, P.; McConnell, H. M. *Proc. Natl. Acad. Sci. U.S.A.* **1972**, *69*, 2056. (b) Sackmann, E.; Trauble, H.; Galla, H. J.; Overath, P. *Biochemistry* **1973**, *12*, 5360.

(28) Irani, R. R.; Callis, C. F. *Particle Size: Measurement, Interpretation and Application*; Wiley: New York, 1963.

ANEXO 2

Available online at www.sciencedirect.com
SCIENCE DIRECT
Polymer 47 (2006) 4531–4536
polymer
www.elsevier.com/locate/polymer

Direct electron paramagnetic resonance monitoring of the peptide synthesis coupling reaction in polymeric support

Clovis R. Nakaie [a,*], Luciana Malavolta [a], Shirley Schreier [b], Eliane Trovatti [c], Reinaldo Marchetto [c]

[a] Department of Biophysics, Universidade Federal de São Paulo, Rua 3 de Maio 100, CEP 04044-020 São Paulo, SP, Brazil
[b] Department of Biochemistry, Institute of Chemistry, Universidade de São Paulo, CP 26077, 05513-970 São Paulo, SP, Brazil
[c] Department of Biochemistry and Technological Chemistry, Institute of Chemistry, UNESP, Araraquara, 14800-900 São Paulo, SP, Brazil

Received 18 January 2006; received in revised form 2 May 2006; accepted 5 May 2006
Available online 22 May 2006

Abstract

This work demonstrates, for the first time, a time-resolved electron paramagnetic resonance (EPR) monitoring of a chemical reaction occurring in a polymeric structure. The progress of the coupling of a N^{α}-*tert*-butyloxycarbonyl-2,2,6,6-tetramethylpiperidine-1-oxyl-4-amino-4-carboxylic acid (Boc-TOAC) spin probe to a model peptide-resin was followed through EPR spectra. Progressive line broadening of EPR peaks was observed, indicative of an increased population of immobilized spin probe molecules attached to the solid support. The time for spectral stabilization of this process coincided with that determined in a previous coupling study, thereby validating this in situ quantitative monitoring of the reaction. In addition, the influence of polymer swelling degree and solvent viscosity, as well as of the steric hindrance within beads, on the rate of coupling reaction was also addressed. A deeper evaluation of the latter effect was possible by determining unusual polymer parameters such as the average site–site distance and site-concentration within resin beads in each solvent system.

Keywords: Peptide; Polymer; Electron paramagnetic resonance

1. Introduction

Despite the great number of studies on the subject, full understanding of the solvation characteristics of polymeric materials continues to be an elusive goal. This is attributable to the high level of complexity of the process and many approaches have been applied to investigate the influence of factor such as the resin, peptide sequence and loading and the solvent system [1–9]. In a conceptual departure from the great majority of these approaches, we have initially focused on correlating this solvation phenomenon of polymers or peptide-polymers with the media polarity. This strategy has been addressed successfully either through measurement of peptide-resin swelling in a microscope [10,11] or combined to the electron paramagnetic resonance (EPR) method, which allows the monitoring of the dynamics of the solvated polymer or peptide-polymer network [12–15] using a paramagnetic amino acid-type spin probe [16,17].

Taking into account that the presence of electrophilic and nucleophilic groups in a peptide bond (N–H and C=O moieties, respectively), might strongly affect the interaction of the peptide-resin with the solvent system, the 1:1 sum of Gutmann's [18] solvent electron acceptor number (AN) and solvent electron donor number (DN) was proposed as a dimensionless and more accurate polarity scale [10,11]. Due to the presence of opposite concepts within the same parameter, the combined polarity term (AN + DN) was adopted as the amphoteric constant [15] and used to build this alternative polarity scale. More recently, these AN and DN concepts have been also applied to aid in predicting the capacity of solvent systems, not only in terms of dissociating peptide chains attached to a polymeric structure but also free in solution [19].

As a natural continuation of this effort to introduce as much variance as possible into the investigation of polymer solvation characteristics, the present study aimed to carry out, for the first time, a real-time monitoring of the coupling reaction within a resin. However, the acylating component for this reaction of binding to the solid support was the spectral probe molecule itself, which will allow in situ monitoring of this coupling

* Corresponding author. Tel.: +55 11 5539 0809; fax: +55 11 5575 9617.
E-mail address: clovis@biofis.epm.br (C.R. Nakaie).

0032-3861/$ - see front matter © 2006 Elsevier Ltd. All rights reserved.
doi:10.1016/j.polymer.2006.05.007

time-resolved experiment. The N^{α}-*tert*-butyloxycarbonyl (Boc)-2,2,6,6-tetramethylpiperidine-1-oxyl-4-amino-4-carboxylic acid (TOAC) amino acid-type paramagnetic probe (Boc-TOAC) [16] was coupled to a model peptide resin, and the progress of this acylation reaction to the polymer backbone was monitored directly by electron paramagnetic resonance (EPR) spectroscopy. In addition, the influence of the degree of peptide-resin swelling, media viscosity and degree of peptide-chain steric hindrance within beads were also examined in this coupling kinetics approach.

2. Experimental

2.1. Materials

Reagents and solvents were of analytical grade, were collected from recently opened containers and were not further purified. The styrene–1% divinylbenzene copolymer attaching phenylmethylamino groups and denoted benzhydrylamino-resin (BHAR) [20] was selected for peptide chain assembly.

2.2. Methods

2.2.1. Peptide synthesis

The (Asn-Ala-Asn-Pro) sequence was synthesized manually by standard Boc-chemistry [21,22] on about 0.5 g of 0.14 and 1.4 mmol/g BHAR. Coupling was performed using a 2.5 excess of Boc-amino acid/DIC/HOBt (1:1:1) in DCM/DMF for approximately 2 h. All couplings were monitored by qualitative ninhydrin test and, when positive, acetylation was performed with 50% acetic anhydride in DCM for 15 min.

2.2.2. Measurement of peptide-resin swelling

Before swelling measurement of resins, all batches of synthesized peptide-BHARs were sized by suspension in ethanol and fine materials were decanted off. The suspension was allowed to stand until approximately 90–95% had settled before decanting the supernatant. This procedure was repeated five times and was followed by suspending the beads in DCM and, solvent containing fine particles was withdrawn. This was also repeated about five times. In order to develop the swelling study with as narrowly sized population of beads as possible, the last purification step of resins involved repeated sifting of dry beads through several 44–88 μm pore metal sieves. This sieving procedure lowered the standard deviation of the resin diameters to about 4%.

Swelling studies of the small-diameter bead populations were performed as published elsewhere [1,10,15] after the resins were dried in vacuum using an Abderhalden-type apparatus. About 200 dry and swollen (allowed to solvate overnight) beads from each resin were spread over a microscope slide and measured directly with a microscope coupled with Image-Pro Plus software. The values of bead diameter distribution were estimated by the geometric means and geometric standard deviations.

2.2.3. EPR studies

EPR measurements were carried out at 9.5 GHz in an EPR spectrometer at room temperature (22 ± 2 °C) using flat quartz cells. Labeled peptide resins were pre-swollen overnight in the solvent under study. The magnetic field was modulated with amplitudes less than one-fifth of the line-widths, and the microwave power was 5 mW to avoid saturation effects. Details of TOAC derivative-labeling of resins have been already reported [12–15].

2.2.4. Yield of the coupling reaction

In a reaction vessel thermostated at 25 °C, 50–100 μmol of peptide-BHAR were equilibrated with the desired solvent. Pre-formed symmetrical anhydride (PSA) of the Boc-TOAC was produced by mixing with DCC in equimolar conditions (for 1 h, at 0 °C). The white precipitate was removed by filtration and the solution was evaporated for further dissolution with the desired solvent for comparative coupling experiments. The PSA method was deliberately chosen for these experiments as it is less susceptible to the effect of the polarity of the solvent [21,22]. The rate of rotation of the reaction flask was 20 rpm. The acylating reagents were dissolved in the solvent under investigation and added in equimolar condition (at 10^{-2} M concentration of reactants) to the reaction vessel, containing peptide resin pre-swollen in the same solvent. The yield of coupling was monitored by the picric acid method [23], and each experiment was performed in duplicate.

3. Results and discussion

Table 1 displays the swelling degrees and the kinetics of the coupling reactions of Boc-TOAC in two $(NANP)_4$–BHAR

Table 1
Correlation between Boc-TOAC coupling yield to $(NANP)_4$–BHAR in different solvents and swelling parameters

Solvent	$(NANP)_4$–BHAR[a]				$(NANP)_4$–BHAR[b]			
	Volume solvent/bead (10^4 μm^3)[c]	Coupling yield (%)			Volume solvent/bead (10^4 μm^3)[c]	Coupling yield (%)		
		30 min	60 min	180 min		30 min	60 min	180 min
DCM	17	54	61	78	12	24	50	74
DMF	28	83	88	93	53	43	82	92
DMSO	17	33	46	65	96	80	87	89

Yield of Boc-TOAC coupling at 25 °C with preformed symmetrical anhydride method in equimolar conditions (2 mM concentration of reactants).
[a] Obtained from a 0.14 mmol/g BHAR.
[b] Obtained from a 1.40 mmol/g BHAR.
[c] Volume of swollen bead − volume of dry bead.

Table 2
Swelling parameters of differently labeled Boc-TOAC–$(NANP)_4$–BHAR in DCM

Sample	Col. 1	Col. 2	Col. 3	Col. 4	Col. 5	Col. 6	Col. 7	Col.8	Col. 9	Col 10
Resin (mmol/g)[a]	Diam. dry bead (μm)	Diam. swollen bead (μm)	Volume solvent/ bead (10^5 μm^3)	Volume dry sample/g copol. (mL)[b]	Weight dry sample/g copol. (g)	Volume dry sample/g sample (mL)	Number of beads/g sample (10^7)	Number of sites/bead (10^{12})	Site–site distance (Å)	Site conc. (M)
0.111[c]	61	82	1.7	2.2	1.48	1.49	1.25	7.0	34.5	0.068
0.385[d]	68	82	1.2	3.1	4.26	0.72	0.44	52.6	17.6	0.730

Calculated according to Ref. [25].
[a] Degree of Boc-TOAC labelling.
[b] Copolymer of styrene–1% divinylbenzene: $d=0.99$ g/mL; average diameter of dry beads $=47$ μm.
[c] Obtained from a 0.14 mmol/g BHAR.
[d] Obtained from a 1.40 mmol/g BHAR.

batches in DCM, DMF and DMSO. The substitution degrees of both solid supports were 0.14 and 1.4 mmol/g, respectively, which allowed final peptide loadings of 14 and 68% (weight/weight). The resin-bound tetradecapeptide sequence corresponds to the antigenic and immunodominant segment of the sporozoite form of *Plasmodium falciparum* involved in malaria transmission [24]. To facilitate the determination of coupling yield, unfavorable experimental conditions were deliberately created, with a low reactant concentration (0.002 M) that was in equimolar proportion with the amount of the amino-group component of the peptide-resin.

The yield of coupling reactions was directly related to the degree of swelling, regardless of the peptide-resin involved (Table 1). Accordingly, DMF and DMSO allowed faster acylation for the lightly- and heavily-peptide-loaded resins, respectively. However, when the swelling degrees were equivalent, as in the case of the lightly- (14%)-peptide-loaded BHAR in DCM and DMSO (1.7×10^5 μm^3 of solvent volume absorbed per bead), the acylation was faster in the less viscous solvent (DCM). This finding indicates that the difference in viscosity between the two solvents (0.4 and 2.0 Cp, respectively), clearly affects the coupling reaction rate, even within the polymer matrix.

In addition to swelling degree and viscosity, the third factor influencing the coupling reaction is the steric hindrance degree within beads, as previously mentioned. The effect of this factor can be seen for example, when the coupling yield of both peptide-resins in DMF is compared (Table 1). The coupling rate of the highly (68%) peptide-loaded resin is slower, although presenting greater swelling than its low (14%) peptide-loaded partner resin (5.3×10^5 and 2.8×10^5 μm^3, respectively).

By considering these swelling values and the degree of substitution of resins and the molecular weight of attached peptides, it was possible to estimate the average distance between peptide chains spread throughout the bead matrices in both peptide-resins, according to our recently published report [25]. Tables 2 and 3 display the calculated values found for the low and highly peptide-loaded resins of Table 1 in DCM and DMF, respectively. In order to detail how the various peptide-resins parameters were sequentially calculated, the detailed procedure will be next described for the 0.111 mmol/g Boc-TOAC–$(NANP)_4$–BHAR batch in DMC (Table 2, row 1).

3.1. Example: 0.111 mmol/g labeled Boc-TOAC–$(NANP)_4$–BHAR swollen in DCM (Table 2)

Columns 1 and 2 list the average diameters of the dry (61 μm) and DCM swollen (82 μm) beads, respectively, measured under the light microscope. The volumes of the dry (1.19×10^5 μm^3) and swollen (2.89×10^5 μm^3) beads were calculated and the volume of solvent/bead (1.7×10^5 μm^3, column 3) was obtained by subtracting the dry bead volume from the swollen bead volume.

Table 3
Swelling parameters of differently labeled Boc-TOAC–$(NANP)_4$–BHAR in DMF

Sample	Col. 1	Col. 2	Col. 3	Col. 4	Col. 5	Col. 6	Col. 7	Col.8	Col. 9	Col 10
Resin (mmol/g)[a]	Diam. dry bead (μm)	Diam. swollen bead (μm)	Volume solvent/ bead (10^5 μm^3)	Volume dry sample/ g copol. (mL)[b]	Weight dry sample/g copol. (g)	Volume dry sample/g sample (mL)	Number of beads/g sample (10^7)	Number of sites/ bead (10^{12})	Site–site distance (Å)	Site conc. (M)
0.111[c]	61	91	2.8	2.2	1.48	1.49	1.25	7.0	38.3	0.042
0.385[d]	68	110	5.3	3.1	4.26	0.72	0.44	52.6	23.7	0.165

Calculated according to Ref. [25].
[a] Degree of Boc-TOAC labeling.
[b] Copolymer of styrene–1% divinylbenzene: $d=0.99$ g/mL; average diameter of dry beads $=47$ μm.
[c] Obtained from a 0.14 mmol/g BHAR.
[d] Obtained from a 1.40 mmol/g BHAR.

3.2. Column 4: volume of dry sample/g of copolymer (2.2 mL/g copolymer)

The ratio (diameter dry sample/diameter dry copolymer)^3 represents the relationship between the volume of the dry macroscopic working sample (0.111 mmol/g Boc-TOAC–$(NANP)_4$–BHAR) and that of the dry copolymer used to synthesize the sample. In the example, since the average diameters of beads of dry sample and dry copolymer are 61 and 47 μm, respectively, the ratio between the dry volumes of both resins is $(61/47)^3=2.18$. Considering that the number of beads in 1 g of copolymer is the same as in the sample synthesized from this amount of copolymer and taking into account that the volume of 1 g of copolymer is 1.01 mL ($d=0.99$ g/mL), the total volume of dry sample containing 1 g of copolymer is therefore 2.18×1.01 mL, or 2.20 mL.

3.3. Column 5: weight of dry sample/g of copolymer (1.48 g/g of copolymer)

The 0.111 mmol Boc-TOAC–$(NANP)_4$–BHAR sample was synthesized by quantitative incorporation of the $(NANP)_4$ peptide and Boc-TOAC in the 0.140 mmol/g BHAR batch. This resin originated from partial phenylmethylamino incorporation into a heavily substituted 1.40 mmol/g benzoyl group-containing copolymer. This copolymer derivative is synthesized in the first step (Friedel–Crafts acylation) necessary to obtain BHAR. Thus, the Boc-TOAC–$(NANP)_4$–BHAR sample under consideration still contains (1.40–0.14) mmol $=1.26$ mmol/g of remaining benzoyl groups attached to its backbone. Considering the total weight of groups added in all the synthetic steps, one can calculate that the sum of Boc-TOAC, $(NANP)_4$ peptide and benzoyl groups attached to the initial copolymer corresponds to 0.325 g. Therefore, in 1 g of sample, the mass of copolymer is $1-0.409$ g $=0.675$ g. Thus, for 1 g of starting copolymer, the weight of the 0.111 mmol Boc-TOAC–$(NANP)_4$–BHAR is 1.48 g.

3.4. Column 6: volume of dry sample/g of sample (1.49 mL/g)

This parameter is calculated by dividing the value of (volume of dry sample/g copolymer), column 4, by (weight of dry sample/g copolymer), column 5. The value obtained (1.49 mL/g) represents the ratio between the volume of the dry sample (2.2 mL) and its total weight (1.48 g), and corresponds to the volume occupied by 1 g of sample in the dry form.

3.5. Column 7: number of beads/g of sample (1.25×10^7 beads/g sample)

This value is calculated by dividing the volume of 1 g of dry sample (1.49 mL, column 6) by the average volume of one dry bead, which is calculated from its diameter (61 μm, column 1). Thus, the volume of one dry bead is 1.19×10^{-7} mL. The ratio 1.49 mL/1.19×10^{-7} mL yields 1.25×10^7 beads in 1 g of sample.

3.6. Column 8: number of sites/bead (7.0×10^{12})

The number of sites per bead is calculated by dividing the number of sites/g of sample by the number of beads/g of sample (column 7). The former value corresponds to $0.145\times 6.02\times10^{20}$ sites/g. Dividing this number by the number of beads in 1 g of sample (1.15×10^{7}, column 7) one obtains 7.0×10^{12} sites/bead.

3.7. Column 9: site–site distance (34.5 Å).

To evaluate this important parameter, we first calculate the average volume per site. This is done by dividing the volume of one swollen bead (2.89×10^{5} μm^3, calculated from the measured diameter of one swollen bead, 82 μm, column 2) by the number of sites/bead (7.0×10^{12}, column 8). Thus, the average volume per site is 4.1×10^{4} Å^3. By assuming a uniformly distributed cubic lattice for the sites within the bead, the site–site distance corresponds to the side of a cube and is given by the cubic root of the volume occupied by one site, i.e. $(4.1\times10^{4}\ \text{Å}^3)^{1/3}=34.5$ Å.

3.8. Column 10: site concentration inside the bead (0.068 mM).

Finally, making use of the parameters calculated in the previous steps, it is possible to determine the site concentration within the bead. Thus, for the 0.145 mmol/g substituted Boc-TOAC–(NANP)$_4$–BHAR, the site concentration is obtained by dividing the number of sites/bead (7.0×10^{12}, column 8) by the volume of solvent/bead (1.7×10^{5} μm^3, column 3), that is, 4.1×10^{7} sites/μm^3, or 4.1×10^{19} sites/mL. Considering that 6.02×10^{20} sites/mL correspond to 1 M concentration, we find that that the site concentration corresponds to an effective Boc-TOAC concentration of 0.068 mM.

Using this calculation strategy also for other data shown either in Tables 2 and 3, it was possible for instance to seen that the average inter-site distance values of 34.5 and 17.6 Å in DCM (Table 2) and 38.3 and 23.7 Å in DMF (Table 3) were determined for these two peptide-bound resins, respectively. In addition, the effective peptide chain concentrations inside the bead were also determined giving the values of 0.068 and 0.730 M in DCM (Table 2) and 0.042 and 0,165 M in DMF (Table 3), respectively. Thus, regardless the peptide-resin, the greater the distance between reactive sites, the faster is the coupling reaction. Taken together, these findings therefore proves clearly the influence of the level of the steric hindrance in neighbouring peptide chains, decreasing the rate of reaction as a consequence of the greater proximity between the chains under conditions of heavier peptide loading.

Following these results, the direct EPR monitoring of the Boc-TOAC spin probe coupling reaction in the (NANP)$_4$–BHAR (1.4 mmol/g) was next tested in DMF, using the same acylation protocol employed for the experiments detailed in Table 1. Fig. 1 reveals a clear line broadening of EPR spectral peaks over the course of the coupling reaction. This line broadening was induced by the increasing immobilization of

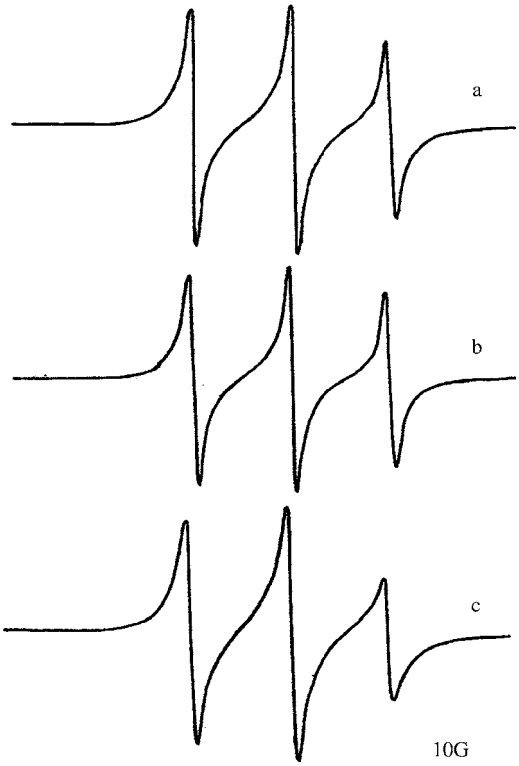

Fig. 1. EPR spectra of Boc-TOAC coupling in (NANP)$_4$–BHAR (1.4 mmol/g) after (a) 0, (b) 60 and (c) 180 min. Reaction at 25 °C in DMF, with preformed symmetrical anhydride method in equimolar conditions and 2 mM concentration of reactants.

the Boc-TOAC molecule population attached to the polymer backbone.

Although most of biradicals known in the literature display a five-line pattern in the EPR spectra, the biradical formed for coupling to resin matrix and corresponding to the reactive symmetrical anhydride of the Boc-TOAC probe gives a three line-type spectrum as can be seen in Fig. 1(a). This result seems to be in accord with the observation that the structure and the average distance between both nitroxide moiety in the biradical

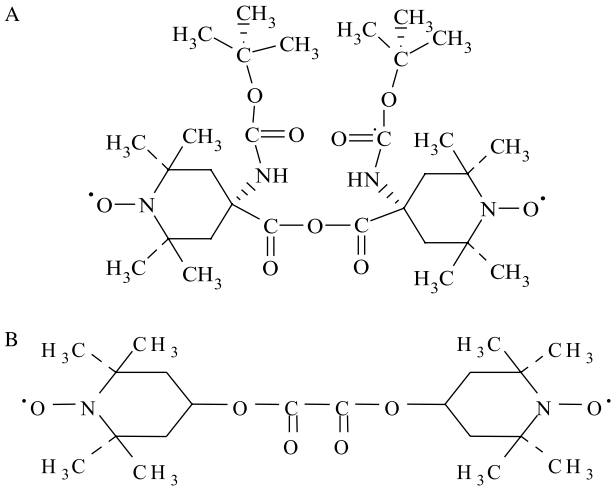

Fig. 2. Molecular structures of the biradicals (A), symmetrical anhydride of N^{α}-*tert*-butyloxycarbonyl-2,2,6,6-tetramethylpiperidine 1-oxyl-4-amino-4-carboxylic acid and (B), bis(2,2,6,6-tetramethylpiperidine-1-oxyl) oxalate.

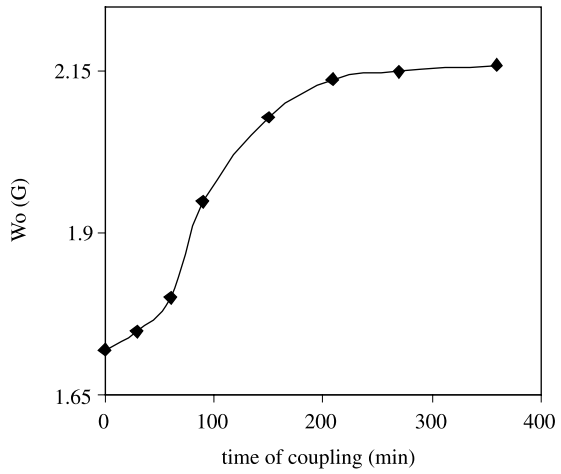

Fig. 3. Correlation between EPR central Wo linewidth values and time of Boc-TOAC coupling to $(NANP)_4$–BHAR (1.4 mmol/g). The reactions were carried out at 25 °C in DMF, with preformed symmetrical anhydride method in equimolar conditions, and 2 mM concentration of reactants.

molecule may affect the EPR spectrum profile [26–28]. To better clarify this issue, the Fig. 2 shows the similarity existing between the structure of Boc-TOAC symmetrical anhydride and that of the bis(2,2,6,6,-tetramethylpiperidine-1-oxyl) oxalate paramagnetic probe. According to the literature, this latter biradical also displays a three line-type EPR spectrum [28].

Next, Fig. 3 shows the correlation between line-width values of the middle-field EPR peak (Wo) and reaction times. This EPR parameter has been often used for determination of the degree of motion of labeled molecules or systems [12–15,25]. As can be seen in the figure, progressive increase in the line-width values of peaks followed by complete stabilization of Wo values (greater immobilization) occurred after 3–4 h of coupling, thus in agreement with data shown in Table 1. These findings therefore, demonstrate the feasibility of carrying out direct, in situ monitoring of a chemical reaction within the polymer structure in which the reacting component is the spectral probe itself.

In summary, our results seem to be of value for increasing the understanding of the solvation characteristics of polymers. We have demonstrated that various physicochemical and structural factors influence the reaction yield in polymers. However, the innovative aspect of the present report is the finding that the EPR approach allows direct time-resolved monitoring of a specific chemical reaction (coupling) occurring throughout the polymer network. The success of this experimental strategy might be of relevance in devising other approaches intended to further investigate, at the microenvironment level, chemical processes in polymers.

Acknowledgements

We gratefully acknowledge FAPESP, CNPq, CAPES and FADA for financial support. All authors are recipients of research fellowships from CNPq.

References

[1] Sarin VK, Kent SBH, Merrifield RB. J Am Chem Soc 1980;102:5463–70.
[2] Fields GB, Fields CG. J Am Chem Soc 1991;113:4202–7.
[3] Kates SA, Albericio F. Solid phase synthesis: a practical guide. New York: Marcel Dekker, Inc.; 2000 p. 275–330.
[4] Vaino AR, Janda KD. J Comb Chem 2000;2:579–96.
[5] Deber CM, Lutek MK, Heimer EP, Felix AM. Peptide Res 1989;2:184–8.
[6] Furrer J, Piotto M, Bourdonneau M, Limal D, Guichard G, Elbayed K, et al. J Am Chem Soc 2001;123:4130–8.
[7] Warrass R, Wieruszeski M, Bouitillon C, Lippens G. J Am Chem Soc 2000;122:1789–95.
[8] Valente AP, Almeida FCL, Nakaie CR, Schreier S, Crusco E, Cilli EM. J Pept Sci 2005;11:556–63.
[9] Yan B. Acc Chem Res 1998;31:621–30.
[10] Cilli EM, Oliveira E, Marchetto R, Nakaie CR. J Org Chem 1996;61:8992–9000.
[11] Malavolta L, Oliveira E, Cilli EM, Nakaie CR. Tetrahedron 2002;58:4383–94.
[12] Cilli EM, Marchetto R, Schreier S, Nakaie CR. Tetrahedron Lett 1997;38:517–20.
[13] Cilli EM, Marchetto R, Schreier S, Nakaie CR. J Org Chem 1999;64:9118–23.
[14] Ribeiro SCF, Schreier S, Nakaie CR, Cilli EM. Tetrahedron Lett 2001;42:3243–6.
[15] Oliveira E, Cilli EM, Miranda A, Jubilut GN, Albericio A, Andreu A, et al. Eur J Org Chem 2002;21:3686–94.
[16] Nakaie CR, Schreier S, Paiva ACM. Braz J Med Biol Res 1981;14:173–80.
[17] Marchetto R, Schreier S, Nakaie CR. J Am Chem Soc 1993;15:11042–3.
[18] Gutmann V. The donor–acceptor approach to molecular interactions. New York: Plenum Press; 1978.
[19] Malavolta L, Nakaie CR. Tetrahedron 2004;60:9417–24.
[20] Pietta PG, Cavallo PF, Takahashi K, Marshall GR. J Org Chem 1974;39:44–8.
[21] Barany G, Merrifield RB. The peptides, vol. 2. New York: Academic Press; 1979 p. 1–284.
[22] Stewart JM, Young JD. Solid phase peptide synthesis. Rockford III: Pierce Chemical Company; 1984.
[23] Gisin BF. Anal Chim Acta 1972;60:248–9.
[24] Dame JB, Williams JL, McCutchan TF, Weber JL, Wirtz RA, Hockmeyer WT, et al. Science 1984;225:593–9.
[25] Marchetto R, Cilli EM, Jubilut GN, Schreie S, Nakaie CR. J Org Chem 2005;70:4561–8.
[26] Calvin M, Wang HH, Entine G, Gill D, Ferruti P, Harpold MA, et al. Proc Natl Acad Sci, USA 1969;63:1–8.
[27] Sankarapandi S, Sukumar M, Balaram P, Manoharan PT. Biochim Biophys Res Commun 1995;213:439–46.
[28] Rozantsev EG. In: Ulrich H, editor. Free radicals. New York: Plenum Press; 1970.

ANEXO 3

Peptides 1998
Sándor Bajusz and Ferenc Hudecz (Eds.)

Interaction Between Quinolone, DNA and a Peptide Analog of DNA Gyrase

REINALDO MARCHETTO[1,3], NÚRIA CASTILLO[1], ERNESTO NICOLÁS[1], MARGARITA NAVIA[2], JORDI VILA[2] and ERNEST GIRALT[1]

[1]*Department of Organic Chemistry, University of Barcelona. Martí i Franqués 1-11, 08028 Barcelona, Spain*
[2]*Department of Microbiology, Faculty of Medicine, University of Barcelona. Villaroel 170, 08036 Barcelona, Spain*
[3]*Department of Biochemistry, Institute of Chemistry, UNESP. Caixa Postal 355, 14801-970 Araraquara, São Paulo, Brazil*

Introduction

The intracellular target of quinolone drugs, is DNA gyrase, an ATP-dependent bacterial type II topoisomerase, able to introduce negative supercoils into covalently closed-circular DNA. The enzyme from *Escherichia coli* consists of two A and two B subunits that form a A_2B_2 complex, and it is believed that subunit A is the direct target for the quinolones [1]. In addition, the ability of quinolones to stabilize the so-called "cleavable complex" indicates that not only the enzyme but also DNA participates in a stable interaction with quinolones [2]. However, exactly how this interaction happens is a matter of controversy and for this reason we have examined the interaction of ciprofloxacin (CFX), closed circular DNA (pBlueScript) and a subunit A DNA gyrase synthetic segment (AGYRA: Figure 1) which contains the important amino acids for the binding of the drug [3], as model to understand this interaction.

Results and Discussion

Prior to investigating the CFX-DNA-AGYRA interaction by affinity chromatography and binding assays, we carried out a series of intrinsic fluorescence measurements of CFX (excitation wavelenght was 330 nm) to analyse the effect of DNA, AGYRA and Mg^{2+} concentration on its emission spectrum (emission wavelenght was 417 nm). The fluorescence emission of CFX was remarkably increased by addition of Mg^{2+} at neutral pH. Saturation occured at a Mg^{2+} concentration of ≈ 5 mM. The intrinsic fluorescence intensity of the CFX in Mg^{2+} solution (concentration in the milimolar range), was quenched when DNA and AGYRA were added, indicating the existence of CFX-DNA and CFX-DNA-AGYRA interaction.

Next we investigated the CFX-DNA-AGYRA complex formation by affinity chromatography with CFX immobilized on epoxy-activated Sepharose. The chromatographic behavior of DNA (absorbance at 260 nm), AGYRA and a mixture of both (fluorescence: excitation at 280 nm, emission at 303 nm) is shown in Figure 1. In the presence of Mg^{2+}, AGYRA had no affinity for the column of immobilized CFX. Under the same conditions,

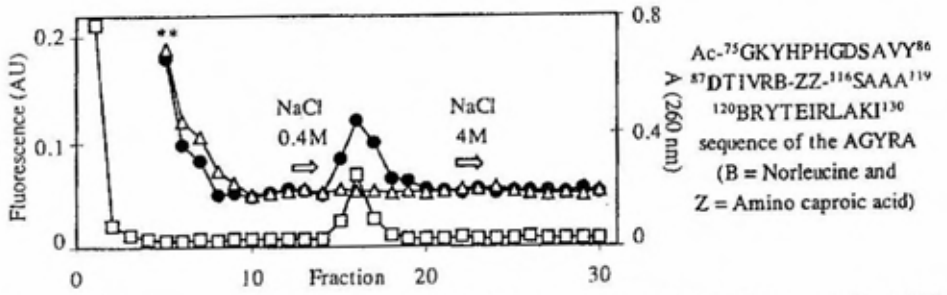

Figure 1. *Chromatography of (Δ) AGYRA, (□) pBS and (•) a mixture of both on immobilized CFX (** indicates that the fluorescence is higher than 0.2). AU = arbitrary unit*

DNA was retained and was eluted by the addition of 0.4 M NaCl in Tris buffer (5 mM Tris.HCl / 20 mM NaCl / 5 mM $MgCl_2$, pH 7.2). When the mixture of DNA and AGYRA was introduced into the column, the complex was retained and eluted with the same 0.4 M NaCl. Experiments carried out without Mg^{2+} showed that DNA, AGYRA or DNA-AGYRA do not bind the CFX-resin. These results suggested interactions between quinolone and AGYRA only in the presence of DNA and Mg^{2+} as shown in the DNA gyrase complex with norfloxacin [4].

Ciprofloxacin binding was determined by a membrane filtration method using Microcon devices which have membranes with molecular weight cutoff of 50 KDa. The amount of CFX bound to the complexes was calculated by subtracting the free CFX concentration in the reaction mixture from the initial CFX concentration, both CFX concentrations were determined by fluorescence. All the binding data were determined by Klotz plots [5]. In the presence of 5 mM Mg^{2+}, the apparent K_d were 1.8×10^{-6} and 1.6×10^{-6} M, for CFX-DNA and CFX-DNA-AGYRA, respectively. In the absence of Mg^{2+}, the binding of CFX to DNA or DNA-AGYRA was negligible.

We conclude that the binding of CFX with DNA and AGYRA, in the presence of Mg^{2+}, implies a quaternary complex formation as DNA gyrase, suggesting that the model presented here is good to study interactions with other quinolones.

Acknowledgements

We thank FAPESP (Brazil) for posdoctoral fellowship to Dr. R. Marchetto, CICYT (PB95-1131) and Generalitat de Catalunya (1995SGR494 and CeRBa).

References

1. Reece, R.J. and Maxwell, A., *Crit. Rev. Biochem. Mol. Biol.*, 26 (1991) 335.
2. Willmott, C.J.R. and Maxwell, A., *Antimicrob. Agents Chemother.*, 37 (1993) 126.
3. Vila, J. et al., *Antimicrob. Agents Chemother.*, 38 (1994) 2477.
4. Bazile-Pham Khac, S. and Moreau, N., *J. Chromatography A*, 668 (1994) 241.
5. Klotz, I.M., *Acc. Chem. Res.*, 7 (1974) 162.

ANEXO 4

Journal of Peptide Science
J. Peptide Sci. **7**: 27–40 (2001)

Two Short Peptides Including Segments of Subunit A of *Escherichia coli* DNA Gyrase as Potential Probes to Evaluate the Antibacterial Activity of Quinolones

REINALDO MARCHETTO[a,c], ERNESTO NICOLÁS[a], NÚRIA CASTILLO[a], JORDI BACARDIT[a], MARGARITA NAVIA[b], JORDI VILA[b] and ERNEST GIRALT[a,*]

[a] Departament de Química Orgànica, Facultat de Química, Universitat de Barcelona, Barcelona, Spain
[b] Departament de Microbiologia, Facultat de Medicina, Universitat de Barcelona, Barcelona, Spain
[c] Departamento de Bioquímica, Instituto de Química, Universidade Estadual Paulista, São Paulo, Brazil

Received 30 June 2000
Accepted 4 August 2000

Abstract: Quinolones constitute a family of compounds with a potent antibiotic activity. The enzyme DNA gyrase, responsible for the replication and transcription processes in DNA of bacteria, is involved in the mechanism of action of these drugs. In this sense, it is believed that quinolones stabilize the so-called 'cleavable complex' formed by DNA and gyrase, but the whole process is still far from being understood at the molecular level. This information is crucial in order to design new biological active products. As an approach to the problem, we have designed and synthesized low molecular weight peptide mimics of DNA gyrase. These peptides correspond to sequences of the subunit A of the enzyme from *Escherichia coli*, that include the quinolone resistance-determining region (positions 75–92) and a segment containing the catalytic Tyr-122 (positions 116–130). The peptide mimic of the non-mutated enzyme binds to ciprofloxin (CFX) only when DNA and Mg^{2+} were present ($K_d = 1.6 \times 10^{-6}$ M), a result previously found with DNA gyrase. On the other hand, binding was reduced when mutations of Ser-83 to Leu-83 and Asp-87 to Asn-87 were introduced, a double change previously found in the subunit A of DNA gyrase from several CFX-resistant clinical isolates of *E. coli*. These results suggest that synthetic peptides designed in a similar way to that described here can be used as mimics of gyrases (topoisomerases) in order to study the binding of the quinolone to the enzyme–DNA complex as well as the mechanism of action of these antibiotics.

Keywords: affinity chromatography; DNA gyrase; *Escherichia coli*; peptide design; peptide synthesis; quinolones; solid phase; topoisomerases

INTRODUCTION

The three-dimensional structure of DNA plays a key role in biological processes such as replication, transcription and recombination. The enzymes responsible for maintaining the topological state of DNA are termed DNA topoisomerases. These proteins are essential to all cells and, as such, they are important targets for many clinically antibacterial drugs. DNA gyrase [1] is one of the most studied enzymes from bacteria and constitutes the intracellular target of quinolones, a group of drugs with a wide-spectrum of antibacterial activity.

Abbreviations: Ahx, ε-aminohexanoic acid; Boc, *tert*-butoxycarbonyl; Bzl, benzyl; CFX, ciprofloxacin; DIEA, *N*,*N*′-diisopropylethylamine; DIPCDI, *N*,*N*′-diisopropylcarbodiimide; *E. coli*, *Escherichia coli*; EDC, 1-ethyl-3(3-dimethylaminopropyl)carbodiimide; gyrA, subunit A of DNA gyrase; gyrB, subunit B of DNA gyrase; HOBt, 1-hydroxy-benzotriazole; *p*-MBHA, *p*-methylbenzhydrylamine; MCA, ε-maleimidocaproic acid; NMP, *N*-methyl-2-pyrrolidone; Pbs, pBlueScript; PyBOP, benzotriazol-1-yl-oxy-*tris*-pyrrolidino-phosphonium; rt, retention time; ssDNA, single-stranded DNA; Tris, 2-amino-2-hydroxymethylpropane-1,3-diol.

* Correspondence to: Departament de Química Orgànica, Facultat de Química, Universitat de Barcelona, Marti i Franquès, 1, 08028, Barcelona, Spain; e-mail: giralt@qo.ub.es

DNA gyrase is a type II topoisomerase consisting of two subunits, A (gyrA) and B (gyrB), which form the active complex A_2B_2 [2]. These subunits have a molecular weight of 97 kD (874 residues) and 90 kD (803 residues), respectively, in the case of *Escherichia coli*. This enzyme introduces negative supercoils into DNA in an adenosine triphosphate (ATP)-dependent manner, catalysing the cleavage of a double-stranded DNA (pBS, pBlueScript) segment and the formation of a transient DNA gate through which another segment is passed. It is known that quinolones inhibit the activity of DNA gyrase through the Mg^{2+}-mediated formation of a tertiary quinolone–enzyme–DNA complex as a key step of the process. However, the way in which the substrates interact [3–9], as well as the functions that the complex develops at the molecular level [10–16], are still matters of controversy.

Finding answers to these questions is crucial in order to design new antibiotic drugs which will prevent bacterial infection or avoid resistance problems. From the structural point of view, this study implies a tremendous difficulty because of the size of the complex. This observation prompted us to consider the possibility of using short peptides containing segments of gyrA involved in the recognition of DNA and quinolones as models to carry out binding studies. In this paper, we report on two 35-residue peptides formed by a *C*-terminal region including the catalytic Tyr residue at position 122 [17] and an *N*-terminal region containing residues 83 and 87, which are believed to be involved in the interaction with quinolones (Figure 1) [18]. Single-stranded DNA (ssDNA) and pBS were used in this work together with the antibiotic ciprofloxacin (CFX) as the quinolone model. Affinity chromatography [19] and membrane filtration techniques were exploited to perform the binding studies [20]. Evidence that these peptides might constitute suitable models to study gyrase–DNA–quinolone interactions as well as the mechanism of action of the drugs is presented.

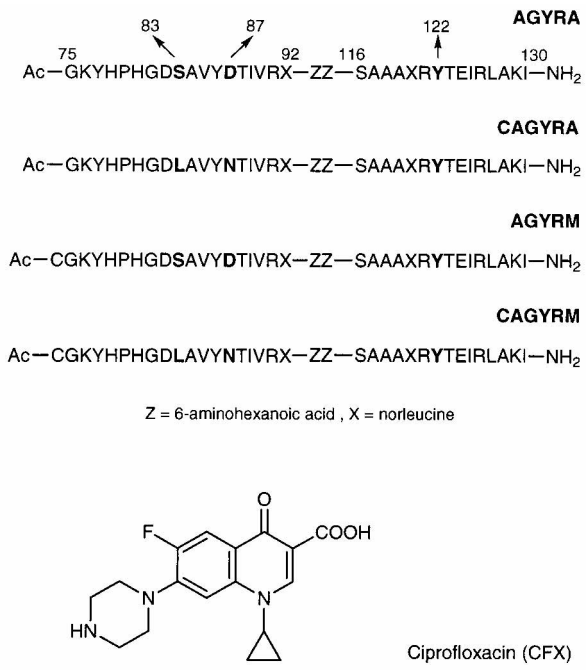

Figure 1

MATERIALS AND METHODS

Tert-butoxycarbonyl (Boc)-amino acids were supplied by Novabiochem AG (Läufelfingen, Switzerland), Bachem Feinchemikalien AG (Bubendorf, Switzerland), Adanced ChemTech (Maidenhead, UK), Propeptide (Vert-le-Petit, France) or Neosystem (Gennevilliers, France).

HF was from UCAR. *P*-Methylbenzhydrylamine (*p*-MBHA) resin (0.45 mmol g^{-1}) was purchased from Bachem, Sepharose 4B (7–12 μmol ml^{-1}) was supplied by Pharmacia Biotech (Sweden) and epoxy-activated Sepharose 6B (19–40 μmol ml^{-1}) was from Sigma–Aldrich Química (Madrid, Spain). Benzotriazol-1-yl-oxy-*tris*-pyrrolidinophosponium (PyBOP) was from Novabiochem. *N*,*N*′-diisopropylcarbodiimide (DIPCDI), 1-hydroxybenzotriazole (HOBt), Ac_2O and propionic acid were supplied by Fluka Chimie AG (Buchs, Switzerland). Dimethylformamide (DMF), supplied by Scharlau (Spain), was bubbled with nitrogen to remove volatile contaminants and kept stored over activated 4 Å molecular sieves. *N*-methyl-2-pyrrolidone (NMP) was from Applied Biosystems. HCl and Tris buffer were from Merck (Darmstadt, Germany). Thiophenol, 1-ethyl-3-(3-dimethylaminopropyl)carbodiimide (EDC) and ε-maleimidocaproic acid (MCA) were obtained from Sigma–Aldrich. *N*,*N*′-diisopropylethylamine (DIEA) was from Acros (Geel, Belgium). MeCN (Scharlau) was high performance liquid chromatography (HPLC) grade; dichloromethane (DCM) (Scharlau) and trifluoroacetic acid (TFA) (Solvay, Germany) were peptide synthesis grade and were used directly. $MgCl_2$-$6H_2O$, NaH_2PO_4 and Na_2HPO_4-$12H_2O$ were supplied by Fluka and NaCl was from J. Escuder (Spain). Bayer (Spain) supplied CFX as a kind gift.

The supercoiled plasmid pBS was prepared in *E. coli* strain DH5α by conventional methods [21] and was purified by the optimized alkaline lysis method [22] followed by purification on a QIAGEN resin (purchased from Qiagen GmbH-Germany). Calf thymus ssDNA was purchased from Sigma–Aldrich. The pBS plasmid and ssDNA mother solutions were diluted with 5 mM Tris–HCl buffer (≈ 4 μg μl^{-1}, pH 7.2), frozen and stored.

Peptide-resins were hydrolysed using 12 M HCl/propionic acid (1:1) at 155°C for 2 h and peptides were hydrolysed in 6 M aqueous HCl solution at 155°C for 90 min. Amino acid analyses were performed on a Beckman System 6300 analyser.

Analytical HPLC was carried out on a Shimadzu apparatus comprising two solvent delivery pumps model LC-6A, automatic injector model SIL-6B69A, variable wavelength detector model SPD-6A, system controller model SCL-6B and plotter model C-R6A. Nucleosil C_{18} reverse-phase columns were used (25 × 0.5 cm, 5 μm). In general, peptides were eluted at a flow rate of 1 ml min^{-1} (A: water, 0.045% of TFA; B: MeCN, 0.036% of TFA) and detection was carried out at 220 nm.

Semi-preparative HPLC and medium performance liquid chromatography (MPLC) techniques were used for purification purposes. The former was performed in a Waters analyser consisting of a fluid unit model 600, automatic injector model 717, variable wavelength detector model 490E, system controller model 600E and a Shimadzu plotter model C-R5A. Nucleosil C_{18} reverse-phase columns were used (25 × 1 cm, 5 μm) at a flow rate of 3 ml min^{-1} and with the eluents mentioned above. Detection was carried out at 220 nm. Reverse-phase MPLC was carried out using a CFG-Prominent/Duramat pump, a 757 ABI variable wavelength detector, an automatic fraction collector model Gilson FC 205 and an Omniscribe rec 101 plotter (Pharmacia Biotech). A glass column (2.5 × 26 cm) packed with reverse-phase Vydac-C_{18} (15–20 μm) was used. A flow rate of 2 ml min^{-1} was utilized (A and B: 400 ml mixtures of water/MeCN with 0.05% of TFA) and the products were detected at 220 nm.

Binding data were determined by the membrane filtration method, using Microcon centrifugal filter units that utilize thin membranes ultracell-YM with a molecular weight cut-off of 50 kD. Centrifugations were carried out in a Beckman GS-15R centrifuge equipped with a fixed angle F2402H rotor. Fluorescence spectroscopy was performed using an Aminco–Bowman AB2 instrument. To carry out the experiments 1 cm-path length cells (1 ml) were used. Spectra were registered between 350 nm and 550 nm in the case of CFX (excitation, 330 nm; emission, 417 nm) and between 280 nm and 303 nm when AGYRA or AGYRM were used (excitation, 280 nm; emission, 303 nm). Ultraviolet spectroscopy was carried out in a Perkin–Elmer Lambda 5 apparatus, using a 1 cm-path length cell (2 ml). Spectra were registered between 230 nm and 280 nm, following the presence of DNA at 260 nm.

General Procedure for the Solid-phase Assembly of Peptides and their Acidolytic Cleavage from the Resin

Peptides were prepared by the solid-phase methodology and following the Boc/Benzyl strategy [23,24]. Protecting groups for amino acids were 2-Cl-Z (Lys), Tos (Arg), OcHx (Asp and Glu), Bzl (Ser and Thr), 2-Br-Z (Tyr), Dnp (His) and MeBzl (Cys). The syntheses were performed manually in polypropylene syringes fitted with a polyethylene disc. Prior to use, the polymeric support (*p*-MBHA resin, 1 g batches) was washed with (1) DCM, 1 × 5 min; (2) 40% TFA in DCM, 1 × 2 min + 1 × 20 min; (3) 5% DIEA in DCM, 3 × 2 min; (4) DCM, 3 × 1 min. Boc-amino acids were assembled using the following protocol: (1) DCM, 2 × 4 min; (2) 40% TFA in DCM, 1 × 2 min + 1 × 20 min; (3) DCM, 3 × 1 min; (4) DMF, 3 × 1 min or NMP, 1 min; (5) Boc-amino acid coupling and (6) DMF, 3 × 1 min; (7) DCM, 3 × 1 min. The fragment Nle-120/Ile-130 was assembled using DIPCDI/HOBt (Boc-AA-OH [5 eq], HOBt [5 eq], DIPCDI [5 eq]; 1 h) and the rest of the amino acids were coupled with PyBOP/DIEA (Boc-AA-OH [3 eq], PyBOP [3 eq], DIEA [6 eq]; 1 h). An additional treatment with 40% TFA in DCM (10 min) was needed in order to achieve α-amino deprotection from position 83. Acetylation was performed as follows: (1) Ac_2O (10 eq) and DIEA (10 eq), 30 min; (2) DMF, 3 × 1 min; (3) DCM, 3 × 1 min.

Deprotection of His residue was performed prior to the cleavage from the resin using the following protocol: (1) DCM, 3 × 1 min; (2) DMF, 3 × 1 min; (3) Thiophenol/DIEA/DMF (3:3:4), 1 × 30 min; (4) DMF, 3 × 1 min; (5) H_2O, 3 × 1 min; (6) MeOH, 3 × 1 min; (7) DCM, 3 × 1 min; (8) 40% TFA in DCM, 3 × 1 min; (9) neat TFA, 1 × 20 min; (10) DCM, 6 × 1 min.

Peptides were cleaved from the resins with HF on a Kel-F Toho–Kasei Ltd (Tokyo, Japan) apparatus. Peptidyl-resins (350–950 mg batches) were treated with 4.5 ml of HF and 500 μl of anisole during 1 h at 0°C. The resins were washed with 10 ml of AcOEt and the resulting suspension was washed with

10 × 5 ml of 10% aqueous AcOH. The fractions were joined and lyophilized. Products were purified by MPLC and/or semipreparative HPLC, volatiles were removed under vacuum and the remaining solutions were lyophilized.

AGYRA

A total of 350 mg of peptidyl-resin were treated with thiophenol following the protocol described above to remove the Dnp protecting group. The acidolytic treatment of the resulting material afforded 118 mg (23 μmol) of the crude peptide (79%), which was eluted under MPLC conditions with a 20–48% convex gradient of organic component. The peptide was further eluted under semi-preparative HPLC conditions with a 25–45% linear gradient of organic component over 30 min to give 30.7 mg (5.1 μmol, 23% recovery; 13% overall yield). HPLC: rt, 20.3 min; 25–45% of B over 30 min. Matrix-assisted laser desorption ionization/time of flight-mass spectrometry (MALDI/TOF-MS): m/z 3952.5; $C_{180}H_{292}N_{51}O_{49}$ requires 3952.2.

AGYRM

A total of 838 mg of peptidyl-resin were treated with thiophenol following the protocol described above to remove the Dnp protecting group. The acidolytic treatment of the resulting material afforded 308 mg (56.9 μmol) of the crude peptide (85%), which was eluted under MPLC conditions with a 23–48% convex gradient of organic component. The peptide was further eluted under semi-preparative HPLC conditions with a 30–40% linear gradient of organic component over 30 min to give 46.5 mg (7.8 μmol, 21% recovery; 12% overall yield). HPLC: rt, 20.9 min; 25–45% of B over 30 min. MALDI/TOF-MS; m/z 3981.1; $C_{183}H_{299}N_{52}O_{47}$ requires 3977.3.

CAGYRA

A total of 957 mg of peptidyl-resin were treated with thiophenol following the protocol described above to remove the Dnp protecting group. The acidolytic treatment of the resulting material afforded 263 mg (56 μmol) of the crude peptide (80%), which was eluted under MPLC conditions with a 23–38% convex gradient of organic component. The peptide was further eluted under semi-preparative HPLC conditions with a 30–40% linear gradient of organic component over 30 min to give 8.3 mg (1.6 μmol, 15% recovery; 7% overall yield). HPLC: rt, 20.2 min; 25–45% of B over 30 min. MALDI/TOF-MS: m/z 4055.2; $C_{183}H_{297}N_{52}O_{50}S$ requires 4055.8.

CAGYRM

A total of 513 mg of peptidyl-resin were treated with thiophenol following the protocol described above to remove the Dnp protecting group. The acidolytic treatment of the resulting material afforded 146 mg (23.5 μmol) of the crude peptide (75%), which was eluted under MPLC conditions with a 18–40% convex gradient of organic component. The peptide was further eluted under semi-preparative HPLC conditions with a 30–40% linear gradient of organic component over 30 min to give 9.2 mg (1.4 μmol, 16% recovery; 6% overall yield). HPLC: rt, 21.5 min; 25–45% of B over 30 min. MALDI/TOF-MS: m/z 4080.5; $C_{186}H_{304}N_{53}O_{48}S$ requires 4080.3.

Affinity Chromatography

CFX Immobilized on Sepharose. CFX was immobilized on epoxy-activated Sepharose as previously reported [19]. To 2 g of the polymeric support were added 200 mg of CFX in 6 ml of 0.3 M carbonate buffer (pH 9.5). The mixture was left for 17 h at 37°C when 0.55 ml of ethanolamine were added and reacted for 4 h at 37°C. After washings with carbonate buffer (pH 9.5), water, acetate buffer (pH 4), water, 5 M urea and water, a 1-ml column was packed and equilibrated with standard buffer (5 mM Tris–HCl, pH 7.2/20 mM NaCl/5 mM $MgCl_2$).

To the column were added DNA (pBS or ssDNA; 20 μl), peptide (AGYRA or AGYRM; 200 μM standard buffer solution) or mixtures of both and the samples were left into the column for 1 h at room temperature under gentle rocking. Further washings with standard buffer were performed until no absorbance at 260 nm (DNA) or no fluorescence at 303 nm were detected. The column was washed with 4 M NaCl before equilibration.

Peptide Immobilized on Sepharose. Peptides CAGYRA and CAGYRM were anchored to a 2 ml batch of Sepharose resin previously functionalized with MCA, following the supplier's recommendations. Before coupling the linker, the polymeric support was put into a polypropylene syringe fitted with a polyethylene disc and washed as follows: (1) 0.5 M aqueous NaCl solution, 10 × 5 ml; (2) overnight equilibraiton with at 4°C with 0.5 M aqueous NaCl solution; (3) 0.5 M aqueos NaCl solution, 10 × 5 ml; (4) water, 10 × 10 ml. The resin was then transferred to a 50 ml round-bottom flask containing a solution of 63 mg (15 eq) of MCA in 4 ml of water/EtOH (2.5:1.5) at pH 4.5. To this mixture were added, with smooth magnetic stirring, 58 mg (15 eq) of EDC. The pH was

adjusted and kept between 4.5 and 6 during 1 h with diluted NaOH solution. After 14 h at room temperature, the slightly ninhydrin-positive functionalized polymeric support [25] was transferred to a syringe fitted with a polyethylene disc and washed as follows: (1) water/EtOH (2.5:1.5), 10 × 10 ml; (2) acetate buffer (0.5 M NaCl, pH 3.8) and Tris–HCl (0.5 M NaCl, pH 7.2), 10 × 10 ml alternatively; (3) water, 10 × 10 ml; (4) EtOH, 3 × 10 ml; (5) water, 10 × 10 ml. To the resulting resin were added 4 ml (2000 eq) of 1 M aqueous AcOH and 387 mg (100 eq) of EDC. A negative ninhydrin test was achieved after leaving the mixture for 5 h with smooth mechanical stirring at room temperature. Then, half of the resin was transferred to a 2 ml polypropylene syringe fitted with a polyethylene disc and 1.5 ml of a peptide (CAGYRA, 0.85 μmols; CAGYRM, 0.71 μmols) solution in phosphate buffer (pH 7.8) with a few drops of 20% aqueous AcOH were added. The mixture was left at room temperature for 16 h with smooth mechanical stirring, when the resin was filtered and washed with water and diluted aqueous AcOH. The resin was packed and equilibrated in a 1 ml column with standard buffer (5 mM Tris–HCl, pH 7.2/20 mM NaCl/5 mM $MgCl_2$). Peptides CAGYRA and CAGYRM were coupled with yields of 67% (0.6 μmols) and 71% (0.55 μmols), respectively, as determined by amino acid analysis of the filtrates. Both peptide-resins were stored in 2 ml of 5 mM Tris–HCl buffer (pH 7.2) at 4°C.

To the columns thus prepared were added the DNA samples (pBS or ssDNA; 20 μl) or the CFX samples (200 μl, 60 μM standard buffer solution), and they were left into the columns for 1 h at room temperature under gentle rocking. Further washings with standard buffer were performed until no absorbance at 260 nm (DNA) or no fluorescence at 417 nm were detected. CFX was added after 30 min of loading the column with DNA when mixtures of DNA and the quinolone were used to carry out the binding experiments. The column was washed with 4 M NaCl before equilibration.

Binding Experiments

The samples consisted of 500 μl reaction mixtures in standard buffer containing: (a) 5 pmol of DNA and different amounts of CFX (binding of CFX to DNA); (b) 5 pmol of DNA and different amounts of AGYRA or AGYRM (binding of the peptide to DNA); (c) 5 pmol of DNA, 1000 pmol of AGYRA or AGYRM and different amounts of CFX (binding of CFX to the DNA/peptide complex). Mixtures (a) and (b) were incubated at 32°C for 60 min and were transferred to the Microcon devices. In the case of mixture (c), DNA and the peptide were preincubated at 32°C for 30 min before adding CFX. A further incubation of 30 min at 32°C was performed and the mixture was transferred to the Microcon device. The membrane lots were tested prior to use following Shen and Pernet's recommendations [26]. Samples were centrifuged at 12.000 rpm (10483 × g) for 15 min and the filtrates were collected in the reservoir on the lower end of the device. The amount of ligand bound was calculated by subtracting the amount of free ligand in the reaction mixture from the initial amount of ligand (both of them determined by measuring the intrinsic fluorescence intensity of CFX and the peptide). All of the binding data were analysed using the Klotz plots [27] in which the apparent dissociation constant is the midpoint of the saturation curve.

RESULTS

Peptide Design

In order to design peptide mimics of DNA gyrase to be used in the study of quinolone/peptide–DNA complex interactions, we focussed our attention on gyrA, which is the subunit of the enzyme where quinolones display their inhibitory effect [2]. Reece and Maxwell [28] identified by protein engineering the fragment 7-523 as the smallest domain in *E. coli* gyrA with DNA-cleavage activity when complexed with gyrB. Recently, the crystal structure determination of this domain has revealed structural details about the sites that are believed to be involved in quinolone/DNA recognition and DNA cleavage [29]. Thus, a helix-turn-helix motif at the *N*-proximal head and a cluster of positively charged residues surrounding Tyr-122 have been proposed as the binding site and the active site of the breakage-reunion reaction, respectively, the two sites being close to each other. The helix-turn-helix motif is also considered the quinolone resistance-determining region since most mutations in resistant strains are located in its sequence (residues 66–92). In this connection, special attention has to be paid to the *C*-terminal helical fragment (residues 81–92) because of the high number of mutations that have been found in this segment so far [8,9,18,30–32].

According to these results, we thought that a good starting point for this study was to consider for peptide design the helix mentioned above and a

short sequence of the native protein containing the active site Tyr-122. Therefore, two fragments of the protein sequence, one including the *C*-terminal helix of the helix-turn-helix motif and the other including Tyr-122, were chosen to be part of the primary structure of the model peptide. Their lengths were set according to the presence of basic residues in the corresponding sequences. In this sense, it has to be pointed out that there are several of such residues (Lys, His and Arg) in the protein at the *N*-proximal extreme of the helix and near Tyr-122 that could be involved in electrostatic interactions with the DNA phosphate groups. Finally, we decided to replace the 23 amino acid long native sequence that connects the two fragments by a flexible linker to simplify the synthetic problem. Taking into account all these considerations, the model peptide AGYRA was built using the natural fragments 75–92 and 116–130, and two residues of Ahx to connect them (Figure 1).

Quinolone resistance seems to be a consequence of the loss of binding of the drug to the gyrase/DNA complex induced by mutations in the enzyme sequence [8]. This observation prompted us to include in this work a comparative study between AGYRA and an analogue that mimic a mutated gyrA. According to what was described in the literature, mutations have been found at positions 83 and 87 in most cases [8,9,18,30,32]. In particular, mutations of Ser-83 to Leu and Asp-87 to Asn induce high levels of resistance to the quinolone CFX [18]. These results prompted us to consider for this study CFX and AGYRA together with its analogue AGYRM, the peptide that mimics the mutated gyrA (Figure 1). Both peptides were acetylated at the *N*-terminus and have a carboxamide group at the *C*-terminus in order to mimic the presence of amide bonds at these positions in the protein. Moreover, Met residues were substituted by Nle residues (Nle can be considered an isoster of Met) in order to prevent undesired oxidation and/or alkylation processes during the synthesis of the peptides.

Our goal was to determine whether CFX could stabilize a ternary complex with DNA and AGYRA, the gyrA model compound, and furthermore, whether such a complex could or could not form in the presence of AGYRM. To this purpose, we designed assays based on affinity chromatography. In doing that, we considered the possibility of having the peptide or the quinolone covalently anchored to the resin in order to know how the substrate bound to a polymeric support affects the experimental results. With the aim of immobilizing the peptides AGYRA and AGYRM on a polymeric support, their analogues with a Cys residue at the *N*-terminal position were also prepared (CAGYRA and CAGYRM, respectively). This residue would allow the binding of the peptide chain to the resin through the thiol function of the Cys side chain.

Peptide Synthesis

The peptides were synthesized by the solid-phase methodology using the Boc/Bzl strategy and *p*-MBHA as the polymeric support (Figure 2). Some difficulties were encountered during the assembling of the peptide chains under the standard conditions. Thus, the DIPCDI/HOBt coupling system proved to be efficient for residues 119–130, but PyBOP had to be used for residues 75 to 92, *ZZ*, and 116–118 in order to get acceptable coupling yields.

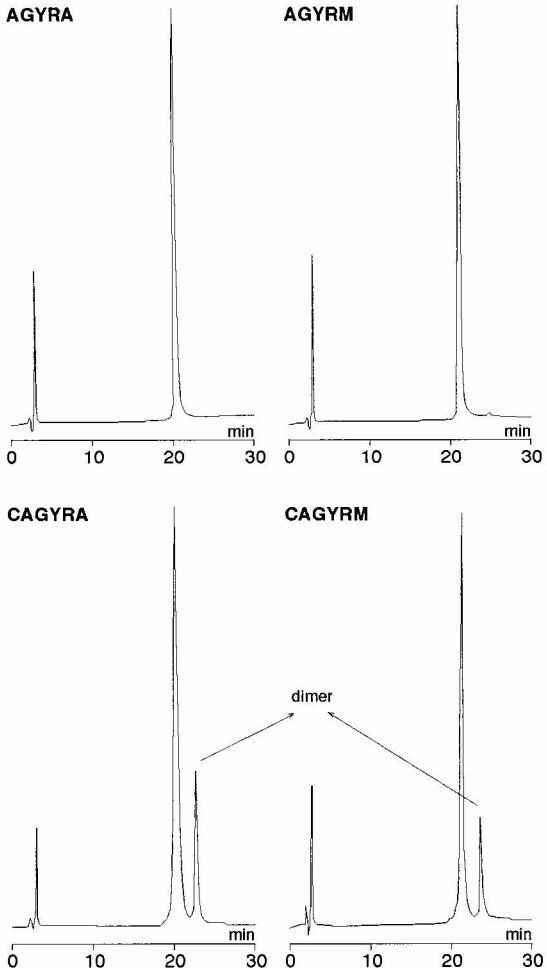

Figure 2 Chromatographic profiles of the peptides used in this study. See 'Materials and Methods' section for HPLC conditions.

On the other hand, additional TFA treatments were necessary from residue 83 to achieve full N^{ε}-amino deprotection.

As revealed by HPLC, in part the Cys containing peptides CAGYRA and CAGYRM underwent oxidation (dimerization) during the purification and the lyophilization steps (Figure 2). The dimers, $[CAGYRA]_2$ and $[CAGYRM]_2$, which were easily identified by MALDI/TOF-MS (8019 and 8162, respectively), had retention times higher than those found for the monomers (22.8 min and 24.0 min, compared to 20.2 min and 21.5 min, respectively). The fact that CAGYRA and CAGYRM have a tendency to aggregate, as revealed by circular dichroism (CD; results not shown), could explain the propensity of these peptides to dimerize.

CFX Affinity Chromatography

With the purpose of obtaining evidence on the formation of a ternary complex among CFX, DNA and the peptide model AGYRA, the first assays were performed using the quinolone bound to a polymeric support. To this aim an epoxy-activated Sepharose was utilized, to which the drug was anchored by alkylation of the secondary amino group under standard conditions (Figure 3(A)).

The peptides and DNA were detected following the fluorescence emission at 303 nm (excitation at 280 nm) and the UV adsorption at 260 nm, respectively. The chromatographic behaviours of peptide and DNA using the drug-immobilized column are shown in Figure 4 (A and B). Both DNAs, pBS and ssDNA (Figure 4(A), see inset for the latter), were retained in the column as demonstrated by their elution when the ionic strength was increased. On the contrary, AGYRA had no affinity for the CFX column in the absence of DNA (Figure 4(A)), but retention of both species was observed when a mixture of the peptide and DNA was utilized (Figure 4(B), see inset for ssDNA). The peptide mimic of the mutant gyrA AGYRM behaved as AGYRA in the absence of DNA (results not shown), but, unfortunately, the assay with a mixture of this peptide with DNA failed due to the insolubility of the components in the standard buffer. The assays with DNA were carried out in the presence of Mg^{2+} since it was reported that this cation stabilizes the quinolone–DNA complex through interactions with both species [4,6,7]. Experiments performed in our laboratory with the column mentioned above in the absence of Mg^{2+} did not show any retention of DNA (results not shown). The peptides and DNA were unable to bind

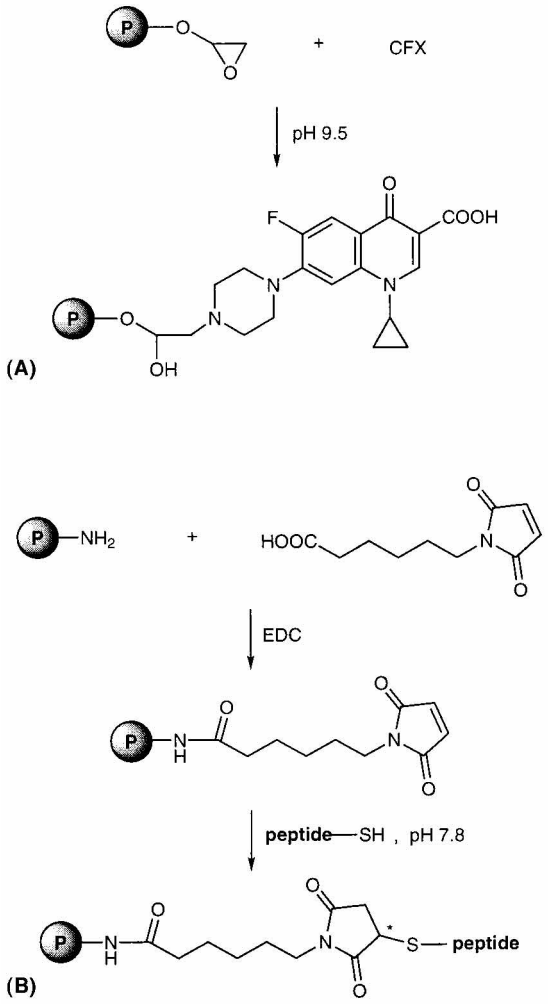

Figure 3 Anchorage of the quinolone CFX (A) and the peptides CAGYRA and CAGYRM (B) to Sepharose. * New chiral centre.

to the resin in a control experiment carried out using unmodified Sepharose.

It is interesting to point up the different chromatographic behaviour of pBS and ssDNA (see for example Figure 4(A)). Thus, DNA was retained in both cases but a higher ionic strength was needed for the total elution of ssDNA, which indicates a preferential binding of the quinolone to ssDNA rather than to pBS.

Peptide Affinity Chromatography

Peptide models were immobilized on a Sepharose resin that was previously functionalized by reaction with MCA (Figure 3(B)). Peptide chains were coupled to the polymeric support using CAGYRA or CAGYRM (Figure 1), by the nucleophilic addition of

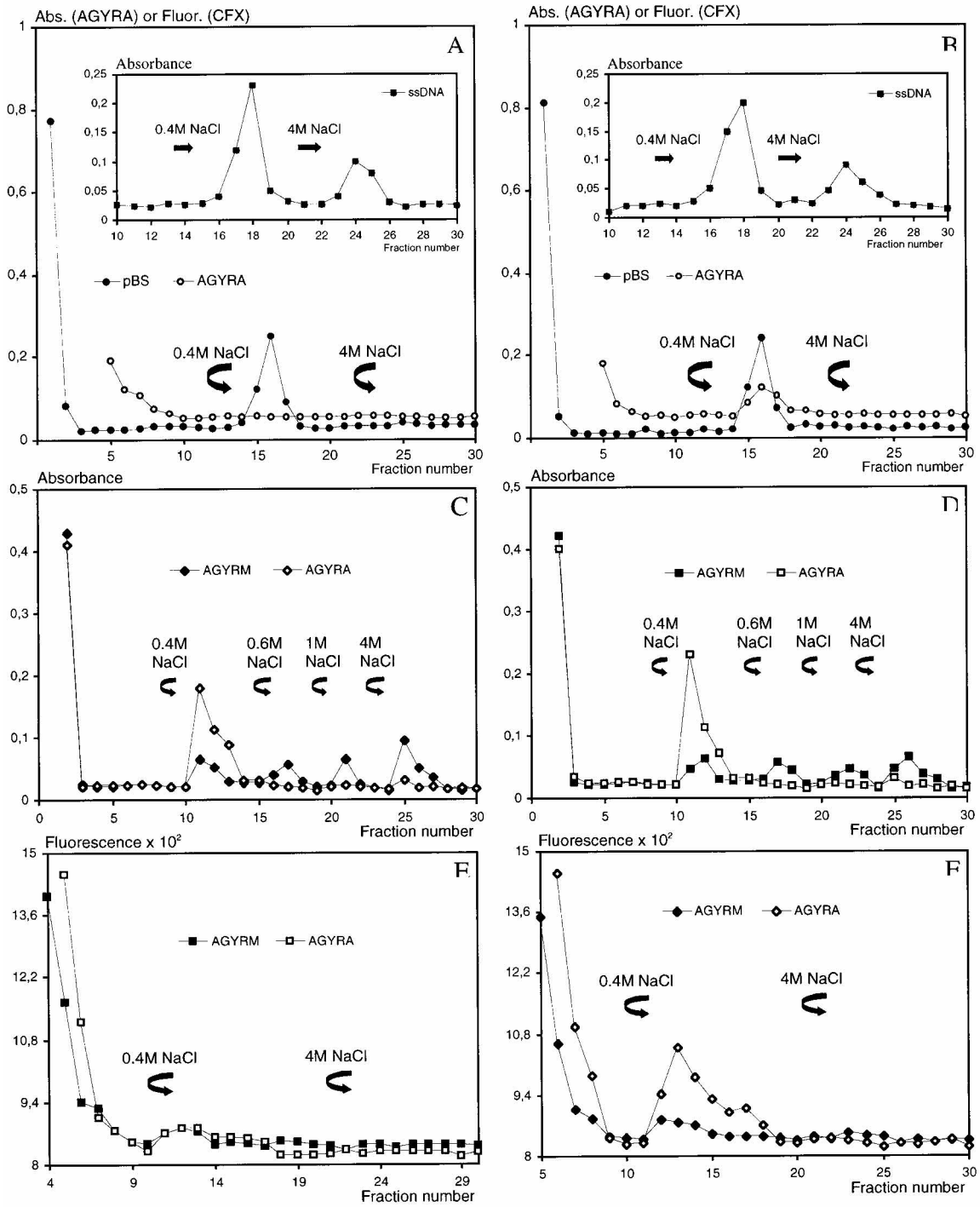

Figure 4 Affinity chromatography experiments with CFX (A and B) and AGYRA or AGYRM (C–F) bound to the polimeric support. (A) AGYRA or DNA alone. (B) A mixture of AGYRA and DNA. (C) pBS. (D) ssDNA. (E) CFX. (F) A mixture of CFX and pBS. The same scale applies for fluorescence and absorbance data in A and B (DNA, absorbance at 260 nm; peptide, fluorescence at 303 nm; CFX, fluorescence at 417 nm). Mobile phase: 5 mM Tris–HCl (pH 7.2), 20 mM NaCl/5 mM $MgCl_2$. Fractions 15–30 (A and B) and 11–30 (C–F) were eluted with the same buffer containing 0.4 or 4 M NaCl and 0.4, 0.6, 1 or 4 M NaCl, respectively, as indicated. Fractions having absorbance or flouresence values out of scale are not presented.

the Cys side-chain thiol group to the double bond of the maleimido function. This process produces a new chiral centre in the pyrrolidinedione ring and, therefore, a mixture of two diastereomeric peptides.

Figure 4(C and D) shows the results concerning the affinity of DNA to the peptide-resins mentioned above. CFX and DNA were detected following the fluorescence emission at 400 nm (excitation at 330 nm) and as already described, respectively. Unlike the study carried out with the drug anchored to a resin, the fact of using the peptides bound to a polymeric support allowed us to determine from a qualitative point of view if they were able to interact with DNA. As indicated by the elution profiles, both DNAs, pBS and ssDNA, were retained in the columns in a similar way, a result that was independent of the presence of Mg^{2+}. On the other hand, DNA was eluted with 0.4 M NaCl when the AGYRA-resin was used, but higher salt concentrations had to be utilized to achieve the complete elution of DNA in the case of the AGYRM-resin (up to 4 M of NaCl). With regard to CFX, no appreciable affinity to the columns was observed even in the presence of Mg^{2+}, as it was found when the drug was bound to the resin (Figure 4(E)). However, CFX retention on the AGYRA-resin was detected when the drug was used together with DNA and in the presence of Mg^{2+}, as when CFX was anchored to the resin (Figure 4(F)). Interestingly, no retention of CFX on the AGYRM-immobilized column was observed under similar conditions (Figure 4(F), the corresponding assay with CFX-resin could not be done because of the insolubility of the DNA/AGYRM mixture). The chromatographic profiles presented in the Figure correspond to pBS, but identical results were obtained in the case of ssDNA. No retention of DNA was observed in a series of control assays that were performed using unmodified resin.

Binding Studies

The experiments carried out using affinity chromatography revealed interactions among DNA and the peptide or CFX. The most interesting result was that the three species studied were able to interact with each other in some way that could result in the formation of a ternary complex when the peptide mimic of gyrA (AGYRA) was utilized. However, this behaviour was not observed in the case of the peptide mimic of the mutant gyrA (AGYRM). This result prompted us to determine the binding parameters for the different systems mentioned above. The measurements were performed using the membrane filtration method [20,26]. The dissociation constants (K_d) were evaluated from the midpoint of the saturation curves resulting from Klotz plots of the amount of free ligand (peptide or CFX) against the molar binding ratio '*r*' (bound peptide or CFX/total DNA) (Figure 5) [27].

As already found using affinity chromatography, CFX binds to both pBS and ssDNA in the presence of Mg^{2+} (Figure 5(A)). A preferential binding of the drug to ssDNA was also observed in this case (2–3-fold in relation to pBS, entry 'a' of the table). As shown in the table of Figure 5 (entries 'b' and 'c'), a similar result was obtained for the interaction of DNA with the model peptides. On the other hand, the peptide mimic of mutated gyrA, AGYRM, binds to DNA more efficiently than AGYRA (Figure 5(B and C); $K_d[\text{AGYRA} - \text{ssDNA}]/K_d[\text{AGYRAM} - \text{ssDNA}] = 7$, $K_d[\text{AGYRA} - \text{pBS}]/K_d[\text{AGYRAM} - \text{pBS}] = 4$), which is in agreement with our observations using affinity chromatography.

Regarding the interaction of CFX with DNA in the presence of peptide, the experiments carried out with mixtures of the three species yielded interesting results. Thus, the drug binds to both pBS and ssDNA when AGYRA is used, as it was expected from the results achieved with the peptide anchored to a polymeric support (Figure 5(D), entry 'd' of the table; the saturation curve that is shown corresponds to pBS). However, the K_d value for this process is similar to that found in the absence of peptide, suggesting that DNA might have different binding sites for CFX and the peptide mimic AGYRA (compare entries 'a' and 'd' of the table). Finally, no interaction of the drug with DNA was detected in the presence of the peptide mimic of the mutant gyrA (AGYRM) in agreement with the results obtained using affinity chromatography (Figure 5(D), entry 'e' of the table).

DISCUSSION

The binding assays carried out with CFX, DNA and the peptide models that were designed as mimics of gyrA (wild type and mutant) confirmed important features already known about the mechanism of action of quinolones. From the point of view of the experimental techniques used in this work, similar conclusions can be drawn from the results achieved with the affinity chromatography approach and the membrane filtration method.

Nowadays, it seems obvious that antibacterial quinolones inhibit DNA gyrase by trapping the

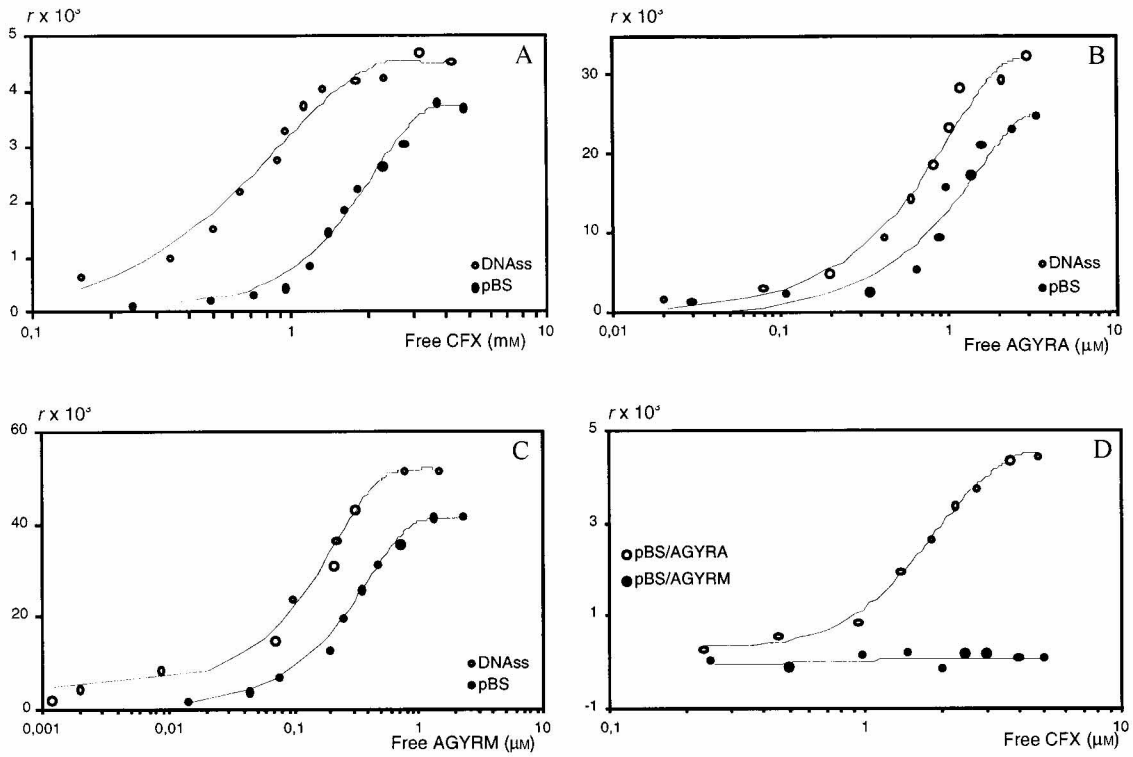

Entry	Ligand	K_d (x 10^{-7} M)	
		Supercoiled plasmid (pBS)	Single-stranded calf thymus DNA (ssDNA)
a	CFX	18.0	8.7
b	AGYRA	10.0	7.0
c	AGYRM	2.5	1.0
d	CFX/AGYRA[a]	16.0	6.9
e	CFX/AGYRM[a]	-[b]	-[b]

[a] CFX was added to a preincubated mixture containing DNA and a peptide mimic.
[b] No binding was observed.

Figure 5 Binding determinations using Klotz plots. (A) pBS (5 pmol) or ssDNA (5 pmol) and CFX (0.25–5 μM). (B) pBS (5 pmol) or ssDNA (5 pmol) and AGYRA (0.1–5 μM). (C) pBS (5 pmol) or ssDNA (5 pmol) and AGYRM. (D) pBS/AGYRA (5 pmol/1 nmol) and CFX (0.25–5 μM) or pBS/AGYRM (5 pmol/1 nmol) and CFX (0.25–5 μM). The midpoint of the saturation curve represents the apparent dissociation constant in all cases ('*r*' stands for molar binding ratio).

enzyme as a complex with DNA, the formation of which is the key event for the topoisomerase to develop its biological activity. The molecular details of the binding site in the ternary complex are unknown, but studies carried out in the absence of gyrase have revealed that the drug interacts with

DNA [5,6,20,26,33]. On the other hand, it is known that the quinolone has low or no affinity for the DNA-free topoisomerase, [8,9,19,26,27] but how the drug binds to the enzyme in the ternary complex still remains unclear.

From a qualitative point of view, a parallel behaviour was found for AGYRA, the peptide mimic of gyrA. Thus, AGYRA is unable to bind CFX, no matter whether the quinolone (Figure 4(A)) or the peptide (Figure 4(E)) are attached to a polymeric support. However, both species bind DNA, as shown by the retention of pBS and ssDNA on the quinolone-immobilized (Figure 4(A)) and peptide-immobilized (Figure 4(C and D)) columns. The affinity chromatography also revealed the formation of a ternary complex when AGYRA (Figure 4(B)) and CFX (Figure 4(F)) were retained into the columns mentioned above, respectively, in the presence of DNA. As already reported in the literature, Mg^{2+} was required in order to promote the interaction of the drug with DNA [4,6,7,19,34,35]. These qualitative results were corroborated by the membrane filtration technique, which allowed K_d values to be determined for the binding of CLX and AGYRA to DNA and the binding of the quinolone to the peptide/DNA complex (table of Figure 5; entries 'b', 'a' and 'd', respectively).

The apparent dissociation constant for the binding of CFX to peptide-free DNA was of the same order of magnitude that the one obtained for the potent DNA gyrase inhibitor norfloxacin (an ethyl group at position N1, Figure 1) using a cooperative binding model (1×10^{-6} M) [26]. In this connection, it has to be pointed out that similar supercoiling inhibition constants have been described for both quinolones [3]. On the other hand, the affinity of AGYRA for DNA ($K_d \approx 10^{-6}$ M for pBS) proved to be much lower than the one reported for DNA gyrase ($K_d \approx 10^{-10}$ M) [36], which is not surprising considering the size of the natural protein.

CFX binds preferentially to ssDNA rather than to pBS, which is in agreement with the data described by other authors [20,26,36]. In this sense, it has been suggested that the drug binds to ssDNA in a non-intercalative way through hydrogen bonds that become available when the bases are unpaired by unwinding of the double strand upon binding of the DNA to gyrase [20,29,37]. The need of 4 M NaCl for full elution of ssDNA from the CFX-immobilized column also revealed a higher affinity of the quinolone for ssDNA since the same result was achieved with 0.4 M NaCl in the case of pBS (Figure 4(A)). However, both techniques afforded different results for the binding of AGYRA to DNA. Thus, the membrane filtration technique showed a preferential binding of the peptide to ssDNA, but similar chromatographic profiles were obtained for both DNAs with the peptide-immobilized column (full elution with 0.4 M NaCl in both cases, Figure 4(C and D)).

According to the K_d values for the AGYRA/DNA and CFX/DNA complexes, the peptide binds to ssDNA and pBS more efficiently than the quinolone, which could be explained in terms of the nature of the interactions that are responsible for binding. As in the case of the binding of basic proteins such as histones to DNA [38], the presence of seven basic residues in AGYRA is probably the key feature for the binding of the peptide to DNA through electrostatic interactions between these residues and the phosphate groups of the nucleic acid [29]. However, experimental data and molecular modelling studies [3,7,34] seem to indicate that the quinolone interacts with DNA through its carboxyl and carbonyl moieties (Figure 1) to form a complex in which Mg^{2+} acts as a bridge between a phosphate group of DNA and the drug.

The fact that AGYRA and CFX had affinity for the quinolone-immobilized and the peptide-immobilized columns, respectively, in the presence of DNA and Mg^{2+} (Figure 4(B and F)) revealed the formation of a ternary complex. This result is not surprising if the retention is a consequence of the simultaneous interaction of DNA with the peptide and the quinolone. It has to be pointed out that the specific interactions involved in the stabilization of the gyrase/DNA/quinolone complex at the quinolone-binding site are still a matter of controversy. In this connection, it has been speculated about the possibility that the binding of the drug to DNA gyrase through hydrogen bonding between the secondary amino group (Figure 1) and Asp-87 might play a crucial role [3,7]. However, AGYRA was retained on the column in spite of having CFX covalently bound to the polymeric support by the piperazine group at this position. Moreover, from a qualitative point of view, similar results were achieved with both columns under the conditions used to carry out the assays, that is, no matter the quinolone or the peptide was anchored to the polymeric support (full elution with 0.4 M NaCl in both cases).

Studies carried out with norfloxacin revealed the appearance of new binding sites for the quinolone in the enzyme–DNA complex as a consequence of the interaction between the two species [3,39]. Interestingly, the formation of a specific binding site by

combination of a gyrase promoted unwound DNA region with number of residues on the protein has been recently suggested [37]. As shown in Figure 4(A and B), the affinity chromatography analysis did not bring any evidence about an increase of the binding of CFX to DNA in the presence of AGYRA (compare the chromatographic profiles for ssDNA and pBS). The results achieved with the membrane filtration technique were not conclusive either, in spite of the fact that the K_d values for the binding of the quinolone to the AGYRA/DNA complex were slightly lower than those found for the binding to the peptide-free DNA (Figure 5, compare entries 'a' and 'd' of the table for both DNAs).

The binding of the peptide mimic of mutated gyrA, AGYRM, to DNA proved to be more efficient than that of AGYRA (Figure 4(C and D) and Figure 5). The change of the effective charge of the peptide from $+2$ to $+3$ as a consequence of the mutation of Asp to Asn at position 87 could explain the higher affinity of AGYRM for DNA in terms of additional electrostatic interactions with the negatively charged phosphate groups. On the other hand, as it was already found for AGYRA, AGYRM had more affinity for ssDNA than for pBS according to the corresponding K_d values, although the chromatographic profiles obtained using the peptide anchored to the polymeric support were not conclusive on this point. However, the most intriguing results were obtained when CFX was used with the model peptide AGYRM. Unlike what was observed in the case of AGYRA, CFX did not bind to DNA in the presence of AGYRM, as revealed by the affinity chromatography and membrane filtration techniques (Figure 4(F) and Figure 5(D), entry 'e' of the table). This behaviour is in agreement with what was found by Willmott and Maxwell [8] for the quinolone norfloxacin and gyrase A with a mutation that confers quinolone resistance (Ser-83 to Trp). In that case, the enzyme showed greatly reduced drug binding. These results indicate that the model peptide AGYRA contains enough structural information to induce the formation of the ternary complex with CFX and DNA through mutual interactions among the three species. Mutations at the critical positions 83 and 87 produce structural changes that result in a destabilization of the complex, as it probably happens in the natural environment [40,41].

Many studies reported in the literature point to the fact that formation of the ternary complex is crucial for the drug to inhibit DNA gyrase activity. If so, according to the results obtained in this work, the use of short peptides such as AGYRA and AGYRM in DNA binding studies could be a suitable approach to a preliminary evaluation of quinolones as potential drugs.

In summary, the binding data reported in this work strongly suggest that the use of short peptides including sequences of gyrA provides an alternative way to study the interaction of quinolones with the DNA/gyrA complex, in order to get an insight into the mechanisms of antibiotic resistance. Moreover, we believe that AGYRA constitutes a starting point for the *de novo* design of peptides able to mimic the structural features of gyrA at the quinolone binding site and, therefore, it is potentially useful in the search for new drugs with antibiotic activity.

Acknowledgements

We thank Carmen Romera for help with the plasmid preparation. We also thank the Brazilian FAPESP (96/4103-1) agency for postdoctoral fellowship to R. Marchetto and CICYT (PB95-1131) and Generalitat de Catalunya (1995SGR494 and CeRBa) for financial support.

REFERENCES

1. Gellert M, Mizuuchi K, O'Dea MH, Nash HA. DNA gyrase: an enzyme that introduces superhelical turns into DNA. *Proc. Natl Acad. Sci. USA* 1976; **73**: 3872–3876.
2. Reece RJ, Maxwell A. DNA gyrase: structure and function. *Crit. Rev. Biochem. Mol. Biol.* 1991; **26**: 335–375.
3. Shen LL, Mitscher LA, Sharma PN, O'Donnell TJ, Chu DWT, Cooper CS, Rosen T, Pernet AG. Mechanism of inhibition of DNA gyrase by quinolone antibacterials: a co-operative drug-DNA binding model. *Biochemistry* 1989; **28**: 3886–3894.
4. Palumbo M, Gatto B, Zagotto G, Palù G. On the mechanism of action of quinolone drugs. *Trends Microbiol.* 1993; **1**: 232–235.
5. Freudenreich CH, Kreuzer KN. Mutational analysis of a type II topoisomerase cleavage site: distinct requirements for enzyme and inhibitors. *EMBO J.* 1993; **12**: 2085–2097.
6. Fan JY, Sun D, Yu H, Kerwin SM, Hurley LH. Self-assembly of a quinobenzoxazine–Mg^{2+} complex on DNA: a new paradigm for the structure of a drug–DNA complex and implications for the structure of the quinolone bacterial gyrase–DNA complex. *J. Med. Chem.* 1995; **38**: 408–424.
7. Llorente B, Leclerc F, Cedergren R. Using SAR and QSAR analysis to model the activity and structure of the quinolone–DNA complex. *Bioorg. Med. Chem.* 1996; **4**: 61–71.

8. Willmott CJR, Maxwell A. A single point mutation in the DNA gyrase A protein greatly reduced binding of fluoroquinolones to the gyrase–DNA complex. *Antimicrob. Agents Chemother.* 1993; **37**: 126–127.
9. Yoshida H, Nakamura M, Bogaki M, Ito H, Kojima T, Hattori H, Nakamura S. Mechanism of action of quinolones against *Escherichia coli* DNA gyrase. *Antimicrob. Agents Chemother.* 1993; **37**: 839–8453.
10. Kreuzer KN, Cozzarelli NR. *Escherichia coli* mutants thermosensitive for deoxyribonucleic acid gyrase subunit A: effects on deoxyribonucleic acid replication, transcription, and bacteriophage growth. *Bacteriol.* 1979; **140**: 424–435.
11. Liu LF. DNA topoisomerase poisons as antitumor drugs. *Annu. Rev. Biochem.* 1989; **58**: 351–375.
12. Maxwell A. The molecular basis of quinolone action. *Antimicrob. Agents Chemother.* 1992; **30**: 409–414.
13. Willmott CJR, Critchlow SE, Eperon IC, Maxwell A. The complex of DNA gyrase and quinolone drugs with DNA forms a barrier to transcription by RNA polymerase. *J. Mol. Biol.* 1994; **242**: 351–363.
14. Critchlow SE, Maxwell A. DNA cleavage is not required for the binding of quinolone drugs to the DNA gyrase–DNA complex. *Biochemistry* 1996; **35**: 7387–7393.
15. Hiasa H, Yousef DO, Marians KJ. DNA strand cleavage is required for replication fork arrest by a frozen topoisomerase–quinolone–DNA ternary complex. *J. Biol. Chem.* 1996; **271**: 26424–26429.
16. Marians KJ, Hiasa H. Mechanism of quinolone action. A drug-induced structural perturbation of the DNA precedes strand cleavage by topoisomerase IV. *J. Biol. Chem.* 1997; **272**: 9401–9409.
17. Horowitz DS, Wang JC. Mapping the active site tyrosine of *Escherichia coli* DNA gyrase. *J. Biol. Chem.* 1987; **262**: 5339–5344.
18. Vila J, Ruiz J, Marco F, Barcelo A, Goñi P, Giralt E, Jimenez De Anta T. Association between double mutation in gyrA gene of ciprofloxacin-resistant clinical isolates of *Escherichia coli* and MICs. *Antimicrob. Agents Chemother.* 1994; **38**: 2477–2479.
19. Khac SBP, Moreau N. Interactions between fluoroquinolones, Mg^{2+}, DNA and DNA gyrase, studied by phase partitioning in an aqueous two-phase system and by affinity chromatography. *J. Chromatogr. A* 1994; **668**: 241–247.
20. Shen LL, Baranowski J, Pernet AG. Mechanism of inhibition of DNA gyrase by quinolone antibacterials: specificity and cooperativity of drug binding to DNA. *Biochemistry* 1989; **28**: 3879–3885.
21. Sambrook J, Fritsch EF, Maniatis T. *Molecular Cloning: A Laboratory Manual* (2nd edn). Cold Spring Harbor Laboratory Press: Cold Spring Harbor, NY, 1989.
22. Birnboim HC, Doly J. A rapid alkaline extraction procedure for screening recombinant plasmid DNA. *Nucleic Acids Res.* 1979; **7**: 1513–1523.
23. Barany G, Merrifield RB. Solid-phase peptide synthesis. In *The Peptides: Analysis, Synthesis and Biology*, Gross E, Meienhofer J (eds). Academic Press: New York, 1980; 3–286.
24. Stewart JM, Young JD. *Solid Phase Peptide Synthesis* (2nd edn). Pierce Chem. Co: Rockford, IL, 1984.
25. Kaiser E, Colescott RL, Bossinger CD, Cook PI. Color test for detection of free terminal amino groups in the solid-phase synthesis of peptides. *Anal. Biochem.* 1970; **34**: 595–598.
26. Shen LL, Pernet AG. Mechanism of inhibition of DNA gyrase by analogues of nalidixic acid: the target of the drugs is DNA. *Proc. Natl. Acad. Sci. USA* 1985; **82**: 307–311.
27. Klotz IM. Protein interactions with small molecules. *Acc. Chem. Res.* 1974; **7**: 162–168.
28. Reece RJ, Maxwell A. Probing the limits of the DNA breakage-reunion domain of the *Escherichia coli* DNA gyrase A protein. *J. Biol. Chem.* 1991; **266**: 3540–3546.
29. Morais Cabral JH, Jackson AP, Smith CV, Shikotra N, Maxwell A, Liddington RC. Crystal structure of the breakage-reunion domain of DNA gyrase. *Nature* 1997; **388**: 903–906.
30. Korten V, Huang WM, Murray BE. Analysis by PCR and direct DNA sequencing of gyrA mutations associated with fluoroquinolone resistance in *Enterococcus faecalis*. *Antimicrob. Agents Chemother.* 1994; **38**: 2091–2094.
31. Ferrero L, Cameron B, Crouzet J. Analysis of gyrA and grlA mutations in stepwise-selected ciprofloxacin-resistant mutants of *Staphylococcus aureus*. *Antimicrob. Agents Chemother.* 1995; **39**: 1554–1558.
32. Reyna F, Huesca M, González V, Fuchs LY. *Salmonella typhimurium* gyrA mutations associated with fluoroquinolone resistance. *Antimicrob. Agents Chemother.* 1995; **39**: 1621–1623.
33. Bailly C, Colson P, Houssier C. The orientation of norfloxacin bound to double-stranded DNA. *Biochem. Biophys. Res. Commun.* 1998; **243**: 844–848.
34. Palù G, Valisena S, Ciarrocchi G, Gatto B, Palumbo M. Quinolone binding to DNA is mediated by magnesium ions. *Proc. Natl. Acad. Sci. USA* 1992; **89**: 9671–9675.
35. Tornaletti S, Pedrini AM. Studies on the interaction of 4-quinolones with DNA by DNA unwinding experiments. *Biochim. Biophys. Acta* 1988; **949**: 279–287.
36. Higgins NP, Cozzarelli NR. The binding of gyrase to DNA: analysis by retention by nitrocellulose filters. *Nucleic Acids Res.* 1982; **10**: 6833–6847.
37. Kampranis SC, Maxwell A. The DNA gyrase–quinolone complex. ATP hydrolysis and the mechanism of DNA cleavage. *J. Biol. Chem.* 1998; **273**: 22615–22626.
38. Wolffe A. *Chromatin Structure and Function*. Academic Press: San Diego, CA, 1992.

39. Shen LL, Kohlbrenner WE, Weigl D, Baranowski J. Mechanism of quinolone inhibition of DNA gyrase. Appearance of unique norfloxacin binding sites in enzyme–DNA complexes. *J. Biol. Chem.* 1989; **264**: 2973–2978.
40. Zunino F, Di Marco A, Zaccara A, Gambetta R. The interaction of daunorubicin and doxorubicin with DNA and chromatin. *Biochim. Biophys. Acta* 1980; **607**: 206–214.
41. Sambrook J, Fritsch EF, Maniatis T. *Molecular Cloning: A Laboratory Manual* (2nd edn). Cold Spring Harbor Laboratory Press: Cold Spring Harbor, NY, 1989.

ANEXO 5

Journal of Peptide Science
J. Peptide Sci. **10**: 566–577 (2004)
Published online 2 April 2004 in Wiley InterScience (www.interscience.wiley.com). DOI: 10.1002/psc.565

JOURNAL OF PEPTIDE SCIENCE

A 4.2 kDa Synthetic Peptide as a Potential Probe to Evaluate the Antibacterial Activity of Coumarin Drugs

ANDREZA C. SCATIGNO,[a,b] SAULO S. GARRIDO[a] and REINALDO MARCHETTO[a]*

[a] Departamento de Bioquímica e Tecnologia Química, Instituto de Química, Universidade Estadual Paulista, Araraquara, São Paulo, Brazil
[b] Área de Ciências Exatas e da Terra, Universidade do Oeste de Santa Catarina, Videira, Santa Catarina, Brazil

Received 10 October 2003
Revised 24 November 2003
Accepted 18 December 2003

Abstract: The coumarin antibiotics are potent inhibitors of DNA replication whose target is the enzyme DNA gyrase, an ATP-dependent bacterial type II topoisomerase. The coumarin drugs inhibit gyrase action by competitive binding to the ATP-binding site of DNA gyrase B protein. The production of new biologically active products has stimulated additional studies on coumarin–gyrase interactions. In this regard, a 4.2 kDa peptide mimic of DNA gyrase B protein from *Escherichia coli* has been designed and synthesized. The peptide sequence includes the natural fragment 131–146 (coumarin resistance-determining region) and a segment containing the gyrase–DNA interaction region (positions 753–770). The peptide mimic binds to novobiocin ($K_a = 1.4 \pm 0.3 \times 10^5$ M^{-1}), plasmid ($K_a = 1.6 \pm 0.5 \times 10^6$ M^{-1}) and ATP ($K_a = 1.9 \pm 0.4 \times 10^3$ M^{-1}), results previously found with the intact B protein. On the other hand, the binding to novobiocin was reduced when a mutation of Arg-136 to Leu-136 was introduced, a change previously found in the DNA gyrase B protein from several coumarin-resistant clinical isolates of *Escherichia coli*. In contrast, the binding to plasmid and to ATP was not altered. These results suggest that synthetic peptides designed in a similar way to that described here could be used as mimics of DNA gyrase in studies which seek a better understanding of the ATP, as well as coumarin, binding to the gyrase and also the mechanism of action of this class of antibacterial drugs. Copyright © 2004 European Peptide Society and John Wiley & Sons, Ltd.

Keywords: peptides; affinity chromatography; fluorescence; peptide synthesis; solid phase; DNA gyrase; coumarins

INTRODUCTION

DNA gyrase is a bacterial type II topoisomerase that is responsible for maintaining the topological state of DNA. Gyrase catalyses the energetically unfavourable negative supercoiling of DNA by coupling this reaction to the hydrolysis of ATP [1,2]. The enzyme from *Escherichia coli* consists of two proteins, A (GyrA) and B (GyrB), of molecular masses 97 and 90 kDa, respectively, which form an A_2B_2 active complex. In addition to DNA supercoiling, gyrase can also catalyse the ATP-independent relaxation of supercoiled DNA. Mechanistic studies have revealed the steps involved in the supercoiling reaction. Briefly, this process involves the wrapping of a segment of DNA around the enzyme, the cleavage of the wrapped DNA in both strands with the formation of covalent bonds between the newly formed 5′ phosphates and Tyr-122 of GyrA, the passage of another segment of DNA through this

*Correspondence to: Dr Reinaldo Marchetto, Departamento de Bioquímica e Tecnologia Química, Instituto de Química, UNESP, Rua Prof. Francisco Degni, s/n° Caixa Postal 355, 14800-900 Araraquara, São Paulo, Brazil; e-mail: marcheto@iq.unesp.br
Contract/grant sponsor: Fundação de Amparo à Pesquisa do Estado de São Paulo (FAPESP); Contract/grant number: 99/02265-2.

double-strand break, and resealing of the broken DNA. The result is the introduction of two negative supercoils whose driving force comes from the hydrolysis of two molecules of ATP [1–3].

A number of researchers have demonstrated that the GyrA and GyrB proteins contain distinct domains. GyrA is functionally divided into a 64 kDa *N*-terminal and a 33 kDa *C*-terminal domain, mainly involved in DNA breakage-reunion and DNA wrapping, respectively [4,5]. The B protein comprises an *N*-terminal domain (43 kDa) containing the ATP-binding site [6] and a 47 kDa *C*-terminal domain that interacts with GyrA and DNA [7]. The *N*-terminal domain includes two subdomains (24 kDa *N*-terminal part and 19 kDa *C*-terminal part). The ATP binding site is located in the first subdomain [8].

Gyrase is a target of several classes of antibacterial agents (for a review, see reference [9]), the best studied being the quinolones (e.g. norfloxacin) [10] and coumarins (e.g. novobiocin) [11] drugs. Quinolones are believed to interfere with the catalytic cycle of gyrase by interactions with subunit A of the enzyme [12], while coumarins interact with the subunit B [13]. The coumarin antibiotics are natural compounds inhibiting the gyrase action by competitively binding to the ATP-binding site in the 24 kDa subdomain of GyrB protein [3,11], as previously shown by the crystal structures of the 24 kDa gyrase subdomain–inhibitor complexes [13,14].

The coumarins are potent inhibitors of the gyrase supercoiling and ATPase reactions, however, they have failed to become clinically successful due to poor cell penetration, low solubility and toxicity in eukaryotes [9]. Despite this, the fact that these compounds are significantly more potent in inhibiting DNA gyrase *in vitro* than the quinolones has stimulated interest with regard to improving their properties in order to produce structurally related compounds suitable for clinical practice. For the design of new antibiotics for this purpose, a total understanding of the structural properties of the enzyme–drug and enzyme–ATP complexes is crucial, which implies a special difficulty because of the size of these complexes. In studies of this nature the 43 or 24 kDa *N*-terminal fragments of B protein from different strains of *Escherichia coli*, have been frequently employed [6,8,11,13,14], but no data are available on the short peptides.

This fact prompted us to consider the possibility of using short synthetic peptides containing segments of GyrB involved in the recognition of coumarins, ATP and DNA as models to carry out interactions

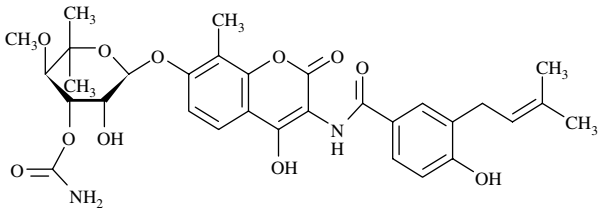

A

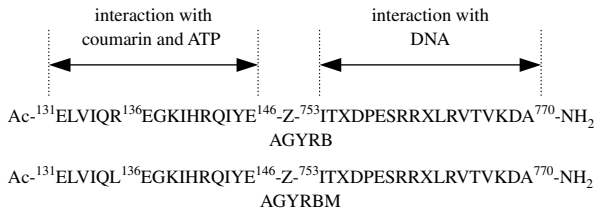

B

Figure 1 Structures of (A) novobiocin and (B) sequences of the peptide mimics of gyrase B protein (X = norleucine and Z = ε-amino caproic acid).

and structural studies. This paper reports a 4.2 kDa synthetic peptide (AGYRB) formed by a *C*-terminal region containing the residues involved in the interaction with DNA [15] and an *N*-terminal region containing the Arg residue at position 136, which is believed to be involved in the coumarin interactions [16] (Figure 1B). Affinity chromatography [17] and fluorescence quenching techniques [18] were exploited to perform the binding studies. Evidence that short peptides might constitute suitable models to study gyrase–coumarin and gyrase–ATP interactions as well as the mechanism of action of the coumarins is presented.

MATERIAL AND METHODS

Chemicals

All chemicals were of analytical grade. 9-fluorenylmethoxycarbonyl (Fmoc)-amino acids were supplied by Novabiochem (San Diego, USA) or Advanced ChemTech (Louisville, USA). 4-(2′,4′-Dimethoxyphenyl-Fmoc-aminomethyl)-phenoxyacetamido- norleucyl-p-methyl-benzhydrylamine (Rink Amide MBHA) resin (0.55 mmol g^{-1}) was purchased from Novabiochem. Epoxy-activated Sepharose 6B (19–40 μmol ml^{-1}), adenosine 5′-triphosphate-agarose (1.3 μmol ml^{-1}) and single stranded deoxyribonucleic acid-cellulose (3.5 μg g^{-1}) were from Sigma-Aldrich Company. 1-Benzotriazolyloxy-tris-pyrrolidinophosphonium hexafluorophosphate

(pyBOP), 1-hydroxybenzotriazole (HOBt) and 1-hydroxy-7-azabenzotriazole (HOAt) were purchased from Novabiochem. The N,N′-diisopropylethylamine (DIEA) and diisopropylcarbodiimide (DIPCI) were supplied by Fluka Chemical Corp. (USA). Trifluoroacetic acid (TFA) and dichloromethane (DCM) (Sigma-Aldrich USA) were peptide synthesis grade and used directly. Dimethylformamide (DMF), supplied by Mallinckrodt, was bubbled with nitrogen to remove volatile contaminants and kept stored over activated 4Å molecular sieves. N-methyl-2-pyrrolidone (NMP) was purchased from Carlo Erba (Italy). Novobiocin (sodium salt) was also from Sigma-Aldrich.

Substrate DNA

The supercoiled plasmid pBS was prepared in *Escherichia coli* strain DH5α by conventional methods [19] and was purified and stored as described by Marchetto *et al.* [17].

Spectroscopic Measurements

Ultraviolet absorbance and fluorescence measurements were made on a Shimadzu UV-visible 1601PC spectrophotometer and a Varian Cary Eclipse fluorescence spectrophotometer, respectively, both equipped with a thermostatted sample compartment, using a 1.5 ml quartz cell for a magnetic stirrer with a 1.0 cm path length. The fluorescence excitation and emission slit widths were set for 5 nm bandpass, for all measurements.

Peptide Synthesis and Purification

The AGYRB and its mutant version (AGYRBM) whose sequences are reported in Figure 1B were prepared manually, according to solid-phase synthesis methodology using Fmoc chemistry [20] with Rink amide MBHA resin and DIPCI/HOBt or pyBOP/DIEA activation. The functional side chains of Fmoc-amino acids were protected by the following groups: Bu^t for Asp, Glu, Ser, Thr and Tyr, Trt for His and Gln, Pmc for Arg and Boc for Lys. Acetylation was performed with acetic anhydride and DIEA (10 eq each). Peptides were cleaved from the resin by a TFA/water/phenol/thioanisole/1,2-ethanedithiol (82.5 : 5 : 5 : 5 : 2.5) treatment for 2 h at room temperature. The resins were washed with diethyl ether and centrifuged (5×) and the resulting suspension was washed with 10% (AGYRB) or 50% (AGYRBM) aqueous acetic acid. Crude peptides were purified by semipreparative HPLC on a Waters system using a reverse-phase Vydac-C_{18} column (25 × 2.5 cm; 10 μm particles; 300 Å porosity) with a linear gradient of 30%–60% of solvent B (A: water, 0.1% TFA; B: acetonitrile (MeCN) 75% in water, 0.1% TFA) over 90 min. The flow rate was 10 ml min^{-1} and detection was carried out at 220 nm. Analytical HPLC was carried out on a Varian ProStar apparatus employing a Nucleosil C_{18} reverse-phase column (25 × 0.46 cm; 5 μm particles; 300 Å porosity) with a 10%–70% linear gradient of solvent B (A: water, 0.045% TFA; B: MeCN, 0.036% TFA) over 30 min, flow rate 1.0 ml min^{-1} and UV detection at 220 nm. Peptide purity was estimated to be higher than 90% by amino acid analysis (6 M aqueous HCl solution at 110 °C for 72 h) on a Beckman System 6300 analyser. The identity of the peptides was confirmed by electrospray ionization mass spectrometry (ESIMS) on a ZMD model apparatus from Micromass.

Affinity Chromatography

Novobiocin immobilized on Sepharose. Novobiocin was immobilized on epoxy-activated Sepharose as previously reported with ciprofloxacin [17]. 100 mg of novobiocin in 8 ml of 0.3 M carbonate buffer (pH 9.5) was added to 1.2 g of the polymeric support. The mixture was left for 20 h at 37 °C when 0.55 ml of ethanolamine was added and reacted for more than 4 h at 37 °C. After washings with carbonate buffer (pH 9.5), water, acetate buffer (pH 4.0), water, 5 M urea and water, a 1 ml column was packed and equilibrated with standard buffer (10 mM Tris-HCl, pH 7.2/20 mM NaCl/5 mM $MgCl_2$). DNA (pBS; 100 μl, 4.37 μg/μl), peptide (AGYRB or AGYRBM; 500 μl, 20 μM standard buffer solution) or a mixture of both, were added to the column. After 1 h at room temperature and gentle rocking, washings with standard buffer were performed until no absorbance at 260 nm or no fluorescence at 304 nm were detected. The column was washed with 4 M NaCl and equilibrated with standard buffer.

DNA immobilized column. A 1 ml column was packed with a commercial single stranded deoxyribonucleic acid-cellulose and equilibrated with standard buffer (10 mM Tris-HCl, pH 7.2/20 mM NaCl/5 mM $MgCl_2$). AGYRB or AGYRBM (500 μl of a 20 μM standard buffer solution) was left in the column for 1 h at room temperature under gentle rocking. Further washings with standard buffer were performed until no fluorescence at 304 nm was

detected. The column was washed with 4 M NaCl before equilibration.

ATP immobilized column. A 1 ml column packed with adenosine 5′-triphosphate-agarose was employed for this assay. The procedures of equilibrium, washings and elution of AGYRB or AGYRBM were the same as described above for the DNA immobilized column.

Binding Experiments

Novobiocin binding to peptide. The quenching of peptide fluorescence by novobiocin was determined as a function of drug concentration as follows. Aliquots (2–50 µl) from a concentrated novobiocin stock solution (100 µM) were added to a solution of 20 µM of AGYRB or AGYRBM in standard buffer, maintained at 37 °C. Prior to measuring the peptide fluorescence, the samples were homogenized and equilibrated in the cell holder for 6 min with the excitation shutter closed. The excitation wavelength was 280 nm with emission measured at 304 nm. The observed fluorescence intensities were corrected for loss of signal due to dilution effect and for optical filtering effects caused by novobiocin absorption at 280 nm [21]. The data were represented in a Stern-Volmer plot, for static quenching, where the relative peptide fluorescence (F_0/F) was plotted against the novobiocin concentration [NB] whose slope is equal to the association constant (K_a) for complex formation [18], according to Equation (1):

$$F_0/F = 1 + K_a[\mathrm{NB}] \quad (1)$$

In this equation F_0 and F are the fluorescence intensities of peptides in the absence and presence of novobiocin, respectively.

Fluorescence quenching data, obtained by intensity measurements alone, can be explained by either a dynamic or static process. To distinguish them the temperature dependence of quenching analysis was used. The increase in the temperature of analysis results in a decrease in the slope of the Stern-Volmer plots. A careful examination of the absorption spectra of the fluorophore was also employed as an additional method to identify static quenching. In contrast to dynamic quenching, ground state complex formation will frequently result in the perturbation of the absorption spectra of the fluorophore.

ATP binding to peptide. ATP binding was quantified by measuring the decrease in the fluorescence intensity of peptides as a function of ATP concentration. Aliquots (2–50 µl) from a concentrated ATP stock solution (5 mM) were added to a solution of 20 µM of AGYRB or AGYRBM in standard buffer. Experimental conditions such as temperature, equilibrium, fluorescence measurements and corrections as well as data analysis were the same as described above for novobiocin binding.

Peptide binding to DNA. This was carried out using aliquots (5–50 µl) of a concentrated pBS plasmid stock solution (4.37 µg/µl). The quenching of peptide fluorescence was determined as for novobiocin and ATP binding experiments.

Competitiveness Assays

For studies of competitiveness binding of novobiocin and ATP, the peptide model AGYRB (20 µM) in standard buffer was incubated with an equal molar excess of novobiocin for 1 h at 37 °C under gentle rocking. Aliquots (2–50 µl) from a concentrated ATP stock solution (5 mM) were then added to the mixture. Fluorescence was measured (excitation, 280 nm; emission, 304 nm) after the addition of each aliquot as described for the binding assays. Alternatively, AGYRB was incubated for 1 h at 37 °C, with an equal molar excess of ATP. Then aliquots (2–50 µl) of a concentrated novobiocin solution were added and the fluorescence measured at the same excitation and emission wavelength. Prior to all measurements of the peptide fluorescence, the samples were homogenized and equilibrated in the cell holder for 6 min with the excitation shutter closed. The observed fluorescence intensities were also corrected for loss of signal due to a dilution effect and for optical filtering effects caused by novobiocin or ATP absorption at 280 nm. The data were represented in a Stern-Volmer plot and compared with the studies carried out without previous incubation with novobiocin or ATP, respectively.

RESULTS

Peptide Design

Analysis of coumarin-resistant bacterial strains from several species has identified a mutation point to coumarin resistance that maps to the 24 kDa amino-terminal subdomain of GyrB protein [22]. The most prevalent of these are mutations of an arginine residue at position 136 (*E. coli* GyrB). This

latter residue was already implicated in coumarin binding since nine independent coumarin-resistant isolates of *E. coli* have mutations at Arg-136 (to His, Ser, Leu or Cys) [16,23]. The most important contacts anchoring the coumarins in the 24 kDa gyrase domains are located in the region covering the ATP-binding site, including residues around Arg-136. The crystal structure determination of this *N*-terminal subdomain (residues 2–220) complexed with novobiocin [14] as well as with chlorobiocin [13] has revealed that the binding sites of ATP and the drug overlap partially. Nevertheless, it has been proposed that residues surrounding Arg-760 [15] or the corresponding region of the *C*-terminal part of C-TERM [24] are related directly to the recognition and/or transportation of DNA to the DNA binding domain of the A subunit.

According to these findings, a good starting point for the study of the interactions of peptide with coumarin, ATP or DNA, was to consider for peptide design the strand sheet 131–135 and 139–146, the loop residues (136 to 138) that connects them, as well as a short sequence of the native protein containing the Arg-760 residue. Therefore, two fragments of the protein sequence, one including a two-stranded sheet and a loop, and the other including Arg-760 were chosen to be part of the primary structure of the peptide model. Their lengths were set according to the presence of basic residues in the corresponding natural sequences. Finally, to simplify the synthetic problems, a flexible linker replaced the 607 amino acid native sequence that connects these two fragments. Taking into account all these considerations, the model peptide AGYRB was built using the natural fragments 131–146 and 753–770, and a residue of ε-amino caproic acid (Z) to connect them (Figure 1B).

Resistance to coumarin drugs seems to be a consequence of the loss of drug binding to the gyrase induced by mutations in the enzymatic sequence. According to the literature, the amino acid usually mutated in spontaneous coumarin-resistance strains is Arg-136 of GyrB [9,16,22,23]. In particular, mutations of Arg-136 to Leu or to His induce high levels of resistance to coumermycin A_1 [25] and novobiocin [26], respectively. These observations prompted us to consider a comparative study between AGYRB and its analogue AGYRBM, the peptide that mimics the Leu-136 mutant GyrB (Figure 1B). Both peptides were acetylated at the *N*-terminus and have a carboxamide group at the *C*-terminus in order to mimic the presence of amide bonds at these positions in the protein. In order to prevent undesired oxidation and/or alkylation processes during the synthesis of the peptides, Met residues were replaced by norleucine. In addition, it was decided not to include any fluorescent probe on the peptides, basically to maintain the primary structure as close as possible to the structural features of coumarin, ATP and DNA binding sites in the gyrase B protein.

The peptides AGYRB and AGYRBM were synthesized and purified by solid phase synthesis, as described in the material and methods. After purification, 27.3 mg of AGYRB (15% overall yield) and 20.6 mg of AGYRBM (12% overall yield) were obtained. HPLC: rt, 16.1 min and 21.1 min to AGYRB and AGYRBM, respectively. Electrospray ionization mass spectrometry (ESIMS): m/z $(M + 2H)^{2+} = 2115$ (AGYRB) and 2093 (AGYRBM); $M_T = 4229.7$ and 4186.2, respectively.

The objective of this study was to determine whether novobiocin or ATP could form a stable complex with AGYRB, as well as whether this complex is stabilized by the presence of DNA. Furthermore, the possibility of the formation of a similar complex, stabilized or not by DNA, with AGYRBM, is also part of this research. For this purpose, assays based on affinity chromatography with novobiocin, ATP and DNA covalently anchored to the resins were designed.

Novobiocin Affinity Chromatography

With the purpose of obtaining evidence on the formation of a complex between novobiocin and the peptide model AGYRB, the first assay was performed using the coumarin bound to the polymeric support. To this aim epoxy-activated Sepharose was utilized, to which the drug was anchored by its nucleophilic phenolic hydroxy group of the 4-hydroxy-3-(3-methyl-2-butenyl)-benzoic acid moiety under weakly alkaline conditions (Figure 2).

The peptides and DNA were detected following the fluorescence emission at 304 nm (excitation at 280 nm) and the UV absorption at 260 nm, respectively. The chromatographic behaviour of peptide and peptide/DNA using the drug-immobilized column are shown in Figure 3 (A and B). In the presence of magnesium and in the absence of DNA, AGYRB had affinity for the novobiocin column (Figure 3A), but when a mixture of the peptide and DNA was employed, the retention was amplified (Figure 3B), as demonstrated by their elution when the ionic strength was increased. On the other hand,

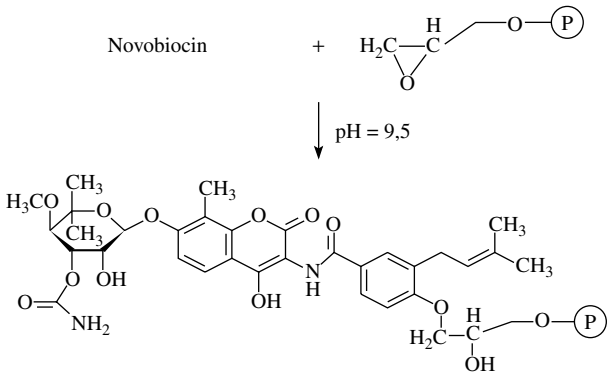

Figure 2 Anchorage of novobiocin to Sepharose.

the peptide mimic of the mutant GyrB (AGYRBM) different to AGYRB was retained in the column only in the presence of DNA. DNA retention was observed in experiments performed in our laboratory under the same conditions and with the column mentioned above (results not shown). All results were dependent on the presence of Mg^{2+}. The peptides and DNA were unable to bind to the resin in a control experiment carried out using unmodified Sepharose.

DNA Affinity Chromatography

The interaction of peptides with DNA was evaluated by the retention in a DNA-cellulose column. Figure 3C shows the results concerning the affinity of peptides to the DNA-resin. The peptides were detected following the fluorescence emission at 304 nm (excitation at 280 nm) as already described. Unlike the study carried out with the drug anchored to a resin, the fact that using DNA bound to a polymeric support allowed us to determine

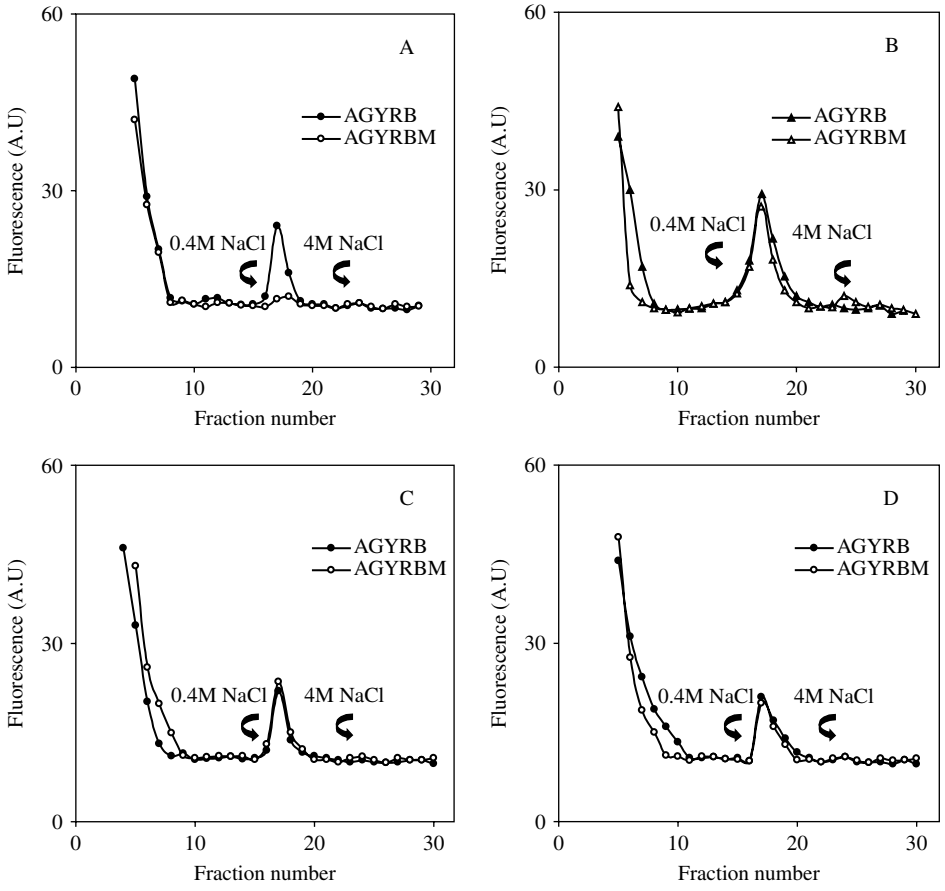

Figure 3 Affinity chromatography experiments with novobiocin (A and B), DNA (C) and ATP (D) bound to the polymeric support. Samples: peptide alone (A, C and D); peptide-DNA (B). The columns were equilibrated with the buffer 5 mM Tris.HCl, pH 7.2/20 mM NaCl/5 mM $MgCl_2$. Elution was carried out with the same buffer containing 0.4 or 4 M NaCl as indicated. The peptide elution was monitored by the intrinsic fluorescence of peptide mimics (excitation at 280 nm and emission at 304 nm). Fractions having fluorescence values out of scale are not presented. AU = Arbitrary units.

qualitatively whether the peptides were able to interact with DNA.

As indicated by the elution profiles, both AGYRB and AGYRBM were retained in the column in a similar way, but the presence of magnesium ions was also essential. Although in the assay conditions used, the effective charge of the peptides was not similar, no difference between the different complexes was observed in terms of stabilization by electrostatic interactions (both were eluted with 0.4 M NaCl). No retention of peptide was observed in a series of control assays that were performed using unmodified resin.

ATP Affinity Chromatography

The binding of the peptides to ATP was assessed using an adenosine 5′-triphosphate affinity column. According to the chromatographic profiles shown in Figure 3D, both peptides, AGYRB and AGYRBM, were retained in the column and were eluted with 0.4 M NaCl. Thus ATP binds, apparently with a similar affinity, to both AGYRB and AGYRBM. With regard to magnesium ions, no appreciable affinity between the peptides and the column with ATP immobilized was observed when the experiments were carried out in the absence of this ion. Control assays carried out using unmodified resin showed no retention of peptides to the column.

Binding Studies

The experiments of affinity chromatography revealed interactions among the peptide mimic AGYRB and novobiocin or ATP. The interesting point was that the interactions were independent of the presence of DNA. However, this behaviour was not observed in the case of the peptide mimic of the mutant GyrB (AGYRBM). This result prompted us to determine the binding parameters for the systems mentioned above. The binding parameters were studied by following the quenching of the intrinsic fluorescence of the peptide upon binding of the novobiocin, ATP or DNA [27]. The plot of the relative peptide fluorescence intensity at an emission wavelength of 304 nm ($\lambda_{ex} = 280$ nm) as a function of total novobiocin, ATP or DNA, is shown in Figure 4. The association constant (K_a) values shown in the Table 1 were obtained from the slope of the Stern-Volmer plot for identified static quenching [18], according to Equation (1). The reported values of

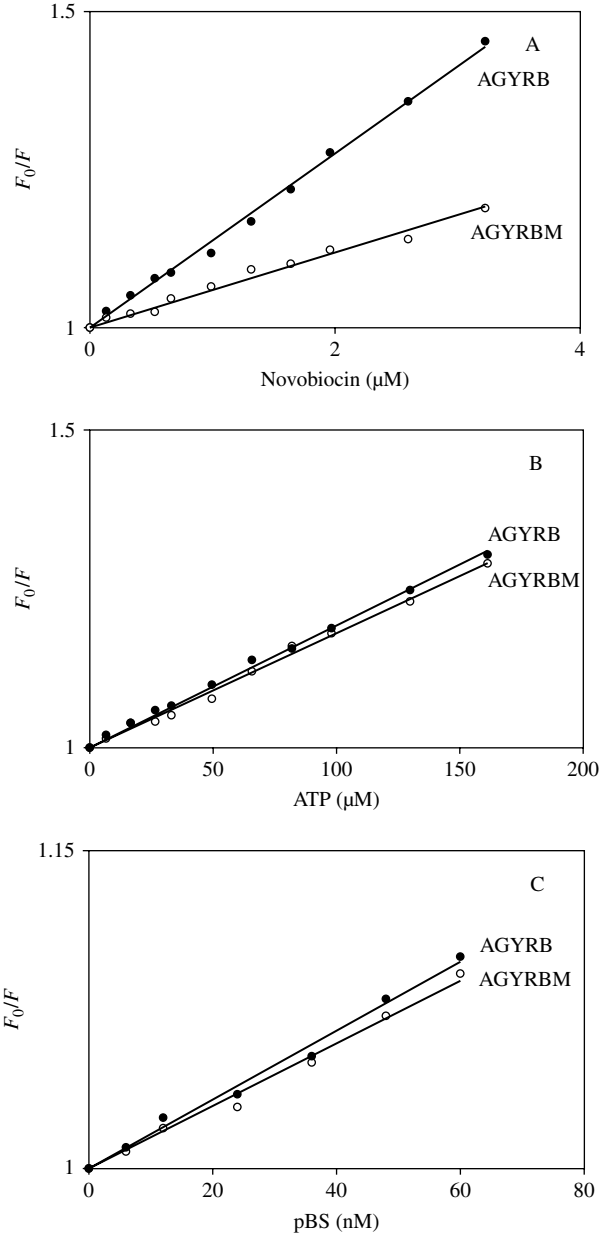

Figure 4 Binding determinations using Stern-Volmer plots. (A) Peptide (30 nmol) and novobiocin (0.13–3.23 μM). (B) Peptide (30 nmol) and ATP (6.65–161.30 μM). (C) Peptide (30 nmol) and pBS (6–60 nM). The slope of the linear Stern-Volmer plot represents the association constant for static quenching. For dynamic quenching the slope represents the Stern-Volmer quenching constant.

K_a are the means of at least five measurements with the standard deviation.

As already found using affinity chromatography, novobiocin and ATP bind to AGYRB in the presence of Mg^{2+}. A preferential binding of the drug to

Table 1 Comparative Binding[a]

Entry	Ligand	$K_a(\times 10^3\ M^{-1})$		$K_d(\mu M)$	
		AGYRB	AGYRBM	AGYRB	AGYRBM
a	Novobiocin	140 ± 30	—[b]	7.1 ± 1.2	—[b]
b	ATP	1.9 ± 0.4	1.7 ± 0.3	530 ± 95	590 ± 90
c	pBS	1600 ± 200	1400 ± 100	0.63 ± 0.08	0.71 ± 0.07

[a] Fluorescence binding assays were performed as described in the Material and Methods section. Reaction mixtures contained 20 μM of one of the peptides and various amounts of ligand. The association constant (K_a) was determined by Stern-Volmer plots [18]. The values of the dissociation constant, K_d ($=1/K_a$), also are shown.
[b] Quenching identified as dynamic quenching, therefore no binding was observed.

peptide was observed in this case (about 70 fold in relation to ATP, entry 'a' and 'b' of Table 1). On the other hand, no binding of novobiocin to the peptide mimic AGYRBM was observed (entry 'a' of Table 1), however, the binding of ATP was identical to both AGYRB and AGYRBM (entry 'b' of Table 1), which is in agreement with our observations using affinity chromatography.

Regarding the interaction of peptides with DNA, the results of binding studies (entry 'c' of Table 1) were consistent with the affinity chromatography studies. Both peptides, with invariable *C*-terminal fragment 753–770, showed identical interactions with DNA. In addition, no change in the binding parameters was observed when the binding assays were carried out with mixtures containing novobiocin or ATP (data not shown).

Competitiveness Assays

To address the question of whether coumarin binds to the peptide mimic AGYRB competitively with ATP, as described for gyrase [14], the binding of novobiocin and ATP to the AGYRB peptide (Figure 5) was examined by fluorescence quenching. When the AGYRB peptide was pre-incubated with ATP and novobiocin was subsequently added for fluorescence quenching analysis, no change in the Stern-Volmer plot was observed when compared with the plot obtained without ATP pre-incubation (Figure 5A). Consequently the association constants were apparently the same for both cases ($1.4 \times 10^5\ M^{-1}$), suggesting that ATP does not affect novobiocin binding. On the other hand, when AGYRB was pre-incubated with novobiocin and ATP was subsequently added for the fluorescence intensity analysis, a lower slope of the Stern-Volmer plot was observed and the association constant was smaller than the corresponding value, obtained without pre-incubation with novobiocin (Figure 5B).

DISCUSSION

The results presented above with peptides designed as mimics of GyrB (wild type and mutant) confirmed important features already known about the mechanism of action of coumarins. In this work, similar conclusions can be drawn from the results achieved with both affinity chromatography and fluorescence quenching methods.

It is well established that the intracellular target of the coumarin group of antibiotics is DNA gyrase and that these compounds inhibit the supercoiling and ATPase reactions of gyrase [28,29]. It is known that residue Arg-136 of the gyrase is a key interaction in terms of the stability of the protein–coumarin complex [16,26], and also that the ATP and coumarin-binding sites are in close proximity [9,14]. Also, it is clear that the presence of DNA is not required for ATP binding [29] but the binding of DNA to B protein is essential for ATP hydrolysis [30]. On the other hand, the DNA dependence of the coumarin interactions remains unclear.

From a qualitative point of view, a parallel behaviour was found for AGYRB, the peptide mimic of GyrB. Thus, AGYRB is able to bind novobiocin and ATP, independently of the DNA presence (Figure 3A,D), consistent with the notion that the *N*-terminal part of the B protein, including Arg-136 residue is concerned with novobiocin and ATP interactions and DNA is not required in order to promote these interactions. The retention increase of the AGYRB on the coumarin-immobilized column in the presence of DNA (Figure 3B) is probably due

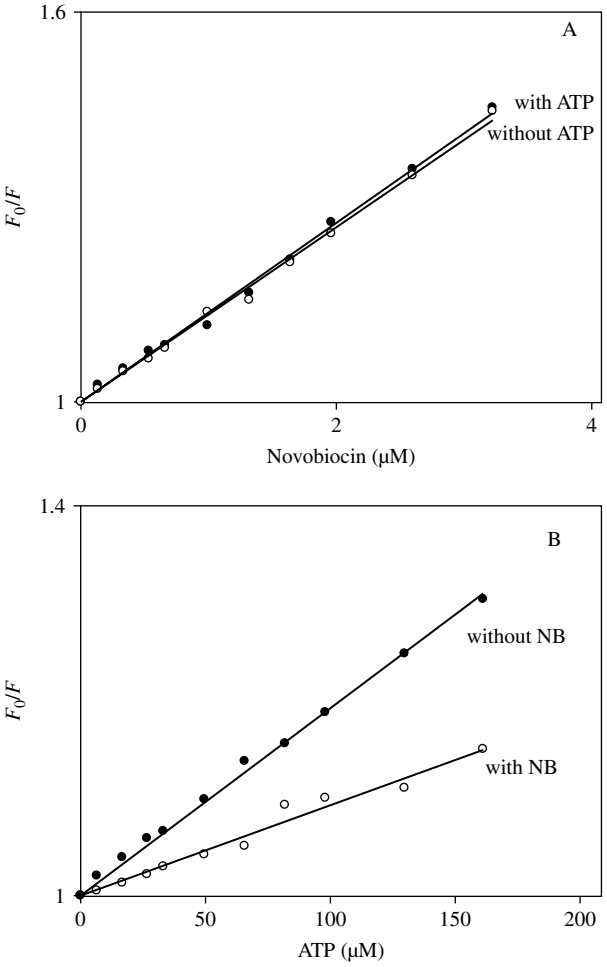

Figure 5 The binding of novobiocin (A) and ATP (B) to the AGYRB peptide. The peptide (20 μM) was incubated with an equal molar excess of ATP for 1 h and novobiocin (0.13–3.23 μM) added (A). The peptide (20 μM) was incubated with an equal molar excess of novobiocin (NB) for 1 h and ATP (6.65–161.30 μM) added (B). Fluorescence was measured (excitation, 280 nm; emission, 304 nm) after each aliquot addition. The slope of the linear Stern-Volmer plot represents the association constant for static quenching.

to simultaneous retention of both the AGYRB and the AGYRB-DNA complex, components of the sample added to the column, in agreement with the binding parameters. As already reported in the literature for B protein, Mg^{2+} was required in order to promote the interactions among the involved species [8,31].

The elution of AGYRB from the novobiocin affinity column by mild conditions suggests that hydrogen bonds are the principal determinants of peptide–drug binding. The importance of Arg-136 might suggest an ionic interaction between this residue and the drug, but in the experimental conditions the drug was unable to interact by this type of interaction due to the absence of a negative effective charge in its structure. Studies carried out with the 24 kDa protein, also suggested that ionic interactions are not likely to be important for drug binding [32]. The Mg^{2+} ion plays an important role in peptide–drug interactions and it can be coordinated with six water molecules, so it is possible that the novobiocin interacts with AGYRB through hydrogen bonds, with Mg^{2+} acting as bridge between the guanidinium group of Arg-136 and the lactone coumarin ring of the drug. The interaction of the AGYRB with the drug produced a quenching in the peptide fluorescence, identified by temperature dependence and absorption spectra analysis as static quenching. Thus, the association constant for the peptide–drug complex was 1.4×10^5 M^{-1}, lower than that reported for 24 and 43 kDa DNA gyrase fragments ($K_a \approx 10^7$ M^{-1}) [8,13,26], which is not surprising considering the size of these fragments (6 and 10-fold bigger, respectively).

In contrast to the novobiocin–AGYRB complex, in the ATP binding electrostatic interactions could be involved. In this case, the phosphate group binds by ionic interactions with Mg^{2+} and the water molecules coordinated to this ion interact with the peptide by hydrogen bonds. ATP binding could also be stabilized by other interactions considering that the adenine rings could make a number of polar contacts with the peptide, in particular with Tyr-145 and the side chain of the glutamic acid residues. The affinity chromatography elution conditions already suggested a weak ATP binding, which was confirmed by the association constant of the ATP–AGYRB complex (1.9×10^3 M^{-1}). Of interest is the fact that the association constant for gyrase is two orders of magnitude higher than the peptide [33], the same difference as observed for the complexes of the peptide or protein with the drug. In addition, the binding of novobiocin to AGYRB is apparently much tighter than for ATP; the K_a for ATP is $\approx 10^3$ M^{-1} compared with 10^5 M^{-1} for novobiocin, in agreement with data described by other authors [3,33,34] for DNA gyrase ($\approx 10^5$ M^{-1} for nucleotides and 10^7–10^9 M^{-1} for coumarins).

According to the K_a values for the AGYRB–DNA, AGYRB–novobiocin and AGYRB–ATP complexes, the peptide binds to DNA more efficiently than the other species, which could be explained in terms of the nature of the interactions that are responsible for binding. The presence of several basic residues in AGYRB is probably the key feature for the binding of

the peptide to DNA through electrostatic interactions between these residues and the phosphate groups of the nucleic acid [17,35]. However, the Mg^{2+} ion dependence observed seems to indicate that the peptide interacts with DNA through its acidic residues within the 753–770 *C*-terminal fragment of AGYRB, to form a complex in which Mg^{2+} acts as a bridge between the phosphate groups of DNA and the peptide, as proposed recently for gyrase [31]. On the other hand, the affinity of AGYRB for DNA ($\kappa_a \approx 10^6\ M^{-1}$ for pBS) proved to be much lower than that reported for DNA gyrase ($\kappa_a \approx 10^{10}\ M^{-1}$) [36], which is not surprising if the size of the natural protein is considered.

The binding of the peptide mimic of mutated GyrB, AGYRBM, to DNA proved to have the same efficiency as AGYRB (Figure 3C and Figure 4C). The change in the effective charge of the peptide from +1 to 0 as a consequence of the mutation of Arg to Leu at position 136 was unable to promote any alteration in the affinity, even with the reduction of the electrostatic interactions with negatively charged phosphate groups. This suggests that the common *C*-terminal fragment in the peptides is concerned with the DNA binding, consistent with the 43 kDa *N*-terminal B fragment that was unable to bind to the DNA [6].

Unlike AGYRB, novobiocin did not bind to AGYRBM, as revealed by the affinity chromatography and fluorescence quenching techniques (Figure 3A, entry 'a' of Table 1). This behaviour is in agreement with several experimental data [22,23,26,36] for the novobiocin and gyrase B fragments with a mutation in Arg-136, that confers coumarin resistance. In those cases, the gyrase B fragments showed greatly reduced drug binding. The retention of the mutated peptide AGYRBM in the novobiocin column in the presence of DNA is additional evidence for the involvement of the *C*-terminal fragment of the peptides with the DNA binding. In this case, the AGYRBM-DNA complex was retained but not the AGYRBM. As with AGYRB, a decrease in the fluorescence intensity of the peptide as a function of the drug concentration was observed (Figure 4A), but the temperature dependence and absorption spectra analysis identified that the quenching was dynamic quenching, resulting from collisional encounters between species and was not due to complex formation. Therefore, the slope of the Stern-Volmer plot is not equal to the association constant, but just to the quenching constant. The reduced affinity displayed by the mutant peptide suggests that the loss of the hydrogen bond between Arg-136 and the drug results in a smaller binding, presumably because of the absence of this important interaction when this residue is changed to Leu. On the other hand, the mutation at the critical position 136 did not produce any change in the ATP binding (Figure 3D and Figure 4B, entry 'b' of the Table 1). This implies that possibly this residue is not a part of the ATP binding site. In fact, a number of the mutations that confer coumarin resistance to DNA gyrase [23,25] lie at the periphery of the ATP binding site.

Many studies reported in the literature have suggested that the ATPase activity of DNA gyrase is inhibited in a competitive manner by novobiocin [3,11,34]. If so, according to the results of competitiveness, the use of short peptides such as AGYRB could be a suitable approach to evaluate the competitive nature of the inhibition of the gyrase by novobiocin. The results of competitiveness assays indicate that, within the limits of experimental error, novobiocin prevents ATP binding, indicating overlapping binding sites, supporting the idea that the novobiocin is competitive with ATP. This conclusion is consistent with x-ray crystallography data on the structure of the complex between the 24 kDa protein and novobiocin [14].

In conclusion, this study has shown that the use of short peptides including sequences of GyrB provides an alternative way to study and better understand the key contacts between the coumarins or ATP and the enzyme, which are especially important for a rational drug design. Moreover, it is believed that these studies provide additional proof that the model of inhibition of coumarin drugs is competitive and that the ATP and novobiocin binding sites are not the same but are in close proximity. Thus, AGYRB constitutes a starting point for the development of peptide models able to mimic the structural features of GyrB at the coumarin and ATP binding sites and, it can be used in the search for new powerful and more specific inhibitors of DNA gyrase.

Acknowledgements

We thank Waldenir Ap. Nunes de Menezes for the technical support. We also thank the Brazilian FAPESP agency for master fellowships to A.C. Scatigno (99/11199-3) and to S.S. Garrido (00/02432-5). R. Marchetto is recipient of research fellowship from CNPq.

REFERENCES

1. Reece RJ, Maxwell A. DNA gyrase: structure and function. *Crit. Rev. Biochem. Mol. Biol* 1991; **26**: 335–375.
2. Wigley DB. Structure and mechanism of DNA gyrase. In *Nucleic Acids and Molecular Biology* Eckstein F, Lilley DMJ (eds). Springer-Verlag: Berlin, Heidelberg 1995; **9**: 165–176.
3. Sugino A, Higgins NP, Brown PO, Peebles CL, Cozzarelli NR. Energy coupling in DNA gyrase and the mechanism of action of novobiocin. *Proc. Natl Acad. Sci. USA* 1978; **75**: 4838–4842.
4. Reece RJ, Maxwell A. Tryptic fragments of the *Escherichia coli* DNA gyrase A protein. *J. Biol. Chem.* 1989; **264**: 19 648–19 653.
5. Reece RJ, Maxwell A. Probing the limits of the DNA breakage-reunion domain of the *Escherichia coli* DNA gyrase A protein. *J. Biol. Chem.* 1991; **266**: 3540–3546.
6. Ali JA, Jackson AP, Howells AJ, Maxwell A. The 43-kilodalton *N*-terminal fragment of DNA gyrase B protein hydrolyses ATP and binds coumarin drugs. *Biochemistry* 1993; **32**: 2717–2724.
7. Brown PO, Peebles CL, Cozzarelli NR. A topoisomerase from *Escherichia coli* related to DNA gyrase. *Proc. Natl Acad. Sci. USA* 1979; **76**: 6110–6114.
8. Wigley DB, Davies GJ, Dodson EJ, Maxwell A, Dodson G. Crystal structure of an *N*-terminal fragment of the DNA gyrase B protein. *Nature* 1991; **351**: 624–629.
9. Maxwell A. DNA gyrase as a drug target. *Trends Microbiol.* 1997; **5**: 102–109.
10. Shen LL, Kohlbrenner WE, Weigl D, Baranowski J. Mechanism of quinolone inhibition of DNA gyrase: appearance of unique norfloxacin binding sites in enzyme-DNA complexes. *J. Biol. Chem.* 1989; **264**: 2973–2978.
11. Gormley NA, Orphanides G, Meyer A, Cullis PM, Maxwell A. The interaction of coumarin antibiotics with fragments of the DNA gyrase B protein. *Biochemistry* 1996; **35**: 5083–5092.
12. Sissi C, Perdona E, Domenici E, Feriani A, Howells AJ, Maxwell A, Palumbo M. Ciprofloxacin affects conformational equilibria of DNA gyrase A in the presence of magnesium ions. *J. Mol. Biol.* 2001; **311**: 195–203.
13. Tsai FTF, Singh OMP, Skarzynsky T, Wonacott AJ, Weston S, Tucker A, Pauptit RA, Breeze AL, Poyser JP, O'Brien R, Ladbury JE, Wigley DB. The high-resolution crystal structure of a 24-kDa gyrase B fragment from *E. coli* complexed with one of the most potent coumarin inhibitors, clorobiocin. *Proteins* 1997; **28**: 41–52.
14. Lewis RJ, Singh OMP, Smith CV, Skarzynski T, Maxwell A, Wonacott AJ, Wigley DB. The nature of inhibition of DNA gyrase by the coumarins and the cyclothialidines revealed by x-ray crystallography. *EMBO J.* 1996; **15**: 1412–1420.
15. Funatsuki K, Tanaka R, Inagaki S, Konno H, Katoh K, Nakamura H. *acrB* Mutation located at carboxy-terminal region of gyrase B subunit reduces DNA binding of DNA gyrase. *J. Biol. Chem.* 1997; **272**: 13 302–13 308.
16. Maxwell A. DNA gyrase as a drug target. *Biochem. Soc. Trans.* 1999; **27**: 48–53.
17. Marchetto R, Nicolas E, Castillo N, Bacardit J, Navia M, Vila J, Giralt E. Two short peptides including segments of subunit A of *Escherichia coli* DNA gyrase as potential probes to evaluate the antibacterial activity of quinolones. *J. Peptide Sci.* 2001; **7**: 27–40.
18. Lacowicz JR. *Principles of Fluorescence Spectroscopy*. Plenum Press: New York, USA, 1987.
19. Sambrook J, Fritsch EF, Maniatis T. *Molecular Cloning: A Laboratory Manual* (2nd edn). Cold Spring Harbor Laboratory Press: Cold Spring Harbor, New York, USA, 1989.
20. Fields GB, Noble RL. Solid-phase peptide synthesis utilizing 9-fluorenyl-methoxycarbonyl amino acids. *Int. J. Peptide Protein Res.* 1990; **35**: 161–214.
21. Borissevitch IE. More about the inner filter effect: corrections of Stern-Volmer fluorescence quenching constants are necessary at very low optical absorption of the quencher. *J. Luminescence* 1999; **81**: 219–224.
22. Maxwell A. The interaction between coumarin drugs and DNA gyrase. *Mol. Microbiol.* 1993; **9**: 681–686.
23. Contreras A, Maxwell A. gyrB mutations which confer coumarin resistance also affect DNA supercoiling and ATP hydrolysis by *Escherichia coli* DNA gyrase. *Mol. Microbiol.* 1992; **6**: 1617–1624.
24. Berger JM, Gamblin SJ, Harrison SC, Wang JC. Structure and mechanism of DNA topoisomerase II. *Nature* 1996; **379**: 225–232.
25. del Castillo I, Vizán JL, Rodríguez-Sáinz MC, Moreno F. An unusual mechanism for resistance to the antibiotic coumermycin A_1. *Proc. Natl Acad. Sci USA* 1991; **88**: 8860–8864.
26. Holdgate GA, Tunnicliffe A, Ward WHJ, Weston SA, Rosembrock G, Barth PT, Taylor IWF, Pauptit RA, Timms D. The entropy penalty of ordered water accounts for weaker binding of the antibiotic novobiocin to a resistant mutant of DNA gyrase: A thermodynamic and crystallographic study. *Biochemistry* 1997; **36**: 9663–9673.
27. Sekiguchi J, Stivers JT, Mildvan AS, Shuman S. Mechanism of inhibition of vaccinia DNA topoisomerase by novobiocin and coumermycin. *J. Biol. Chem.* 1996; **271**: 2313–2322.
28. Gellert M, O'Dea MH, Itoh T, Tomizawa J. Novobiocin and coumermycin inhibit DNA supercoiling catalysed by DNA gyrase. *Proc. Natl Acad. Sci. USA* 1976; **73**: 4474–4478.
29. Mizuuchi K, O'Dea MH, Gellert M. DNA gyrase: subunit structure and ATPase activity of the purified enzyme. *Proc. Natl Acad. Sci. USA* 1978; **75**: 5960–5963.

30. Maxwell A, Gellert M. The DNA dependence of the ATPase activity of DNA gyrase. *J. Biol. Chem.* 1984; **259**: 14 472–14 480.
31. Noble CG, Maxwell A. The role of GyrB in the DNA cleavage-religation reaction of DNA gyrase: a proposed two metal-ion mechanism. *J. Mol. Biol.* 2002; **318**: 361–371.
32. Gilbert EJ, Maxwell A. The 24kDa *N*-terminal subdomain of the DNA gyrase B protein binds coumarin drugs. *Mol. Microbiol.* 1994; **12**: 365–373.
33. Tamura JK, Bates AD, Gellert M. Slow interaction of 5′-adenylyl-β,γ-imido-diphosphate with *Escherichia coli* DNA gyrase. *J. Biol. Chem.* 1992; **267**: 9214–9222.
34. Sugino A, Cozzarelli NR. The intrinsic ATPase of DNA gyrase. *J. Biol. Chem.* 1980; **255**: 6299–6306.
35. Morais Cabral JH, Jackson AP, Smith CV, Shikotra N, Maxwell A, Liddington RC. Crystal structure of the breakage-reunion domain of DNA gyrase. *Nature* 1997; **388**: 903–906.
36. Kampranis SC, Gormley NA, Tranter R, Orphanides G, Maxwell A. Probing the binding of coumarins and cyclothialidines to DNA gyrase. *Biochemistry* 1999; **38**: 1967–1976.

ANEXO 6

S.S. Garrido
A.C. Scatigno
E. Trovatti
D.C. Carvalho
R. Marchetto

Probing the binding of the coumarin drugs using peptide fragments of DNA gyrase B protein

Authors' affiliations:
S.S. Garrido, E. Trovatti, D.C. Carvalho and R. Marchetto, Department of Biochemistry and Technological Chemistry, UNESP – Institute of Chemistry, Caixa Postal 355, 14800-900 Araraquara, São Paulo, Brazil

A. C. Scatigno, Area of Earth and Exact Sciences, University of West of Santa Catarina, Rua Paese, 198, Videira, Santa Catarina, Brazil

Correspondence to:
R. Marchetto
Department of Biochemistry and Technological Chemistry
UNESP – Institute of Chemistry
Caixa Postal 355
14800-900 Araraquara
SP
Brazil
Tel.: 55-16-3301-6670
Fax: 55-16-3322-7932
E-mail: marcheto@iq.unesp.br

Dates:
Received 2 September 2004
Revised 2 September 2004
Accepted 7 March 2005

To cite this article:
Garrido, S.S., Scatigno, A.C., Trovatti, E., Carvalho, D.C. & Marchetto, R. Probing the binding of the coumarin drugs using peptide fragments of DNA gyrase B protein.
J. Peptide Res., 2005, **65**, 502–511.
DOI 10.1111/j.1399-3011.2005.00264.x

Key words: affinity chromatography; coumarins; DNA gyrase; fluorescence; peptide synthesis; quenching

Abstract: Bacterial DNA gyrase, has been identified as the target of several antibacterial agents, including the coumarin drugs. The coumarins inhibit the gyrase action by competitive binding to the ATP-binding site of DNA gyrase B (GyrB) protein. The high in vitro inhibitory potency of coumarins against DNA gyrase reactions has raised interest in studies on coumarin–gyrase interactions. In this context, a series of low-molecular weight peptides, including the coumarin resistance-determining region of subunit B of *Escherichia coli* gyrase, has been designed and synthesized. The first peptide model was built using the natural fragment 131–146 of GyrB and was able to bind to novobiocin ($K_a = 1.8 \pm 0.2 \times 10^5$/M) and ATP ($K_a = 1.9 \pm 0.4 \times 10^3$/M). To build the other sequences, changes in the Arg^{136} residue were introduced so that the binding to the drug was progressively reduced with the hydrophobicity of this residue ($K_a = 1.3 \pm 0.1 \times 10^5$/M and $1.0 \pm 0.2 \times 10^5$/M for Ser and His, respectively). No binding was observed for the change Arg^{136} to Leu. In contrast, the binding to ATP was not altered, independently of the changes promoted. On the contrary, for peptide–coumarin and peptide–ATP complexes, Mg^{2+} appears to modulate the binding process. Our results demonstrate the crucial role of Arg^{136} residue for the stability of coumarin–gyrase complex as well as suggest a different binding site for ATP and in both cases the interactions are mediated by magnesium ions.

Abbreviations: The symbolic representations of the amino acids and its protecting groups as well as abbreviations of techniques, reagents and solvents are is accordance with 'A Revised Guide to Abbreviations in Peptide Science' published in *J. Pept. Sci.* **9**, 1–8 (2003). Rink amide MBHA resin, 4-(2′,4′-dimethoxyphenyl-Fmoc-aminomethyl)-phenoxyacetamido-norleucyl-4-methylbenzhydrylamine resin; NMP, 1-methyl-2-pyrrolidone; ACN, acetonitrile.

Introduction

The intracellular target of the coumarin group of antibacterial agents is DNA gyrase. Gyrase is an essential bacterial protein of the topoisomerase family which uniquely catalyses the negative supercoiling of DNA using the free energy released by ATP hydrolysis (1,2). The structural and biochemical functions of the *Escherichia coli* DNA gyrase have been extensively studied. This enzyme consists of two proteins, A (GyrA) and B (GyrB), of molecular masses 97- and 90-kDa, respectively, which form an A_2B_2 active complex (1,3). The A subunit is functionally divided into a 64-kDa N-terminal and a 33-kDa C-terminal domain, mainly involved in DNA breakage-reunion and DNA wrapping, respectively (4,5). The B protein contains a 43-kDa N-terminal domain, which includes the ATP-binding site, and a 47-kDa C-terminal domain which interacts with GyrA and DNA (6,7). The N-terminal domain includes two subdomains (24-kDa N-terminal part and 19-kDa C-terminal part). The ATP-binding site is located in the first subdomain (7).

Because gyrase is an essential enzyme in prokaryotes but is not found in eukaryotes, it is an ideal target for several classes of antibacterial agents, including the quinolone and coumarin groups (8,9). The coumarins (e.g. novobiocin; Fig. 1A) are naturally occurring compounds that inhibit the gyrase action by competitively binding to the ATP-binding site (10–13).

A

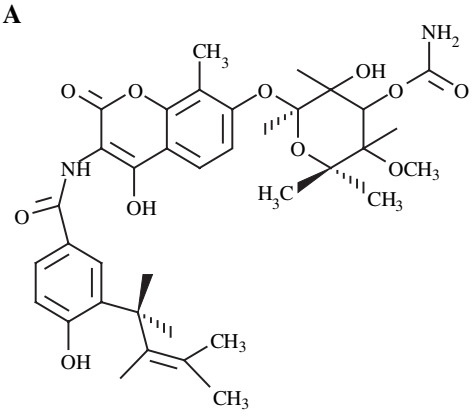

B

Ac-E[131]LVIQ**R**[136]EGKIHRQIYE[146]-NH_2 ***agbN***

Ac-E[131]LVIQ**S**[136]EGKIHRQIYE[146]-NH_2 ***agbS***

Ac-E[131]LVIQ**H**[136]EGKIHRQIYE[146]-NH_2 ***agbH***

Ac-E[131]LVIQ**L**[136]EGKIHRQIYE[146]-NH_2 ***agbL***

Figure 1. Structures of (A) novobiocin and (B) sequences of the synthetic peptide fragments of gyrase B protein.

Information regarding the amino acid residues important in coumarin interaction has come firstly from studies on coumarin-resistant bacterial strains. Point mutations of GyrB that confer resistance to the coumarins all lies at the 24-kDa subdomain of GyrB protein. One residue in particular, Arg^{136}, appears to play an important role in determining coumarin resistance as mutations at this residue have been found in several coumarin-resistant clinical isolates of *E. coli* (14,15). X-ray crystallographic studies (16–18) have also been revealing Arg^{136} as a fundamental residue for coumarin interactions, as well as an indirect link of the enzyme with the ATP (3).

The coumarins are powerful inhibitors of the gyrase supercoiling and ATPase reactions however, they have not enjoyed the same pharmaceutical success as the quinolones: toxicity, permeability and solubility problems have prevented widespread clinical use. Despite this, the interest regarding the production of new biologically active products has stimulated additional studies on molecular mechanism of coumarin binding, including a better understanding of the key contacts between the coumarins and the enzyme. In studies for this purpose, the 43- and 24-kDa N-terminal fragments of GyrB prepared from different *E. coli* strains have been frequently employed (6,7,12,13,17,19), but short peptides have not been used.

Recently, we have reported the synthesis of a 4.2-kDa peptide as a suitable model to study gyrase–coumarin and gyrase–ATP interactions (20). To corroborate the possibility of using short synthetic peptides as models to carry out interactions and structural studies and to elucidate more details about the importance of Arg^{136} residue in the drug–protein and ATP–protein interactions, the drug- and ATP-binding properties of short synthetic peptides (Fig. 1B) bearing a series of mutations in this position have been determined. Affinity chromatography (21) and fluorescence quenching techniques (20,22) were exploited to perform the binding studies. Evidence is presented suggesting that the Arg^{136} residue is at the coumarin and not at the ATP-binding site of gyrase, however both binding sites are in overlapping. A model with Mg^{2+} bridges between the guanidinium group of Arg^{136} and the lactone coumarin ring of the drug is proposed.

Experimental Procedures

N-α-Fluorenylmethoxycarbonyl-amino acids, 4-(2′,4′-dimethoxyphenyl-Fmoc-aminomethyl)-phenoxyacetamido-norleucyl-4-methylbenzhydrylamine resin (Rink amide MBHA resin; 0.55 mmol/g) and 2-(1H-Benzotrizole-1-

yl)-1,1,3,3-tetramethyl-uronium hexafluorophosphate (HBTU) were supplied by Novabiochem (Läufelfingen, Switzerland). Epoxy-activated Sepharose 6B (19–40 μmol/mL), ATP-agarose (1.3 μmol/mL) and single-stranded DNA-cellulose (3.5 μg/g) were provided by Sigma-Aldrich Company (St Louis, MO, USA). *N*,*N*-diisopropylethylmine (DIEA) and trifluoroacetic acid (TFA) were supplied by Fluka Chemical Corp. (New York, NY, USA). Dichloromethane (DCM; Sigma-Aldrich) was peptide synthesis grade and used directly. N,N-dimethyl formamide (DMF), supplied by Mallinckrodt (Phillipsburg, NJ, USA), was bubbled with nitrogen to remove volatile contaminants and kept stored over activated 4 Å molecular sieves. 1-Methyl-2-pyrrolidone (NMP) and acetonitrile (ACN) were purchased from Carlo Erba (Rodano, Milan, Italy). Novobiocin (sodium salt) was also provided by Sigma-Aldrich.

Spectroscopic measurements

Ultraviolet absorbance and fluorescence measurements were made on a Shimadzu (Kyoto, Japan) UV-visible 1601PC spectrophotometer and a Varian (Palo Alto, CA, USA) Cary Eclipse fluorescence spectrophotometer, respectively, both equipped with a thermostated sample compartment, using a 1.5 mL quartz cell for a magnetic stirrer with a 1.0 cm path length. The fluorescence excitation and emission slit widths were set for 5 nm bandpass, for all measurements.

Peptide synthesis

All peptides whose sequences are reported in Fig. 1B were synthesized manually by the solid-phase method according to the standard Fmoc protocol (23) using Rink amide MBHA resin and HBTU/DIEA as coupling reagents. The functional side chains of Fmoc-amino acids were protected by the following groups: Bu^t for Glu, Ser and Tyr, Trt for His and Gln, Pmc for Arg and Boc for Lys. Couplings were performed in all cases using 4 eq of Fmoc-amino acid and 4 eq of coupling reagents in DMF/NMP (1 : 1, v/v) for 1 h. The assembly was monitored by the qualitative Kaiser test and, if positive, the process was repeated with a 50% of reactants. Acetylation was performed with acetic anhydride and DIEA (10 eq each) in DMF, for 30 min. Cleavage and total deprotection of the peptide from the resin were performed with reagent K (TFA/water/phenol/thioanisole/EDT, 82.5 : 5 : 5 : 5 : 2.5, v/v), 10 mL/g peptidyl-resin, 2 h treatment at room temperature. Crude peptides were precipitated in cold diethyl ether and centrifuged (four times), dissolved in 10% aqueous acetic acid and lyophilized. Yields of crude peptides (in weight) ranged between 78 and 90%.

Purification of peptides was carried out by preparative high-performance liquid chromatography (HPLC) on a Waters (Milford, MA, USA) chromatograph using a reverse-phase Vydac-C_{18} column (25 × 2.5 cm; 10 μm; 300 Å) with a linear gradient of 30–60% of solvent B (A: water, 0.1% TFA; B: ACN 60% in water, 0.1% TFA) over 90 min. The flow rate was 10 mL/min and UV detection at 220 nm. Analytical HPLC was carried out on a Varian (Palo Alto, CA, USA) ProStar apparatus employing a Nucleosil C_{18} reverse-phase column (25 × 0.46 cm; 5 μm; 300 Å) with a 5–70% linear gradient of solvent B (A: water, 0.045% TFA; B: ACN, 0.036% TFA) over 30 min, flow rate 1.0 mL/min and UV detection at 220 nm.

Amino acid analysis found are in concordance with the theoric (hydrolysis: 6 M aqueous HCl solution at 110 °C for 72 h; analyzer: Beckman (Fullerton, CA, USA) System 6300). The identity of the peptides was confirmed by electrospray mass spectrometry (ESI-MS) on a ZMD model apparatus from Micromass (Manchester, UK).

Affinity chromatography studies

Novobiocin immobilized on Sepharose

Novobiocin was immobilized on epoxy-activated Sepharose as previously reported (20). Briefly, 100 mg of novobiocin in 8 mL of 0.3 M carbonate buffer (pH 9.5) was added to 1.2 g of the polymeric support. The mixture was left for 20 h at 37 °C when ethanolamine was added for blocking the epoxy-groups excess. After washings, a 1 mL column was packed and equilibrated with standard buffer (10 mM Tris-HCl, pH 7.2/20 mM NaCl/5 mM $MgCl_2$). Peptide sample (500 μL of a 100 μM standard buffer solution) was added to the column. After 1 h at room temperature and gentle rocking, washings with standard buffer were performed until no fluorescence at 304 nm (excitation at 280 nm) was detected. The peptide elution was carried out with 0.4 M NaCl and the column was finally washed with 4 M NaCl and equilibrated with standard buffer.

ATP immobilized column

A 1 mL column was packed with a commercial ATP-agarose and equilibrated with standard buffer. Peptide sample (500 μL of a 100 μM standard buffer solution) was left in the column for 1 h at room temperature under gentle rocking. Further washings with standard buffer were

performed until no fluorescence at 304 nm (excitation at 280 nm) was detected. The peptide elution was carried out with 0.4 M NaCl. The column was washed with 4 M NaCl before equilibration.

DNA immobilized column

A 1 mL column packed with single-stranded DNA-cellulose was employed for this assay. The procedures of equilibrium, washings and elution of peptides were the same as described above for the ATP immobilized column.

Binding experiments

Novobiocin binding to peptide

The quenching of peptide fluorescence by novobiocin was determined as a function of drug concentration as follows. Aliquots (2–50 μL) from a concentrated novobiocin stock solution (100 μM) were added to a solution of 100 μM (1.5 mL) of each peptide in standard buffer, maintained at 37 °C. Prior to measuring the peptide fluorescence, the samples were homogenized and equilibrated in the cell holder for 6 min with the excitation shutter closed. The excitation wavelength was 280 nm with emission measured at 304 nm. The observed fluorescence intensities were corrected for loss of signal because of dilution effect and for optical filtering effects caused by a possible optical absorption of the novobiocin in the emission region (24). The data were represented in a Stern-Volmer plot, for static quenching, where the relative peptide fluorescence (F_o/F) was plotted against the novobiocin concentration [NB] whose slope is equal to the association constant (K_a) for complex formation (22), according to the equation:

$$F_o/F = 1 + K_a[\mathrm{NB}]$$

In this equation, F_o and F are the fluorescence intensities of peptides in the absence and presence of novobiocin, respectively.

Fluorescence quenching data, obtained by intensity measurements alone, can be explained by either a dynamic or static process. To distinguish them, the temperature dependence of quenching analysis was used. Dynamic quenching depends upon diffusion. Because higher temperatures result in larger diffusion coefficients, the bimolecular quenching constants are expected to increase with the increasing temperature. In contrast, increased temperature is likely to result in decreased stability of complexes, and thus lower values of the static quenching constants. So, for static quenching, the increase in the temperature of analysis results in a decrease in the slope of the Stern-Volmer plots. A careful examination of the absorption spectra of the fluorophore was also employed as an additional method to identify static quenching. In contrast to dynamic quenching, ground state complex formation will frequently result in perturbation of the absorption spectra of the fluorophore.

ATP binding to peptide

The ATP binding was quantified by measuring the decrease in the fluorescence intensity of peptides as a function of ATP concentration. Aliquots (2–50 μL) from a concentrated ATP stock solution (5 mM) were added to a solution of 100 μM (1.5 mL) of each peptide in standard buffer. Experimental conditions such as temperature, equilibrium, fluorescence measurements and corrections as well as data analysis were the same as described above for Novobiocin Binding.

Competitiveness assays

For studies of competitiveness binding of novobiocin and ATP, the peptide model *agbN* (100 μM) in standard buffer was incubated with an equal molar excess of novobiocin for 1 h at 37 °C under gentle rocking. Aliquots (2–50 μL) from a concentrated ATP stock solution (5 mM) were then added to the mixture. Fluorescence was measured (excitation, 280 nm; emission, 304 nm) after the addition of each aliquot as described for the binding assays. Alternatively, *agbN* was incubated for 1 h at 37 °C, with an equal molar excess of ATP. Then aliquots (2–50 μL) of a concentrated novobiocin solution (100 μM) were added and the fluorescence measured at the same excitation and emission wavelength. Prior to all measurements of the peptide fluorescence, the samples were homogenized and equilibrated in the cell holder for 6 min with the excitation shutter closed. The observed fluorescence intensities were also corrected for loss of signal because of a dilution effect and for optical filtering effects caused by novobiocin or ATP absorption in the emission region. The data were represented in a Stern-Volmer plot and compared with the studies carried out without previous incubation with novobiocin or ATP, respectively.

Results

Design strategy

Four low-molecular weight peptides were selected and synthesized according to the solid-phase procedure: *agbN*,

agbS, *agbH* and *agbL* (Fig. 1B). The *agbN* was selected because its amino acid sequence reproduces the amino acid sequence of the 131–146 segment (16 residues) of *E. coli* gyrase B (GyrB) protein, including the Arg^{136} residue, thankfully essential for coumarin interactions.

Analysis of coumarin-resistant bacterial strains from several species has identified mutation point to coumarin resistance that maps to the 24-kDa amino-terminal subdomain of GyrB protein (8). The most prevalent of these are mutations of an arginine residue at the position 136. This latter residue was already implicated in coumarin binding as nine independent coumarin-resistant isolates of *E. coli* have mutations at Arg^{136} (to His, Ser, Leu or Cys) (15,16). The most important contacts anchoring the coumarins in the 24-kDa gyrase domains are located in the region covering the ATP-binding site, including residues around Arg^{136}. The crystal structure determination of this N-terminal subdomain (residues 2–220) complexed with novobiocin (16) as well as with chlorobiocin (17) has revealed that the binding sites of ATP and the drug overlap partially.

According to these considerations, the peptide model *agbN* was built using the strand sheets 131–135 and 139–146 and the loop residues (136–138) that connect them. The *agbS*, *agbH* and *agbL* peptides are analogues of *agbN* in which the arginine residue at position 136 was substituted by Ser, His and Leu residues, respectively. All peptides were acetylated at the N-terminus and have a carboxamide group at the C-terminus in order to mimic the presence of amide bonds at these positions in the protein. In addition, it was decided not to include any fluorescent probe on the peptides, basically to maintain the primary structure as close as possible to the structural features of coumarin- and ATP-binding sites in the GyrB protein.

The peptides were synthesized and purified as described in the Experimental Procedures. After purification, 7.3 mg (15% overall yield), 7.6 mg (12% overall yield), 8.1 mg (17% overall yield) and 7.7 mg (16% overall yield) of *agbN*, *agbS*, *agbH* and *agbL*, respectively, were obtained. HPLC: Rt, 14.4 min, 14.9 min, 15.1 min and 20.1 min to *agbN*, *agbS*, *agbH* and *agbL*, respectively. ESI-MS: m/z $(M + H)^+ = 2051$ (*agbN*), 1982 (*agbS*), 2033 (*agbH*) and 2009 (*agbL*); $M_T = 2051.4$, 1982.3, 2032.3 and 2008.3, respectively.

Affinity chromatography measurements

Bearing in mind that affinity chromatography is a good qualitative analysis method, assays based on this technique were designed for interaction processes identification. The first assay was performed using the novobiocin bound to the polymeric support. To this aim epoxy-activated Sepharose was used, in which the drug was anchored by its nucleophilic phenolic hydroxy group of the 4-hydroxy-3-(3-methyl-2-butenyl)-benzoic acid moiety under weakly alkaline conditions (20).

The peptides were detected following the fluorescence emission at 304 nm (excitation at 280 nm). The chromatographic behaviours of peptides using the drug-immobilized column are shown in Fig. 2A. In the magnesium presence, *agbN* had affinity for the novobiocin column, as demonstrated by their elution when the ionic strength was

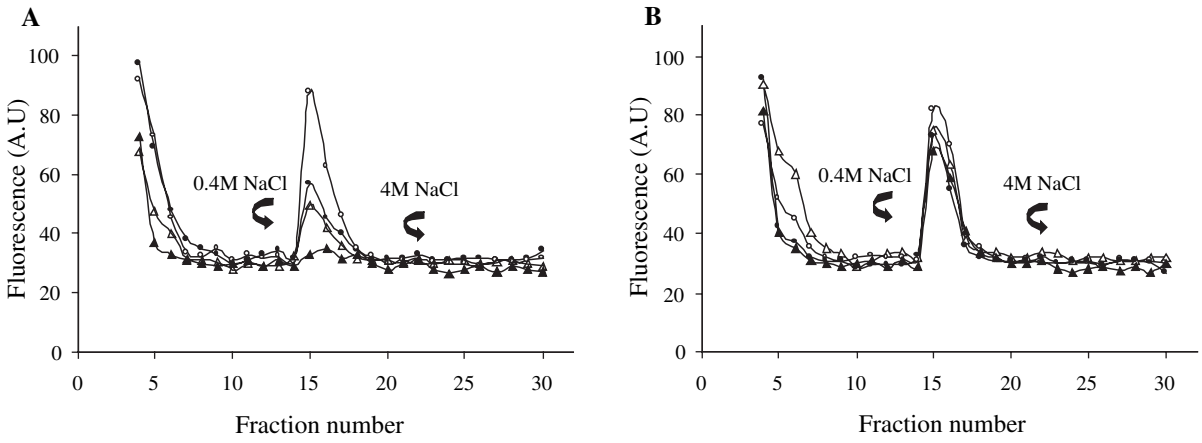

Figure 2. Affinity chromatography experiments with novobiocin (A) and ATP (B) bound to the polymeric support. Samples: *agbN*, ○; *agbS*, •; *agbH*, Δ; *agbL*, ▲. The columns were equilibrated with the buffer 5 mM Tris-HCl, pH 7.2/20 mM NaCl/5 mM $MgCl_2$. Elution was carried out with the same buffer containing 0.4 or 4 M NaCl as indicated. The peptide elution was monitored by the intrinsic fluorescence of peptide fragments (excitation at 280 nm and emission at 304 nm). Fractions having fluorescence values out of scale are not presented (AU, arbitrary units).

increased. For the peptide mimics of the mutant GyrB (*agbS* and *agbH*), the affinity was relatively smaller than *agbN*. On the contrary, the mutant *agbL* peptide, differently from the others, was not retained in the column. All results were dependent on the presence of Mg^{2+}. The peptides were unable to bind to the resin in a control experiment carried out using unmodified Sepharose.

The binding of the peptides to ATP was assessed using an ATP affinity column. According to the chromatographic profiles shown in Fig. 2B, all peptides independently of residue at position 136, were retained in the column and were eluted with 0.4 M NaCl. Thus, ATP binds apparently with a similar affinity to both *agbN* and its variable mutants. In regard to magnesium ions, no appreciable affinity between peptides and the column with ATP immobilized was observed when the experiments were carried out in the absence of this ion. Unlike ATP immobilized column, the *agbN* as well as its mutagenic forms were not retained in the DNA-cellulose column, evidencing that the peptides are not able to interact with DNA, independently of the magnesium presence. Control assays carried out using unmodified resins showed no retention of peptides to the columns.

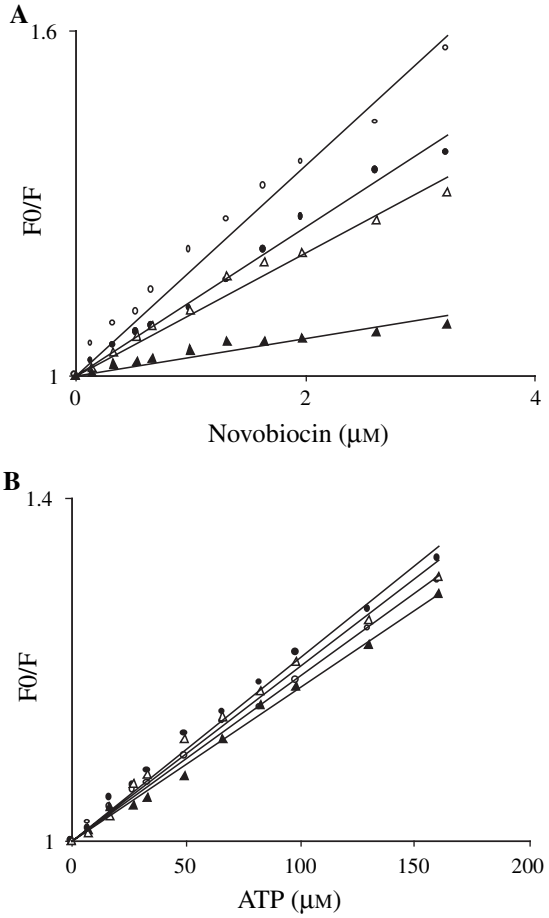

Figure 3. Binding determinations using Stern-Volmer plots. 150 nmol of *agbN*, ○; *agbS*, •; *agbH*, Δ; *agbL*, ▲ and (A) novobiocin (0.13–3.23 μM) or (B) ATP (6.65–161.30 μM). Fluorescence was measured (excitation, 280 nm; emission, 304 nm) after each aliquot addition for each peptide sample. The slope of the linear Stern-Volmer plot represents the association constant for static quenching. For dynamic quenching the slope represents the Stern-Volmer quenching constant.

Binding studies

The affinity chromatography studies revealed interactions among the peptide mimic *agbN* and novobiocin or ATP. The interesting point was that the novobiocin interactions were dependent on the amino acid residue at position 136. This result prompted us to determine the binding parameters for the systems mentioned above. The binding parameters were studied by following the quenching of the intrinsic fluorescence of the peptides upon binding of the novobiocin or ATP (25). The plot of the relative peptide fluorescence intensity at the emission wavelength of 304 nm ($\lambda_{ex} = 280$ nm) as a function of total novobiocin or ATP, is shown in Fig. 3. The association constant (K_a) values shown in the Table 1 were obtained from the slope of the Stern-Volmer plot for identified static quenching (22), according to equation described in the Experimental Procedures. The reported values of K_a are the mean values of at least five measurements with the standard deviation.

As already found using affinity chromatography, novobiocin and ATP bind to *agbN* in the presence of Mg^{2+}. A preferential binding of the drug to peptide was observed in this case (about 80-fold in relation to ATP, entry 'a' of Table 1). The binding of the novobiocin to *agbS* and *agbH* was very close, but smaller than *agbN*. On the contrary, no binding of novobiocin to the peptide mimic *agbL* was observed (entry 'd' of Table 1), however the binding of ATP was identical independently of the peptide sequence ($K_a \cong 2.0 \times 10^3$/M), which is in agreement with our observations using affinity chromatography.

Competitiveness assays

To clarify definitively the role of Arg^{136} residue in the coumarin–protein and ATP–protein interactions and to address the question as to whether coumarin binds to peptide mimic *agbN* competitively with ATP, as described for GyrB protein (16) and its fragments (13,20), the binding of novobiocin and ATP to the *agbN* peptide (Fig. 4) was examined by fluorescence quenching. When the *agbN* peptide was

Table 1. **Comparative binding**[a]

		K_a ($\times 10^3$/M)		K_d (μM)	
Entry	Peptide	Novobiocin	ATP	Novobiocin	ATP
a	*agbN*	180 ± 20	1.9 ± 0.4	5.5 ± 0.5	526 ± 90
b	*agbS*	130 ± 10	2.1 ± 0.3	7.7 ± 0.8	476 ± 70
c	*agbH*	100 ± 20	2.0 ± 0.3	10.0 ± 0.9	500 ± 75
d	*agbL*	–[b]	1.8 ± 0.2	–[b]	555 ± 65

a. Fluorescence-binding assays were performed as described in the Experimental Procedures. Reaction mixtures contained 100 μM of one of the peptides and various amounts of novobiocin or ATP. The association constant (K_a) was determined by Stern-Volmer plots (22). The values of the dissociation constant, K_d (=1/K_a), are also shown.
b. Quenching identified as dynamic quenching, therefore no binding was observed.

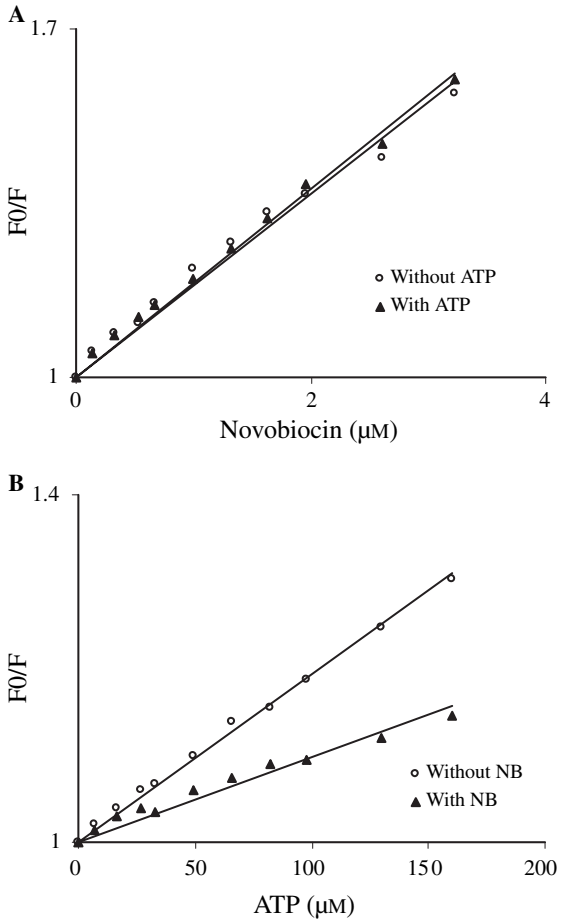

Figure 4. The binding of novobiocin (A) and ATP (B) to the *agbN* peptide. The peptide (100 μM) was incubated with an equal molar excess of ATP for 1 h and novobiocin (0.13–3.23 μM) added (A). The peptide (100 μM) was incubated with an equal molar excess of novobiocin (NB) for 1 h and ATP (6.65–161.30 μM) was added (B). Fluorescence was measured (excitation, 280 nm; emission, 304 nm) after each aliquot addition. The slope of the linear Stern-Volmer plot represents the association constant for static quenching.

pre-incubated with ATP and novobiocin subsequently added for fluorescence quenching analysis, no change in the Stern-Volmer plot was observed if compared with the plot obtained without ATP pre-incubation (Fig. 4A). Consequently the association constants were apparently the same for both cases (1.8×10^5/M), suggesting that ATP does not affect novobiocin binding. On the contrary, when *agbN* was pre-incubated with novobiocin and ATP subsequently added for the fluorescence intensity analysis, a lower slope of the Stern-Volmer plot was observed and the association constant was smaller than the corresponding value, obtained without pre-incubation with novobiocin (Fig. 4B).

Discussion

The Arg^{136} residue of the DNA GyrB protein constitutes the principal point of interactions of the enzyme and the coumarin drugs. Affinity chromatography and fluorescence quenching experiments presented here confirm the important features about the role of the Arg^{136} residue in the mechanism of action of the coumarins.

It is already known that intracellular target of coumarin group of antibiotics is DNA gyrase and that these compounds inhibit the supercoiling and ATPase reactions of gyrase (11,26). It is established that the residue Arg^{136} of the gyrase is a key interaction in terms of the stability of the protein–coumarin complex (18,27), and also that the ATP- and coumarin-binding sites are in close proximity (9,16). Also, its clear that the DNA presence is not required for ATP and coumarin binding but the binding of DNA to B protein is essential for ATP hydrolysis (28).

A similar behaviour, from a qualitative point of view was recently found for a 4.2-kDa synthetic peptide (20). Here, we found a parallel behaviour for *agbN*, the new peptide mimic of wild-type GyrB. Thus, *agbN* is able to bind novobiocin and ATP, independently of the DNA presence (Fig. 2A,B), consistent with the notion that N-terminal part of the B protein, including Arg^{136} residue is concerned with

novobiocin and ATP interactions and DNA is not required in order to promote these interactions. As already reported in the literature for B protein, Mg^{2+} was required in order to promote the interactions among the involved species (6,29).

The elution of *agbN* from novobiocin affinity column by mild conditions suggests that hydrogen bonds, and not ionic interactions, are the main determinants of peptide–drug binding. Studies carried out with 24-kDa protein, also suggested that ionic interactions are not likely to be important for drug binding (12). Once Mg^{2+} ion plays an important role for peptide–drug interactions, it is possible that the Mg^{2+} acts as a bridge between the guanidinium group of Arg^{136} and the lactone coumarin ring of the drug. In this model, two water molecules coordinated with Mg^{2+} forms hydrogen bonds to the guanidinium group of Arg^{136} and other two with the ester and carbonyl oxygens of the coumarin ring (Fig. 5). It is possible that in the molecular adjustment, the 2′-hydroxyl group of novobiose forms one direct hydrogen bond to the carbonyl oxygen of Gln^{143}. The 3′-carbamoyl group of novobiose forms one water-mediated hydrogen bonds with Mg^{2+} coordinate with the side chain of Glu^{146}. In addition, the ether oxygen that bridges the coumarin rings and the novobiose sugar can form a hydrogen bond to an ordered water molecule, which in turn forms a hydrogen bond to the side chain of Gln^{143}. The interaction of the *agbN* with the drug produced a quenching in the

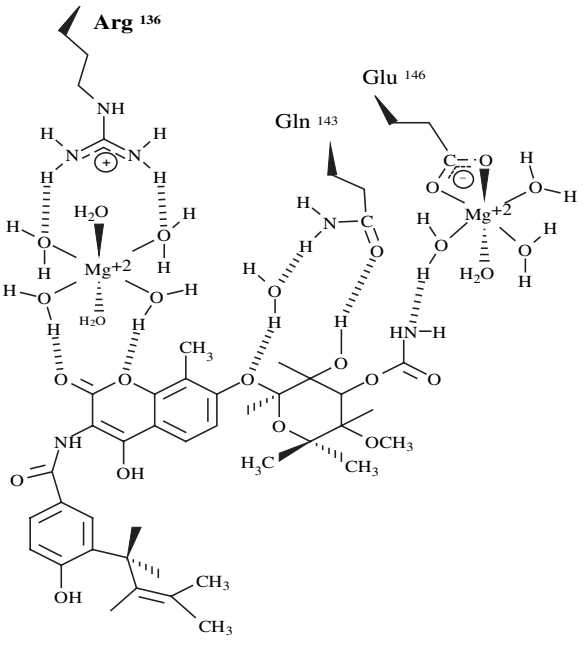

Figure 5. Proposed hydrogen bonds (dashed lines) between novobiocin and amino acid residues in *agbN*. In the proposed model the Mg^{2+} acts as bridge between the guanidinium group of Arg^{136} and the lactone coumarin ring of the drug. Other water-mediated hydrogen bonds act in the molecular adjustment of the novobiocin to its binding site.

peptide fluorescence (Fig. 3A), identified by temperature dependence and absorption spectra analysis as static quenching. Thus, the association constant for peptide–drug complex was 1.8×10^5/M, lower than the one reported for 24- and 43-kDa DNA gyrase fragments ($K_a \approx 10^7$/M) (6,17,18) but of the same order of magnitude as the recent reported 4.2-kDa synthetic GyrB fragment (20).

Differently from the novobiocin–*agbN* complex, in the ATP binding electrostatic interactions could be involved. In this case, the phosphate group binds by ionic interactions with Mg^{2+} which in turn also binds by ionic interactions with the side chains of glutamic acid residues specifically at the positions 131 and 146. ATP binding could also be stabilized by other interactions considering that the adenine rings can make a number of polar contacts with the peptide, in particular with Tyr^{145}. The affinity chromatography elution conditions already suggested a weak ATP binding, which was confirmed by the association constant of the ATP–*agbN* complex (1.9×10^3/M). Interesting is the fact that the association constant for gyrase is two orders of magnitude higher than the peptide (30), the same difference observed for the complexes of the peptide or protein with the drug. In addition, the binding of the novobiocin to *agbN* is apparently much tighter than for ATP; the K_a for ATP is $\cong 10^3$/M compared with 10^5/M for the novobiocin, in agreement with data described for gyrase ($\cong 10^5$/M for nucleotides and 10^7–10^9/M for coumarins) (10,30,31) and for the short synthetic peptide AGYRB ($\cong 10^3$ and 10^5/M for ATP and novobiocin respectively) (20).

Regarding the interactions with DNA, recent studies with two peptide fragments of GyrB, with an invariable C-terminal fragments 753–770 (20), confirmed the proposal that the residues surrounding Arg^{760} are related directly to the recognition and/or transportation of DNA to the DNA-binding domain of A subunit of gyrase. The interaction lack between *agbN* and the DNA described here intensifies this hypothesis.

For mutagenic forms of *agbN*, novobiocin binding was progressively reduced with the hydrophobicity of the residue at the position 136 ($\cong$30 and 50% for Ser and His respectively). Novobiocin did not bind to *agbL*, as revealed by the affinity chromatography and fluorescence quenching techniques (Fig. 2A,entry 'd' of Table 1). This behaviour is in agreement with several experimental data (8,15,18,32) for the novobiocin and GyrB fragments with a mutation in Arg^{136}, that confers coumarin resistance. In those cases, the GyrB fragments showed greatly reduced drug binding. Apparently the affinity of novobiocin to the peptide is related to the number of hydrogen bonds of the drug to

amino acid residue at position 136. Ser and His, unlike Arg, forms only a single hydrogen bond with water molecules coordinated with Mg^{2+} which in turn form two hydrogen bonds with the ester and carbonyl oxygens of the coumarin ring (Fig. 5). However, in the experimental conditions, Ser amino acid acts as a hydrogen bond donor while His as hydrogen bond acceptor, resulting in the little difference in the novobiocin binding observed for *agbS* and *agbH*. The lack of the hydrogen bond between novobiocin and the Leu mutant peptide can also explain the reduced affinity displayed by this peptide. With the increase of the hydrophobicity of the residues at position 136 (Arg < Ser ≤ His < Leu) (33–35), there is a decrease in the tendency of the hydrogen bonds formation and consequently in the novobiocin binding. Thus, apparently there is a relationship between the number of hydrogen bonds of novobiocin to the peptide and the corresponding binding affinity, consistent with X-ray crystallographic data on the complex between the 24-kDa protein and novobiocin (16).

As with *agbN*, a decrease in the fluorescence intensity of peptide as a function of the drug concentration was observed for all peptide mimics of mutagenic GyrB (Fig. 3A). But differently from *agbN* and its mutagenic forms *agbS* and *agbH*, the temperature dependence studies and absorption spectra analysis for *agbL* identified that the quenching was dynamic quenching, resulting from collisional encounters between species and was not due to complex formation. Therefore, the slope of the Stern-Volmer plot is not equal to the association constant, but just the quenching constant. This result intensifies the hypothesis that the affinity of novobiocin to its binding site depends on the hydrogen bonds, as the absence of this important interaction promoted a complete loss of binding when Arg^{136} was changed to Leu.

On the contrary, the mutations at the critical position 136 did not produce any change in the ATP binding (Figs 2B and 3B; columns 4 and 6 of Table 1). This implies that possibly this residue is not a part of the ATP-binding site. In fact, a number of the mutations that confer coumarin resistance to DNA gyrase (14,15) lies at the periphery of the ATP-binding site.

Studies from different researches have been suggesting that the ATPase activity of DNA gyrase is inhibited in a competitive manner by novobiocin (10,13,31). If so, recent studies (20) together with the results of competitiveness presented here, the use of short peptides as *agbN* could be a suitable approach to evaluate the competitive nature of the inhibition of the gyrase by novobiocin. The results of competitiveness assays indicate that, within the limits of experimental error, novobiocin prevent the ATP binding, indicating overlapping binding sites, supporting the idea that the novobiocin is competitive with ATP. This conclusion is also consistent with crystallographic studies of the structure of the complex between the 24-kDa protein and coumarin drugs (16,17).

In conclusion, we have corroborated that the use of short peptides including sequences of GyrB provides an alternative way to study and better understand the key contacts between the coumarins or ATP and the enzyme, which are especially important for a rational drug design. Moreover, our studies provide an additional proof that the model of inhibition of coumarins drugs is competitive and that ATP- and novobiocin-binding sites are not the same but are in close proximity. Perhaps the most important conclusion that emerges from this work is the supposed role that the Mg^{2+} and its coordinated water molecules play in the hydrogen bonding network formation which is necessary for the stability of coumarin–gyrase complex. The Mg^{2+} bridge model provides some clues of the essential importance of Arg^{136} residue for coumarin binding.

Acknowledgements: This work was funded by FAPESP agency in the form of grant (99/02265-2) and master fellowships to A. C. Scatigno (99/11199-3) and to S. S. Garrido (00/02432-5). R. Marchetto is recipient of CNPq research fellowship.

References

1. Reece, R.J. & Maxwell, A. (1991) DNA gyrase: structure and function. *Crit. Rev. Biochem. Mol. Biol.* **26**, 335–375.
2. Wang, J.C. (1996) DNA topoisomerases. *Annu. Rev. Biochem.* **54**, 665–697.
3. Wigley, D.B. (1995) Structure and mechanism of DNA gyrase. In: *Nucleic Acids and Molecular Biology*, Vol. 9 (Eckstein, F. & Lilley, D.M.J., eds), pp. 165–176. Springer-Verlag, Heidelberg, Berlin.
4. Reece, R.J. & Maxwell, A. (1989) Tryptic fragments of the *Escherichia coli* DNA gyrase A protein. *J. Biol. Chem.* **264**, 19648–19653.
5. Reece, R.J. & Maxwell, A. (1991) Probing the limits of the DNA breakage-reunion domain of the *Escherichia coli* DNA gyrase A protein. *J. Biol. Chem.* **266**, 3540–3546.
6. Wigley, D.B., Davies, G.J., Dodson, E.J., Maxwell, A. & Dodson, G. (1991) Crystal structure of an N-terminal fragment of the DNA gyrase B protein. *Nature* **351**, 624–629.

7. Ali, J.A., Jackson, A.P., Howells, A.J. & Maxwell, A. (1993) The 43-kilodalton N-terminal fragment of DNA gyrase B protein hydrolyses ATP and binds coumarin drugs. *Biochemistry* **32**, 2717–2724.
8. Maxwell, A. (1993) The interaction between coumarin drugs and DNA gyrase. *Mol. Microbiol.* **9**, 681–686.
9. Maxwell, A. (1997) DNA gyrase as a drug target. *Trends Microbiol.* **5**, 102–109.
10. Sugino, A., Higgins, N.P., Brown, P.O., Peebles, C.L. & Cozzarelli, N.R. (1978) Energy coupling in DNA gyrase and the mechanism of action of novobiocin. *Proc. Natl Acad. Sci. U S A* **75**, 4838–4842.
11. Mizuuchi, K., O'Dea, M.H. & Gellert, M. (1978) DNA gyrase: subunit structure and ATPase activity of the purified enzyme. *Proc. Natl Acad. Sci. U S A* **75**, 5960–5963.
12. Gilbert, E.J. & Maxwell, A. (1994) The 24 kDa N-terminal sub-domain of the DNA gyrase B protein binds coumarin drugs. *Mol. Microbiol.* **12**, 365–373.
13. Gormley, N.A., Orphanides, G., Meyer, A., Cullis, P.M. & Maxwell A. (1996) The interaction of coumarin antibiotics with fragments of the DNA gyrase B protein. *Biochemistry* **35**, 5083–5092.
14. del Castillo, I., Vizán, J.L., Rodríguez-Sáinz, M.C. & Moreno, F. (1991) An unusual mechanism for resistance to the antibiotic coumermycin A_1. *Proc. Natl Acad. Sci. U S A* **88**, 8860–8864.
15. Contreras, A. & Maxwell, A. (1992) GyrB mutations which confer coumarin resistance also affect DNA supercoiling and ATP hydrolysis by *Escherichia coli* DNA gyrase. *Mol. Microbiol.* **6**, 1617–1624.
16. Lewis, R.J., Singh, O.M.P., Smith, C.V., Skarzynski, T., Maxwell, A., Wonacott, A.J. & Wigley, D.B. (1996) The nature of inhibition of DNA gyrase by the coumarins and the cyclothialidines revealed by X-ray crystallography. *EMBO J.* **15**, 1412–1420.
17. Tsai, F.T.F., Singh, O.M.P., Skarzynsky, T., Wonacott, A.J., Weston, S., Tucker, A., Pauptit, R.A., Breeze, A.L., Poyser, J.P., O'Brien, R., Ladbury, J.E. & Wigley, D.B. (1997) The high-resolution crystal structure of a 24-kDa gyrase B fragment from *E. coli* complexed with one of the most potent coumarin inhibitors, clorobiocin. *Proteins* **28**, 41–52.
18. Holdgate, G.A., Tunnicliffe, A., Ward, W.H.J, Weston, S.A., Rosembrock, G., Barth, P.T., Taylor, I.W.F., Pauptit, R.A. & Timms, D. (1997) The entropy penalty of ordered water accounts for weaker binding of the antibiotic novobiocin to a resistant mutant of DNA gyrase: a thermodynamic and crystallographic study. *Biochemistry* **36**, 9663–9673.
19. Laffite, D., Lamour, V., Tsvetkov, P.O., Makarov, A.A., Klich, M., Deprez, P., Moras, D., Briand, C. & Gilli, R. (2002) DNA gyrase interaction with coumarin-based inhibitors: the role of the hydroxybenzoate isopentenyl moiety and the 5′-methyl group of the noviose. *Biochemistry* **41**, 7217–7223.
20. Scatigno, A.C., Garrido, S.S. & Marchetto, R. (2004) A 4.2 kDa synthetic peptide as potential probe to evaluate the antibacterial activity of coumarin drugs. *J. Pept. Sci.* **10**, 566–577.
21. Marchetto, R., Nicolas, E., Castillo, N., Bacardit, J., Navia, M., Vila, J. & Giralt, E. (2001) Two short peptides including segments of subunit A of *Escherichia coli* DNA gyrase as potential probes to evaluate the antibacterial activity of quinolones. *J. Pept. Sci.* **7**, 27–40.
22. Lacowicz, J.R. (ed.) (1987) *Principles of Fluorescence Spectroscopy*. Plenum Press, New York, USA, p. 496.
23. Fields, G.B. & Noble, R.L. (1990) Solid-phase peptide synthesis utilizing 9-fluorenyl-methoxycarbonyl amino acids. *Int. J. Pept. Protein Res.* **35**, 161–214.
24. Borissevitch, I.E. (1999) More about the inner filter effect: corrections of Stern-Volmer fluorescence quenching constants are necessary at very low optical absorption of the quencher. *J. Luminescence* **81**, 219–224.
25. Sekiguchi, J., Stivers, J.T., Mildvan, A.S. & Shuman, S. (1996) Mechanism of inhibition of vaccinia DNA topoisomerase by novobiocin and coumermycin. *J. Biol. Chem.* **271**, 2313–2322.
26. Gellert, M., O'Dea, M.H., Itoh, T. & Tomizawa, J. (1976) Novobiocin and coumermycin inhibit DNA supercoiling catalysed by DNA gyrase. *Proc. Natl Acad. Sci. U S A* **73**, 4474–4478.
27. Maxwell, A. (1999) DNA gyrase as a drug target. *Biochem. Soc. Trans.* **27**, 48–53.
28. Maxwell, A. & Gellert M. (1984) The DNA dependence of the ATPase activity of DNA gyrase. *J. Biol. Chem.* **259**, 14472–14480.
29. Noble, C.G. & Maxwell, A. (2002) The role of GyrB in the DNA cleavage-religation reaction of DNA gyrase: a proposed two metal-ion mechanism. *J. Mol. Biol.* **318**, 361–371.
30. Tamura, J.K., Bates, A.D. & Gellert, M. (1992) Slow interaction of 5′-adenylyl-β,γ-imido-diphosphate with *Escherichia coli* DNA gyrase. *J. Biol. Chem.* **267**, 9214–9222.
31. Sugino, A. & Cozzarelli, N.R. (1980) The intrinsic ATPase of DNA gyrase. *J. Biol. Chem.* **255**, 6299–6306.
32. Kampranis, S.C., Gormley, N.A., Tranter, R., Orphanides, G. & Maxwell, A. (1999) Probing the binding of coumarins and cyclothialidines to DNA gyrase. *Biochemistry* **38**, 1967–1976.
33. Guy, H.R. (1985) Amino acid side-chain partition energies and distribution of residues in soluble proteins. *Biophys. J.* **47**, 61–70.
34. Abraham, D.J. & Leo, A.J. (1987) Extension of the fragment method to calculate amino acid zwitterion and side chain partition coefficients. *Proteins* **2**, 130–152.
35. Roseman, M.A. (1988) Hydrophilicity of polar amino acid side-chains is markedly reduced by flanking peptide bonds. *J. Mol. Biol.* **200**, 513–522.